

GI_Forum

Journal for Geographic Information Science



Table of Content

Learning with Geomedia

Robert Vogler (Ed.)

Josef Buchner – Peter Michael Jeremias – Nikola Kobzare – Lelia König – Sebastian Oberreiter – Stefan Reiter – Bernd Resch

An Augmented Reality Learning Environment for Informal Geoinformatics Education

Page 3 - 17

DOI: 10.1553/giscience2021_02_s3

Jana Pokraka – Torsten Kralemann–Poppell – Inga Gryl – Paula Schmidt

'This is a Great Place for Children. Here, They Can Play, Do What They Want, Have Fun and Other Things.' Mapping Primary School Children's Everyday Spaces

Page 18 - 33

DOI: 10.1553/giscience2021_02_s18

Torben Foehrder – Jan–Peter Mund – Peter Spathelf

Advantages of 360° Virtual Forest Tours to Supplement Academic Forestry Education

Page 34 - 44

DOI: 10.1553/giscience2021_02_s34

Daniel Raithofer – Christiane Hintermann

Intellectual Resilience – Draft of a New Educational Approach for the Geography Classroom

Page 45 - 53

DOI: 10.1553/giscience2021_02_s45

Leon Fuchs – Detlef Kanwischer – Christian Dorsch

Algorithmic Cultures: A Missing Link of Spatial Citizenship Education

Page 54 - 64

DOI: 10.1553/giscience2021_02_s54

Advances in GI Science

Adrijana Car – Gerald Griesebner (Eds.)

Alois Simon

Modelling Climate–Sensitive Forest Succession to Assess Impacts of Climate Change and Support Decision Making

Page 65 - 81

DOI: 10.1553/giscience2021_02_s65

Sabine Hennig

Orchard Meadow Trees: Tree Detection Using Deep Learning in ArcGIS Pro

Page 82 - 93

DOI: 10.1553/giscience2021_02_s82

Victoria Chmarycz – K. Wayne Forsythe

Examining Wildfire Spread Variables for Assessing Forest Burn Vulnerability

Page 94 - 107

DOI: 10.1553/giscience2021_02_s94

Vincenza Ferrara – Anders Wästfelt

Unpacking Layers of Space–Time Complexity in Land–Use Dynamics. A Case Study from the Olive Agroecosystems of Sicily (Italy)

Page 108 - 121

DOI: 10.1553/giscience2021_02_s108

Jakub Růžička – Lukáš Brůha

Automatic Detection of Driving–Lane Geometry Based on Aerial Images and Existing Spatial Data

Page 122 - 135

DOI: 10.1553/giscience2021_02_s122

Oliver Hennhöfer – Julian Bruns – Peter Ullrich – Andreas Heiß – Galibjon Sharipov – Dimitrios Paraforos

Multidimensional Exploratory Spatial Data Analysis

Page 136 - 151

DOI: 10.1553/giscience2021_02_s136

Mohammad Mustafa Sa'doun – Christopher D. Lippitt – Gernot Paulus – Karl–Heinrich Anders
A Comparison of Convolutional Neural Network Architectures for Automated Detection and Identification of Waterfowl in Complex Environments

Page 152 - 166

DOI: 10.1553/giscience2021_02_s152

Helen Ngonidzashe Serere – Bernd Resch – Clemens Rudolf Havas – Andreas Petutschnig
Extracting and Geocoding Locations in Social Media Posts: A Comparative Analysis

Page 167 - 173

DOI: 10.1553/giscience2021_02_s167

Christoph Traun – Gudrun Wallentin – Manuela Larissa Schreyer

Design of an Experiment to Evaluate Modes of Value Generalization in Animated Choropleth Maps

Page 174 - 192

DOI: 10.1553/giscience2021_02_s174

David Li – Matthias Budde – Julian Bruns

Towards Dynamic Isochrone Mapping Accounting for Uncertainty

Page 193 - 201

DOI: 10.1553/giscience2021_02_s193

Gulam Mohiuddin – Jan–Peter Mund

Application of Land Surface Temperature Analysis in Urban Green Spaces: Case Studies from South Asia

Page 202 - 214

DOI: 10.1553/giscience2021_02_s202

Yingwen Deng – Wolfgang Spitzer – Sabine Gadocha – Thomas Prinz

A Web Application for Simulating Future Settlement Development

Page 215 - 227

DOI: 10.1553/giscience2021_02_s215

Meng–Chin Tsai – Stephan van Gassel – Tzu–Chin Lin

Towards Sustainable Urban Car–Parking Solutions: Exploring Effects of Parking Policies Using Spatial Regression Analysis

Page 228 - 241

DOI: 10.1553/giscience2021_02_s228

Victoria Fast – Jiaao Guo

Putting Pedestrians First: Sidewalk Infrastructures, Width Patterns and COVID–19

Page 242 -250

DOI: 10.1553/giscience2021_02_s242

Claudia Luger–Bazinger – Veronika Hornung–Prähauser

Innovation for Sustainable Cities: The Effects of Nudging and Gamification Methods on Urban Mobility and Sustainability Behaviour

Page 2051 - 258

DOI: 10.1553/giscience2021_02_s251

An Augmented Reality Learning Environment for Informal Geoinformatics Education

Josef Buchner¹, Peter Michael Jeremias², Nikola Kobzare², Lelia König², Sebastian Oberreiter², Stefan Reiter² and Bernd Resch²

¹University of Duisburg-Essen, Germany

²University of Salzburg, Austria

Abstract

In this paper, we describe an interactive learning environment for geoinformatics enriched by Augmented Reality (AR) that was designed by researchers and practitioners using a design-based research approach. In total, four AR modules were developed to engage learners physically, cognitively and emotionally in the learning process. AR is thus used not merely as a visualization technology, but also to initiate and scaffold learning activities. To address the known challenges of learning with AR, we designed our learning environment to be used by teams of students. This can counteract the problem of cognitive overload, or frustration due to technical problems. We examined our technological and pedagogical framework in an evaluation with 12 learners. The results show that our design did not lead to cognitive overload; technological aspects, such as usability, were also evaluated positively. However, we also detected possible improvements to our design, such as using AR glasses to free the hands for task completion. Overall, it was shown that AR is a good way to expand traditional learning opportunities with digital ones and to enable holistic learning experiences.

Keywords:

geoinformatics, augmented reality, collaborative learning, education, interactive learning

1 Introduction

In science education, students often struggle to understand the complexity and interrelationships of natural phenomena, since these are not immediately perceivable or tangible. Consequently, educators increasingly report misconceptions on the part of students, and a decline in their interest and motivation with regard to science learning (see e.g. Sahin & Yilmaz, 2020). To counteract this, researchers are calling for science learning to be student-centred and to use an active learning paradigm (Deslauriers et al., 2011), in which learners become (co-)designers of the learning process by asking questions, hypothesizing, and planning experiments with which to test predictions (Goff et al., 2020). The use of technology can support these self-regulated learning activities in a variety of ways, including just-in-time

feedback, scaffolding, making non-visible phenomena visible, and giving students the feeling of experiencing an authentic situation that requires real-life problem-solving (Yannier et al., 2020).

In recent years, augmented reality (AR) technology has proved particularly promising for this purpose because, in contrast to immersive virtual reality (iVR), reality is not completely replaced but enhanced by digital elements (Cheng & Tsai, 2013). Hence, learners can still explore the real world, but at the same time they can see underlying relationships; helpful information can be displayed directly on an object, and students can even make changes to both the object and the information that are displayed in real time and can thus be observed (Dunleavy et al., 2009). Moreover, many studies have demonstrated that learners find AR motivating, satisfying and interesting, which in turn has led to improved attitudes towards science learning (Ibáñez & Delgado-Kloos, 2018).

In addition to these potentials, researchers also point to challenges when using AR in learning environments. From a technical perspective, particular attention must be paid to the usability of the AR application employed. If the operation is perceived as difficult and complicated, negative effects on both affective and cognitive learning outcomes can be observed. For example, the usefulness of the technology for one's own learning is then questioned, satisfaction decreases, and further use of the application becomes less likely (Ibili et al., 2019). Another factor that must be considered is cognitive load. AR learning environments integrate different media and require self-directed learning, which could lead to cognitive overload for students (Lai et al., 2019).

Based on these affordances of science education and AR learning, we developed an AR learning environment for geoinformatics using a design-based research approach. In this study, we present a design consisting of four AR modules. In addition, we report the results of our initial evaluation, in which 12 learners tested the first iteration of the modules. The goal of the evaluation was to find out whether the AR modules are perceived as cognitively demanding, and whether the technical framework used is suitable, acceptable to students, and perceived as user-friendly.

2 Design Process

The development and design of the AR-enhanced learning modules for geoinformatics was part of the ARED project (Augmented Reality for Education), which is being carried out in cooperation with the iDEAS:lab Salzburg¹. In this project researchers from the fields of educational technology and geoinformatics, practitioners, university students and AR developers collaborate to design meaningful and exciting educational experiences for school students and the public. This merging of research and practice can help to ensure that innovative educational practice persists beyond the duration of the project itself (Bell, 2004). One approach that is explicitly suitable for projects with theory–practice linkages is the design-based research approach (DBR), in which concrete educational problems are first analysed together with practitioners, and concrete solutions for the problems are then worked on

¹ <https://ideaslab.sbg.ac.at>

(McKenney & Reeves, 2019). Next, the solution is tested and evaluated in practice. Since the DBR procedure is cyclical, the findings from the evaluation are used to make any necessary adjustments. At the end of this process, design principles are derived that expand both the theoretical and the practical understanding of teaching and learning (McKenney & Reeves, 2019).

2.1 Development of the pedagogical framework

Following the generic model of DBR (McKenney & Reeves, 2019), first we analysed and explored the learning activities and materials that are already to be found in the iDEAS:lab Salzburg. This phase consists of a visit to the iDEAS:lab and intensive discussions with practitioners, including educators and ICT experts. This helps the research team to understand the educational problem(s). For example, one installation in the iDEAS:lab aimed to visualize the functional principle of satellite-based positioning, a 3-dimensional phenomenon. However, at the beginning of the project this phenomenon was introduced using 2-dimensional representations on a computer screen, making it hard for learners to understand it. As a team, we identified three other installations with similar deficiencies, such as a lack of illustration of spatial concepts, and either insufficient information or a presentation of information that was too demanding, cognitively, to perform learning tasks effectively. These inadequacies can come to light thanks to experience and evidence from the science of instruction and can be mitigated by redesign. According to cognitive load theory (CLT) (Sweller et al., 2019), well-designed instructional materials can help learners to manage the cognitive demand induced by a learning activity and thus promote better learning. For example, the split-attention effect states that information to be learned or that is needed to perform a task should be presented close in space and time to the equipment and materials required (Ayres & Sweller, 2014). Furthermore, effective learning environments are ones that provide tasks which engage learners cognitively, emotionally and physically (Domagk et al., 2010). For example, Lindgren et al. (2016) developed a mixed-reality platform for learning about the path of asteroids and its consequences for planets. Learners simulated the path of the asteroid through movements with their bodies and immediately observed how their movements affected the asteroid's speed and trajectory. Compared to a control group, the learners in the mixed-reality simulation (i.e. which included movements) performed significantly better on a post-test. Lindgren et al. (2016) conclude that body movements are a promising way for supporting learners' understanding of spatial phenomena.

Based on the practical and theoretical considerations explored, we started the second phase of the DBR model, namely design and construction, and generated solutions to address the deficiencies we have mentioned. We decided to use AR, as this technology had been used in previous studies to address similar problems. AR is defined as the computer-supported extension of the real world by virtual objects, resulting in a situation in which reality and virtuality coexist in both time and space (Azuma et al., 2001). Sommerauer and Müller (2014) used AR in a museum to visualize mathematical concepts in a more effective way, for example by integrating 3-dimensional objects or displaying additional information directly on a real-world object. In a similar way, Chang and Hwang (2018) used AR to provide immediate feedback to learners in a physics class. For example, the students conducted an experiment about magnetic fields using physical materials, and with the help of AR they could see whether

their constructions were correct. In Yoon et al. (2017), visualizing the invisible in science education, such as air streams, was found to be a major potential of AR when compared to more traditional instructional materials and methods. However, researchers also reported negative effects of AR-enhanced learning environments that need to be considered in their design. Ibili et al. (2019) point out that any AR system implemented must be easy to use. Otherwise, frustration can arise, which has a negative effect on learning. Additionally, the self-directed nature of AR learning environments, combined with technical affordances, can be cognitively demanding and consequently may result in poor learning (Dunleavy et al., 2009; Lai et al., 2019). To overcome these issues, we designed the AR modules in such a way that they can also be worked on collaboratively. Collaborative learning is not only highly effective but can also reduce the risk of cognitive overload (Janssen & Kirschner, 2020). Learners help each other with the tasks, and technical problems are also solved as a team.

With these potentials and challenges of AR-enhanced learning environments in mind, we constructed four AR modules which include learning tasks and virtual elements that can address the shortcomings mentioned earlier, and therefore contribute to solving our educational problem(s). An overview of the AR modules is given in Table 1.

Table 1: Overview of the modules, problems identified, solutions developed and learning tasks

Module	Problem	Solution	Learning task(s)
Visualizing the functional principle of GNSS	Limited representation of a 3D phenomenon.	Visualization of the signal processing and trilateration using 3D AR objects	Collaborative documentation of the satellite signals and their positions
Construction of a sensing station	Cognitively demanding instructional manual	AR-based guidance directly on the hardware	Construction of the sensing station
Performing geospatial tasks with the AR sandbox	Lack of information to set the heights of the sand landscapes in relation to each other	Complementing the sandbox with an AR-based legend containing elevation scales	Collaborative landscape modelling, and comparison with locally relevant information
Spatial-temporal distribution of geo-social media	The non-visibility of social media postings and location	Visualization of social media posts as AR objects directly on a physical map	Collaborative search for specific locations, e.g. streets with high volume of traffic

2.2 Technical development of the AR modules

In this study, we chose to use the Wikitude software development kit (SDK), version 8.10, which provides a cross-platform AR environment and is combinable with multiple development engines. We used the Wikitude SDK primarily for the integration of virtual elements into the AR-based visualization, making use of Wikitude’s image- and object-tracking capabilities, which we realized differently for each module. The common guiding principle in

our design was to use markers of various kinds and thus to transform real-world objects into recognizable virtual objects.

To create a comprehensive AR experience for our learners, we designed and generated virtual objects to be displayed in the AR environment. Unity supports the development of VR applications and allows the use of the Wikitude SDK as an add-on package. For this purpose, we chose Unity version 2018.4.22f1 because of its extensive functionalities, which we required for the goals of our research, and due to its strong user-base and support. The Unity Editor was used to generate virtual objects, design actions (including triggers and loops), and to build the AR application. In practice, following the Module functional principles of GNSS (Section 3.1) as an example, we used this AR foundation as follows. In Unity, satellite vectors were imported from the library and positioned; spheres and signal features were created and integrated into an animation of the positioning workflow. Using the Wikitude SDK, a QR code was generated, which served as a marker for the AR app and was defined as the trigger for the application.

To give the reader a more precise illustration of the AR modules, we describe two of them in the following section. A detailed description of the other two modules can be found in the Appendix, and a video demonstration of all modules can be found here: t1p.de/aredu

3 Sample AR modules

3.1 Visualizing the functional principle of GNSS

Signal processing and the principle of trilateration are key to satellite-based positioning (Teunissen & Montenbruck, 2017). Although the GNSS communication principle is one-directional, learners often assume bi-directional communication between satellites and mobile devices. Thus, transparently communicating the GNSS trilateration principle is key to understanding the technology, but it is typically limited by how 3-dimensional phenomena are represented in a 2-dimensional learning environment (e.g., a computer screen). Intersecting spheres that represent omnidirectional satellite signal propagation are difficult to visualize in a 2-dimensional representation, resulting in the risk of misunderstandings and of generating incorrect information. Using an AR-based 3-dimensional representation of the trilateration may simplify the learning of the underlying principle through an improved spatial perception of this process. Students' spatial imagination is thus supported through AR, which in turn leads to an increased understanding of more advanced topics, such as possible problems with signal propagation or possible location-specific inaccuracies.

In practical terms, the GNSS AR module functioned as follows. Upon successful detection of the marker (in this instance a QR code on the ceiling) by pointing the camera of a mobile device (e.g. a tablet) at it, the AR app visualizes four virtual satellites, and the signal transmission of each satellite is displayed schematically, in a single direction. The visualization clearly shows the intersection points of the distance spheres, representing potential GNSS position candidates. The three-dimensionality of these signal transmissions is underpinned by the use of a distance sphere around each satellite (the centre), which gradually increase in size to represent the distance to the satellite. The surfaces of these semi-transparent spheres and

the schematic signal paths, represented as coloured lines, intersect at a certain point, which represents an exemplary GNSS position. In this use case, the QR code on the lab's ceiling emulates the elevated position of the satellites; the subsequent trilateration animation was designed to be seen from below the marker. After the students had generated new virtual objects, or acquired existing ones, the main focus was on the illustration of the positioning workflow. This included the correct placement of satellites in a circle around the marker, the definition of an exemplary positioning-target, and the animation sequence of spheres and signals. This animation element is especially important to ensure students' proper understanding of the workflow in GNSS. Figure 1 shows an illustration of the virtual elements in the preparatory phase (left), and of the in-app visualization in a real environment (right). A video demonstration of the GNSS module is available here: t1p.de/gps6

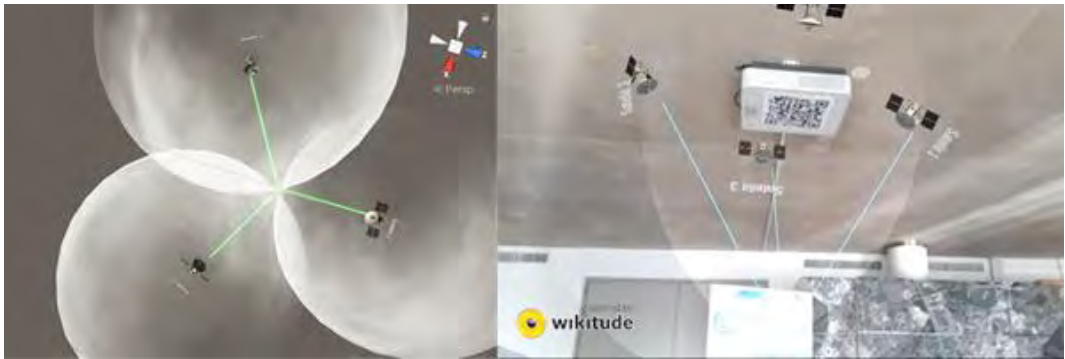


Figure 11: Illustration of the virtual elements (left) and of the in-app visualization in a real environment (right).

3.2 Visualizing the spatial-temporal distribution of geo-social media

Geo-social media have recently been widely used in scientific research in a variety of fields, from disaster management, epidemiology and urban planning, to communication science and political science. However, the geospatial nature and the wider implications of social media data and their usage (i.e. the benefits and risks of social media) are mostly not transparently communicated. In fact, geo-social media data can be used to extract thematically relevant information from personal data to investigate spatial-temporal phenomena, for example in urban science and urban planning (Resch et al., 2016). Using digital media in a citizen-centred approach to planning promotes the discussion of publicly relevant issues in a more inclusive development environment and the integration of the voices of members of the public.

The AR visualization created for our study aims to illustrate the spatial-temporal patterns of social media usage graphically together with the semantic content of social media posts, i.e. what opinions and sentiments people express at and about different locations. The cartographic challenge in this case was to find a balance between maintaining the overview of larger geographical areas for reasons of orientation in geographical space, and the detailed visualization of individual locations and social media posts, while also keeping information density at a digestible level.

We therefore created an AR visualization that used a marker-based approach and existing physical maps as triggers. The maps also provided the spatial reference for the AR-based illustration of social media posts. Figure 2 shows these physical map elements (left), which are parts of the city of Salzburg. For reasons of information readability and spatial assignability, a simplified representation of the city was used (i.e., a graphically appealing city map). Sample posts were created as virtual objects, and position icons were placed on the digital representation of the map tile, used as the marker. As before, animation effects were used to represent positions of posts, which in this case was carried out by having parts of the texts rise vertically from the position icons. In this scenario, the marker was used not only as a trigger, but also as a base layer for the overlaid information – which is precisely what constitutes the novelty in the merged visualization of real and virtual objects (see Figure 2, right). A video demonstration of the geo-social media module is available here: t1p.de/mediar

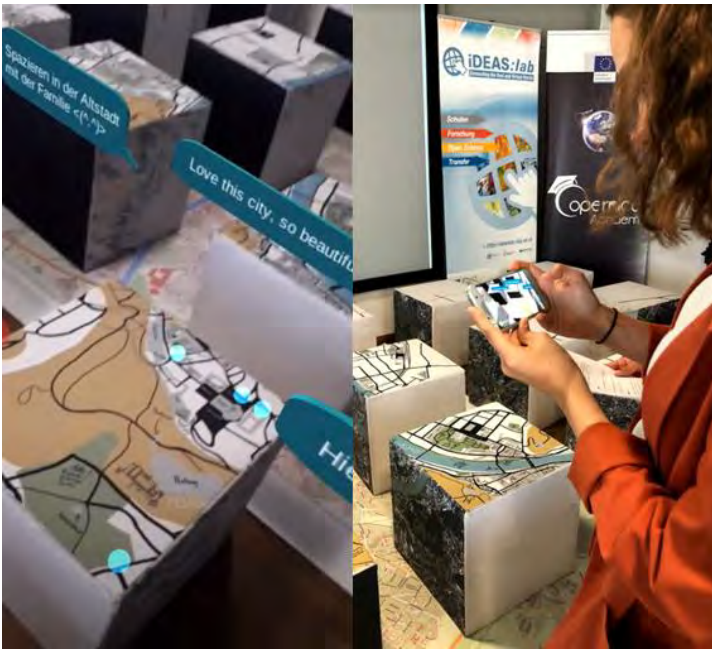


Figure 2: Physical map elements serve as markers (left), which are overlaid by virtual objects and displayed on the users' devices (right).

4 Evaluation

4.1 Participants and instruments

To test our first iteration, we recruited five women and seven men ($n = 12$) with a mean age of 20.58 (SD = 0.99). They participated as volunteers; they received no gratuity or similar. As usual in DBR, a mixed-method approach of data collection was chosen. Quantitative data was

collected using questionnaires on cognitive load and acceptance of AR technology; qualitative data was collected through group discussions.

To measure cognitive load, we used the Nasa Task Load Index (Nasa-TLX) (Hart, 2006), the questionnaire used most frequently to measure cognitive load in human–computer studies, because it allows the multidimensional assessment of cognitive load (Grier, 2015). The sub-scales survey participants' perceptions regarding mental, physical and temporal demands, performance, effort and frustration. Together they add up to the overall cognitive load.

To find out whether the AR learning environment we had designed was acceptable to the participants, we used an adapted version of the Technology Usage Inventory (TUI) developed by Kothgassner et al. (2013). This version includes the scales for the Usability and Usefulness of AR for learning, and for Skepticism towards the use of AR in learning environments. In addition, we also asked participants whether they would be happy to continue using AR in other learning settings. They completed the questions on a scale of 1 (strongly disagree) to 7 (strongly agree). An example of an item from the usefulness scale is ‘The use of augmented reality could help me to complete the learning tasks more efficiently’.

4.2 Procedure

The trial session took place in summer 2020 and complied with the COVID-related hygiene requirements. At the beginning of the trial, the participants were welcomed and briefly introduced to the AR application. Subsequently, the four AR modules were tested collaboratively. At the end, students completed the questionnaire, which included TUI as well as Nasa-TLX items.

4.3 Data analysis

The data was processed and analysed using the statistical software SPSS 27. Scales were first calculated using items from the TUI sub-scales (e.g., the usability scale was formed from three items on the use of the AR application). In total, the four scales Usability, Usefulness, Skepticism and Intention to Use were evaluated; Cronbach’s alpha ranged from 0.6 to 0.8, which indicates sufficient reliability of the measurement instrument. The six items from the Nasa-TLX were aggregated into an overall scale of cognitive load, for which Cronbach’s alpha = 0.8. The Performance sub-scale was recoded according to the questionnaire design; low values here stand for a positive assessment of one’s own performance during learning in the AR environment.

5 Results

5.1 Cognitive load

Table 2 shows the mean values with standard deviation for the sub-scales from the Nasa-TLX and the total cognitive load scale. The participants perceived the AR learning environment as not cognitively demanding; the overall cognitive load was reported as being low, with $M = 3.17$ ($SD = 1.51$). This is also reflected in the values of the sub-scales; for example, the learners

did not feel any time pressure or excessive physical strain. The values for the Performance scale ($M = 3.08$, $SD = 1.38$) indicate that the learners were able to learn successfully with the help of the AR modules.

Table 1: Descriptive statistics of the Nasa-TLX scales with means and standard deviations.

Variable	M	SD
Mental Demand	4.42	2.07
Physical Demand	2.50	2.20
Temporal Demand	2.92	2.61
Performance	3.08	1.38
Effort	2.75	2.34
Frustration	3.33	2.67
Overall Cognitive Load	3.17	1.51

Note: Scales range from 1 to 10. Scale Performance is reverse-coded.

5.2 Acceptance of the technology

In terms of its technical requirements, the AR learning environment was predominantly rated positively by participants, with Usability ($M = 6.08$, $SD = 0.64$) being rated a little higher than Usefulness ($M = 5.56$, $SD = 0.70$) (see Table 3). The value for the Skepticism scale ($M = 3.50$, $SD = 0.69$) is in the middle of the seven-point Likert-scale, so there were different opinions within the group. The results for Intention to Use ($M = 5.42$, $SD = 1.02$) allow the conclusion that the participants' willingness to use AR in the context of future learning activities is high.

Table 3: Descriptive statistics of the TUI scales, with means and standard deviations.

Variable	M	SD
Usability	6.08	0.64
Usefulness	5.56	0.70
Skepticism	3.50	0.69
Intention to Use	5.42	1.02

Note: Scales range from 1 to 7.

6 Discussion and outlook

In this study, we have presented the development and design of four AR modules in the context of an informal educational programme in geoinformatics. We considered the requirement for active learning in science education as well as the potential risks of using AR in education and based our pedagogical framework on this. In order not to overburden students in an AR learning environment, we focused on collaborative learning. The individual elements in the AR modules were designed in such a way that they do not overwhelm learners; rather, they enable students to learn in a holistic, interactive way (behaviourally, cognitively and emotionally). The results of the evaluation regarding cognitive load reflect the careful planning that went into our design: the participants did not experience cognitive overload in this first pilot. They rated their own performance on the tasks to be completed using AR as high. These results are in line with other studies on the use of AR. For example, Turan et al. (2018) showed that an evidence-informed AR learning environment in geography was not perceived as cognitively demanding. Lin et al. (2015) draw the same conclusion for AR learning in geometry, especially when learning is collaborative.

For the technical implementation, we used marker-based AR technology. The combination of Wikitude and Unity proved to be successful. We were able to create the three-dimensional and animated visualizations necessary for understanding the content of the modules, and to make them accessible via mobile devices without technical difficulties. The evaluation showed that this form of presentation was perceived as useful and user-friendly. The willingness to continue learning using AR was very high, and scepticism about AR as an educational medium was low.

Although our results demonstrate that the use of AR in informal learning settings is very much welcomed, we should also point out that such learning opportunities would have to be made accessible for all schools – not only for privileged schools but for everyone, avoiding any further technological and social divides. Consideration of this social aspect was essential for us and our ARED project. First, we learnt that informal learning spaces can be of particular importance in the educational process. It is all the more essential that educational institutions present innovative concepts and make these available in schools. This is also the conclusion of Yoon et al. (2017), who used AR installations in various museums. Secondly, we took away from our experience that a project like this should also think about how we can access schools directly. Mund and Müller (2019) report how difficult it can be to integrate AR-supported learning offers into the regular classroom. We are taking this as a mission and intend to create AR-enhanced learning materials that can be used regardless of time and place. We will also further revise the AR modules. For example, it became clear that the construction task in one module (see Appendix: Citizen sensing platform) could be improved if the learners had their hands completely free for the task. Here, the use of AR glasses would be a possible improvement, which we would like to test in the next iteration. In addition, we will include a control group in the next run to test our pedagogical framework. For example, we will compare individual vs. collaborative learning using the AR modules. In our next study, we also plan to record other variables, e.g. learning achievement, task performance or motivation. In this study, only cognitive load and acceptance were investigated, which must be considered a limitation. A further limitation of this first prototype study is the small sample size. The results must therefore be interpreted with caution; further studies are required to learn more about

the effects of our design. Additionally, in a future study we will test the learning environment with school students in order to gain insights into how to improve the design for this target group.

In summary, the possible uses of AR in geoinformatics education go beyond those of mere visualization of complex phenomena. Our project shows that with the help of an AR learning environment, designed by a multidisciplinary team, holistic learning experiences can be initiated that learners are happy to engage in and do not perceive as overwhelming. Informal educational institutions can use AR-based pedagogical approaches as a welcome alternative to everyday school life to inspire students for science and research.

Acknowledgement

We would like to thank the volunteers who made the evaluation of the first implementation possible. We would especially like to thank Philipp Nagele from Wikitude, who allowed us to use Wikitude AR and supported us in creating the AR objects.

Appendix

Module: Performing geospatial tasks with the augmented reality sandbox

The AR Sandbox has a built-in AR component, which is the main element of this learning environment. The equipment consists of a computer and a projector, as well as a structured light range sensor mounted above a sand surface (in our case, a Microsoft Kinect for XBOX 360). In a structured light-based approach, the Kinect emits a narrow band of light towards a surface. The surface relief, in this case a sand landscape, changes the patterns of light and shade, which are observed from multiple cameras at different positions on the Kinect device. The distortion between the expected and the observed pattern is used to calculate the physical offsets on the surface, in this case the depth or height of the surface relief. Using the calculated height, an isopleth map is rendered in the backend computer and then projected onto the sand surface, thus visualizing a digital elevation model. Additional interaction capabilities are implemented based on object recognition.

The sandbox offers a broad range of possibilities to perform small-scale landscape modelling in an interactive way, based on subjective decisions and actions. Using this technology without additional instructions, however, limits the capabilities and learning targets. For example, no classification can be derived from the colour assignment of the corresponding heights. Consequently, it is difficult to assess the heights of the summits in the sand landscape in relation to each other, which is an obstacle in landscape modelling. Thus, the goal of our study is to provide additional information and learning tasks in an AR-based application in order to improve the communication of height information. This additional information is displayed in written form and superimposed on the surface (see Figure 3, right). It allows better understanding of height differences and thus also allows more realistic landscape modelling through the representation of elevation scales.

A critical question in the implementation of this use-case was information density. The existing AR component of the sandbox requires some further information in order not to draw attention away from the application itself. For this reason, we decided to illustrate aggregated elevation levels using multiple markers. Depending on the elevation levels, markers were designed as triggers for displaying specific, locally relevant information. For example, for elevations between 706 and 1,519 metres, the Gaisberg mountain was set as the reference. In total, we created descriptions for eight markers, representing the height of different topographical features like mountains or lakes. After the AR app has recognized the marker, the information is displayed without any additional user interaction. Figure 3 shows the markers for the altitude levels (left), and the exemplary application (right). A video demonstration of the sandbox module is available here: t1p.de/sandbox1



Figure 3: Markers (left) and demonstration of the additional information superimposed on the sandbox (right).

Module: AR-based construction guidance for a Citizen Sensing platform

In this module, learners are introduced to measurable environmental phenomena on the one hand, and to the concepts of Citizen Sensing more broadly on the other. Learners use our AR app to assemble a sensing station in a self-guided manner. For this, we used the senseBox:Edu, which was designed to enable the construction and operation of different sensing stations with a variety of measurement parameters and a broadly variable degree of difficulty. The hardware kit used consists of (often combined) sensors for different measurement variables, various connection cables, a circuit board and the central Micro Control Unit (MCU). For advanced learners, the measurement application can be programmed in the MCU itself. The measurement setup includes pre-designed instructions for specific measurement stations. This means alternating attention between the instructions that need to be read and understood, and the measurement hardware that is being assembled. This continuously shifting attention is a typical source of errors and increases the time needed to complete the task of assembling the sensing station. Furthermore, the various sensors require close inspection for identification because of similarities in appearance. Therefore, the goal of this scenario is to keep the learner's focus on the senseBox (Figure 4, left) with the help of the presentation of AR-based information. Installation steps are interactively displayed in the AR environment through object identification; individual sensors are identified by their shape and texture. To reach these goals, we designed a dual approach to augmentation. First, the installation instructions (several

consecutive steps) were transferred to virtual text objects. For this marker-based approach, the step numbers of the installation were used as triggers. As soon as the AR app recognizes a marker, it initializes the display of the current installation step. These basic-level steps include the simple identification of hardware pieces, for which the second approach was designed: previously generated digital models of each element of the hardware were used to enable the recognition-based identification of objects. This means that the actual object (a sensor, the MCU, the display, etc.) were recognized by the AR app. The combination of these two approaches leads to an AR-based installation tutorial that includes hardware identification, preventing the learner from making assembly errors and hardware mix-ups. The two approaches with sensor identification (centre) and AR-based manual (right) are shown in Figure 4. A video demonstration of the senseBox module is available here: t1p.de/sensebox

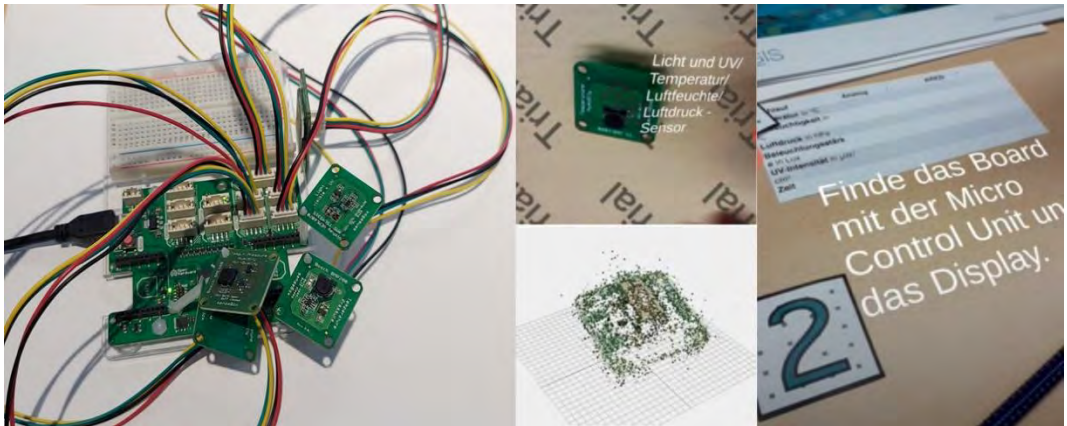


Figure 4: SenseBox (left), with sensor identification (centre), and the AR-based construction manual (right).

References

- Ayres, P., & Sweller, J. (2014). The Split-Attention Principle in Multimedia Learning. In R. E. Mayer (Ed.), *The Cambridge Handbook of Multimedia Learning* (Second Edition, pp. 206–226). Cambridge University Press.
- Azuma, R., Baillot, Y., Behringer, R., Feiner, S., Julier, S., & MacIntyre, B. (2001). Recent advances in augmented reality. *IEEE Computer Graphics and Applications*, 21(6), 34–47. <https://doi.org/10.1109/38.963459>
- Bell, P. (2004). On the Theoretical Breadth of Design-Based Research in Education. *Educational Psychologist*, 39(4), 243–253. https://doi.org/10.1207/s15326985ep3904_6
- Chang, S.-C., & Hwang, G.-J. (2018). Impacts of an augmented reality-based flipped learning guiding approach on students' scientific project performance and perceptions. *Computers & Education*, 125, 226–239. <https://doi.org/10.1016/j.compedu.2018.06.007>
- Cheng, K.-H., & Tsai, C.-C. (2013). Affordances of Augmented Reality in Science Learning: Suggestions for Future Research. *Journal of Science Education and Technology*, 22(4), 449–462. <https://doi.org/10.1007/s10956-012-9405-9>

- Deslauriers, L., Schelew, E., & Wieman, C. (2011). Improved Learning in a Large-Enrollment Physics Class. *Science*, 332(6031), 862–864. <https://doi.org/10.1126/science.1202043>
- Domagk, S., Schwartz, R. N., & Plass, J. L. (2010). Interactivity in multimedia learning: An integrated model. *Computers in Human Behavior*, 26(5), 1024–1033. <https://doi.org/10.1016/j.chb.2010.03.003>
- Dunleavy, M., Dede, C., & Mitchell, R. (2009). Affordances and Limitations of Immersive Participatory Augmented Reality Simulations for Teaching and Learning. *Journal of Science Education and Technology*, 18(1), 7–22. <https://doi.org/10.1007/s10956-008-9119-1>
- Goff, E. E., Hartstone-Rose, A., Irvin, M. J., & Mulvey, K. L. (2020). Using Augmented Reality to Promote Active Learning in College Science. In J. J. Mintzes & E. M. Walter (Eds.), *Active Learning in College Science* (pp. 741–755). Springer International Publishing. https://doi.org/10.1007/978-3-030-33600-4_46
- Grier, R. A. (2015). How High is High? A Meta-Analysis of NASA-TLX Global Workload Scores. *Proceedings of the Human Factors and Ergonomics Society Annual Meeting*, 59(1), 1727–1731. <https://doi.org/10.1177/1541931215591373>
- Hart, S. G. (2006). NASA-Task Load Index (NASA-TLX); 20 Years Later. *Proceedings of the Human Factors and Ergonomics Society 50th Annual Meeting*, 904–908.
- Ibáñez, M.-B., & Delgado-Kloos, C. (2018). Augmented reality for STEM learning: A systematic review. *Computers & Education*, 123, 109–123. <https://doi.org/10.1016/j.compedu.2018.05.002>
- Ibili, E., Resnyansky, D., & Billingham, M. (2019). Applying the technology acceptance model to understand maths teachers' perceptions towards an augmented reality tutoring system. *Education and Information Technologies*, 24(5), 2653–2675. <https://doi.org/10.1007/s10639-019-09925-z>
- Janssen, J., & Kirschner, P. A. (2020). Applying collaborative cognitive load theory to computer-supported collaborative learning: Towards a research agenda. *Educational Technology Research and Development*, 68(2), 783–805. <https://doi.org/10.1007/s11423-019-09729-5>
- Kothgassner, O. D., Felnhofer, A., Hauk, N., Kastenhofer, E., Gomm, J., & Kryspin-Exner, I. (2013). TUI: Technology Usage Inventory. https://www.ffg.at/sites/default/files/allgemeine_downloads/thematische%20programme/progr_ammtdokumente/tui_manual.pdf
- Lai, A.-F., Chen, C.-H., & Lee, G.-Y. (2019). An augmented reality-based learning approach to enhancing students' science reading performances from the perspective of the cognitive load theory. *British Journal of Educational Technology*, 50(1), 232–247. <https://doi.org/10.1111/bjet.12716>
- Lin, H.-C. K., Chen, M.-C., & Chang, C.-K. (2015). Assessing the effectiveness of learning solid geometry by using an augmented reality-assisted learning system. *Interactive Learning Environments*, 23(6), 799–810. <https://doi.org/10.1080/10494820.2013.817435>
- Lindgren, R., Tscholl, M., Wang, S., & Johnson, E. (2016). Enhancing learning and engagement through embodied interaction within a mixed reality simulation. *Computers & Education*, 95, 174–187. <https://doi.org/10.1016/j.compedu.2016.01.001>
- McKenney, S., & Reeves, T. C. (2019). *Conducting Educational Design Research* (2.). Routledge.
- Mund, J.-P., & Müller, S. (2019). Augmented Reality and Mobile GIS as Tools for Teaching Data-collection in the Context of Forest Inventories. *GI_Forum*, 1, 129–143. https://doi.org/10.1553/giscience2019_02_s129
- Resch, B., Summa, A., Zeile, P., & Strube, M. (2016). Citizen-Centric Urban Planning through Extracting Emotion Information from Twitter in an Interdisciplinary Space-Time-Linguistics Algorithm. *Urban Planning*, 1(2), 114–127. <https://doi.org/10.17645/up.v1i2.617>
- Sahin, D., & Yilmaz, R. M. (2020). The effect of Augmented Reality Technology on middle school students' achievements and attitudes towards science education. *Computers & Education*, 144, 103710. <https://doi.org/10.1016/j.compedu.2019.103710>

- Sommerauer, P., & Müller, O. (2014). Augmented reality in informal learning environments: A field experiment in a mathematics exhibition. *Computers & Education*, 79, 59–68. <https://doi.org/10.1016/j.compedu.2014.07.013>
- Sweller, J., van Merriënboer, J., & Paas, F. G. W. C. (2019). Cognitive Architecture and Instructional Design: 20 Years Later. *Educational Psychology Review*, 31(2), 261–292. <https://doi.org/10.1007/s10648-019-09465-5>
- Teunissen, P. J. G., & Montenbruck, O. (Eds.). (2017). *Springer Handbook of Global Navigation Satellite Systems*. Springer International Publishing. <https://doi.org/10.1007/978-3-319-42928-1>
- Turan, Z., Meral, E., & Sahin, I. F. (2018). The impact of mobile augmented reality in geography education: Achievements, cognitive loads and views of university students. *Journal of Geography in Higher Education*, 42(3), 427–441. <https://doi.org/10.1080/03098265.2018.1455174>
- Wikitude. (2021). Wikitude Augmented Reality SDK. Wikitude. <https://www.wikitude.com/>
- Yannier, N., Hudson, S. E., & Koedinger, K. R. (2020). Active Learning is About More Than Hands-On: A Mixed-Reality AI System to Support STEM Education. *International Journal of Artificial Intelligence in Education*, 30(1), 74–96. <https://doi.org/10.1007/s40593-020-00194-3>
- Yoon, S., Anderson, E., Lin, J., & Elinich, K. (2017). How Augmented Reality Enables Conceptual Understanding of Challenging Science Content. *Educational Technology & Society*, 20(1), 156–168.

'This is a Great Place for Children. Here, They Can Play, Do What They Want, Have Fun and Other Things.'

Mapping Primary School
Children's Everyday Spaces

Jana Pokraka, Torsten Kraleman-Poppell, Inga Gryl and Paula Schmidt
University of Duisburg-Essen, Germany

Abstract

This article presents empirical findings from a learning environment based on education for Spatial Citizenship (Gryl & Jekel, 2012; Schulze et al., 2015) conducted with primary school children (6 to 10 years of age) in the city of Essen, Germany. In workshops comprising three stages, participants used an easy-to-use mapping application to trace significant places and objects in their school surroundings in relation to the workshops' overall topic of envisioning designs and features of a 'city for children'. This paper focuses on the analysis of collaborative maps created from children's perspectives on urban space in their own life-worlds.

Keywords:

mapping, spatial citizenship, primary school, digital geomedial, VGI

1 Introduction

Digital media are a ubiquitous element of our information society and familiar tools in children's everyday life-worlds, not only for communication purposes but also as sources of information for extra-curricular or educational purposes (GDSU, 2013). According to a study on the media use of primary school children (Prasse et al., 2017), half of primary school pupils in Germany stated that they use the internet at least once a week for information research. It is this exposure to and interaction with media content that calls for media-related education in primary schools, and therefore also within the subject of Primary Social and Science Education ('Sachunterricht'). Media-related Primary Social and Science Education has to react to changing, mediatized life-worlds through pupil-centred adaptation of the subject contents (Peschel, 2015). The changes in structure and type of media always go along with changes in the ways that the media are used. This is particularly evident in the omnipresence of (mobile) digital media, especially social media, in private and public spaces (Gervé & Peschel, 2013). Kanwischer & Schlottmann (2017) describe social media and their relation to physical space as 'both part of the world and "creators of world"' (p. 62; authors' translation). This relation

also becomes evident in the structural media education approach of Jörissen and Marotzki (2009), who describe how everyday life is permeated by digital media, and the educational implications of this for self–world relations. This permeation, or ubiquity, of digital media provides a fruitful opportunity for Primary Social and Science Education to draw on pupils’ experiences and interests in an action-oriented way (Gervé & Peschel, 2013), especially in the context of digital geomeia education.

The focus of this paper is to present an outline for, and an analysis of, a learning environment that links an education for Spatial Citizenship (Schulze et al., 2015) with a life-world-centred approach in Primary Social and Science Education. The aim is to provide an insight into children’s spatial perceptions as a starting point for fostering reflexive spatial-appropriation processes. We will first provide a brief explanation of the link between digital geomeia education and Primary Social and Science Education, and then delve into the methodology of subjective neogeography, which derives from the paper-based approach of subjective mapping (Daum, 2010) (Section 2). We next present our methodology (Section 3), and in Section 4 analysis and discussion of and reflection on a geomeia-based research project: during workshops comprising three phases, participants from primary schools in Essen, Germany used tablets equipped with an easy-to-use mapping application, based on Survey123 by ArcGIS, to create maps of their schools’ surroundings. The data gathered from these collaborative maps were analysed to explore the children’s perspectives on spatial challenges in their life-worlds.

2 Digital geomeia in Primary Social and Science Education

Digital geomeia, as representations of ‘digitally coded, spatially-referenced data [...] as well as the technological devices and software necessary for their administration, analysis and visualization’ (Rinschede et al., 2020: 372), hold a crucial position in the geographical dimension of Primary Social and Science Education. The need for appropriate, reflexive and critical use of omnipresent digital geomeia supports the subject’s aim of fostering elementary geographical literacy skills for the longer term (Schmeinck, 2013). In the context of digital geomeia as cultural technology, Schulze et al. (2020) emphasize the need to foster communication aspects, such as negotiation, reflection and mature participation through the use of digital geomeia, rather than exclusively focusing on competences in the realm of ‘simple’ data processing. The aim of contextualizing the use of digital geomeia as cultural technology within the users’ own life-worlds is in line with an education for Spatial Citizenship (Gryl & Jekel, 2012),¹ which aims to achieve a mature appropriation of space and participation through the use of digital geomeia. Spatial Citizenship is based on three pillars: 1) relational concepts of space that regard spaces as socially constructed and, thus, changeable (Lefebvre, 1991); 2) neocartography, which aims to re-centre everyday geographical problems rather than focus on the use of high-tech approaches, which used to dominate GIS education; 3) a contemporary understanding of citizenship education that pays more attention to informal

¹ The concept of Spatial Citizenship education has also been embraced by Shin & Bednarz (2019), who emphasize the importance of geographical knowledge in relation to formal citizenship competences.

participation paths, such as in fluid web entities (Bennett et al., 2009). Gryl (2016) developed the first theoretical and empirical approaches for interlinking Spatial Citizenship and primary education, especially opportunities for mapping practices, with children of primary school age. Following the Spatial Citizenship competence model, Bach and Peschel (2019) examined primary school children's mapping competences using a mapping application within the kidipedia platform, which is intended specifically for use in primary school contexts. They showed that, for final-year primary school students, digital maps had a stronger positive effect on the acquisition of both media- and geography-related competences than analogue maps.

2.1 Digital (geo)media and Spatial Citizenship in primary school curricula

The German Primary Social and Science Education curriculum (GDSU, 2013) comprises five subject-specific 'perspectives'. Each represents one of the subject's reference subjects in secondary education (geography, history, natural sciences, social sciences and technical instruction). Additionally, the curriculum features five topics (one of which is called 'media') that relate to two or more of the 'perspectives'. In the curriculum, media education follows an integrated approach that aims to incorporate the complexity of 'traditional' and digital media into classroom practice, focusing both on learning with and learning about media as relevant competences for discovering the world (Gervé & Peschel, 2013).²

In geomeia-based learning within the curriculum's spatial perspective, the central aim is to foster students' spatial orientation competences, including through the production of maps:

'Students are confronted with maps, images and large- and small-scale 'constructions' and orientate themselves in their own ways following different strategies. [...]

Students become increasingly familiarized with spatial phenomena and situations of their natural and built environment by actively engaging with them through [...] making observations, gathering data, mapping, interviewing individuals and presenting their results.'

(GDSU, 2013: 46; authors' translation)

However, the importance of the consumption and production of *digital* geo-media is not explicitly emphasized within the framework.

As an important feature of early geographical education, the acquisition of media-related competences (notably the prosumption [production and consumption] of geomeia) can be subsumed under the term of 'cartographic/geomeia-based learning' (Gryl & Naumann, 2016: 20; authors' translation). Acquiring media-related competences should be embedded more

² Other approaches incorporate these two dimensions into the dimension of learning through (geo)media (e.g. Demirci 2015; Kanwischer 2014; Gryl & Schulze 2013). This focuses more on the use of (geo)media as a tool for world-exploration than as an end in itself.

fully within the framework in face of the everyday digital geomeia that are already embedded in children's life-worlds.

2.2 Subjective neogeography in primary schools

With the paradigm shift in the school subject of Geography that impacted not only subject-related modes of thinking and acting but also the choice of subject-related media to incorporate into teaching and learning, Kanwischer (2013: 80) proposes a 'shift of leading media' from analogue to digital maps. Maps have always been the central medium of geography (or geography education) and play a central role in human orientation. Based on individual perceptions, they represent the spatial constructions of a single cartographer or of a collective, and communicate individually-perceived perspectives on imagined (spatial) realities (Gryl, 2010). The shift from analogue maps to digital geomeia provides opportunities to create convincing forms of lay cartography (as opposed to those of 'expert' cartographers), as has already been acknowledged in the Spatial Citizenship approach, paving the way for digital forms of subjective mapping (Daum, 2010), or 'subjective neogeography'.

In subjective mapping, children draw maps of their life-worlds based on their cognitive models, which can then be analysed, deconstructed and discussed. Reflection on these mental representations of space provides insights into children's appropriation of space and how they attach meaning to physical-material space. By observing, giving expression to, and reflecting on one's own perception of one's (constructed) life-world, a shift of perspective becomes possible and conscious (Rhode-Jüchtern, 2004; Daum, 2010). This process is crucial for children's spatial appropriation as they position themselves, or 'stage themselves' (Daum, 2010: 125; authors' translation), in their life-worlds through cartographic practice (Löw, 2001).

Subjective neogeography incorporates central elements of Volunteered Geographic Information (VGI) into the method of subjective mapping. The aim is to incorporate easy-to-use digital geomeia applications into primary school education in the context of Spatial Citizenship to foster the mature appropriation of space and spatial/public participation. In the wake of neogeography, the possibility for spatial and public participation in the construction of space has already been greatly enhanced by the rise of VGI (Elwood & Mitchell, 2013), as have emancipatory approaches that provide 'new spaces of civic engagement' (ibid.: 276). Using VGI, Spatial Citizenship can offer increased access to, and promote credibility in, traditional processes of spatial negotiation through competences in geomeia prosumption, reflection and communication (Schulze et al., 2015). Because these spatial communications are articulations of identity that are capable of promoting 'social and political awareness' (Elwood & Mitchell, 2012: 4), they have the potential to visualize subjective perceptions (e.g. children's maps), and to question power (im-)balances and interpretational sovereignty in planning processes (Ramasubramanian, 2010). The digital context, in which spatial representations are shared and negotiated using various platforms, has already changed the scope of children's participation, making way for new forms of 'global citizenship' (Tuukkanen et al., 2012: 144). At the same time, critical reflection on processes of inequality that emerge from the interplay of the prosumption of geomeia, constructions of childhood, participation and intersectional power relations must be taken into consideration in the context of VGI (Pokraka, 2016; Pokraka & Gryl, 2017; Pokraka, 2021).

3 Methodology and research design

3.1 Research context

The empirical research was conducted at before- and after-school childcare facilities at three schools in two different neighbourhoods of Essen, Germany: Altenessen and Rüttenscheid. As a former coal-mining city in the heart of the Ruhr, Essen has been transformed structurally since the pit closures of the late 1980s. The city itself is divided economically and socially by the A40 motorway. To the south is a high-income, almost bourgeois area, where Rüttenscheid is located; north of the motorway lies a low-income area that includes Altenessen. According to data derived from the education report published by Essen municipality in 2011, there are striking socio-economic and educational differences between the two neighbourhoods: in Rüttenscheid, almost 50% of primary school students will continue to higher secondary education, compared to only 25% in Altenessen. 11% of Altenessen's pupils leave school after lower secondary education ('Hauptschule'), in contrast to only 2% of the pupils in Rüttenscheid (Essen, 2011: 113).³

The seven groups participating in the project consisted of 40 children in total, ranging in age from 6 to 10. The participants joined the workshops voluntarily after one of the authors had run information sessions, at before- and after-school childcare facilities, about the workshops' topics and research context. As the participants spent time with each other at school and in the before- and after-school settings, they knew each other. All the groups except one were mixed-age and mixed-gender.

3.2 Workshop design and data analysis

The learning environment consisted of workshops, with three stages each, that aimed to establish a space for reflection on, and the communication of the participants' perspectives on their own neighbourhoods, and the perceived spatial challenges and power-relations therein. In a participation-based environment, the aim was to gather the participants' life-world experience through geomeia-based communication and negotiation (see Figure 1).

The initial phase was a group discussion based on the creation of paper-based subjective maps (Daum, 2010): the participating children drew their own visions of a 'Perfect city for children'. The subjective maps were presented and compared for the central elements they contained, so that central issues and points of discussion evolved spontaneously from the participants' own materials. The issues and subjects of discussion were noted on paper for later reference during the final phase of reflection.

During the workshop's second phase, the participants conducted a mapping excursion (Pettig, 2016; Gryl, 2016) based on the approach of subjective neogeography. Using tablets equipped with Survey 123 by ArcGIS, the children discovered and mapped places and objects in their

³ The different neighbourhoods for this research were chosen not in order to reproduce negative, mediated stereotypes, but rather in order to avoid research bias and to tackle the connotations associated with the northern part of the city.

schools' surroundings that were significant in their life-worlds. The choices were based on the participants' positively or negatively connoted perceptions. To support the mapping process, the app featured a tool for geo-localization, the possibility of taking and uploading pictures of the geo-localized object or place, and a text field to include a description of the place or object.⁴ Thus, the app supports the communication of issues and of the spatially ascribed meanings of the children's life-worlds (Gryl, 2010). It also allows for the analysis (by the researchers) of the data gathered, in the context of geomeia-based communication in primary school settings (Schmeinck, 2013).

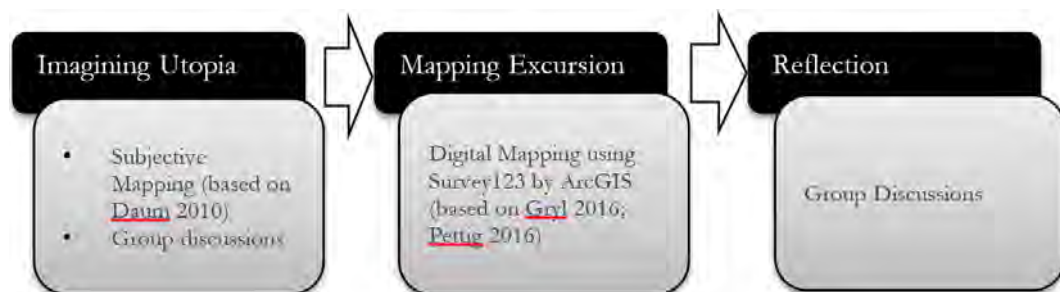


Figure 1: Workshop design (own figure)

The third and final stage of each workshop was another group discussion, aiming for reflection on, and connection between, the findings of the first two phases. During this stage, participants explored the collaboratively created digital maps and their notes from the initial discussions. They then created posters of their research environments, pointing out positive features and issues that they felt had to be addressed. The posters were then exhibited inside the school buildings for the attention of the wider school community.

The workshops were accompanied by student assistants whose role was to observe the participants (Bachmann, 2009). They also transcribed the audio recordings of the group discussions for analysis. Pokraka (2021) focuses on the oral processes that emerged in the group discussions. In this context, the students' subjective paper and digital maps had served as the basis for oral, spatial reasoning and negotiation (Kanwischer & Gryl, 2012; Vogler, 2012).

The focus of this paper now lies on the children's perspectives on the spatial conditions of their everyday life-worlds, as derived from the analysis of their collaborative maps. The maps' text-based entries and photographs (approx. 420 map entries in total) were interpreted by comparing cases with each other (Kelle & Kluge, 1999). That is, all the map entries were first considered as individual, single, cases. Case-specific categories and subcategories were then formed (see Section 4), and these then underwent an inter-case comparison to identify thematic differences and similarities.

⁴ For reasons of data privacy, user accounts were created for the children by the workshop organizers using blank e-mail addresses.

4 Results

During the mapping excursion, the participating children researched their spaces of everyday experience (Kogler, 2019). These spaces and places are significant for children’s continuous processes of the appropriation of space; they are the children’s residential environment and familiar stretches of road (ibid.). During the mapping process, participants researched, discovered and mapped aspects of their environment and points of reference that might not have come to their consciousness in their everyday movements. As a result, they exposed spatial challenges but also aspects of their life-worlds that they really appreciated. In many cases, the children also formulated specific demands for spatially related changes in their environments.

Table 1: Category system

Categories	Subcategories
Environment / environmental protection	Waste of resources
	Increase of e-mobility Increase of infrastructure for waste disposal
Health	Smoking Ban
Threats	Cars Animals Lack of secure infrastructure
Vandalism	Damage to public infrastructure
Social Issues	Distribution of wealth and private property Increase of infrastructure for children Design of public space for children Increase of leisure-time infrastructure for children
Institutional settings	Approval of infrastructure Spaces of relative freedom
Aesthetics	Graffiti Commercial Space
	Flora and Fauna
	Environmental Pollution
Positive Connotations Negative Connotations Demands 	

Table 1 presents an overview of the spatial aspects that the participants discovered during mapping. The following sub-sections illustrate the different subcategories with specific examples, discussion and reflection.

4.1 Environment/environmental protection: increase of infrastructure for waste disposal

The participants evaluated the state of the environment (or environmental protection) in their school's proximity critically, especially in terms of the waste of resources and fossil-fuelled individual transport. In this context, they formulated demands for an increase of both e-mobility and infrastructure for waste disposal. Figure 2 is one of a series of map entries that depict waste bins that are locked behind a metal fence. They belong to a local supermarket and have probably been fenced to prevent illegal waste disposal by third parties, as this seems to be a problem in the neighbourhood (WAZ, 2020). However, these inaccessible waste bins seem to issue a challenge, or cognitive conflict, to the participants: in their everyday lives, be it at school or in their private lives, they are probably confronted with questions of sustainability and environmental protection. For example, the disposal of waste and its significance in relation to sustainability is part of the Primary Social and Science curriculum (GDSU, 2013: 76). Pursuing this line of enquiry could provide a good opportunity to question the scope of individual action in relation to environmental protection, and to question spheres of environmental protection that students cannot influence immediately in that particular neighbourhood.

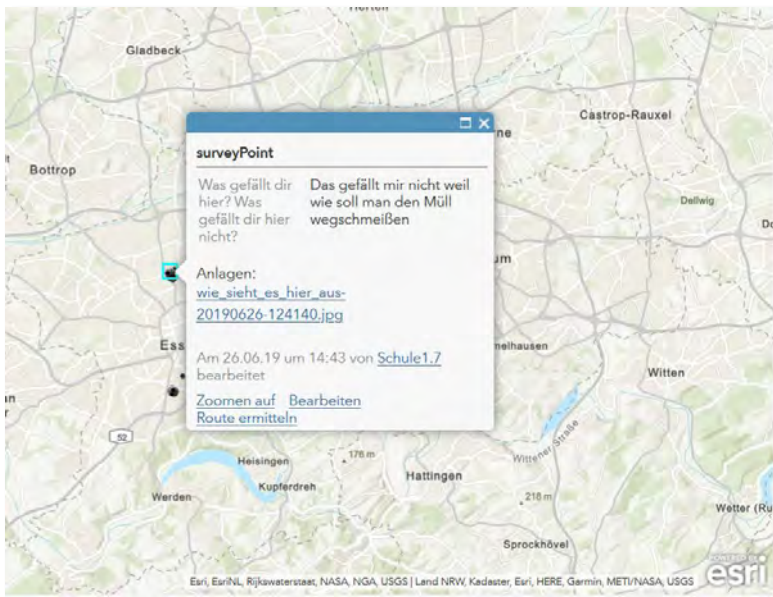


Figure 2: Extract from collaborative map in ArcGIS-Online (© Esri)⁵

⁵ Data sources for this and the following ArcGIS maps: Esri Community Maps Contributors, Land NRW, Kadaster, Esri, HERE, Garmin, INCREMENT P, METI/NASA, USGS | Esri Community Maps Contributors, Land NRW, Kadaster, Esri, HERE, Garmin, INCREMENT P, METI/NASA, USGS. In cases where a large-scale map would have revealed the school's location, a smaller scale was used to ensure anonymity. The map's entries were translated from German into English by the authors.

4.2 Threats: lack of secure infrastructure

The category ‘Threats’ consists of objects in public spaces that the participants have evaluated as being dangerous. These range from relatively vague ascriptions (‘bumblebees are dangerous animals’) to criticism of specific elements of infrastructure that pose a possible threat, especially to children. Such criticisms draw attention to generational differences between children and adults, and seemingly re-affirm public spaces as potentially dangerous for children (Evans, 2008; Holloway, 2014). Figure 3 shows an example of a perceived threat in relation to a lack of safe infrastructure for children. The fact that the school playground’s side entrance gate does not feature a child safety lock is perceived negatively, although it remains unclear whether such a lock would be intended to prevent children from leaving the school grounds or intruders from entering. In mapping the lack of a lock, the participant communicates a need for protection. The expression of that need could derive from prior negative experiences or the internalization of patronizing perceptions (Pokraka & Gryl, 2018) of the possible threats that public spaces hold, especially for children.

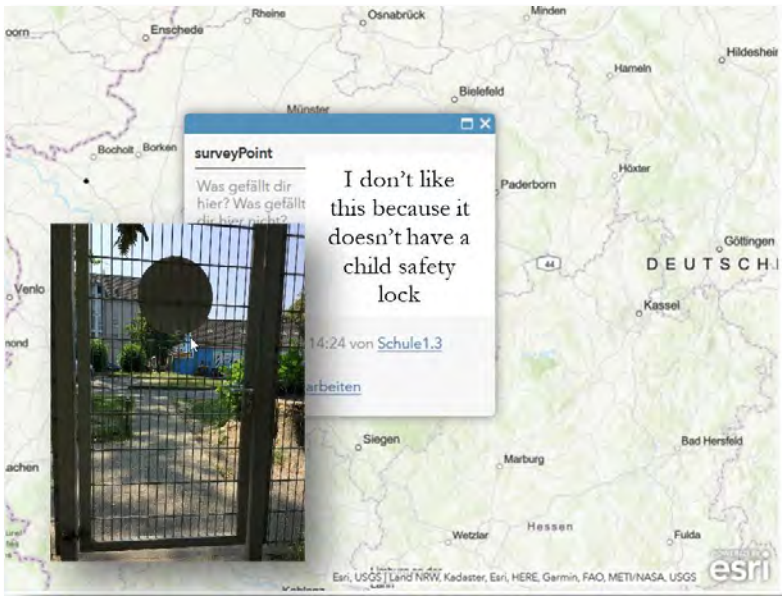


Figure 3: Extract from collaborative map in ArcGIS-Online (© Esri).

4.3 Social issues: distribution of wealth and property

In the category ‘Social Issues’, the participants’ perceptions of social inequalities, which manifest themselves spatially, become evident, especially through questions around the design of public spaces in relation to children’s needs (e.g. the provision of free leisure facilities, usability of public spaces for children, and the increase of infrastructure that caters specifically for children’s needs). Furthermore, the participants expressed strong criticism of the distribution of wealth and private property, an issue that was present in the group discussions

that took place before the mapping excursions (Pokraka & Gryl, under review). The criticism of the distribution of wealth ranged from specific disapproval of the cost of Pokémon trading cards, which are very popular among several of the participating children, to very general demands for income equality at the level of individuals (see Figure 4) or for a reduction in living costs. Interestingly, these demands can be traced in the maps made by groups from both the wealthier southern neighbourhood of Rüttenscheid and the lower-income Altenessen, although no data was gathered on the socio-economic backgrounds of the individual mappers.



Figure 4: Extract from collaborative map in ArcGIS-Online (© Esri).

4.4 Institutional settings: spaces of relative freedom

In terms of institutional settings, many participants mapped objects and places within their school grounds. This is not surprising, as all of the excursions started in the schools' day-care facilities. However, it is interesting to examine what specific elements of their school environment the students mapped: Tonucci & Rissotto (2001) have summarized the increasing importance of institutional settings within children's life-worlds and their exposure to adults' control as the shift from playground to 'sandbox city'. However, the collaborative maps show that the participants create and value their own free spaces within supervised institutional settings. Figure 5 shows a geo-referenced picture of the school's toilets, which were mapped by several participants. The toilets potentially provide a space within the school environment where pupils are not subject to supervision and regulation. Going to the toilet unsupervised provides opportunities to increase their sphere of action and autonomous spatial appropriation.



Figure 5: Extract from collaborative map in ArcGIS-Online (© Esri).

4.5 Aesthetics: flora and fauna

'Aesthetics' is probably the most ambiguous category to have emerged from the data: many places and objects were mapped and annotated with either positive or negative associations according to whether the individual participant considered them 'pretty' or 'ugly'. The sub-categories 'graffiti' and 'commercial space' are connoted both positively and negatively in Table 1. However, almost every point that was mapped in the sub-category 'Flora and Fauna' was evaluated positively in terms of aesthetics. Participants emphasized the importance and their appreciation of urban green spaces, as well as of domestic animals (dogs, cats, animals at an urban petting zoo) and of wild animals (insects) which they encountered. Herlyn et al. (2003) have already noted the demand for urban green spaces in the context of children's participation in urban planning processes.

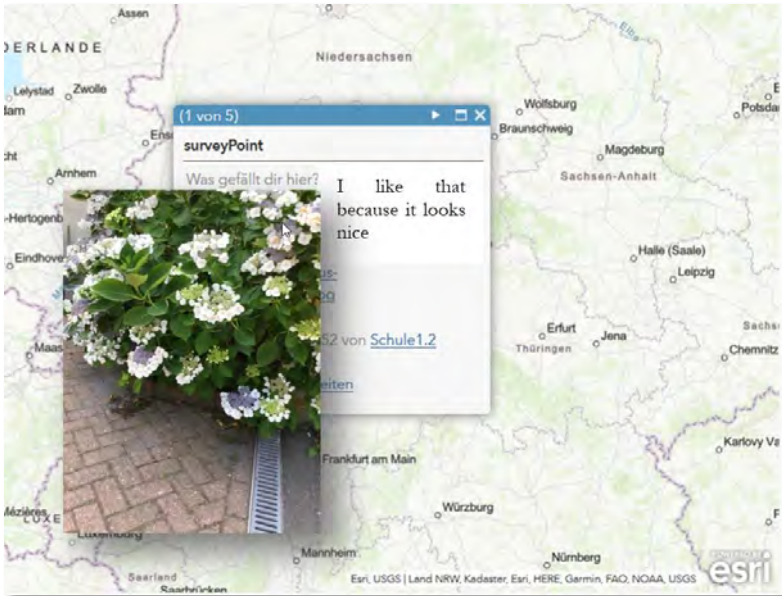


Figure 6: Extract from collaborative map in ArcGIS-Online (© Esri).

4.6 Discussion

The data analysis has shown that incorporating digital geomedia into a primary school-based learning environment can be beneficial for exploring their spatial appropriation processes with children. Using digital geomedia in the ways outlined is part of an education for Spatial Citizenship based on subjective neogeography. Through the creation of collaborative, mash-up maps that incorporate geo-referenced pictures along with text annotations, which could be added either by typing or by using voice recognition, participants were able to record and communicate a collective perspective on their life-worlds.

The critical examination and formulation of specific demands for spatial and social change which are evident especially in the categories of environment/environmental protection and social issues can provide a starting point for socio-spatial participation. Such demands are also vivid examples of the students' spatial appropriation processes: they identify life-world challenges but at the same time acknowledge their own relation to these life-worlds and the opportunity for change (Rhode-Jüchtern, 2004; Daum, 2010; Jaeggi, 2016). The results also make clear that paradigms of the institutionalization of childhood (see Tonucci & Rissotto, 2001) are ambivalent: children's life-worlds are subjected to processes of institutionalization; at the same time, children undermine these processes through the creation and validation of free spaces within institutionalized restrictions, as became evident in the school toilets examples. At the same time, guarded and secure spaces for children are sometimes perceived very positively due to imagined, or experienced, threats in public space (see the child safety lock example above). In the analysis of the workshop discussions (Pokraka, 2021), we identified the importance of private gardens as places for free exploration and as extended

spheres of action in lieu of public spaces, which were perceived as potentially dangerous. Acknowledging and supporting the search for these free spaces within the power-related restrictions of a neoliberal school system (Gryl & Naumann, 2016) can encourage the mature appropriation of space (Dorsch & Kanwischer, 2019) within an education for Spatial Citizenship. However, exposing children's 'hidden' spaces of autonomy always runs the risk of these spaces being eliminated. This makes weighing the interests of the children, their right to privacy, and the search for fields of autonomy in education (and research) a crucial point for consideration.

At the same time, the suggested mapping process provides opportunities to incorporate these challenges in the Primary Social and Science Education classroom: using the point-maps to identify spatial clusters and thematic points of interest offers a student-centred approach for learning. For example, the Primary Social and Science curriculum focuses on questions of economic action in relation to the distribution of material resources (GDSU, 2013: 32), which can be linked with issues of social inequality through the question of the distribution of wealth. Furthermore, the demand for an increase of e-mobility can be linked with the perspective-connecting topic of sustainable development (GDSU, 2013: 75–76). Here, one could also focus on the climate-related importance of urban green spaces beyond their mere aesthetic or recreational functions. However, one must note that learning environments tend to promote solely the impact of the individual's actions on climate change and sustainability, which Kehren (2016: 151) calls the 'privatization of sustainability': the implication is that as soon as students separate their waste, avoid fossil-fuelled individual transport and remember to turn off the lights when leaving the room, climate change is solved. There are several recent approaches that could be useful for tackling these issues, which stem from a de-politicized examination of highly political, global issues: transformation in geography education (Rohmann, 2021) proposes a systemic perspective on an education for sustainable development that reflects on both the scope of individual action and political dimensions. Furthermore, an approach of immanent critique in social geography didactics (Lehner et al., in preparation) can support the process of uncovering immanent contradictions in global environmental issues – e.g. the promotion of e-mobility which still relies on the production of electricity using fossil fuels.

5 Conclusion

We have presented the conceptualization of a learning environment based on an education for Spatial Citizenship: the incorporation of geomedia education in primary school teaching and learning. The analysis of the learning environment has shown that using simple web mapping applications can support student-based enquiry into spatial challenges in the children's own life-worlds, as well as the exploration of global challenges that manifest themselves spatially on a local level. We would like to encourage the use of digital mapping, especially for initiating and supporting processes of spatial appropriation and of exploring the world, within Primary Social and Science Education.

References

- Bach, S., & M. Peschel (2019): Erweiterung des Medienangebotes in kidipedia – Entwicklung, Implementierung, Erprobung und Evaluation eines Mapping-Tools in Form digitaler, interaktiver Karten. In: Praxisforschung Sachunterricht, 137-152.
- Bachmann G. (2009): Teilnehmende Beobachtung. In: Kühl S., Strodtholz P. & A. Taffertshofer (Hrsg.): Handbuch Methoden der Organisationsforschung. Wiesbaden, 248-271.
- Bennett, Lance, Wells, Chris, and Allison Park. 2009. 'Young citizens and civic learning: Two paradigms of citizenship in the digital age.' *Citizenship Studies*, 13(2): 105-120.
- Daum, E. (2010): Heimatmachen durch subjektives Kartographieren. In: Grundschulunterricht Sachunterricht 2. S. 17-21.
- Demirci, A. (2015): The Effectiveness of Geospatial Practices in Education. In: Solari, O.M., Demirci, A. & J. van der Schee (eds.): *Geospatial Technologies and Geography Education in a Changing World*. Tokyo: Springer, 141–153.
- Dorsch, C. & D. Kanwischer (2019): Mündigkeitsorientierte Bildung in der geographischen Lehrkräftebildung – Zum Potential von E-Portfolios. In: *Zeitschrift für Geographiedidaktik (zgd)*, 47 (3), 98-116.
- Elwood, S. & K. Mitchell, (2012): Mapping Children's Politics. In: *Geografiska Annaler, Series B* 94 (1), 1-15.
- Elwood, S., & K. Mitchell (2013): Another politics is possible. Neogeographies, visual spatial tactics, and political formation. In: *Cartographica*, 48 (4), 275-292.
- Essen. Oberbürgermeister Essen, Amt für Statistik, Stadtforschung und Wahlen (2011): *Der Bildungsbericht 2011*.
- Evans, B. (2008): Geographies of youth/young people. In: *Geography Compass*, 2 (5), 1659-1680.
- Gervé, F., & Peschel, M. (2013). Medien im Sachunterricht. In E. Gläser & Schönknecht, G. (Hrsg.), *Sachunterricht in der Grundschule* (S. 58-79). Arbeitskreis Grundschule – Der Grundschulverband.
- Gesellschaft für Didaktik des Sachunterrichts (GDSU) (2013): *Perspektivrahmen Sachunterricht*. Bad Heilbrunn: Klinkhardt.
- Gryl, I. (2010): Mündigkeit durch Reflexion. Überlegungen zu einer multiperspektivischen Kartendarstellung. In: *GW-Unterricht* 2010, 118, 20-37.
- Gryl, I. (2016): Der Schulhof. Erleben, Teilhaben und Gestalten zwischen pädagogischem Schutzraum und Öffentlichkeit. In: Adamina, Marco [Hrsg.], Hemmer, Michael [Hrsg.], & Schubert, Jan Christoph [Hrsg.]. (2016). *Die geographische Perspektive konkret*. Bad Heilbrunn: Verlag Julius Klinkhardt.
- Gryl, I. & T. Jekel. (2012): 'Re-centering geoinformation in secondary education: Toward a spatial citizenship approach.' In: *Cartographica*, 47(1): 18-28.
- Gryl, I. & J. Naumann (2016): Mündigkeit im Zeitalter des ökonomischen Selbst? Blinde Flecken des Geographielernens bildungstheoretisch durchdacht. In: *GW-Unterricht* 141. 19-30.
- Gryl, I. & U. Schulze (2013): Geomedien und Geographieunterricht. In: Kanwischer, D. (Ed.): *Geographiedidaktik. Ein Arbeitsbuch zur Gestaltung des Geographieunterrichts*. Stuttgart: Gebrüder Bornträger, 209-218.
- Herlyn, Ulfert, Hille Von Seggern, Claudia Heinzlmann, and Daniela Karow (2003). *Jugendliche in öffentlichen Räumen Der Stadt: Chancen Und Restriktionen Der Raumeignung*. Wiesbaden: VS Verlag Für Sozialwissenschaften, 2003.
- Holloway, S. L. (2014): Changing children's geographies. In: *Children's Geographies*, 12 (4), 377-392.
- Jaeggi, R. (2016): *Entfremdung: Zur Aktualität eines sozialphilosophischen Problems*. Suhrkamp, Berlin.
- Jörissen, B. & W. Marotzki (2009): *Medienbildung - eine Einführung. Theorie - Methoden- Analysen*. Bad Heilbrunn.

- Kanwischer, D. (2013): Informations- und Kommunikationstechnologien im Geographieunterricht. In: Rolfes, M. & A. Uhlenwinkel (Hrsg.): Metzler Handbuch 2.0 Geographieunterricht. Ein Leitfaden für Praxis und Ausbildung. Braunschweig, S. 79 - 86.
- Kanwischer, D. (2014): Digitale Geomedien und Gesellschaft. Zum veränderten Status geographischen Wissens in der Bildung. In: Geographische Rundschau, 66(6), 12-17.
- Kanwischer, D. & I. Gryl (2012): Der Einsatz von digitalen Karten und Globen zur Förderung der Argumentationskompetenz. In: Budke, A. (Hrsg.): Diercke Kommunikation und Argumentation. Braunschweig.
- Kanwischer, D. & A. Schlottmann (2017): Virale Raumkonstruktionen – Soziale Medien und Mündigkeit im Kontext gesellschaftswissenschaftlicher Medienbildung. In: zdg, Zeitschrift für Didaktik der Gesellschaftswissenschaften, 8 (2), 60-78.
- Kehren, Y. (2016). Bildung für nachhaltige Entwicklung. Zur Kritik eines pädagogischen Programms. Baltmannsweiler: Schneider Verlag Hohengehren.
- Kelle, Udo. Kluge, Susann (1999). Vom Einzelfall Zum Typus: Fallvergleich Und Fallkontrastierung in Der Qualitativen Sozialforschung. Opladen: Leske Budrich, Print.
- Kogler, Raphaela. (2019). Räume für Kinder - Räume der Kinder. Typologien urbaner Kinderräume. Lefebvre, Henri. 1991. The production of space. Oxford: UP.
- Lehner, M., Gruber, D. & I. Gryl (in preparation): Vom Widerspruch zum Widersprechen. Ansätze einer immanent-kritischen sozialgeographischen Didaktik.
- Löw, M. (2001): Raumsoziologie. Frankfurt am Main.
- Gervé, F. (2015): Digitale Medien. In: Kahlert, J./Fölling-Albers, M./Götz, M./Hartinger, A. u.a. (Hrsg.): Handbuch Didaktik des Sachunterrichts 2. Aufl. Bad Heilbrunn: Klinkhardt, S. 496-500
- Peschel, M. (2015). Medien im Sachunterricht – Unterricht gestalten – Lernkulturen entwickeln. In (Grundschule aktuell., Bd. 131, S. 10-14).
- Pettig, F. (2016): Mapping - Möglichkeitsräume erfahren. An- und Aufsichten im Geographieunterricht am Beispiel Berlins. In: Gryl, I. (Hrsg.): Diercke. Reflexive Kartenarbeit. Methoden und Aufgaben. Braunschweig, 194-198.
- Pokraka, J. (2016): Spatial Citizenship for All? Impulses from an Intersectionality Approach. In: GI_Forum 2016, 1, 262-268.
- Pokraka, J. (2021): Researching the Margins - Theoretische und empirische Betrachtungen differenz- und machtkritischer Perspektiven auf Bildung zu Spatial Citizenship. Dissertation, Universität Duisburg-Essen.
Online unter: https://duepublico2.uni-due.de/receive/duepublico_mods_00074724.
- Pokraka, J. & I. Gryl (2017): KinderSpielRäume. Kinder als Spatial Citizens im Spiegel von Intersektionalität, Medialität und Mündigkeit. In: zdg, Zeitschrift für Didaktik der Gesellschaftswissenschaften, 8 (2), 79-101.
- Pokraka, J. & I. Gryl (2018): Kinder:Karten:Kommunikation – Spatial Citizenship zwischen Partizipation und Paternalismus. In: Kartographische Nachrichten, 3, 140 – 146.
- Prasse Doreen, Egger Nives, Honegger Beat (2017). Mobiles Lernen. Auch zu Hause? In: Bastian Jasmin, Aufenanger Stefan [Hrsg.]. Tablets in Schule und Unterricht. Springer VS, Wiesbaden.
- Ramasubramanian, Laxmi. 2010. Geographic Information Science and Public Participation. Berlin: Springer.
- Rhode-Jüchtern, Tillmann (2004): Derselbe Himmel, verschiedene Horizonte. Zehn Werkstücke zu einer Geographiedidaktik der Unterscheidung. Materialien zur Didaktik der Geographie und Wirtschaftskunde 18. Wien: Universität Wien Institut für Geographie und Regionalforschung.
- Rinschede, Gisbert. Siegmund, Alexander. Ditter, Raimund (2020). Geographiedidaktik. 4.völlig neu bearbeitete und erweiterte Auflage ed. Paderborn: Ferdinand Schöningh, Print.
- Rohmann, N. (2021): Bringt Transformation in die Schulgeographie. OpenSpaces-Zeitschrift für Didaktiken der Geographie 1(21), 9-16.

- Schmeinck, Daniela (2013): Digitale Geomedien und Realtime Geographies. Konsequenzen für den Sachunterricht. In: Fischer, H.-J.; Giest, H. & Pech, D. (Hrsg.): Sachunterricht und seine Didaktik. Bestände prüfen und Perspektiven entwickeln. Bad Heilbrunn, S. 187-194
- Schröder, C. (2016): Mediale Verantwortung 2.0. In: Peschel, M. & T. Irion (Hrsg.): Neue Medien in der Grundschule 2.0. Frankfurt, 202-211.
- Schulze, Uwe, Gryl, Inga, and Detlef Kanwischer. 2015. 'Spatial Citizenship, Kompetenzmodellierung und Lehrerbildung. Zur curricularen Einbindung von digitalen Geomedien.' In: Zeitschrift für Geographiedidaktik 43(2): 139-164.
- Schulze, U., Kanwischer, D., Gryl, I. & Budke, A. (2020): Mündigkeit und digitale Geomedien – Implementation eines digitalen Fachkonzepts in der geographischen Lehrkräftebildung. Journal für Angewandte Geoinformatik, 43(2), S. 139–164.
- Shin, E. E. & S. W. Bednarz (2019): Spatial Citizenship Education. Citizenship through Geography. New York: Routledge.
- Tonucci, F. & A. Rissotto (2001): Why do we need children's participation? The importance of children's participation in changing the city. In: Journal of Community & Applied Social Psychology 11, 407-419.
- Tuukkanen, T., Kankaanranta, M. & T.-A. Wilska (2012): Children's life world as a perspective on their citizenship: The case of the Finnish Children's Parliament. In: Childhood, 20 (1), 131-147.
- Vogler, R. (2012): Schüler:Stad/tt:Planer. Web2.0 mapping environments in Planung und Bildung. In: Hüttermann, A. u.a. (Hrsg.): Räumliche Orientierung, Karten und Geoinformation im Unterricht. Geographiedidaktische Forschungen, Band 49. Braunschweig, 290-298 & 387-388.
- WAZ (2020). Illegaler Müll: Stadt Essen verhängt über 200 Bußgelder.
<https://www.waz.de/staedte/essen/illegaler-muell-stadt-essen-verhaengt-ueber-200-bussgel-der-id230632276.html>

Advantages of 360° Virtual Forest Tours to Supplement Academic Forestry Education

Torben Foehrder, Jan-Peter Mund and Peter Spathelf
Eberswalde University for Sustainable Development, Germany

Abstract

360° virtual forest tours (VFTs), created by state-of-the-art virtual reality technology, contribute to the progression of academic e-learning and forest management. The article proposes a conceptual framework for 360° VFT production and use to supplement field courses. Reflective insights into the authors' own learning process in the production of 360° VFTs, and a consideration of the general challenges of the medium are also presented. To conclude, the article summarizes the advantages of 360° VFTs for forestry education in an academic context.

Keywords:

virtual forest tours, forestry education, virtual reality, e-learning

1 Introduction

Excursions, field exercises and real-world laboratories are core elements of practice-oriented university didactics in education for sustainable development (ESD). The context-sensitive learning objectives of ESD cover knowledge transfer and cognitive experience, especially in the areas of nature conservation, ecology and forestry. Immersive and interactive learning is a modern didactic method in which 3D animation technology can be used to immerse learners in virtual realities (VR) and enable them to interact with so-called digital twins. This method is already widely used in technical sciences. It has been proven to promote learning efficiency by allowing learners to revisit the VR experience multiple times, in combination with more traditional forms of learning – or to use Pantelidis's terminology, through the combination of symbolic and experiential information (Pantelidis, 2009). The technological advancements in augmented, mixed and virtual reality (AR/MR/VR) applications support learning in cases of the physical or ethical inaccessibility of the object of study. Interactive 3D 'immersive learning spaces' bridge barriers of space and time, and enable focusing via AR/MR/VR on parameters or ratios in ecosystems that are invisible or not immediately comparable (e.g. size of tree stems compared to crown height; or crown size in relation to leaf cover, which can only be determined in different seasons). In the light of ongoing developments by the GIS Laboratory of the University for Sustainable Development Eberswalde, this article describes the creation

of a practical 360° virtual forest tour (360° VFT), which can be used as a tool for teaching and project coordination in forestry education. With suitable AR solutions already available (Mund & Müller, 2019), the development of VR teaching methods is the next logical step. The scope of the article includes the practical integration of the technology for individuals and institutions interested in the possibilities that 360° VFTs have to offer. An analysis of the didactical methods and advantages of the medium is not part of this article, as this would considerably extend the cover of the research. For an examination of immersive VR technology and learning theories for implementation in higher education contexts, see e.g. Radianti et al. (2020).

360° VFTs have become popular in environmental education as a way of informing people about how forestry benefits humans and wildlife (Kershaw, 2020). Transferring the didactic tool into an academic context serves as a supplement for field trips and partially solves limitations on financial and logistical resources (Reque Kilchenmann, García Ochoa, & Spathelf, 2017). To identify the contributions of 360° VFTs to higher education in forestry, the authors examined their personal experiences of 360° VFT production and the technical long-term implementation of the tours. A basic framework for the creation and comparison of 360° VFTs is presented, and the advantages of the medium are critically assessed in relation to the efforts required for successfully producing VFTs.

2 Materials and methods

Investigation into 360° VFTs as a possible tool for academic research and teaching was carried out using a basic technical setup. The equipment consisted of various digital single-lens reflex (DSLR) cameras, positioned in a panoramic head (Manfrotto, Cassola, Italy), mounted on a standard tripod in the field, and operated manually. Execution was constantly refined to evaluate the quickest and most reliable routine for photographing spots of interest for later digitalization. The image data acquired were then processed in PTGui (a software package that is currently available) and Panotour Pro (which is no longer released). This allowed the two-dimensional pictures to be re-arranged in a virtual simulation of the precise locations photographed.

Using PTGui, the photographs taken in the field were merged to create a spherical simulation of the site (see Figure 1). The software includes an additional masking tool for favouring or excluding areas in individual source images, as is found in most types of image-editing software. Basic functions such as the manual adjustment of anchor points shared by images and their placement within the virtual sphere, as well as simple graphic-adjustment tools, are also part of PTGui. The files produced allow a 360° experience of the virtual replica of a real-world location. To connect these files to an interactive tour, implement additional digital content, and generate a publishable HTML file, the Panotour Pro software by Kolor (Figure 2) proved sufficient, but distribution of the product was suspended and technical support discontinued during the period when this study was being carried out.



Figure 1: Transformation and distortion of single photographs taken by DSLR cameras in the creation of a spherical virtual replica using PTGui. From top left to bottom right: generation of photographic source files; merged images in spherical simulation; mosaic display of source files; distortion of source files within the panorama

The combined efforts of several projects allowed the production of various 360° VFTs for the purposes of academic knowledge transfer and project transparency. In this way, methods of large-scale forestry management could be visualized and compared. The aspects looked at included areas for practical fieldwork in forestry (marteloscopes), international ecosystem comparison, reforestation areas, and areas of storm damage and their structural development over time. Various ways of making the tours available for user interaction were compared and tested for accessibility, ease of application and sustainable data management.

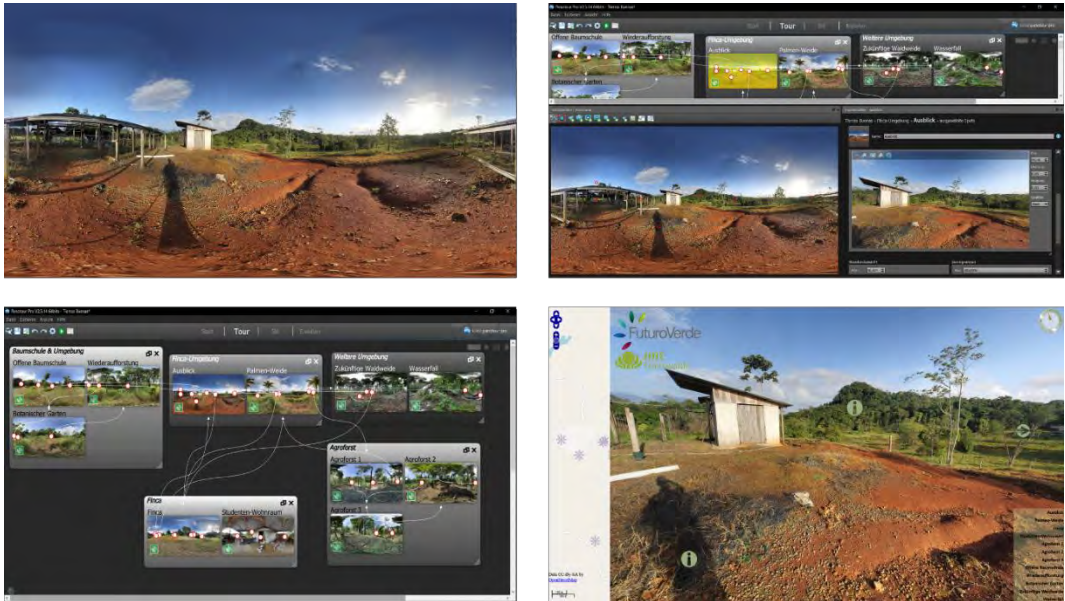


Figure 2: Implementation of the previously generated panoramic image into a virtual tour, including interactive and connective elements, using Panotour Pro. From top left to bottom right: panoramic image generated; implementation of spatial references and information; combining scenes into a tour; final tour as viewed in a web browser.

2.1 Subsequent reflexion

Based on their experiences in the projects undertaken, the authors refined the conceptual framework for the content-related production of a 360° VFT. After understanding the technological conditions needed to produce photographic material which meets the requirements for digital progression, the authors next examined the viewer's experience of the tour. For academic e-learning concepts in relation to forestry, tours that are publicly available were compared to the project results in order to extract preferred features. Additionally, a review of scientific and popular literature connected to forest-related VR research was carried out with a view to identifying possible implementations of 360° VFTs and their academic value.

3 360° VFT production

The production of a 360° VFT requires the same conceptual framework as that found in most projects focusing on public interaction and media presentation. Informational content, contextual storyboard, publishing environment and technological capacities are defining factors for the composition of the tour. The extent of the information and additional data to include can then be determined. Interested parties may consider outsourcing the creation of a 360° VFT as a way of reducing time, effort and costs while still achieving satisfactory results; indeed, there are more and more professional service providers creating virtual tours. The

most prominent companies in this domain are Google Tour Creator, RICOH360 and 3DVista. To create or modify a 360° VFT, using a third party or in-house resources, a sound understanding of the basic procedures may shorten the development process and aid in the design of a working concept.

For the creation of a 360° VFT, interested parties first need to generate suitable visual content for the spherical replication – i.e. panoramic photographic images. This is followed by the implementation of additional information, choosing a didactic connection between scenes, and embedding the tour in its publishing environment. The continuous development of equipment and software makes the technical procedures in 360° VFT production increasingly easy, but creative decisions for the integration of content require a further skill set in addition to subject-knowledge of forestry. Depending on the target group and the purpose of a 360° VFT, creators may consider deepening their understanding of digital and visual media, immersive didactics and interdisciplinary knowledge transfer.

3.1 Preparatory framework

Most important during the outlining phase of a 360° VFT is determining how much time will have to be invested for individual stages of the project. Furthermore, it must be kept in mind that acquiring appropriate image data requires favourable weather conditions. To avoid accumulating unnecessary data, the number and location of scenes to be shot should be established before starting the fieldwork. The choice of equipment and software (see Section 3.2) determines how the tour will be published and what modifications will be possible, and should therefore be addressed as early as possible.

3.2 Technical requirements

Integrated functions for the generation of panoramic image files can be found in conventional hand-held photographic devices (mobile phones, compact cameras, or point-and-shoot devices like GoPro models). Unmanned aerial vehicles (UAVs) are the most convenient way to inspect hard-to-reach locations while assuring exact geographical references. Higher-priced models commonly include settings for panorama shots (Muliawan, 2017). For high-resolution image data and the option to adjust settings according to the circumstances in the field, manually operated DSLR cameras are sufficient. However, full-panoramic (360°) footage can only be produced by specific state-of-the-art cameras. These are not currently available commercially as integrated components of UAVs (Feist, 2020).

Digital processing of the photographs to create spherical virtual environments requires less computing capacity than, for example, editing movie clips, but extracting clipped scenes from high-resolution image data is still very time-consuming. To guarantee fluid progress on the technical work involved and editing procedures, devices rely mainly on graphic components, such as high GPU capacities, and adequate virtual working storage. The accumulation of data can cause files for a single VFT to quickly exceed 10GB. Adequate hard-drive space therefore needs to be ensured.

3.3 Project stages of VFT production

These basic guidelines offer the essential procedures for producing a 360° VFT. The concept can be applied to any location and desired subject.

Draft of the project's scope

A preliminary definition of the 360° VFT subject is reached by consolidating the knowledge that is to be transferred and identifying the geographical references to be included. Also during the planning phase, the means of transport to the locations for photographic fieldwork, the creative partners in the project and their intentions for specific content, and the choice of equipment and publication platform need to be decided. The conceptual framework determining how many scenes to create and their sequence also need to be decided in relation to the target viewers of the 360° VFT.

Fieldwork and post-processing

A basic understanding of photography is necessary to achieve suitable photographic image data at the geographic location of interest. Differing weather and light conditions require constant adaptation for optimal source material. The effort invested may vary widely based on the equipment used and the desired level of detail.

The individual photographic image files are merged into a single larger image file, which can be displayed using specific software as a virtual 360° spatial experience of the scene. Given appropriate source material and software, creating a spherical combination of the individual files requires minimal manual graphical corrections or selection/omission of individual source files in the mosaic display (Figure 1).

Tour creation and publication

Subsequently, the individual scenes are connected to form a virtual tour. If augmented by geographical references, the sequence of the individual scenes can deliver an understanding of the environmental conditions at the geolocation, at a specific point in time (Figure 2). Metadata or the appropriate EXIF files should therefore always be accessible for auxiliary information – but via icons or other interactive functions, so as not to obstruct the viewer's undisturbed field of vision. Trade-offs between fostering the benefits of an intuitive understanding of the virtual replicated environment, ease of access to supplementary technological components, and software limitations are to be expected during this phase.

When a 360° VFT is created for public access, online lessons or as a stand-alone production, webhosting, remote access or a server structure is necessary to deliver the tour to interested viewers. Hosting services like WordPress or Wix have published technical expansions to integrate virtual 360° content. Software that can produce virtual tours generates usable data formats (HTML5 or JavaScript are common) and may include complementary software to present the created tour via an Intranet or a local host. If technical training and resources are available, the tours may also be made available through in-house webhosting.

4 Utilization of 360° VFT

Especially in the context of a worldwide pandemic, the advantages of remote-access study courses and virtual excursions have become ever more apparent. A virtual replication of real-world forest stands allows for repeatable experience in a specific area of interest, independently of the current weather conditions, season of the year or transport. The exchange of (detailed, computerized) academic knowledge in connection to forestry (e.g. types of vegetation and structural composition, growth over time, or effects of natural disasters) can be fostered by the opportunities offered by 360° VFT, and vice versa.

One example of 360° VFTs being used to supplement or complement traditional courses of study, classroom teaching methods and fieldwork are the teaching units designed by the Institute for Sustainable Forest Management Research, University of Valladolid, Spain (Figure 3), which are based on interactive online walks through real forest stands (Instituto Universitario de Investigación Gestión Forestal Sostenible (iuFOR), 2018). Documentation of experiments, of extraordinary events such wildfires or storms, of harvesting, planting or fencing allows for immediate visual comparison of plant growth, for example, and offers a holistic perspective on the ecosystem (Figure 4). The European-Vietnamese Higher Education Network for Sustainable Forest- and Bio-Economy, another instance of a 360° VFT used in education, aims to examine issues in a multidisciplinary fashion and to compare different forest ecosystems on a global scale.



Didactic materials

Virtual Visits

MARTELOSCOPE XAMK_South-Eastern Finland University of Applied Sciences (Mikkeli)

Marteloscope XAMK (Mikkeli, Finland)

Key words: Forestry, silviculture, harvesting, thinning, clear-cut, tending, regeneration, Hippala, Mikkeli, BIOECON.EU, ERASMUS MUNDUS

[HOME](#)

Fullscreen: http://sostenible.palencia.uva.es/rutas/Marteloscope_XAMK/index.html

[View Virtual Visit >>](#)

MARTELOSCOPE Thai Nguyen University of Forestry_Vietnam (Virtual Forest Tour)

[MARTELOSCOPE TUAF Thai Nguyen University of Forestry, Vietnam](#)

Figure 3: Screen shot of 360° VFT to supplement academic field courses sostenible.palencia.uva.es (Instituto Universitario de Investigación Gestión Forestal Sostenible (iuFOR), 2018)



Figure 4: Sample images showing different site conditions after storm damage (Mund, Beiler, & Manh, BioEcoN, 2019)

The development of a virtual teaching environment for owners of small-scale forests to ensure adaptation of their stands to future conditions caused by climate change is the subject of a recent project by the Department of Information Management and Information Systems at the University of Osnabrück (Thomas, 2021). This example of the use of 360° VFTs in higher education is aimed at young forest owners who have little forest management experience, for the identification of tree species, assessment of forest stands, identification of habitats, timber harvesting, and rejuvenation.

5 Discussion

Setting up a suitable collection of 360° VFTs for academic e-learning and knowledge transfer requires a considerable investment of time, suitable equipment, relevant media competence, photography and programming skills, and secure web hosting. Consequently, virtual tour production and webhosting are now carried out predominantly by businesses instead of individual creators. Cancellation of support for the Panotour Pro production software by developer Kolor was a further complexity encountered during the learning process.

The importance of ethics and moral sensitivity to be integrated into new technologies reached new levels with the development of VR. Referred to as ‘anticipatory technology ethics’ by Philip A. E. Brey (Brey, 2012) and ‘responsible research and innovation’ by Hilary Sutcliffe (Sutcliffe, 2011), the responsibilities and moral obligations of technology designers to the public may include a wider long-term view, taking into account social involvement, environmental impacts and other repercussions. Predictions, forecasting impacts, and evaluating and elaborating on possible consequences need to be integrated into the development of VR applications to guarantee early identification of issues with openness and transparency. Additionally, profound acknowledgement of active, real, lived experience needs to be a fundamental psychological element in VR development for the provision of a ‘positive’

experience in a virtual environment, which is supposed to stay as close to reality as possible (Kenwright, 2019).

5.1 Advantages of 360° VFT in forestry education

The potential of 360° VFTs to offer visual impressions of environmental conditions at a particular geographical location that can be compared with each other makes this a holistic and comprehensive medium for understanding the complex interdependencies that exist within a forest ecosystem. The level of immersion provided by 360° VFTs cannot be accomplished by traditional textual or photographic learning materials. By connecting geographical references, extracted in semi-autonomous fashion from existing image metadata, and photo-optic panoramic portrayals of a location, remote users are able to immerse themselves in the scene and to experience its content in an interdisciplinary and unbiased way. Further implemented data, accessed via intuitive and meaningfully (spatially) oriented links/icons within the scenes, can supplement a tour. In this way, the visual concept of a 360° VFT supports memorizing, understanding, and the creation of links between different pieces of information (Kouyoumdjian, 2012). VR implementations, due to their intuitive, digital and transdisciplinary nature, facilitate increased learning engagement, higher accuracy in planning processes, decreased costs of prototype development, as well as the generation of new ways of communicating and interacting between collections of data, products, locations and stakeholders (Marr, 2017).

Regarding forestry education specifically, the digital recreation of real-world forest structures in a 360° VFT provides an objective picture to unify all available data, combined with analytical tools to support collaborative decision-making and stakeholder engagement. Cost reduction and increased productivity are possible by minimizing the reliance on field trips and using 360° VFT for forest management decisions (Roeser, 2020). Current 360° VFT applications include updating forest asset information, automatization of data integration via remote sensing, and improvement of forest machinery and management simulators for staff training (Fabrika, Valent, & Mokroš, 2016). Highly immersive VR simulations are of increasing value for school purposes due to their independence of time and location. They also provide a risk-free environment and room for mistake-driven experiences (Pappas, 2017). In the long term, ambitions are set to create digital replicas of forests, including the modelling of every tree in terms of its location, height, diameter and species. It will become possible to visit timber transactions virtually and compare management decisions. The simulation of stand conditions after the application of different management decisions will be another convenience of 360° VFTs (Hofmann & Jumppanen, 2017).

6 Prospects and developments

Digital replications of real-world forest stands are expected to become further enhanced. They will provide geospatial references for silvicultural objects improved by the integration of multi-sensory data, generated by autonomous and manually-operated vehicles in forest operations. Using photogrammetric or LiDAR technology in 360° VFT could allow the display of point cloud data in a graphically enhanced way within a tour. Viewers would be able to carry out

assessment tasks for which natural human perceptual skills are required, without the restrictions of a conventional display screen (Chinthammit, 2017). Calculations performed by integrated functions within the software could reduce manual documentation and automate basic assessments (Fabrika, Valent, & Mokroš, 2016). It may soon be possible to create autonomous inventories, as shown by developments discussed in (Mohan, et al., 2017). Given the increasing accuracy of sensor technologies, inventories will achieve greater levels of reliability through autonomous, technological means than human observation alone is able to accomplish.

References

- Bardi, J. (2020, 09 21). Marxent. (Marxent, Editor) Retrieved 01 31, 2021, from What is Virtual Reality? VR Definition and Examples: <https://www.marxentlabs.com/what-is-virtual-reality/>
- Brey, P. A. (2012, 04 04). Anticipatory ethics for emerging technologies. *NanoEthics*, 6(1-13). doi:<https://doi.org/10.1007/s11569-012-0141-7>
- Chinthammit, D. W. (2017). ForestTECH. (I. Ltd., Interviewer) Retrieved 01 31, 2021, from Virtual reality and it's use in local forests: https://fridayoffcuts.com/dsp_article.cfm?id=745&aid=8903
- Fabrika, M., Valent, P., & Mokroš, M. (2016). Sektion Ertragskunde im Verband Deutscher Forstlicher Versuchs- und Forschungsanstalten. (T. U. Faculty of Forestry, Ed.) Retrieved 01 31, 2021, from Forest Landscape Simulations in Immersive Virtual Reality: http://sektionertragskunde.fvabw.de/2016/08_Fabrika_et_al.pdf
- Feist, J. (2020, 07 27). Drone Rush. Retrieved 01 31, 2021, from Best drones with 360 degree camera: <https://dronerush.com/best-drones-360-degree-camera-10725/>
- Google Street View. (2021). Google Street View. (Google Street View) Retrieved 01 31, 2021, from Take a look at all the Street View mapping stories: <https://www.google.com/intl/en-GB/streetview/case-studies/>
- GoPro, Inc. (2020). Kolor Panotour. (GoPro, Inc.) Retrieved September 16th, 2020, from Kolor: <https://www.kolor.com/>
- Hofmann, C., & Jumppanen, J. (2017). Metsä Group - Forerunner in sustainable bioeconomy. (M. Group, Editor) Retrieved 01 31, 2021, from Virtual forests are coming: <https://www.metsagroup.com/en/Campaigns/IntelligentMetsa/intelligentforest/Virtual-forests-are-coming/Pages/default.aspx>
- Instituto Universitario de Investigación Gestión Forestal Sostenible (iuFOR). (2018, 01 11). INICIO | Gestión Forestal Sostenible. Retrieved 01 31, 2021, from Virtual Forest Tours: <http://sostenible.palencia.uva.es/content/virtual-forest-tours>
- Kenwright, B. (2019, 01 14). Technology and Society. Retrieved 01 31, 2021, from Virtual Reality: Ethical Challenges and Dangers: <https://technologyandsociety.org/virtual-reality-ethical-challenges-and-dangers/>
- Kershaw, A. (2020, 01 14). The Ecologist. (T. Ecologist, Editor) Retrieved 01 31, 2021, from Virtual forest tours for children: <https://theecologist.org/2020/jan/14/virtual-forest-tours-children>
- Kouyoumdjian, H. (2012, 07 20). Psychology Today. Retrieved 01 31, 2021, from Learning Through Visuals: <https://www.psychologytoday.com/us/blog/get-psyched/201207/learning-through-visuals>
- Marr, B. (2017, 07 31). Forbes. (Forbes, Editor) Retrieved 01 31, 2021, from The Amazing Ways Companies Use Virtual Reality For Business Success: <https://www.forbes.com/sites/bernardmarr/2017/07/31/the-amazing-ways-companies-use-virtual-reality-for-business-success/>

- Mohan, M., Silva, C. A., Klauberg, C., Jat, P., Catts, G., Cardil, A., . . . Dia, M. (2017, 09 11). Individual Tree Detection from Unmanned Aerial Vehicle (UAV) Derived Canopy Height Model in an Open Canopy Mixed Conifer Forest. *Forests*, 8(9). doi:<https://doi.org/10.3390/f8090340>
- Muliawan, R. C. (2017, 05 08). SkyPixel. Retrieved 01 31, 2021, from Tips for 360-Degree Aerial Photography: <https://store.dji.com/guides/tips-360-degree-aerial-photography/>
- Mund, J.-P., Beiler, K., & Manh, V. V. (2019). BioEcoN. Retrieved 07 15, 2021, from Virtual Forest Tours: <http://bioecon.eu/virtual-forest-tours/>
- Mund, J.-P., & Müller, S. (2019). Augmented Reality and Mobile GIS as Tools for Teaching Data-collection in the Context of Forest Inventories. (U. f. Eberswalde, Ed.) *GI_Forum*, pp. 129-143. doi:10.1553/giscience2019_02_s129
- New House Internet Services B.V. (2020). PTGui. (New House Internet Services B.V.) Retrieved September 16th, 2020, from PTGui: <https://www.ptgui.com/>
- Pantelidis, V. S. (2009). Reasons to Use Virtual Reality in Education and Training Courses and a Model to Determine When to Use Virtual Reality. (C. o. Department of Library Science, Ed.) *THEMES IN SCIENCE AND TECHNOLOGY EDUCATION*, 2(Special Issue), pp. 59-70. Retrieved 07 15, 2021, from <https://files.eric.ed.gov/fulltext/EJ1131313.pdf>
- Pappas, C. (2017, 02 11). eLearning Industry. Retrieved 01 31, 2021, from 6 Tips To Use Virtual Reality In Online Training: <https://elearningindustry.com/tips-use-virtual-reality-online-training>
- Radianti, J., Majchrzak, T. A., Fromm, J., & Wohlgenannt, I. (2020, April). A systematic review of immersive virtual reality applications for higher education: Design elements, lessons learned, and research agenda. *Computers & Education*, 147. doi:<https://doi.org/10.1016/j.compedu.2019.103778>
- Reque Kilchenmann, J., García Ochoa, M., & Spathelf, P. (2017). Bringing the forest to the classroom: developing virtual tours in forestry. In 1. I. (ICEE21C) (Ed.), *New competences in Engineering Education in the area of sustainability and university social responsibility* (pp. 23-26). Castelló de la Plana: Universitat Jaume I.
- Roeser, D. (2020, 04 17). The University of British Columbia. Retrieved from How Virtual Reality Can Aid Land-Based Resource Management and Operation Planning: <https://forestry.ubc.ca/research/how-virtual-reality-can-aid-forest-operations/>
- Sutcliffe, H. (2011, 05 16-17). European Commission. Retrieved from Responsible Research and Innovation Report: https://ec.europa.eu/programmes/horizon2020/sites/default/files/rri-report-hilary-sutcliffe_en.pdf
- Thomas, O. (2021, 05 01). Universität Osnabrück. Retrieved 007 15, 2021, from Department of Information Management and Information Systems (IMWI): https://www.wiwi.uni-osnabrueck.de/fachgebiete_und_institute/informationsmanagement_und_wirtschaftsinformatik_prof_thomas/projekte/virtual_reality_forestry_training.html
- Vitec Imaging Solutions Spa. (2021). Manfrotto. Retrieved 07 15, 2021, from Virtual reality panoramic head w/ multiple sliding plates: <https://www.manfrotto.com/global/virtual-reality-panoramic-head-w-multiple-sliding-plates-mhpanovr/>

Intellectual Resilience – Draft of a New Educational Approach for the Geography Classroom

GI_Forum 2021, Issue 2

Page: 45 - 53

Full Paper

Corresponding Author:

daniel.raithofer@univie.ac.at

DOI: 10.1553/giscience2021_02_s45

Daniel Raithofer and Christiane Hintermann
University of Vienna, Austria

Abstract

Major crises such as the Covid-19 pandemic put societies to the test. The conjuncture of globalization, with all its challenging transformation processes, social inequality, and the epidemic spread of a new (viral) pathogen has fuelled feelings of uncertainty and insecurity in virtually every part of society, on a global scale. Focusing on learners, this paper proposes 'intellectual resilience' as a new educational concept aiming to empower learners to more fully comprehend and navigate global crises. An intellectually resilient person is defined as someone who can use multiple scientific approaches and concepts in a participative, democratically informed way. The aim is to explore the potential of school geography education to support young learners in handling crisis situations

Keywords:

resilience, geography education, crises, Covid-19

1 Introduction

With the Covid-19-pandemic, we are currently facing the severest social and economic crisis on a global scale since the end of World War II. Even though the pandemic is first and foremost a health crisis, there can be no doubt that Covid-19 affects every part of our lives. Unlike other global challenges such as the financial meltdown in 2008, it affects everybody's wellbeing, albeit to different degrees. As the UNHCR emphasizes, more vulnerable groups in society, such as 'people living in poverty situations, older persons, persons with disabilities, youth, and indigenous peoples' (UN, 2020), are hit harder. Everybody has to cope with the effects of Covid-19, although not everyone has the same possibilities and abilities to do so. In what follows, we will outline a new educational concept aiming to foster learners' intellectual resilience.¹ The intention of this approach is to empower learners to more fully comprehend, negotiate and shape today's 'super-complex' crises (Barnett, 2000). The concept will be elaborated from the perspective of the geography classroom and uses the current Covid-19

¹ The conceptualization and implementation of the approach will be undertaken within the context of a PhD project.

situation as an example of a global crisis that increases feelings of uncertainty in wide parts of society.

However, before Covid-19, other risks had spread from their geographic sources and become global threats. The SARS outbreak (2002/03), MERS (2012) and the Ebola virus (e.g. 2018–2020) epidemic drew attention years ago to the fact that the conjuncture of globalization, social inequality and the epidemic spread of a pathogen is a potentially dangerous mix. The need to permanently deal with hazards and insecurities resulting from the modernization process itself is a characteristic of modern ‘risk societies’ (Beck, 1992) and inherent to ‘liquid’ or ‘reflexive’ modernity (Baumann, 2000), where everything undergoes constant processes of transformation.

Discourses of danger, risk and hazards are permanently spread via the media. Nature being ‘out of control’ makes front-page news, and increasingly such discourse, through people’s participation in social media, influences signification in the world of social media. Whilst traditional media form and disseminate representations and significations of what is and could be, an ever-growing number of media producers spread mis- and disinformation. This also holds true for maps, which are never just representations of the physical world but are always instruments of power (Pavlovskaya, 2018). GIS offers new possibilities to negotiate and shape power relations, since digital and online mapping can be used as tools for social transformation, but also to spread mis- and disinformation. Being able to distinguish between fact and fake is more and more difficult in times ‘where nothing can be taken for granted, where no frame of understanding or of action can be entertained with any security, [...] in which we are conceptually challenged, and continually so’ (Barnett, 2000: 257).

When anything can change from one day to the next, as during the current Covid-19 pandemic (e.g. restrictions on movement and social life), concepts of flexibility, adaptability and resilience become of key importance. Resilience especially became very popular in numerous academic disciplines and beyond academia. Runguis et al. (2018) argue that resilience and its popularity can be understood as an answer to uncertainty, crisis and reflexive modernity.

Crisis situations like the current pandemic entail numerous consequences in different societal spheres. From an educational perspective, school shutdowns are among the most obvious and most challenging, especially, as early research into the pandemic shows, for learners with limited access to technology and little parental support (Huber et al., 2020). It has also been pointed out that trainee teachers in Austria have not been familiarized with the concepts and practices of distance learning (Jekel et al., 2020). Nevertheless, lockdown led to increased use of digital devices and social media among (young) people for daily information and communication (ibid). Children and young people rely heavily on media channels like YouTube as major sources of information (Medienpädagogischer Forschungsverbund Südwest, 2020: 38ff). One effect of this development is the accelerated spread of misinformation about COVID-19.

School shutdowns and the implementation of distance learning can be seen as a particular form of crisis management that is closely linked to the Covid-19 pandemic. Together with the ever-growing importance of social media as places where feelings of insecurity and uncertainty are fuelled, the pandemic points to the need to develop new educational concepts to equip young people with the skills for informed decision making, creative problem solving, and the

ability to shape change. Intellectual resilience is one competence that will be explored and conceptualized as being important for students (not only) in times of crisis.

2 Intellectual Resilience – Draft of a new educational approach

In an educational context, resilience has mostly been addressed in connection with young people who have experienced personal difficulties or trauma, who therefore need to build up skills to cope with these situations. (For an overview, see Hess 2019.) Contrary to approaches which are based on a pedagogy of vulnerability and which tend to shift responsibility from society to the individual (Pollard, 2014), our approach to resilience education is informed by critical pedagogy (Freire, [1997] 2000) and civic education (Giroux, 2011); it is also linked to the social resilience approach (Keck & Sakdapolrak, 2013), which focuses on actors and their (cap)abilities.

Education for intellectual resilience is embedded in, and linked to, several general pedagogical concepts (and others) that have been developed within the field of geography education. So far, however, none of these approaches have been operationalized in terms of education confronting crises, or global challenges and transformations. One of these approaches is the **capabilities approach** (Nussbaum & Sen, 1993; Sen, 1999; Nussbaum, 2013). Originally conceived as an alternative economic approach to human welfare, it has also been adopted by social sciences more widely and used in an educational context. The concept of **geocapabilities** (Lambert et al., 2015) is closely linked to the capabilities approach and focuses the contribution of geography education on a person's capabilities. The geocapabilities approach aims to help learners reach their full human potential in a highly interdependent world by using the **powerful disciplinary knowledge** (Young, 2008) offered by geography education.

The notion of powerful disciplinary knowledge is also represented in the development of specific **key concepts** (Lambert, 2013) and their implementation in school curricula. (For a discussion of this in relation to Geography and Economics education in Austria, see Jekel & Pichler, 2017). Learning with key concepts (or conceptual thinking) can support learners in understanding complex processes, foster critical thinking, help learners to deconstruct pre-given questions or solutions, as well as enable them to actively participate in societal negotiation processes.

Intellectual resilience is closely linked to concepts from **civic and citizenship education** (Sander, 2010; Bennett et al., 2009). The work of Bennett et al. (2009) is an important point of reference. They stress changes in young people's civic orientation, which led to two different types of citizen identity: the 'dutiful citizen' and the 'actualizing citizen' (Bennett et al., 2009: 106). Today's younger generations mostly belong to the latter group, which is characterized by less political participation in traditional ways (e.g. voting, following issues in the news) and a focus on lifestyle politics such as political consumerism, volunteering or social activism. Other attributes of the group are a mistrust of traditional media and the widespread use of digital media for communication. Bennet et al. stress the need for interactive and project-based learning environments for citizenship education.

Interaction and learners' agency are also central to the concepts of **innovativeness** or **education for innovation** (Golser et al., 2019; Shavinina 2013), which can also be linked to intellectual resilience. Innovativeness strives to integrate the process of innovation in learning situations. It aims to improve learners' creativity, reflexivity and innovativeness by fostering critical and constructivist thinking, but also by encouraging learners to use their capabilities to find new and creative solutions to problems which they have identified themselves.

Critical spatial learning (Gordon et al., 2016) and **education for spatial citizenship** (Gryl & Jekel, 2012) are further important reference points. Gordon et al. aim to foster young learners' civic engagement through critical spatial thinking. They use processes of critical digital mapping to emphasize 'how social and spatial processes intertwine to generate societal inequalities and show how this learning informs students' social and spatial civic responses' (Gordon et al., 2016: 558). These approaches also link to **critical GIS** (Pavlovskaya, 2018), which strives to reveal how spatial inequalities are produced and maintained. Gryl & Jekel (2012) add a more spatial view to citizenship education in general. Their main objective is to enable learners not simply to take part in society more actively, but to do this by critically using geoinformation and geomedial. Education for spatial citizenship and critical GIS could thus be used to bridge geoinformation and intellectual resilience.

Education for intellectual resilience can further be linked to the notion of the **viral construction of space** (Kanwischer & Schlottmann, 2017). This concept can be positioned at the intersection of spatial learning or education for spatial citizenship and critical (geographic) media literacy. It focuses on the changing ascriptions of the meanings of places in social media and how these meanings can go viral by being shared. To better comprehend how spatial ascriptions may go viral, reflective approaches connected to **structural media theory** (Jörissen & Marotzki, 2009) are useful, since structural media theory aims to analyse changes in our conception of ourselves and our views of the world.

Finally, we draw on concepts of **critical (geographic) media literacy** (Kellner & Share, 2005, 2007; Hintermann et al., 2020). Kellner & Share point out that critical media literacy 'involves gaining the skills and knowledge to read, interpret, and produce certain types of texts and artifacts and to gain the intellectual tools and capacities to fully participate in one's culture and society' (Kellner & Share, 2005: 365). Transferred to the field of geography education, this means the competences to read, interpret and produce spatially and economically embedded media representations as a means of participating in society in a more informed and emancipatory way (Hintermann et al., 2020).

The concept of intellectual resilience is elaborated in the context of the school subject Geography and Economics. School geography in Austria is an interdisciplinary subject that combines geography, economics and civic education with the aim of empowering learners to actively and responsibly participate in society at local and wider levels, including the global level (BGBl. II Nr. 219/2016). Taking these aims seriously means focusing on students' own (political) agency, building on their own experiences, supporting critical and conceptual thinking, and empowering them to deal with uncertainty and contingency as basic conditions in society and preconditions to improve knowledge. Intellectual resilience, then, would comprise not only the ability to adapt to difficult circumstances but also skills to question these circumstances, to perceive supposedly 'given' situations and narratives as constructed and

changeable, and to intervene responsibly in societal transformation processes. An intellectually resilient person can therefore be defined as someone who can make use of multiple scientific approaches and concepts in a participative, democratically informed way. Table 1 gives an overview of the (cap)abilities that students need to acquire in order to become intellectually resilient. The table also outlines pedagogical and educational approaches related to these (cap)abilities.

Table 1: (Cap)abilities fostered by intellectual resilience, and corresponding educational/pedagogical approaches

(Cap)ability	Corresponding approach
ability to question and challenge ‘crisis’, ‘risk’ and ‘threat’ as concepts: Who defines a situation as a crisis/risk/threat? When is a crisis (/risk/threat) a crisis (/risk/threat)? Who is affected by the crisis (/risk/threat), and to what extent?	critical (geographic) media literacy, civic and citizenship education
ability to understand the contingent nature of debates and to decode propositions as context-sensitive	critical pedagogy, critical (geographic) media literacy
ability to deconstruct (political) crisis-driven rhetoric	critical (geographic) media literacy, civic and citizenship education
ability to realize that crises involve change, and that change and transformation are constants in society	civic and citizenship education, innovativeness, education for innovation
ability to intervene and participate responsibly in societal negotiation processes	critical pedagogy, geocapabilities, civic and citizenship education
ability to identify (social) media as major actors and players in the negotiation and (re)construction of ‘crises’, ‘risks’ or ‘threats’	critical (geographic) media literacy, viral construction of space
ability to work out the spatial dimensions of crises	critical spatial learning, education for spatial citizenship, critical GIS, viral construction of space
ability to phrase questions instead of accepting pre-given answers	critical pedagogy, civic and citizenship education, innovativeness, education for innovation

The (cap)abilities specified in Table 1 are not presented in any hierarchical order: education for intellectual resilience aims to strengthen all of them. Different approaches can support the acquisition or strengthening of each individual capability. In the context of education for intellectual resilience, these approaches will further be linked to the concept of social resilience.

3 Connecting resilience to current educational approaches

It has been pointed out that intellectual resilience as a new educational approach needs further in-depth conceptualization. However, in what follows, and taking the Covid-19 pandemic as an example, we will illustrate how the notion of resilience can be linked with present educational concepts in order to enhance learners' knowledge and (cap)abilities. First, we need to figure out reasons for students' feelings of insecurity or uncertainty in relation to the pandemic, not simply as a health hazard. That might be the loss of financial security when parents become unemployed; changing daily routines when distance learning replaces regular school classes; issues that might occur when learning and living routines are shifted from physical to virtual space; an overload of information spread via diverse media channels, and the closely related questions of which information is to be trusted, and what is fact and what is fake.

For the sake of exemplification, we now focus on the questions of information spread, overload and trustworthiness. The ability to deal with information spread by media is clearly connected to strategies or core concepts inherent to critical media literacy. According to Kellner & Share (2005: 375), **non-transparency** is the first core concept to be applied in dealing with media products. Media products, as is widely acknowledged, do not reflect reality but are representations of reality and imply construction processes (see Luhmann, 2017). Making this process visible or transparent helps to deconstruct media messages, for instance with regard to what is conveyed by a message and what is left out. In the context of the coronavirus pandemic, one could ask: What information about Covid-19 is being transmitted? What aspects are *not* being focused upon, or are even missing? Such questions are valid for information based on provable facts as well as for fake news.

Another important core concept in media literacy is **audience decoding** (Kellner & Share, 2005: 375). The various processes of encoding and decoding media messages never provide congruency, leading to a pluralistic interpretation of media products. In other words, it is possible to gain different information from the same media product depending on the way the audience decodes the message. Learners who are aware of the concepts of non-transparency and audience decoding might handle the steady information stream on Covid-19 more easily. It is precisely at this point that critical media literacy as an educational approach and social resilience intertwine. Social resilience as Keck & Sakdapolrak (2013) describe it is characterized by three main capacities: coping capacities, adapting capacities and transformative capacities. Coping capacities aim to restore a status quo of wellbeing, as experienced before a threat or crisis occurred. The temporal scope is short-term, and the degree of change of social structures is rather low. Linked to critical media literacy, coping capacities would imply the ability to decode media messages in a way that increases transparency and allows for a more personal reading of the information transmitted. This might lead to a restoration of former feelings of security or certainty. On a meta-level, this restoration of wellbeing could be expressed as a new capability that aims to identify (social) media as main actors and players in the negotiation and (re)construction of 'crises', 'risk' or 'threats'.

Social resilience targets not only short-term coping capacities but also adapting and transformative capacities. Applied to the Covid-19 pandemic and the trustworthiness and spread of information, we will now briefly address the interrelation of transformative capacities

and critical media literacy. Critical media literacy and its two core concepts of **content and message** and **motivation** (Kellner & Share, 2005: 376–77) are strongly connected to critical thinking (Dewey, 1910), which encourages values and power relations to be questioned or contested. Both **content and message** and **motivation** serve to reflect on ideologies or bias transmitted in media products and the roles that media play in the process of negotiating power. Applying these two concepts to feelings of uncertainty or insecurity caused by the pandemic opens up new, completely different, questions: Who has the power to select the information which is transmitted and how is it selected and transmitted? What interests are pursued through the communication of certain pieces of information? What possibilities are there to foster a broader participation in the process of media production? From a social resilience perspective, these questions can be addressed within the realm of transformative capacities. In order to improve individual welfare but also to strengthen societies as such against future crises, there needs to be more participation in decision-making processes (Keck & Saksdapolrak, 2013: 11). It becomes clear that transformative capacities relate to the long term, having a high potential to change the structures of a social system. Applied to the Covid-19 situation, linking critical media literacy and social resilience can be used to foster a new capability which aims to question and challenge ‘crises’, ‘risk’ or ‘threat’ as concepts: Who defines which situations as crises (/risks/threats)? When is a crisis a crisis? Who is affected by the crisis and to what extent?

In brief, education for intellectual resilience aims to enhance learners’ participative skills and agency in order to empower them to participate in ongoing processes of change and transformation and to navigate through a crisis like the Covid-19 pandemic towards a state of increased wellbeing, security and certainty.

4 Outlook

The conceptualization of intellectual resilience as a new educational approach focuses on how geography education can promote a more comprehensive understanding of crises and the complex conjuncture of risk, uncertainty, liquid modernity and (fake) news through the use of (social) media, including geomeia. In future work, based on the principles of Participatory Action Research (Coghlan & Brydon-Miller, 2014), the concept will be elaborated collaboratively in a workshop setting with students in higher secondary education. Strategies and methods to facilitate intellectual resilience will be explored and implemented, with the aim of developing a practical and adaptive tool kit that can readily be employed in the classroom.

References

- Barnett, R. (2000). Supercomplexity and the Curriculum. *Studies in Higher Education* 25(3), 255-265. DOI: 10.1080/713696156.
- Baumann, Z. (2000): *Liquid Modernity*. Cambridge: Polity Press.
- Beck, U. (1992). *Risk Society: Towards a New Modernity*. London: Sage.
- Bennett, W. L., Wells, C., & Rank, A. (2009). Young Citizens and Civic Learning: Two Paradigms of Citizenship in the Digital Age. *Citizenship Studies* 13(2), 105-120. DOI: 10.1080/13621020902731116.
- BGBI. II Nr. 219/2016: Änderung der Verordnung über die Lehrpläne der allgemeinbildenden höheren Schulen; Änderung der Bekanntmachung der Lehrpläne für den Religionsunterricht an diesen Schulen.
- Coghlan, D., & Brydon-Miller, M. (Eds.) (2014). *The Sage Encyclopedia of Action Research*. Los Angeles, London, New Dehli, Singapore & Washington DC: Sage.
- Dewey, J. (1910). *How we think*. Lexington: DC Heath.
- Freire, P. (2000). *Pedagogy of the Oppressed*. New York: Continuum Publishing.
- Giroux, H. A. (2011). *On Critical Pedagogy*. New York: Continuum.
- Golser, K., Scharf, C., & Jekel, T. (2019). Schüler*innen als Innovator*innen: Das Projekt Innovativitäts_Schulen (Inno_Schools). *OpenSpaces* 01/2019, 60-70.
- Gordon, E., Elwood, S., & Mitchell, K. (2016). Critical spatial learning: participatory mapping, spatial histories, and youth civic engagement. *Children's Geographies* 14(5), 558-572. DOI: 10.1080/14733285.2015.1136736.
- Gryl, I., & Jekel, T. (2012). Re-centering GI in secondary education. Towards a spatial citizenship approach. *Cartographica* 47(1): 18–28. DOI: 10.3138/cart0.47.1.18.
- Hess, J. (2019). Moving beyond resilience education: musical counterstorytelling. *Music Education Research* 21(5), 488-502. DOI: 10.1080/14613808.2019.1647153.
- Hintermann, C., Bergmeister, F. M., & Kessel, V. A. (2020). Critical Geographic Media Literacy in Geography Education: Findings from the MiDENTITY Project in Austria. *Journal of Geography* 119(4): 115-126. DOI: 10.1080/00221341.2020.1761430.
- Huber, S. G., Günther, P.S., Schneider, N., Helm, C., Schwander, M., Schneider, J. A., & Pruitt, J. (2020). COVID-19 und aktuelle Herausforderungen in Schule und Bildung: Erste Befunde des Schul-Barometers in Deutschland, Österreich und der Schweiz. Münster/New York: Waxmann.
- Jekel, T., Oberrauch, A. & Breitfuss-Horner, C. (2020). „Ich habe unbekannte Seiten und Talente meiner Schüler/innen entdeckt“: Eine Delphi-Studie zum Ist-Stand und Entwicklungsstrategien zur fachspezifischen Fernlehre an österreichischen Sekundarschulen. *GW-Unterricht* 158, 57-67. DOI: 10.1553/gw- unterricht158s57.
- Jekel, T., & Pichler, H. (2017). Vom GW-Unterrichten zum Unterrichten mit geographischen und ökonomischen Konzepten: Zu den neuen Basiskonzepten im österreichischen GW-Lehrplan AHS Sek II, *GW-Unterricht* 147, 5- 15. DOI: 10.1553/gw-unterricht147s5.
- Jörissen, B., & Marotzki, W. (2009). *Medienbildung - eine Einführung: Theorie - Methoden - Analysen*. Bad Heilbrunn: Klinkhardt.
- Kanwischer, D., & Schlottmann, A. (2017). Virale Raumkonstruktionen: Soziale Medien und Mündigkeit im Kontext gesellschaftswissenschaftlicher Medienbildung. *ZDG* 8(2), 60–78.
- Keck, M., & Sakdapolrak, P. (2013). What is social resilience?: Lessons learned and ways forward. *Erdkunde* 67(1), 5-19. DOI: 10.3112/erdkunde.2013.01.02.
- Kellner, D., & Share, J. (2005). Toward critical media literacy: Core concepts, debates, organizations, and policy. *Discourse: Studies in the Cultural Politics of Education* 26(3), 369-386. DOI: 10.1080/01596300500200169.

- Kellner, D., & Share, J. (2007). Critical media literacy is not an option. *Learn Inquiry* 1(1), 59-69. DOI: 10.1007/s11519-007-0004-2.
- Lambert, D. (2013). Geographical concepts. In M. Rolfes and A. Uhlenwinkel (Eds.) *Metzler Handbuch 2.0 Geographieunterricht: Ein Leitfaden für Praxis und Ausbildung*. Braunschweig: Westermann.
- Lambert, D., Solem, M., & Tani, S. (2015). Achieving Human Potential Through Geography Education: A Capabilities Approach to Curriculum Making in Schools. *Annals of the Association of American Geographers* 105(4), 723–735. DOI: 10.1080/00045608.2015.1022128.
- Luhmann, N. (2017). *Die Realität der Massenmedien* (5th edition). Wiesbaden: Springer.
- Medienpädagogischer Forschungsverbund Südwest. (2020). *JIM-Studie 2019: Jugend, Information, Medien: Basisuntersuchung zum Medienumgang 12- bis 19-Jähriger*. Retrieved from https://www.mpfs.de/fileadmin/files/Studien/JIM/2019/JIM_2019.pdf.
- Nussbaum, M. (2013). *Creating capabilities: The human development approach*. Cambridge, MA: Routledge. OECD. 2020. *Economic Outlook, Interim Report September 2020*. Paris: OECD Publishing. DOI: 10.1787/34ffc900-en.
- Nussbaum, M., & Sen, A. (1993). *The quality of life*. Oxford, UK: Routledge.
- Pavlovskaya, M. (2018). Critical GIS as a tool for social transformation. *The Canadian Geographer* 62(1), 40-54. DOI: 10.1111/cag.12438.
- Pollard, T. J. (2014). Education, the Politics of Resilience, and the War on Youth: A Conversation with Brad Evans. *Review of Education, Pedagogy, and Cultural Studies* 36(3), 193-213. DOI: 10.1080/10714413.2014.917902.
- Runguis, C., Schneider, E., & Weller, C. (2018). Resilienz - Macht - Hoffnung: Der Resilienz begriff als diskursive Verarbeitung einer verunsichernden Moderne. In M. Karidi, M. Schneider, & R. Gutwald (Eds.), *Resilienz: Interdisziplinäre Perspektiven zu Wandel und Transformation*. Wiesbaden: Springer.
- Sander, W. (2010). Wissen im kompetenzorientierten Unterricht – Konzepte, Basiskonzepte, Kontroversen in den gesellschaftswissenschaftlichen Fächern. *ZDG* 1(1), 42–66.
- Sen, A. (1999). *Development as freedom*. New Delhi: Routledge.
- Shavinina, L. (2013). The Routledge international Handbook of Innovation Education. London & New York: Routledge.
- UN Department of Economic and Social Affairs. (2020). *Everyone Included: Social Impact of COVID-19*. Retrieved from <https://www.un.org/development/desa/dspd/everyone-included-covid-19.html>
- Young, M. (2008). From constructivism to realism in the sociology of the curriculum. *Review of research in education* 32, 1-28.

Algorithmic Cultures: A Missing Link of Spatial Citizenship Education

Leon Fuchs, Detlef Kanwischer and Christian Dorsch
Goethe University Frankfurt/Main, Germany

Abstract

This article addresses the current challenges for geographical educational science brought about by algorithmic cultures. It argues from different theoretical perspectives. First, we discuss sociological, cultural and geographical perspectives on algorithmic cultures and link them to selected approaches of media education in general and geographical media education in particular. We conclude from the discussion that Spatial Citizenship Education is especially suitable to address the challenges. This leads to the question of what aspects of Spatial Citizenship Education need to be supplemented to address algorithmic cultures. We therefore examined the curriculum of Spatial Citizenship Education. The analysis demonstrated that the approach is a sound basis for coping with the developments seen in the context of algorithmic cultures. Nevertheless, algorithmic cultures are accompanied by some changes in social and geographical structures that have not yet been captured by the approach. For example, there is no consideration of geomedias as algorithmic, semi-autonomous systems. Further implications also emerge. In this context, the investigation into the practicability and relevance of algorithmic cultures for the practical learning process is of particular interest.

Keywords:

algorithms, spatial citizenship education, geography, digital sovereignty

1 Introduction: Black boxes, sovereignty and education

Algorithms can be defined as sets of rules that control the behaviour of machines or people. The simplest algorithms, such as rules of behaviour, commandments and laws, have shaped human history from the beginning. Stalder (2018) argues that in digital conditions, algorithmicity has become the distinctive cultural form of expression: 'Faced with the enormous amount of data generated by people and machines, we would be blind were it not for algorithms' (Stalder, 2018: 6). We understand algorithms as decision-making systems based on machine learning neural networks. These kinds of algorithmic assemblages are characterized by recursive operations that allow the systems to develop themselves iteratively (Patterson & Gibson, 2017). Although the individual algorithms of the systems still follow specific rules of behaviour, by influencing each other a distinct constellation of individual algorithms can morph into a (semi-)autonomous system regarding situated decision-making.

As a result, these algorithmic assemblages shape infrastructures, practices and daily life around the world. For example, the specific algorithms of various social networks determine the spatial information we receive as well as when and where we receive it. Therefore, algorithms configure the informational basis of our spatial actions. The problem is that in most cases algorithms are black boxes. An algorithm's manner of functioning is known only to the organization that uses it. Sometimes, it is not even known to them. Consequently, our actions are shaped by rules we do not know. Nor do we know what happens to the digital data we produce. As '[a]lgorithms are part of a broader array of performativities that includes, for example, rituals, narratives, and symbolic experiences' (Rauer, 2016: 142), we use the term 'algorithmic cultures'.

Seyfert and Roberge (2016: 6) stated that

instead of treating algorithms as mere utilitarian devices, the study of algorithmic cultures [...] identifies the meaningfully performative effects that accompany algorithmic access to the world: What is it that they do, culturally speaking? How do they make sense of their surroundings and the different categories people use to interpret them?

From the perspective of geographical media education, the examination and discussion of algorithmic cultures represent a new central topic, as algorithms not only influence students' everyday lives but also shape political and geographical discussions. Every individual requires certain abilities to ensure their digital sovereignty. Gryl et al. (2020) therefore view it as a responsibility of formal education to introduce students to algorithmic cultures at an early stage. Dorsch and Kanwischer (2020) underline the importance of harnessing the potential of digital cultures for educational processes. This should enable pupils, university students and teachers to reflect on algorithms as entities that shape their daily lives. In this context, personal confrontation with algorithms is of particular relevance for the anchoring of algorithmic cultures in educational processes. On the educational level, this is not completely new: we can draw on a variety of approaches that have been developed and introduced in media education and geographical education in recent years. One of the most important approaches is Spatial Citizenship Education (Gryl & Jekel, 2012; Schulze et al., 2015). The spatial citizen is able to initiate social discourses with the help of digital geomedial. In this way, citizens should be empowered to take ownership of public spaces and to participate in spatial planning processes. The unreflective and merely technical-methodological use of digital geomedial that is frequently observed in geography education has led Gryl, Jekel, Schulze et al. to conceptualize the Spatial Citizenship approach, which is based on a constructivist view of geomedial and learning. In recent years, the approach has been widely adopted in geography education on both theoretical and practical levels. This was accompanied by the continuous development of the approach against the background of technological developments, social changes in everyday life, theoretical aspects, and target-group-specific criteria. However, so far there has been no consideration of geomedial as algorithmic, semi-autonomous systems, as described, for example, in the GIS&T Body of Knowledge (gistbok.ucgis.org). In other words, a concrete confrontation and examination of algorithmic cultures is a missing link.

This marks the starting point of our contribution, which addresses in particular the following questions. What challenges do algorithmic cultures pose for geography education processes?

Building on that question: what content-related aspects of Spatial Citizenship Education need to be supplemented in order to address algorithmic cultures? To answer these questions, we will first outline central developments for the appearance of algorithmic cultures and analyse them from a geographical perspective. Based on the results, various media education concepts will be presented. These will provide starting points for integrating algorithmic cultures in educational processes. The approach of Spatial Citizenship Education will also be related to the results. Finally, we will draw a brief conclusion.

2 Sociological, cultural and geographical perspectives on algorithms

While computer science and informatics view algorithms primarily in utilitarian terms, social and cultural studies focus on the consequences and meanings that algorithms have for the relationships between technology, humans and society. Seyfert and Roberge (2016: 4) state: 'Indeed, a cultural sociology of the algorithm is possible only insofar as algorithms are considered as both meaningful and performative, that is to say, performative for the very reason that they are meaningful, and vice versa.' Thus, algorithms do not have a causal effect on culture but determine – to use Foucault's term – its *dispositifs*. In this sense, algorithms not only aggregate, select and produce digital data, but also generate cultural identities. They do this in a variety of ways. As digital gatekeepers, algorithms curate cultural artefacts (e.g. social media posts), and thereby assume the roles of human curators, like art patrons or newspaper critics. Through the attribution of popularity and the creation of trending lists, algorithms construct trends within certain (sub-)publics, which are not usually transparently delimited. Recommendations of trends within digital services, with the help of recommendation systems, can contribute to the creation of filter bubbles and echo chambers (Gillespie, 2016), i.e. the sorting of personal newsfeeds, e.g. on social media platforms, according to the user's preferences assumed by algorithms.

The co-constitutive character of algorithmic systems and the dynamic flow of agency complicate the categorization of roles that algorithms play in socio-cultural processes. As a guide to the different roles, Figure 1 outlines the continuum between social and technological determinism from a geographical perspective.

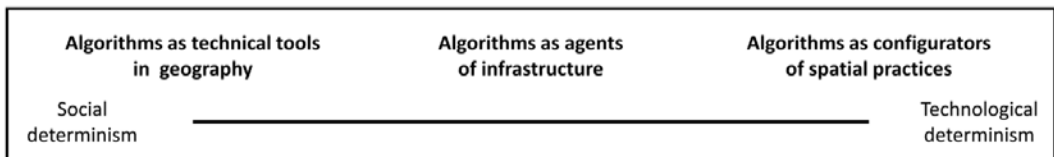


Figure 1: The role of algorithms in socio-technical systems from a geographical perspective (own figure).

The three areas are not to be understood as discrete or strictly delineated classifications but as signposts for orientation within the continuum. The presumed impact of algorithms on human action and social practices increases from left to right. The exact location of the algorithm in the schema depends on the particular situation and the actor who is confronted with it. For

example, a student who has the ability to understand and reflect on the impact of algorithms on his or her behaviour might handle an algorithm-induced situation in a more competent way than a novice.

Algorithms as technical tools in geography

The evaluation of satellite data is an example of how algorithms and machine-learning systems are used as geographic tools (Ash et al., 2019, Brandt et al., 2020). With the help of high-resolution images, image recognition systems can be trained to determine different landscape forms and surface conditions. Thus, they replace manual classifications by geographers and become a decisive component of the gaining of geographical knowledge. When algorithms are being used as tools, the use of automated image recognition software also changes geographical research practice. This leads to algorithms becoming agents of infrastructures that support action.

Algorithms as agents of infrastructure

Kitchen and Dodge (2011: 16) developed the term ‘code/space’ to describe algorithms as part of agents of infrastructure: ‘Code/space occurs when software and the spatiality of everyday life become mutually constituted, that is, produced through one another.’ The fact that code is written explicitly for the production of space and that algorithmic systems are entering spatial planning processes as carriers of action becomes particularly clear in the example of smart cities. Against the background of the smart city, cities and urban planning concepts are being developed in which algorithms are closely interwoven with urban infrastructure. Algorithms are thus increasingly finding their way into the management of spatial usage data within the city. Analogous to code/space, space and algorithms thus constitute each other.

Algorithms as configurators of spatial practices

Bots are another example of the dominance of algorithmic cultures in the urban environment. For example, in the context of protest cultures, bots are programmed to collect digital warnings from citizens about ticket inspections on public transport and to disseminate them via Twitter. With the help of these alerts, other passengers on public transport can locate ticket controls roughly and avoid them (Krempl, 2020). This type of bot exemplifies how algorithms can influence and transform communication and mobility practices.

Social transition processes in the geographical context of algorithmic cultures also place new demands on the design and orientation of geography education and learning processes, which are explained below.

3 Media education, geography and algorithmic cultures

Concerning educational processes, the influences of algorithms unfold in two ways. On the one hand, algorithms have an impact on educational *processes*. They can serve as digital tools for the innovation of teaching situations (e.g. learning analytics software) for teachers and learners. In addition, they confront students in their role as decision-makers (e.g. in social networks) with indeterminacy and therefore offer occasions for creative debates, which in turn

can initiate learning processes. On the other hand, algorithms represent a content-related *subject area* that has to be made relevant for educational processes in subject-specific contexts.

In the German-language debate on how educational processes can be beneficial in the digital society, the approach of structural media education (*Strukturelle Medienbildung*) by Jörissen and Marotzki (2009) has been widely adopted, and further developed over the years. The approach assumes that media determine the structures of worldviews on a fundamental level. This means that we do not react *to* media and algorithms but behave as part of them. In this sense, media education is defined as the structural changes in patterns of reference to oneself, and to the world, brought in by the media. Consequently, this change in the defining form of media (as is currently happening with the shift from the ‘Gutenberg Galaxy’ to the ‘Internet Galaxy’) also necessitates the development of new conceptual forms of media education, including ones which focus on dealing with indeterminacy in educational and subjectification processes. Therefore, media education cannot be reduced to a ‘know-what’ and ‘know-how’ basis. The concept (with reference to Kant) draws special attention to critical analysis of, and autonomous reflection on, knowledge-, action-, boundary- and biography-related aspects of human life (Jörissen & Marotzki, 2009: 30–32). When media education is transferred to algorithmic cultures in geography education processes, the following reflexive orientation dimensions result:

1. Reflection on the terms and limits of knowledge (e.g., on the question of how algorithms make multiple and different spatial interpretations possible).
2. Reflection on the moral consequences of one’s actions that result from concrete social contexts (e.g., when the focus is on spatial options for action carried out through the use of algorithms).
3. Reflection on boundaries as the fundamental structure of education when algorithms reconfigure the relationship between subject and space.
4. Reflection on the process of creating a biography when the question of one’s socio-spatial identity and its biographical conditions become virulent in the context of algorithms.

These four dimensions of orientation and reflection provide a means for individuals to grasp and assess the power of digital geomediality and the algorithms involved as channels that structure reality in, and deliver it to, the world. However, at the same time, these dimensions can also serve as an analysis matrix for investigating individual uses and the effectiveness of algorithms regarding educational purposes.

Allert and Richter (2017: 28) also place confronting indeterminacy at the centre of media education, but at the same time understand educational processes as being interwoven in inherently indeterminate social practices that are constantly in the process of being constituted. This relational understanding of education in the context of social practice goes beyond Jörissen and Marotzki’s (2009) third dimension (reflection on boundaries), which results in the idea of the autonomous subject being relativized. Therefore, learners are, rather, semi-autonomous subjects in the educational process. This gives additional relevance to the abilities of creativity and resistance. A concrete example in the context of algorithms and social networks is the protection of privacy from the state and commercial interests.

Geographical media education has taken up these approaches in recent years. The effects of algorithmic cultures are approached in different ways. Kanwischer and Schlottmann (2017) and Reithmeier and Kanwischer (2020) show how digital spatial constructions in social networks can find their way into geographic education processes against the background of structural media education. Dorsch and Kanwischer (2020) and Gryl et al. (2020), on the other hand, approach algorithmic cultures via the various dimensions of maturity-oriented education and its relevance for educational processes in the context of digital conditions (Stalder, 2018). However, individual phenomena of algorithmic cultures are mostly dealt with by way of example. A systematic approach in terms of content, starting from algorithmic cultures, which generates subject-specific, subject-didactic and pedagogical discussions, is still lacking. For a concretization and systematization from a geographical perspective, the Spatial Citizenship approach is a good choice.

4 Spatial Citizenship and algorithmic cultures

The Spatial Citizenship approach (Gryl & Jekel, 2012) focuses on the role of the ‘spatial citizen’ and his or her appropriation of the spatial area for social life. A spatial citizen should know how to navigate everyday life in relation to the physical world, know the meanings associated with the physical objects and the environment, and, eventually, understand the balance of power involved in the production of meaning. The approach includes geotechnologies and related tools for assigning meaning, and newer forms of collaboration and negotiation using Web 2.0 applications. The Spatial Citizenship competence model (Schulze et al., 2015) presents an individual’s overall competence as an overlapping arrangement of discrete dimensions of subject-specific as well as generic competences.

The model consists of six major dimensions: ‘Technology and Methodology’, ‘Reflection’ and ‘Communication’, which represent instrumental and interpersonal competences, and form the core competences, or nucleus, of the Spatial Citizenship competence model. These three dimensions include the generic ability to apply technical knowledge and skills using web-2.0-based geomedia reflectively. Additionally, the ‘spatial citizen’ is able to communicate alternative spatial visions and constructions autonomously and collaboratively. The dimensions ‘Spatial Domain’ and ‘Citizenship Education Domain’ provide theoretical aspects in content knowledge areas. They are thus related to subject-specific competences and underpin the core competences. Finally, the dimension ‘Implementation Strategies’ functions as a framing category necessary to link teachers’ pedagogical content knowledge and motivational orientations of teaching and learning to the field of Spatial Citizenship (Schulze et al., 2014a).

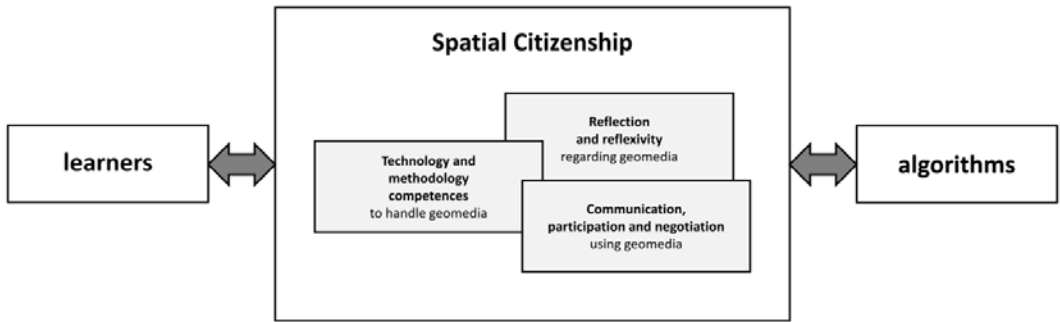


Figure 2: The Spatial Citizenship competence model as intervention between learners and algorithms (own figure based on Jekel et al. 2015: 7).

The competence model serves as the starting point for curriculum development for Spatial Citizenship in teacher education and training (Schulze et al., 2014a). The structure of the learning fields in this curriculum corresponds to the structure of the Spatial Citizenship competence model. Schulze et al. (2014b) formulated a description of particular learning outcomes for every single competence. In what follows, these descriptions are confronted with the theoretical conclusions presented above regarding algorithmic cultures. The Spatial Citizenship approach in our concept intervenes in the relationship between learners and algorithms (see Figure 2). The aim is to empower students to participate in spatial negotiation processes by reflecting on, and (where necessary) rejecting, algorithmic influence, and to use algorithms for their own purposes. At the same time, the Spatial Citizenship dimensions themselves are affected by algorithmic systems.

Technology and methodology

In the field of geomeia technology and methodology, geomeia must be seen as more than just instruments. By focusing on the use of geomeia, the interaction with algorithmic systems relativizes the relationship between individual and medium. A stronger orientation towards relational interactions *with* geomeia rather than the one-sided use *of* geomeia would be helpful. This does not exclude the use of geomeia to fulfil a certain purpose, but suggests a relation between media and individuals. For example, users react to the recommendations made by algorithmic systems when using navigation tools for sightseeing, either by visiting the suggested places or by ignoring the suggestions. Furthermore, the integration of machine learning systems in digital geomeia requires additional knowledge of how information is generated from geodata and about algorithmic mechanisms that serve to retrieve geoinformation.

Reflection

In the field of reflection, geomeia are predominantly seen as passive platforms and sites of negotiation (Schulze et al., 2014b: 370). Although a central focus is on the reflection of digital spatial constructions as products of actions, the view is limited to human or institutionalized actors (Schulze et al., 2014b: 370). In this context, algorithms are not considered as (partially) autonomous, space-constructing actors, as in the co-construction of places by users and algorithms on Instagram (Reithmeier & Dorsch, 2021). Nevertheless, reflection encourages

consideration of algorithms as configurators of spatially related practice by encompassing awareness of the influence of geomediality on everyday practices (Schulze et al., 2014b: 370).

Communication

This dimension emphasizes the relevance of specific digital competences and digital literacy for communication in digital environments. Here, reference is made to the social, action-oriented communication concept of language use as defined in the Common European Framework of Reference for Languages (Schulze et al., 2014b: 371). As algorithmic cultures are not specifically mentioned in this context, it depends on individual interpretation and the design of the curriculum whether algorithmic logic is referred to explicitly or not in an educational context. Furthermore, only other citizens and public authorities are mentioned as communication partners (Schulze et al., 2014b: 372). Algorithmic communication systems, such as social bots, are not mentioned as communication partners. However, learning outcomes that include reflections on socio-cultural aspects such as the structuring of one's own and other cultures can be found in the subordinate area of socio-linguistic competences (Schulze et al., 2014b: 373). These competences offer a starting point for discussing algorithmically-constructed realities and their reproduction in digital filter bubbles and echo chambers. In addition, we would like to suggest that the curriculum's understanding of communication could be expanded to include current and future technological aspects (e.g. bots).

Spatial domain

Within the spatial domain, the deconstruction of digital spatial constructions as products of power relations is envisaged (Schulze et al., 2014b: 375). In the context of algorithmic cultures, this offers opportunities to reflect on algorithmically-driven business models in social media and on the power of the platforms' operators. In addition, the spatial domain highlights the importance of digital constructions of space for the formation of social rules. The domain includes not only absolute but also relational concepts of space. Hence, the actions of human individuals are seen as spatially constitutive in the context of relational concepts of space. This can serve as a starting point for the discussion of algorithms as configurators of social practice. However, no attention is paid to algorithms as agents of infrastructure or to their constitutive influence on space and spatiality.

Citizenship education domain

The domain of citizenship education includes basic skills for negotiating the learners' roles within social structures (Schulze et al., 2014b: 377). In this context, as in the previous dimensions, geomediality are only mentioned as instruments for participation. In addition, a stronger focus in this domain should be placed on complex relationships, and algorithms should be seen as a constituting element of social relations.

Implementation Strategies

The dimension of didactic implementation strategies already contains many connectable points for implementation in the classroom. In many respects, it also takes the requirements of education of algorithmic cultures into account. These include, for example, encouraging teachers to find educational opportunities to encourage students to engage independently with digital technologies (Schulze et al., 2014b: 379), and reflexive engagement with digital technologies in the context of educational processes inside and outside school (ibid.). Furthermore, the

dimension includes reflection on one's competences concerning the design of educational processes. In designing a curriculum, one should focus explicitly on the influence of algorithmic cultures on the design of lessons, especially when using digital tools.

The analysis shows that Spatial Citizenship Education lends itself well to drawing on the content of algorithm cultures. Nevertheless, some adjustments have to be made to take into account the transformative power of algorithmic cultures in the educational process.

5 Conclusion: There is still a long way to go

The development of curricular documents is a permanent construction site, as new social, subject-specific, technical and educational developments must be taken into account continuously. To stimulate the discussion on algorithmic cultures and geography education processes, we have presented an analysis of the curriculum from Spatial Citizenship Education in relation to the discussion on algorithms and education. Our analysis has demonstrated that the Spatial Citizenship approach is a sound basis to do justice to the developments shown in the context of an algorithm culture. Nevertheless, algorithm cultures are accompanied by some changes in social and geographical structures that have not yet been captured by the approach. For example, the approach regards digital geomeia primarily as instruments used by individuals for participation. There is no consideration of geomeia as algorithmic, semi-autonomous systems. This results in desiderata that should be addressed in a revision of the curriculum – for example, the competence to analyse the role of algorithms as configurators of social practices should be a part of the curriculum.¹

The latest position paper of the Hochschulverband für Geographiedidaktik on the educational contribution of the subject of geography in a world shaped by digitalization and mediatization stresses the importance of this process: 'Geography education in a world shaped by mediatization [...] enables students to critically examine their role, the role of others and the significance of algorithms and artificial intelligence for the construction of identity, social realities and knowledge using geomeia' (Hochschulverband für Geographiedidaktik, 2020: 6, author's translation from German). However, against the backdrop of the traditional location of algorithms in mathematics and computer science education in schools, there have so far been few discussions about anchoring them in the context of social science subjects. But this is necessary to enable relational learning processes within algorithmic cultures, so that children and adolescents acquire the ability to develop digital sovereignty at an early stage. In this regard, appropriate media education also holds the potential for transforming the role of algorithms. Media education can help to initiate discussions about the effects of machine data analysis, to regulate or question algorithmically-supported business models, and to reveal and contain the power structures behind algorithmic systems (Kurz & Rieger, 2017: 95). This can enable users to participate actively in shaping digital cultures and in negotiating the roles of algorithmic systems in the socio-material world.

¹ For a complete list of competences, see Fuchs 2021 (https://www.researchgate.net/publication/352680439_Algorithmuskulturen_in_der_geographischen_Bildung (in German)).

The various roles of algorithms as technical tools, agents and configurators of social practices demonstrate that to describe algorithms in dichotomous terms of social and technological determinism is inadequate. Even if the role definitions have more of an analytical character (and algorithms can be assigned different roles in practice – depending on the research question), they offer guidance for educational processes to clarify which type of algorithmic transition process takes place. These different aspects need to be further sharpened and differentiated in more in-depth considerations to make algorithmic cultures tangible for geography education on the content level. Algorithmic systems that move between two or three role tendencies and are therefore more difficult to grasp represent an exciting field for further discussions. Moreover, the normatively-developed requirements of education regarding algorithmic cultures should be examined for their practicability and relevance in the context of the learning process in the real-life classroom.

This paper is a small step towards a structured approach to the field of algorithmic cultures from geography education perspective. The theoretical lines of argumentation that emerge can be seen as an impetus for further reflection to supply the missing link of Spatial Citizenship Education.

Acknowledgment

The project ‘Digi_Gap’ is part of the ‘Qualitätsoffensive Lehrerbildung’, a joint initiative of the Federal Government and the Länder, which aims to improve the quality of teacher training. The programme is funded by the Federal Ministry of Education and Research. The authors are responsible for the content of this publication.

References

- Allert, H., & Richter, C. (2017). Kultur der Digitalität statt digitaler Bildungsrevolution. *Pädagogische Rundschau*, 71(1), 19-32.
- Ash, J., Kitchin, R., & Leszczynski, A. (2019). Introducing digital geographies. In Ash, J., Kitchin, R. & Leszczynski, A. (Eds.): *Digital Geographies*. Los Angeles: SAGE. 1-10.
- Couture, S., & Toupin, S. (2019). What does the notion of ‘sovereignty’ mean when referring to the digital? *New Media & Society*, 21(10), 2305-2322. doi:10.1177/1461444819865984
- Brandt, M., C. J., Tucker, A., Kariryaa, K., Rasmussen, C., Abel, J., Small, J., Chave, L. V., Rasmussen, H., Pierre, A. A., Diouf, L., Kergoat, O., Mertz, C., Igel, F., Gieseke, J., Schöning, S., Li, K., Melocik, J., Meyer, S., Sinno, E., Romero, E., Glennie, A., Montagu, M., Dendoncker, & Fensholt, R. (2020). An unexpectedly large count of trees in the West African Sahara and Sahel. *Nature*, 587, 78-82. doi:10.1038/s41586-020-2824-5
- Dorsch, C., & Kanwischer, D. (2020). Mündigkeit in einer Kultur der Digitalität: Geographische Bildung und ‚Spatial Citizenship‘. *Zeitschrift für Didaktik der Gesellschaftswissenschaften*, 11(1), 23-40.
- Gillespie, T. (2016). #trendingistrending: When Algorithms become Culture. In Seyfert, R., & Roberge, J. (Eds.). *Algorithmic Cultures. Essays on Meaning, Performance and New Technologies*. London: Routledge, 52-75.

- Gryl, I., & Jekel, T. (2012). Re-centering GI in secondary education: Towards a spatial citizenship approach. *Cartographica*, 47, 18-28.
- Gryl, I., Dorsch, C., Lehner, M., Pokraka, J. & Zimmer, J. (2020). Technologie, Medien, Mündigkeit: Integration autonomieförderlicher Haltungen und Kompetenzen in die fachliche Vermittlung. In Beißwenger, M., Bulizek, B., Gryl, I. & Schacht, F. (Eds.). *Digitale Innovationen und Kompetenzen in der Lehramtsausbildung*. Duisburg: Universitätsverlag Rhein-Ruhr, 121-146.
- Hochschulverband für Geographiedidaktik (2020). *Der Beitrag des Fachs Geographie zur Bildung in einer durch Digitalisierung und Mediatisierung geprägten Welt*. Positionspapier des Hochschulverbands für Geographiedidaktik (HGD) e.V.
- Jekel, T., Gryl, I. & Oberrauch, A. (2015). Education for Spatial Citizenship: Versuch einer Einordnung. *GW-Unterricht*, 137(1), 5-13. Retrieved from: http://www.gw-unterricht.at/images/pdf/gwu_137_05_13_jekel_gryl_oberrauch.pdf
- Jörissen, B., & Marotzki, W. (2009). *Medienbildung – eine Einführung. Theorie – Methoden – Analysen*. Stuttgart: UTB.
- Kanwischer, D., & Schlottmann, A. (2017). Virale Raumkonstruktionen – Soziale Medien und Mündigkeit im Kontext gesellschaftswissenschaftlicher Medienbildung. *Zeitschrift für Didaktik der Gesellschaftswissenschaften*, 8(2), 60-78.
- Kitchin, R., & Dodge, M. (2011). *Code/Space. Software and Everyday Life*. Cambridge, USA: MIT Press.
- Krempel, S. (2020). Data Cities: Wie Hacktivist*innen Smart-City-Konzepte unterwandern. Retrieved from https://www.heise.de/news/Data-Cities-Wie-Hacktivist*innen-Smart-City-Konzepte-unterwandern-4913295.html?utm_source=pocket-newtab-global-de-DE
- Kurz, C. & Rieger, F. (2017). Autonomie und Handlungsfähigkeit in der digitalen Welt. Crossing the creepy line? In Augstein, J. (Eds.): *Reclaim autonomy. Selbstermächtigung in der digitalen Weltordnung*. Berlin: Suhrkamp, 85-97.
- Patterson, J., & Gibson, A. (2017). *Deep Learning*. Sebastopol: O'Reilly Media.
- Rauer, V. (2016). Drones: The mobilization of algorithms. In Seyfert, R & Roberge, J. (Eds.). *Algorithmic Cultures. Essays on Meaning, Performance and New Technologies*. London: Routledge, 140-157.
- Reithmeier, C. & Dorsch C. (2021). Soziale Medien. In Bork-Hüffer, T., Füller, H., & Straube, T. (Eds.): *Handbuch Digitale Geographien: Welt - Wissen – Werkzeuge*. Stuttgart: UTB, 231-243.
- Reithmeier, C., & Kanwischer, D. (2020). Adolescents and the 'Instagramability' of Places – An Explorative Study on Spatial Practices in Social Media. *GI_Forum, Journal for Geographic Information Science*, 2, 96-106. doi: 10.1553/giscience2020_02_s96
- Schulze, U., Gryl, I., & Kanwischer, D. (2014a). Spatial Citizenship – Creating a Curriculum for Teacher Education. In Vogler, R., Car, A., Strobl, J., & Griesebner, G. (Eds.): *GI_Forum 2014. Geospatial Innovation for Society*. Berlin: Herbert Wichmann Verlag, VDE Verlag GMBH, 230-241. doi:10.1553/giscience2014s230
- Schulze, U., Gryl, I., & Kanwischer, D. (2014b). A Curriculum for Spatial Citizenship Education. In Vogler, R., Car, A., Strobl, J., & Griesebner, G. (Eds.): *GI_Forum 2014. Geospatial Innovation for Society*. Berlin: Herbert Wichmann Verlag, VDE Verlag GMBH. 362-380. doi: 10.1553/giscience2014s362
- Schulze, U., Gryl, I., & Kanwischer, D. (2015). Spatial Citizenship education and digital geomediation: composing competences for teacher education and training. *Journal of Geography in Higher Education*, 39(3), 369-385. doi: 10.1080/03098265.2015.1048506
- Seyfert, R., & Roberge, J. (2016). What are algorithmic cultures? In Seyfert, R & Roberge, J. (Eds.). *Algorithmic Cultures. Essays on Meaning, Performance and New Technologies*. London: Routledge. 1-25.
- Stalder, F. (2018). *The digital condition*. Cambridge, UK: Polity.

Modelling Climate-Sensitive Forest Succession to Assess Impacts of Climate Change and Support Decision Making

Alois Simon^{1,2}

¹University of Natural Resources and Life Sciences Vienna, Austria

²Office of the Tyrolean government, Innsbruck, Austria

Abstract

Mountain forests provide a wide variety of ecosystem services to society. In light of the trend of temperature increase and related climatic extremes in the Greater Alpine Area, mountain forests are likely to undergo dramatic changes in the coming centuries. Therefore, forest managers face the challenge of adapting forests to support resilience to climate change. To facilitate this process, the forest gap model ForClim, a process-based forest succession model, was applied to generate site-specific information on future forest stand development and species composition. The tree species composition without management activities was predicted up to 2100 assuming a stable climate, and for both moderate and severe climate-change scenarios. Furthermore, three different forest stand development scenarios were implemented. The forest stand investigated in our research shows significant climate-sensitivity. Results demonstrate that deciduous mixed forest stands are necessary to increase resilience and manage forests for climate change. Using active silvicultural measures, such as assisted migration through planting thermophilus species, negative effects of climate change could be reduced. The modelling approach presented here is appropriate for assessing the impacts of climate change and supporting decision making by local forest managers.

Keywords:

dynamic vegetation model, mountain forest, long-term development, tree species composition, Austria

1 Introduction

Predicting forest growth and stock volume is an age-old task in forestry science, going back to the first yield tables in the 19th century, e.g. Hartig (1847); Lorey (1878); Weisse (1880); Schwappach (1890). With these early attempts to quantify forest productivity, the foundations for sustainable management of natural resources were laid. Static yield tables for single-species, evenly-aged forest stands (Assmann & Franz, 1963) are still widely used. However, the high proportion of mixed-species, unevenly-aged, structurally diverse forest stands in mountain areas have always hampered their implementation in mountain forests. Besides static yield

tables, dynamic models for predicting forest growth were also developed and gained increasing popularity (Röhle, 2004). The general shift in forestry towards mixed-species forests (BFW, 2019), and the fact of heterogeneous and non-static environmental conditions, enhanced the demand for dynamic growth models for forest management.

In addition to sustainable timber production (BMNT, 2018), mountain forests provide a wide variety of ecosystem services, e.g. prevention of natural hazards (Berger et al., 2013), recreation, welfare (Forest Act, 1975) and carbon storage (Prietzl & Christophel, 2014). In view of the trend of temperature increase and related climatic extremes in the Greater Alpine Area (Auer et al., 2014), and the continuously increasing global carbon emissions (Le Quéré et al., 2018), mountain forests are likely to undergo dramatic changes in the coming centuries (Allen et al., 2010). Therefore, forest managers face the challenge of adapting forests and supporting resilience to climate change (Rasche et al., 2011). To facilitate this process, dynamic vegetation models can generate site-specific information on future forest stand development and species composition (Seidl et al., 2011). Alongside process-based models, correlative species distribution models (Guisan et al., 2017) are widely used; an overview of the applications in forest management is given by Pecchi et al. (2019).

The development of decision support systems in forest management is reviewed by Vacik and Lexer (2014), who identified the main challenge as balancing ease-of-use and model complexity due to users' growing information demands. As well as applications in practical management, model-based decision support also has the potential to be used in forest policy-making (Linkevičius et al., 2019).

As year-round settlements in mountain areas are primarily located at lower elevations, public demands on lower-altitude forests are especially high. Predictions of climate change impacts (Remund & Augustin, 2015) and forest disturbances in recent decades (e.g. Bigler et al. (2006); Jump et al. (2006)) suggest that forests at lower elevations are especially susceptible. Hence, investigating the impacts of climate scenarios at drought-prone low-elevation sites is crucial for forest management.

By applying a process-based, climate-sensitive forest succession model, this study investigates future tree species composition and growth at sites that may be critically affected by drought stress under climate change. To guarantee the transferability of the approach and to increase its usability, open-source products were used in designing the workflow. Demonstrating the expected change in tree species composition will support decision making in the context of adaptations for climate change.

2 Material and Methods

2.1 Study site and data recording

The forest investigated is located in the valley of the river Inn in the province of Tyrol, Austria (Figure 1). The study site is at an elevation of 670 m asl and has a steep (30°), south-west facing (200°) slope. The average annual rainfall is c. 1160 mm, and the annual mean temperature c. 8.1°C (ZAMG, 2015). The geological bedrock material consists of calcareous, coarse, fluvial

sediments which develop to a mosaic of Renzic Leptosols and Calcareous Cambisols (IUSS Working Group WRB, 2014). The potential natural vegetation type of the study site is classified as forest dominated by European beech (*Fagus sylvatica* (L.)), ranging from *Carici albae-Fagetum* on the slightly drier ridge and the upper slope, to *Mercuriali-Fagetum caricetosum albae* from mid-slope down to the bottom of the slope (Forest Site Classification Tyrol, 2018). The forest stand is dominated by Scots pine (*Pinus sylvestris* (L.)) and Norway spruce (*Picea abies* ((L.) Karts)). In the understorey, *P. abies* dominates, with occasional common oak (*Quercus robur* (L.)) and *F. sylvatica*. The only occurring black pine (*Pinus nigra* (J.F.Arnold)) is combined with *P. sylvestris* for further analysis.

A plot of 10,000 m² (180 x 55 m) was marked out at the study site; each tree above 7 cm in diameter at breast height (DBH) was recorded, and along with its DBH (cm), its height (m) and x-y location were also noted. To describe the soil properties, two soil profiles were excavated, described according to the Austrian soil classification (Nestroy et al., 2011) a plant-available water storage capacity of 85 dm³*m⁻² was calculated according to Arbeitskreis Standortkartierung (2003). The 60 kg*ha⁻¹ nitrogen stock available for plant growth was estimated to be 2% of the total nitrogen in the soil (Blume et al., 2009), based on the analysis of soil-profile data with comparable bedrock material (Simon et al., 2021).

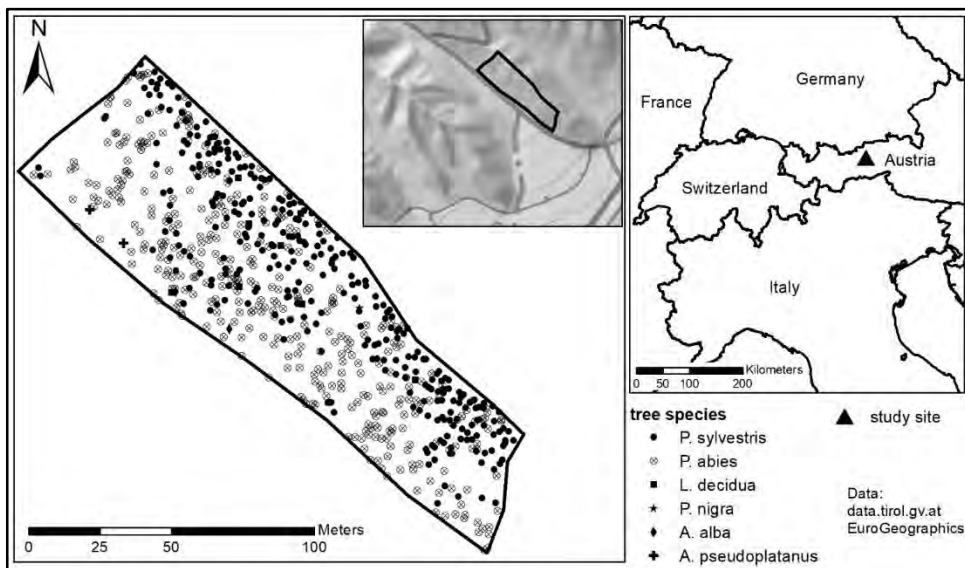


Figure 1: Location of the study site and current tree-species distribution of the forest stand.

2.2 Dynamic forest model

To model the future tree species composition, the tried and tested forest gap model ForClim (Bugmann, 1996), developed by the Forest Ecology Group of ETH Zurich, was used. Forest gap models in general are widely used by forest ecologists to address a large number of applied research questions. In these models, forests are represented as a composite of many small patches of the same size, usually defined by the crown size of an adult tree. Each patch can be

of a different age and successional stage, and is horizontally homogeneous; exact tree position within the patch is not taken into account. All patches have the same resource level, and patches do not interact with each other. Tree establishment, growth and mortality are modelled for each patch individually (Bugmann, 2001).

ForClim Vers. 4.0.1 (Huber, 2019) consists of four submodels, namely WEATHER, PLANT, WATER and MANAGEMENT. The present study considers only the first three of these. The PLANT submodel was initialized using data for the current forest stands (Figure 1). By default, 30 tree species are parametrized for central Europe (Huber, 2019). Of these, the tree species that are currently found at the site and a set of naturally occurring tree species (Forest Site Classification Tyrol, 2018) were selected for modelling. For the current forest stand, a patch size of 400 m² was selected with which to initialize the model. Due to the irregular shape of the forest stand (Figure 1), the total area was divided into just 24 patches (9,600 m²). In order to upscale to the recommended 200 modelling patches (Forest Ecology Group, 2019), representing an area of 8 ha, the patches were repeated, each eight times, to which were added eight randomly selected patches. To account for the regeneration of trees between 1 cm DBH and the recording threshold of 7 cm DBH, individuals were added to the patches based on field estimations.

The input data for the WEATHER (Table 1) and WATER submodels are derived from the recorded site data and climatic data. The general model variant ‘24’ was implemented (Huber et al., 2020) to define the regeneration routine, the allocation of growth to height and diameter, and the background mortality (Forest Ecology Group, 2019). This variant reduces the strong differences between shade-tolerant and shade-intolerant species through recruitment limitation of shade-tolerant species (E6*) and growth allocation (A2). These assumptions are in line with empirical findings on regeneration patterns of the shade-tolerant species *Fagus sylvatica* and *Abies alba* (Nagel et al., 2010). The background mortality (M1) of this model variant is described as a u-shaped relationship between DBH and mortality probability. This relationship represents high mortality in the early life-stages of saplings, and increased mortality of mature trees (Monserud & Sterba, 1999).

2.3 Simulation scenarios and climate data

Tree species composition was predicted in annual timesteps from 2020 to 2100. Three different climate scenarios were applied for the simulation: a stable climate with an extrapolation of the current climate (A) (data for 1 January 1981 to 31 December 2010); a moderate climate-change scenario (B), and a severe climate-change scenario (C), represented by Representative Concentration Pathways (RCPs) of 4.5 and 8.5 (IPCC, 2014) for B and C respectively. Since the different RCPs do not start to show greater differentiations before 2050 (IPCC, 2014), two timesteps were implemented for the climate-change scenarios (Figure 2). These time steps were 1 January 2020 to 31 December 2070, and 1 January 2071 to 31 December 2100. All necessary climate data (Table 1) were selected from the ÖKS15 datasets (ÖKS15, 2016) with a 1x1 km spatial resolution, provided by the Climate Change Centre Austria (data.CCCA). The reference period of these datasets is 1961–2005, with a temporal resolution of 24h. The data are generated by the EURO-CORDEX model ‘cncm-cerfacs-cncm-cm5’ using the ‘r1i1p1’ ensemble; they are corrected for bias (in scaled distribution mapping) using observations from Spartacus or GPARD (ZAMG, 2015). The climate data

used in scenario A give a mean annual temperature (MAT) of 9.2°C and a mean annual precipitation (MAP) of 1,127 dm³*m⁻² for the period 1981–2010. These serve as a baseline in the model. The MAP is thus similar to the 1,079 dm³*m⁻² given by the 3PClim dataset (ZAMG, 2015); for the MAT, the same data source gives slightly cooler conditions, of 8.6°C. For scenario A, monthly data is used; for scenarios B and C, only seasonal data are needed (Table 1) by ForClim. For the last decade of the modelling period, Scenario B (for moderate climate change) shows a MAT increase of 1.7°C, and scenario C (for severe climate change) shows a MAT increase of 3.5°C (see Figure 2). The MAT thus increases progressively from the start of the modelling period. For precipitation, the climate scenarios show a slight increase, of around 1–4%, especially during winter.

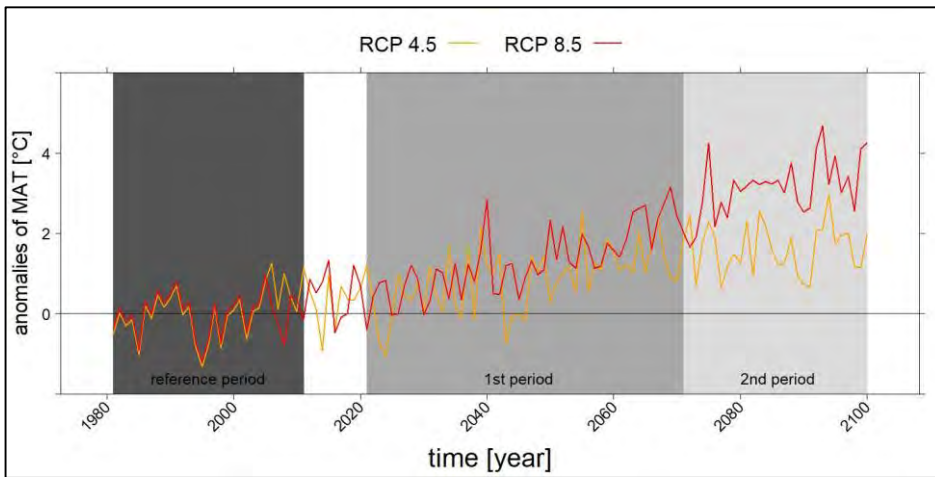


Figure 2: Predicted changes of Mean Annual Temperature (MAT) for the climate-change scenarios. The baseline is the MAT for 1981–2010.

Based on the current stand data, three different forest stand development scenarios were developed for the simulation: a business-as-usual scenario (I), allowing only currently-present species to grow and regenerate; a mixed species scenario (II), allowing for migration of species through natural regeneration; and a mixed species scenario with assisted migration (III) in which the best-performing species of scenario II are planted at the beginning of the modelling period. The trees planted in scenario III are considered to have a DBH of 1 cm and height of 150 cm; they are added to the present forest stand. The species for planting in scenario III are chosen from among those with the best performance in the mixed species scenario (II); how many were planted and the proportions of different species are based on the current forest stand structure and the silvicultural requirements of the species selected. In the present case, 400 *Quercus petraea* and 200 *Tilia cordata* saplings*ha⁻¹ were planted at the beginning of the modelling period. This corresponds to 3 groups of 8 saplings for each patch (400 m²) (2 groups of *Q. petraea*, and one 1 of *T. cordata*), or a total of 75 groups*ha⁻¹, 50 of which were comprised of *Q. petraea*, and 25 of *T. cordata*.

Table 1: Climate data for *ForClim* simulation scenarios, with data sources.

variable	data source
current climate (A) (Jan, Feb, Mar, Apr, May, Jun, Jul, Aug, Sep, Oct, Nov, Dec)	
monthly mean temperature (mT)	https://hdl.handle.net/20.500.11756/1dba52b2
monthly temperature standard deviation (sdT)	https://hdl.handle.net/20.500.11756/1dba52b2
monthly mean precipitation (mP)	https://hdl.handle.net/20.500.11756/9df12611
monthly precipitation standard deviation (sdP)	https://hdl.handle.net/20.500.11756/9df12611
monthly temperature-precipitation cross-correlation (rTP)	calculated from mT and mP
climate change RCP 4.5 (B) (Spring: Mar, Apr, May; Summer: Jun, Jul, Aug; Autumn: Sep, Oct, Nov; Winter: Dec, Jan, Feb)	
seasonal mean temperature (CC_mT)	https://hdl.handle.net/20.500.11756/1dba52b2
seasonal temperature standard deviation (CC_sdT)	https://hdl.handle.net/20.500.11756/1dba52b2
seasonal mean precipitation (CC_mP)	https://hdl.handle.net/20.500.11756/9df12611
seasonal precipitation standard deviation (CC_sdP)	https://hdl.handle.net/20.500.11756/9df12611
seasonal temperature-precipitation cross-correlation (CC_rTP)	calculated from CC_mT and CC_mP
climate change RCP 8.5 (C) (Spring: Mar, Apr, May; Summer: Jun, Jul, Aug; Autumn: Sep, Oct, Nov; Winter: Dec, Jan, Feb)	
seasonal mean temperature (CC_mT)	https://hdl.handle.net/20.500.11756/dd922ed4
seasonal temperature standard deviation (CC_sdT)	https://hdl.handle.net/20.500.11756/dd922ed4
seasonal mean precipitation (CC_mP)	https://hdl.handle.net/20.500.11756/b1899294
seasonal precipitation standard deviation (CC_sdP)	https://hdl.handle.net/20.500.11756/b1899294
seasonal temperature-precipitation cross-correlation (CC_rTP)	calculated from CC_mT and CC_mP

2.4 Data processing and modelling

The data and output processing as well as the model runs were performed using the statistical software R (R Core Team, 2019). The climate data (Table 1) were accessed in netCDF format using the R package *ncdf4* (Pierce, 2017). The transformation of the climate and stand data into XML structure for the *ForClim* model input was carried out using the R package *XML* (Duncan, 2020). To capture stochastic processes (e.g. recruitment, mortality) in the model, each model run was repeated 100 times, changing the seed of the random generator (*seedValue*) in the *ForClim* setup file. The upscaling of the present forest stand was repeated 100 times to test for random effects in the model initialization. The aggregation of the multiple iterations was carried out using R package *matrixStats* (Bengtsson, 2020). For graphical output, the R package *lattice* (Sarkar, 2008) was used. The modelling workflow was documented using a business process model and notation (see the supplements).

3 Results

3.1 Growth patterns of individual species

For the prediction of the tree species composition, the following species from the present forest stand were selected: Silver fir (*Abies alba* (Mill.)), sycamore maple (*Acer pseudoplatanus* (L.)), European larch (*Larix decidua* (Mill.)), Norway spruce (*Picea abies*) and Scots pine (*Pinus sylvestris*) (Figure 1); also selected were: European beech (*Fagus sylvatica*) and common oak (*Quercus robur*), which were occasionally present in the regeneration; sessile oak (*Quercus petraea* ((Matt.) Liebl.)), small-leaved lime (*Tilia cordata* (Mill.)), and large-leaved lime (*Tilia platyphyllos* (Scop.)) as thermophilus trees of lower elevations; and silver birch (*Betula pendula* (Roth)) and whitebeam (*Sorbus aria* (Crantz)) as typical pioneer species. The predicted tree species composition is characterized by the total volume [$\text{m}^3\cdot\text{ha}^{-1}$], which describes the stock of the forest stand. The temporal response pattern of the growth parameters for the mixed species scenario with natural regeneration (scenario II) under different climate conditions is illustrated in Figure 3. Of the tree species investigated that are not currently present in the forest stand, *Q. petraea* and *T. cordata* showed the best growing performance in terms of volume increment (Figure 3). Replacing *Q. robur* by *Q. petraea* in the model showed that the latter performed significantly better than the former. The same was true for the two lime species: *T. cordata* was superior to *T. platyphyllos*. The pioneer species are not shown in Figure 3 as they reach only very low values in all climate scenarios, with a maximum of $0.16 \text{ m}^3\cdot\text{ha}^{-1}$ under the current climate scenario. All tree species currently present in the forest stand (Figure 1) showed a reduction in volume under the severe climate-change scenario (RCP 8.5, Figure 3C) compared to the current climate (Figure 3A) up to the end of the prediction period. Even under the moderate climate-change scenario (RCP 4.5, Figure 3B), a negative trend is observed for *L. decidua* and above all for *P. abies*, which is the only species that already shows a negative trend under current climate conditions. The decline of *P. abies* shows a very low standard deviation over the whole modelling period. *P. sylvestris* turned out to be the most resilient species at the site, increasing its share significantly under all climate scenarios. It is only at the end of the modelling period that it shows a slight decline in volume for all climate scenarios.

3.2 Growth patterns of stand development scenarios

The development of the growing stock under the three different stand development scenarios is illustrated in Figure 4. For the tree species currently present and their natural regeneration (I), a decrease of volume is predicted for climate-change scenarios B and C compared to the growth pattern under current climate conditions. For the last decade (2090–2100), for the moderate and severe climate-change scenarios, the mean decreases are 2.9 ± 31.8 and $21.9 \pm 29.7 \text{ m}^3\cdot\text{ha}^{-1}$ (\pm standard deviation) respectively. The second stand development scenario (Figure 4, II), which allows for the natural regeneration of mixed species, was developed from the results of the individual species' performances (Figure 3). The increasing volume, especially of *Q. petraea* and *T. cordata* and to a certain extent of *F. sylvatica* (Figure 3), counteracts the negative development of the climate-change scenarios. For the RCP 8.5 scenario, a decrease of $3.8 \pm 33.7 \text{ m}^3\cdot\text{ha}^{-1}$ is predicted for the last decade; for the current climate and for the RCP 4.5 scenario, increases of 14.0 ± 30.5 and $12.4 \pm 29.3 \text{ m}^3\cdot\text{ha}^{-1}$ (mean \pm standard deviation) are

predicted for the last decade. The third stand development scenario, with planting at the beginning of the modelling period, leads to an increase in stock for all climate scenarios (Figure 4, III) compared to the baseline. The increases for the last modelling decade (mean \pm standard deviation) are as follows. For the current climate: 61.0 ± 36.0 ; for the moderate climate-change scenario (RCP 4.5): 59.8 ± 31.4 ; for the severe climate-change scenario (RCP 8.5): 37.2 ± 36.7 $\text{m}^3 \cdot \text{ha}^{-1}$.

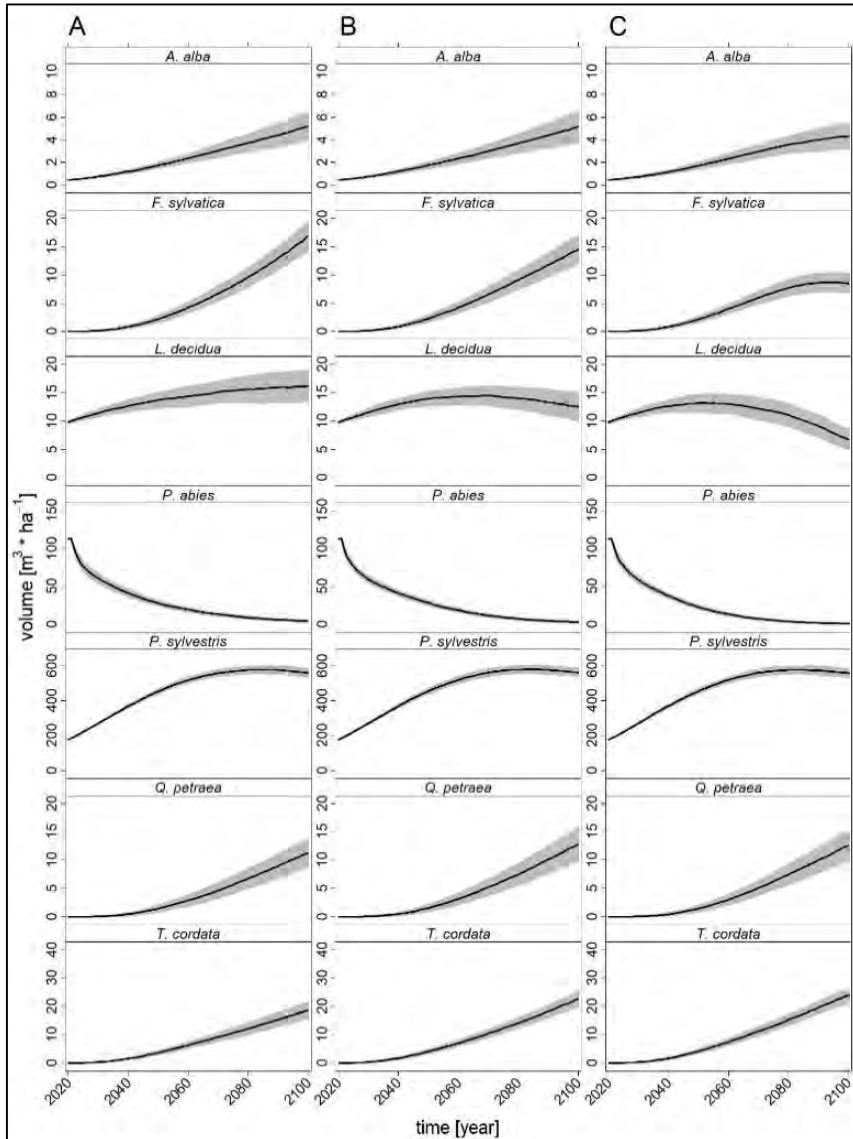


Figure 3: Predicted tree species composition of the mixed-species regeneration scenario (II) for the study site under different climate scenarios. A: current climate, B: moderate climate-change scenario (RCP 4.5), C: severe climate-change scenario (RCP 8.5); black line: mean of 100 model runs; shaded area: standard deviation of 100 model runs.

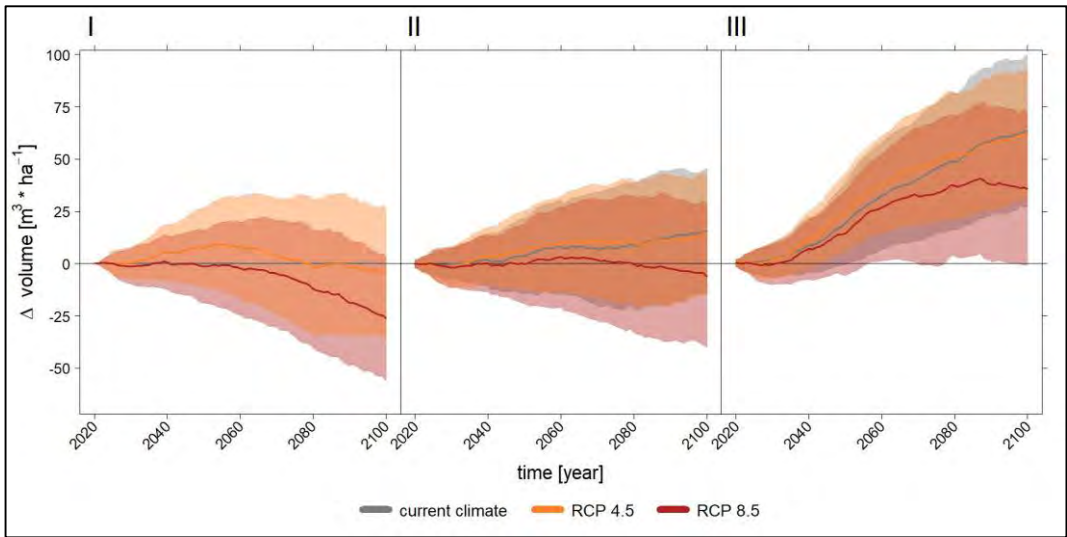


Figure 4: Change in growing stock for different stand development and climate scenarios in relation to the predictions for stand development scenario I under current climate scenario (A). I: present species regeneration only; II: mixed species regeneration; III: mixed species regeneration and planting. Solid line: mean of 100 model runs; shaded area: standard deviation of 100 model runs for current climate (grey), RCP 4.5 (light orange), and RCP 8.5 (light red).

4 Results

4.1 Methodological considerations

In this study, the dynamic forest succession was modelled up to the end of the twenty-first century. The forest stand responses are driven by the establishment, growth and mortality of individual trees related to climate scenarios (e.g. length of growing season) or soil moisture (Forest Ecology Group, 2019). The effects of forest disease (Sturrock et al., 2011) or outbreaks of bark beetle or defoliating insects are not considered in the modelling approach presented here, although these disturbance agents can change the competitive relationship between species and the pathways of stand development quite dramatically (Seidl et al., 2017).

Furthermore, the parametrization of the *ForClim* model for the tree species characteristics does not contain intraspecific variation resulting from different tree provenances, although these can modify the response to extreme climatic events (Wang et al., 2020). However, more detailed parametrization would not be beneficial if the origin of the forest stand under investigation is unknown, as in the majority of forest stands. A trade-off between general validity and specialization is ubiquitous in dynamic vegetation models and many other modelling approaches. A recent evaluation of various forest ecosystem models that use long-term inventory data (Irauschek et al., 2021) evidenced *ForClim*'s suitability for stand development projections. To assess the impacts of climate change, raise awareness and support decision making, predicting general growth patterns of species and forest stands is considered perfectly adequate.

As reproducibility in research is also an increasingly important topic in geographic information science (Nüst et al., 2018), the modelling workflow was implemented using Free/Libre and Open Source Software (FLOSS). This should guarantee the transferability of the application and increase its usability.

As the mean and standard deviation of 100 iterations of the model runs are shown, the change in species composition and growth seem to be gradual, rather than abrupt, after the disturbance of stands or removal of single species. Although the prediction uncertainty is high, extreme climatic events, like heatwaves and droughts, will shape forest ecosystems to a greater extent than gradual changes in average conditions (Fuhrer et al., 2006). Such tipping-point dynamics, resulting in sudden drought-related tree mortality, become very likely with progressing climate change (Allen et al., 2015). Therefore, non-linear responses of ecosystems should also be considered in the management recommendation.

4.2 Species-specific growth patterns

Although the trajectories of temperature changes (Figure 2) show relatively small differences between the emission scenarios (RCP 4.5 and 8.5) for the first half of the century (IPCC, 2014), the impacts on the species differ. The growth responses intensify as time goes on, and at the end of the century clear trends in species-specific growth patterns can be identified.

The most notable development was for *Picea abies*, which shows a strong reduction in volume under all climate scenarios (Figure 3 A–C). The low standard deviation of this growth patterns indicates a high correspondence between all model runs. It is predicted that *P. abies* will be almost absent from the site by the end of the century. In the face of the extensive dieback of *P. abies* at lower elevations of Central Europe, initiated by the drought in 2018 (Krejza et al., 2020), a strong decline is likely. As *P. abies* was for a long time planted far beyond its natural distribution range (Spiecker, 2000), it also occurs at marginal sites where a general withdrawal is observed (BFW, 2019). *P. abies* seems to be at high risk in the study site, in terms of its resilience and adaptation to climate change, as well as in terms of sustainable timber production and provision of ecosystem services.

The temporal pattern for volume growth of *Larix decidua* was not as clear as for *P. abies*, but it did show a slightly negative trend up to 2070, which strengthened over time (Figure 3, B and C). This is interpreted as the high climate-sensitivity of *L. decidua* at the study site. The response of *L. decidua* to drought and therefore its silvicultural suitability under climate change need to be studied more closely. The results are in line with the findings of Lévesque et al. (2013), who reported growth reduction of *L. decidua* for a mesic lowland site in Switzerland, and a xeric, mid-elevation, inner-alpine site in Italy. The same response was observed by Obojes et al. (2018) investigating the radial growth of *L. decidua* in mid-elevation to high-elevation forests in another xeric inner-alpine valley in Italy. Accordingly, these findings might also be valid for drought-prone mountain forests at lower elevations in the transition zone between the Atlantic- or Mediterranean-influenced fringes of the Alps and the continental inner-alpine areas.

A typical tree species for this transition zone is *Fagus sylvatica*, which is highly competitive in the lowlands of Central Europe and the fringes of the Alps, but is known to be drought-sensitive (Leuschner, 2020). Thus, *F. sylvatica* shows an increase in volume under the current

climate scenario (Figure 3A), but this trend weakens already under the moderate climate-change scenario (Figure 3B). Furthermore, in the severe climate-change scenario (Figure 3C), a significant reduction in growth from 2080 onwards is predicted. Given the negative impact of the 2018 drought on *F. sylvatica* (Schuldt et al., 2020), the predicted growth pattern could be ascribed to climate change-related heatwaves and drought periods.

For *Abies alba*, most of the increase in volume relates to the growth of the two existing juvenile individuals at the study site; results should therefore not be overinterpreted. Nevertheless, in contradiction to the findings of Thurm et al. (2020), *A. alba* seems to be more resilient than *L. decidua* to climate change (Figure 3, B and C).

The only species of conifer tree with an increasing growth pattern is *Pinus sylvestris*, which is known to be highly drought-tolerant (Krakau et al., 2013). In the present forest stand, it is the dominant tree species and has an almost normal distribution of DBH classes, up to a maximum of 25–30 cm. The stock at the beginning of the modelling period is only 200 m³·ha⁻¹. This is predicted to almost triple by the end of the century, regardless of the climate scenario (Figure 3, A–C). On the one hand, this is a result of the present forest structure, with low stock and a favourable DBH distribution of *P. sylvestris*, a structure which generally allows high annual increments. Compared with the recommended yield tables for *P. sylvestris* in Tyrol (Eckmüller, 2004), the predicted growth in volume is at the upper end of the range, but possible at sites with favourable conditions. On the other hand, *P. sylvestris* seems to suffer fewer adverse effects from climate change than other species, as there are no significant differences between the scenarios. Rather, *P. sylvestris* could benefit from the decline of other competing species, such as *P. abies* and *L. decidua*, and improved access to resources. Nevertheless, the predicted growth of *P. sylvestris* seems to be overestimated as site conditions are not among the best regarding increased growth. This is also evidenced by an average age of *P. sylvestris* above 20 cm DBH of around 110 years, which indicates a generally low growth rate and age-related flattening of it (Eckmüller, 2004). As current age is not considered in the model initialization, this could lead to misjudgement of the growth pattern. Regardless of the exact stock, it continues to be an important species and ensures continuity of the forest cover at the sites studied.

The thermophilous deciduous tree species *Quercus petraea* and *Tilia cordata*, which are both absent from the present forest stand, proved to be highly suitable under all climate scenarios (Figure 3, A–C). A comparison of the two sympatric oak species demonstrated the superiority of *Q. petraea* over *Q. robur* with the increasing severity of the climate scenario. Differences between these two oak species are also reflected in the findings of Vivin et al. (1993), who showed that the shoot growth of *Q. petraea* is less sensitive to water deficit than the shoot growth of *Q. robur*. Ponton et al. (2002) summarized that the lower growth rate of *Q. petraea* compared to *Q. robur* is associated with the greater long-term survival of adult *Q. petraea* trees in drought-prone environments. While literature on the direct comparison of the drought tolerance of *T. cordata* and *T. platyphyllos* is scarce, Hölscher et al. (2005) confirmed a high drought tolerance of *T. cordata*, which has a distribution range far beyond that of *T. platyphyllos*: it extends into the continental zone of Europe, which has regular or episodic summer drought. According to the findings presented here, *Q. petraea* and *T. cordata* form an important basis for building climate-smart forests; they are predestined for stand development scenario (III), in which the best-performing species from the mixed-species scenario are planted at the beginning of the modelling period.

4.3 Change patterns in the development of stands

The modelling results of the current climate scenario showed a discrepancy between those trees actually present and the natural tree species composition in the forest stand investigated. The predicted increase of *F. sylvatica* (Figure 3A), under the elimination of seed limitation, is in line with dry beech forest having been classified as potential natural vegetation (Forest Site Classification Tyrol, 2018). Likewise, more thermophilic deciduous trees (e.g. oak, lime) are already feasible under current climate conditions. Nevertheless, the observed growth potential of *F. sylvatica* is weakening (Figure 3, B and C), and thus the potential natural vegetation type may also change. Considering the high growth potential of thermophilus oak and lime species at the site, a shift towards an oak-dominated mixed forest is likely. The reasons for the present dominance of *P. sylvestris* and *P. abies* and the absence of deciduous trees could be numerous, ranging from effects of historical forest use (e.g. forest pasture, litter removal, clear-cuts), high browsing pressure preventing regeneration of deciduous trees, to the silvicultural objectives or preferences of the forest owner.

In all stand development scenarios (Figure 4, I–III), growth increases until around 2080 for the moderate climate-change scenario (scenario B, RCP 4.5), and then falls below the stocks predicted under current climate conditions (scenario A). This indicates that the current growth conditions are slightly temperature-limited, and a moderate temperature increase can foster tree growth, e.g. through an extension of the growing period. In addition, the severe climate-change scenario (scenario C, RCP 8.5) showed the lowest stock development in all cases. Especially in the 2nd time period (2071–2100) (Figure 2), the predictions reveal major differences and point towards a degradation of growing conditions (Figure 4, I–III). This pattern, with substantial differences between climate-change scenarios from 2050 onwards, was also shown by Thrippleton et al. (2020), in a similar study carried out in Switzerland.

Taking a closer look at the different stand development scenarios reveals that the differences between these are greater (appr. $50 \text{ m}^3 \cdot \text{ha}^{-1}$) than those between the climate scenarios (appr. $25 \text{ m}^3 \cdot \text{ha}^{-1}$). This shows the great advantages of mixed-tree forest stands for climate change mitigation. While the predictions, which are based only on those species that are currently present, show a negative growth pattern (Figure 4, I), allowing natural regeneration of deciduous tree species can stabilize growing stock (Figure 4, II). Developing mixed forests with a high proportion of thermophilus species, above all *Q. petraea*, can foster stable forest stands and sustainable yield. This finding is in line with Steckel et al. (2020), who stated that mixing of *P. sylvestris* and oak species (*Q. robur*, *Q. petraea*) can play a considerable role in creating climate-smart forests. The necessity for actively converting forests became even more apparent in view of large outbreaks of bark beetle and defoliating insects, which can trigger abrupt ecosystem changes (Campbell et al., 2009). This risk is especially high in anthropogenic, pure *P. abies* stands at lower elevations (e.g. Lévesque et al. (2013); Krejza et al. (2020)). Thus the stand development scenario that involves planting climatically suitable tree species (Figure 4, III) will significantly reduce the risk of abrupt changes in forest productivity and other forest ecosystem services.

4.4 Supra-regional embedding and international relevance

In 2020, the Department of Forest Planning of the Office of the Tyrolean Government launched the initiative ‘climate adapted mountain forests Tyrol’ (Ziegner, 2020). The present study contributes to the scientific basis of the management advice and activities promoted by this initiative. In addition, the study also addresses the Climate Smart Forestry Policy (Kauppi et al., 2018) of the European Union, which consists of three pillars: (i) reduction and sequestration of greenhouse gases; (ii) resilience; (iii) adaptation to change, and the sustainable increase of productivity and welfare. The results presented here directly contribute to the improvement of resilience and adaptation of forests to climate change, and therefore foster stable forest stands and sustainable yield.

5 Conclusion

The modelling approach discussed here can be used to assess the impacts of climate change on forest growth at selected sites, and therefore to support decision making at all levels, from forest owners to provincial forest authorities. Target groups are all parties interested in forest ecology and management. Through a set of best-practice recommendations, awareness raising can also reach stakeholder groups beyond the forest sector – in nature conservation, natural hazard protection or regional planning, for example.

The forest stand investigated in this research indicates significant climate-sensitivity, with different reactions by different tree species. Among the tree species present, Norway spruce (*Picea abies*) and European larch (*Larix decidua*) are not recommended for drought-prone mountain forests at lower elevations similar to the study site. European beech (*Fagus sylvatica*), common oak (*Quercus robur*) and large-leaved lime (*Tilia platyphyllos*) turned out to be unsuitable under future climate conditions at the site. Scots pine (*Pinus sylvestris*) continues to be an important species and ensures continuity of the forest cover at the study site. The results seem to be transferable to comparable sites that have artificial Scots pine forests, which are frequent in alpine valleys at low elevation. Considering the high growth potential of sessile oak (*Quercus petraea*) and small-leaved lime (*Tilia cordata*), a shift towards mixed forest in which oak dominates would be desirable. Therefore, the potential natural vegetation type under current climate conditions is not always appropriate as a silvicultural objective for future stand composition. To support decision making, development objectives based on the characteristics of specific forest sites must be provided for the total area of forested land.

It has been demonstrated that mixed forest stands that include broadleaved species are necessary to increase the resilience and adapt managed forests to climate change. With active silvicultural measures such as assisted migration through planting thermophilus species, negative effects of climate change could be diminished.

Supplements

Supplemental information is available at: <https://github.com/simonalois/cliffs>

References

- Allen, C., D. Breshears & N. McDowell (2015), On underestimation of global vulnerability to tree mortality and forest die-off from hotter drought in the Anthropocene. *Ecosphere* Nr. 6, p. art129; 1-55, 10.1890/ES15-00203.1.
- Allen, C. D., A. K. Macalady, H. Chenchouni, D. Bachelet, N. McDowell, M. Vennetier, T. Kitzberger, A. Rigling, D. D. Breshears, E. H. Hogg, P. Gonzalez, R. Fensham, Z. Zhang, J. Castro, N. Demidova, J.-H. Lim, G. Allard, S. W. Running, A. Semerci & N. Cobb (2010), A global overview of drought and heat-induced tree mortality reveals emerging climate change risks for forests. *Forest Ecology and Management* Nr. 259(4), p. 660-684, <https://doi.org/10.1016/j.foreco.2009.09.001>.
- Arbeitskreis Standortskartierung (2003), Forstliche Standortsaufnahme. IHW-Verlag, Eching, Germany.
- Assmann, E. & F. Franz (1963), Vorläufige Fichten-Ertragstafel für Bayern 1963. Institut für Ertragskunde der Forstlichen Forschungsanstalt München, Munich, GER.
- Auer, I., U. Foelsche, R. Böhm, B. Chimani, L. Haimberger, H. Kerschner, K. A. Koinig, K. Nicolussi & C. Spötl (2014), Vergangene Klimaänderungen in Österreich. In: (APCC), A. P. o. C. C. (Hrsg.).): Österreichischer Sachstandsbericht Klimawandel 2014 (AAR14). Vienna, Austria, Verlag der Österreichischen Akademie der Wissenschaften.
- Bengtsson, H. (2020), matrixStats: Functions that Apply to Rows and Columns of Matrices (and to Vectors).
- Berger, F., L. Dorren, K. Kleemayer, B. Maier, S. Planinsek, C. Bigot, F. Bourrier, O. Jancke, D. Toe & C. G. (2013), Eco-Engineering and Protection Forests Against Rockfalls and Snow Avalanches. In: Cerbu, G., Hanewinkler, M. & Gerosa, G. (Hrsg.). Management Strategies to Adapt Alpine Space Forests to Climate Change Risks, Intech Open.
- BFW (2019), Zwischenauswertung der Waldinventur 2016/18. BFW Praxisinformation Vienna, AT, Bundesforschungszentrum für Wald. Nr. 50.
- Bigler, C., O. U. Bräker, H. Bugmann, M. Dobbertin & A. Rigling (2006), Drought as an Inciting Mortality Factor in Scots Pine Stands of the Valais, Switzerland. *Ecosystems* Nr. 9(3), p. 330-343, 10.1007/s10021-005-0126-2.
- Blume, H. P., G. W. Brümmer, R. Horn, E. Kandeler, I. Kögel-Knabner, R. Kretschmar, K. Stahr & B.-M. Wilke (2009), Scheffer/Schachtschabel: Lehrbuch der Bodenkunde. Spektrum Akademischer Verlag Heidelberg, Germany.
- BMNT (2018), Österreichische Waldstrategie 2020+, Bundesministerium für Nachhaltigkeit und Tourismus.
- Bugmann, H. (1996), A Simplified Forest Model to Study Species Composition Along Climate Gradients. *Ecology* Nr. 77, 10.2307/2265700.
- Bugmann, H. (2001), A Review of Forest Gap Models. *Climatic Change* Nr. 51(3), p. 259-305, 10.1023/A:1012525626267.
- Campbell, E., S. C. Saunders, D. Coates, D. Meidinger, A. MacKinnon, G. O'Neil, D. MacKillop & C. DeLong (2009), Ecological resilience and complexity: a theoretical framework for understanding and managing British Columbia's forest ecosystems in a changing climate. Technical Report 055. Victoria, B.C., B.C. Min. For. Range, For. Sci. Prog. . Nr. 55.
- Duncan, T. L. (2020), XML: Tools for Parsing and Generating XML Within R and S-Plus.
- Eckmüllner, O. (2004), Empfohlene Ertragstafeln für Nord- und Osttirol. Amt der Tiroler Landesregierung, Abt. Forstplanung, Innsbruck, AT.
- Forest Act (1975), Forstgesetz. Government, A. Vienna, AT. Nr. StF: BGBl. Nr. 440/1975; NR: GP XIII RV 1266 AB 1677 S. 150. BR: 1392 AB 1425, p. 344.
- Forest Ecology Group (2019), ForClim Documentation, Release 4.0. Zürich, CH, ETH Zürich.

- Forest Site Classification Tyrol (2018), Waldtypisierung Tirol. Planning, D. o. F., Office of the Tyrolean government.
- Fuhrer, J., M. Beniston, A. Fischlin, C. Frei, S. Goyette, K. Jasper & C. Pfister (2006), Climate risks and their impact on agriculture and forests in Switzerland. *Climatic Change* Nr. 79, p. 79-102.
- Guisan, A., W. Thuiller & N. E. Zimmermann (2017), *Habitat Suitability and Distribution Models: With Applications in R*. Cambridge University Press, Cambridge.
- Hartig, T. (1847), Vergleichende Untersuchungen über den Ertrag der Rothbuche im Hoch- und Pflanz-Walde, im Mittel- und Niederwald-Betriebe nebst Anleitung zu vergleichenden Ertragsforschungen. Förstner, Berlin, GER.
- Hölscher, D., O. Koch, S. Korn & C. Leuschner (2005), Sap flux of five co-occurring tree species in a temperate broad-leaved forest during seasonal soil drought. *Trees* Nr. 19, p. 628-637, 10.1007/s00468-005-0426-3.
- Huber, N. (2019), Towards robust projections of future forest dynamics: why there is no silver bullet to cope with complexity. Thesis, ETH Zurich.
- Huber, N., H. Bugmann & V. Lafond (2020), Capturing ecological processes in dynamic forest models: why there is no silver bullet to cope with complexity. *Ecosphere* Nr. 11(5), <https://doi.org/10.1002/ecs2.3109>.
- IPCC (2014), *Climate Change 2014: Synthesis Report. Contribution of Working Groups I, II and III to the Fifth Assessment Report of the Intergovernmental Panel on Climate Change*. Pachauri, R. K. & Meyer, L. A. Geneva, CH, p. 151.
- Irauschek, F., I. Barka, H. Bugmann, B. Courbaud, C. Elkin, T. Hlásny, M. Klopčič, M. Mína, W. Rammer & M. J. Lexer (2021), Evaluating five forest models using multi-decadal inventory data from mountain forests. *Ecological Modelling* Nr. 445, p. 109493, <https://doi.org/10.1016/j.ecolmodel.2021.109493>.
- IUSS Working Group WRB (2014), *World Reference Base for Soil Resources 2014: international soil classification system for naming soils and creating legends for soil maps*. FAO, Rome, IT.
- Jump, A. S., J. M. Hunt & J. Penuelas (2006), Rapid climate change-related growth decline at the southern range edge of *Fagus sylvatica*. *Global Change Biology* Nr. 12(11), p. 2163-2174.
- Kauppi, P., H. Hanewinkel, T. Lundmark, L. Hetemäki, H. Peltola & A. Trasobares (2018), *Climate Smart Forestry in Europe*. Joensuu, FIN, European Forest Institute.
- Krakau, U.-K., M. Liesebach, T. Aronen, M.-A. Lelu-Walter & V. Schneck (2013), Scots Pine (*Pinus sylvestris* L.). In: Pâques, L. E. (Hrsg.). *Forest Tree Breeding in Europe*, Springer Netherlands, p. 267-323.
- Krejza, J., E. Cienciala, J. Světlík, M. Bellan, E. Noyer, P. Horáček, P. Štěpánek & M. V. Marek (2020), Evidence of climate-induced stress of Norway spruce along elevation gradient preceding the current dieback in Central Europe. *Trees*, 10.1007/s00468-020-02022-6.
- Le Quéré, C., R. M. Andrew, P. Friedlingstein, S. Sitch, J. Hauck, J. Pongratz, P. A. Pickers, J. I. Korsbakken, G. P. Peters, J. G. Canadell, A. Arneth, V. K. Arora, L. Barbero, A. Bastos, L. Bopp, F. Chevallier, L. P. Chini, P. Ciais, S. C. Doney, T. Gkritzalis, D. S. Goll, I. Harris, V. Haverd, F. M. Hoffman, M. Hoppema, R. A. Houghton, G. Hurtt, T. Ilyina, A. K. Jain, T. Johannessen, C. D. Jones, E. Kato, R. F. Keeling, K. K. Goldewijk, P. Landschützer, N. Lefèvre, S. Lienert, Z. Liu, D. Lombardozzi, N. Metz, D. R. Munro, J. E. M. S. Nabel, S. Nakaoka, C. Neill, A. Olsen, T. Ono, P. Patra, A. Peregón, W. Peters, P. Peylin, B. Pfeil, D. Pierrot, B. Poulter, G. Rehder, L. Resplandy, E. Robertson, M. Rocher, C. Rödenbeck, U. Schuster, J. Schwinger, R. Séférian, I. Skjelvan, T. Steinhoff, A. Sutton, P. P. Tans, H. Tian, B. Tilbrook, F. N. Tubiello, I. T. van der Laan-Luijkx, G. R. van der Werf, N. Viovy, A. P. Walker, A. J. Wiltshire, R. Wright, S. Zaehle & B. Zheng (2018), *Global Carbon Budget 2018*. *Earth Syst. Sci. Data* Nr. 10(4), p. 2141-2194, 10.5194/essd-10-2141-2018.

- Leuschner, C. (2020), Drought response of European beech (*Fagus sylvatica* L.)—A review. *Perspectives in Plant Ecology, Evolution and Systematics* Nr. 47, p. 125576, <https://doi.org/10.1016/j.ppees.2020.125576>.
- Lévesque, M., M. Saurer, R. Siegwolf, B. Eilmann, P. Brang, H. Bugmann & A. Rigling (2013), Drought response of five conifer species under contrasting water availability suggests high vulnerability of Norway spruce and European larch. *Global Change Biology* Nr. 19(10), p. 3184-3199, <https://doi.org/10.1111/gcb.12268>.
- Linkevičius, E., J. G. Borges, M. Doyle, H. Püzl, E.-M. Nordström, H. Vacik, V. Brukas, P. Biber, M. Teder, P. Kaimre, M. Synek & J. Garcia-Gonzalo (2019), Linking forest policy issues and decision support tools in Europe. *Forest Policy and Economics* Nr. 103, p. 4-16, <https://doi.org/10.1016/j.forpol.2018.05.014>.
- Lorey, T. (1878), Die mittlere Bestandeshöhe. *Allgemeine Forst- und Jagdzeitung* Nr. 54, p. 149-155.
- Monserud, R. A. & H. Sterba (1999), Modeling individual tree mortality for Austrian forest species. *Forest Ecology and Management* Nr. 113(2), p. 109-123, [https://doi.org/10.1016/S0378-1127\(98\)00419-8](https://doi.org/10.1016/S0378-1127(98)00419-8).
- Nagel, T. A., S. Miroslav, T. Rugani & J. Diaci (2010), Gap regeneration and replacement patterns in an old-growth *Fagus*–*Abies* forest of Bosnia–Herzegovina. *Plant Ecology* Nr. 208, p. 307-318.
- Nestroy, O., G. Aust, W. Blum, M. Englisch, H. Hager, E. Herzberger, W. Kilian, P. Nelhiebel, G. Ortner, E. Pecina, A. Pehamberger, W. Schneider & J. Wagner (2000, 2011), Systematische Gliederung der Böden Österreichs. *Österreichische Bodensystematik 2000 in der revidierten Fassung von 2011. Mitteilungen der Österreichischen Bodenkundlichen Gesellschaft* Nr. 79.
- Nüst, D., C. Granell, B. Hofer, M. Konkol, F. Ostermann, R. Sileryte & V. Cerutti (2018), Reproducible research and GIScience: An evaluation using AGILE conference papers. *PeerJ* Nr. 6, p. e5072, [10.7717/peerj.5072](https://doi.org/10.7717/peerj.5072).
- Obojes, N., A. Meurer, C. Newesely, E. Tasser, W. Oberhuber, S. Mayr & U. Tappeiner (2018), Water stress transpiration and growth of European larch up to the lower subalpine belt in an inner-alpine dry valley. *New Phytologist* Nr. 220(2), [10.1111/nph.15348](https://doi.org/10.1111/nph.15348).
- ÖKS15 (2016), Klimaszenarien für Österreich - Daten - Methoden - Klimaanalyse. Vienna, AT, Ministerium für ein Lebenswertes Österreich.
- Pecchi, M., M. Marchi, V. Burton, F. Giannetti, M. Moriondo, I. Bernetti, M. Bindi & G. Chirici (2019), Species distribution modelling to support forest management. A literature review. *Ecological Modelling* Nr. 411, p. 108817, <https://doi.org/10.1016/j.ecolmodel.2019.108817>.
- Pierce, D. (2017), *ncdf4: Interface to Unidata netCDF (Version 4 or Earlier) Format Data*.
- Ponton, S., J.-L. Dupouey, B. Nathalie & E. Dreyer (2002), Comparison of water-use efficiency of seedlings from two sympatric oak species: Genotype x environment interactions. *Tree physiology* Nr. 22, p. 413-22, [10.1093/treephys/22.6.413](https://doi.org/10.1093/treephys/22.6.413).
- Prietzl, J. & D. Christophel (2014), Organic carbon stock in forest soils of the German Alps. *Geoderma* Nr. 221-222, p. 28-39.
- R Core Team (2019), *R: A language and environment for statistical computing*. R Foundation for Statistical Computing, Vienna, AT.
- Rasche, L., L. Fahse, A. Zingg & H. Bugmann (2011), Getting a virtual forester fit for the challenge of climatic change. *Journal of Applied Ecology* Nr. 48, p. 1174-1186, [10.1111/j.1365-2664.2011.02014.x](https://doi.org/10.1111/j.1365-2664.2011.02014.x).
- Remund, J. & S. Augustin (2015), Zustand und Entwicklung der Trockenheit in Schweizer Wäldern. *Schweizerische Zeitschrift für Forstwesen* Nr. 166, p. 352-360.
- Röhle, H. (2004), Wachstumsmodelle und Umweltfaktoren - Möglichkeiten und Grenzen der forstlichen Modellierung. *Forst und Holz* Nr. 59, p. 480-484.
- Sarkar, D. (2008), *Lattice: Multivariate Data Visualization with R*. Springer, NY, USA.
- Schuldt, B., A. Buras, M. Arend, Y. Vitasse, C. Beierkuhnlein, A. Damm, M. Gharun, T. E. E. Grams, M. Hauck, P. Hajek, H. Hartmann, E. Hiltbrunner, G. Hoch, M. Holloway-Phillips, C. Körner, E.

- Larysch, T. Lübbe, D. B. Nelson, A. Rammig, A. Rigling, L. Rose, N. K. Ruehr, K. Schumann, F. Weiser, C. Werner, T. Wohlgemuth, C. S. Zang & A. Kahmen (2020), A first assessment of the impact of the extreme 2018 summer drought on Central European forests. *Basic and Applied Ecology* Nr. 45, p. 86-103, <https://doi.org/10.1016/j.baae.2020.04.003>.
- Schwappach, A. (1890), *Wachstum und Ertrag normaler Fichtenbestände*. Springer, Berlin, GER.
- Seidl, R., W. Rammer & M. Lexer (2011), Climate change vulnerability of sustainable forest management in the Eastern Alps. *Climatic Change* Nr. 106, p. 225-254.
- Seidl, R., D. Thom, M. Kautz, D. Martin-Benito, M. Peltoniemi, G. Vacchiano, J. Wild, D. Ascoli, M. Petr, J. Honkaniemi, M. J. Lexer, V. Trotsiuk, P. Mairota, M. Svoboda, M. Fabrika, T. A. Nagel & C. P. O. Reyer (2017), Forest disturbances under climate change. *Nature Climate Change* Nr. 7(6), p. 395-402, [10.1038/nclimate3303](https://doi.org/10.1038/nclimate3303).
- Simon, A., M. Wilhelmy, R. Klosterhuber, E. Cocuzza, C. Geitner & K. Katzensteiner (2021), A system for classifying subsolum geological substrates as a basis for describing soil formation. *Catena* Nr. 198, p. 105026, <https://doi.org/10.1016/j.catena.2020.105026>.
- Spiecker, H. (2000), Growth of Norway spruce (*Picea abies* [L.] Karst.) under changing environmental conditions in Europe. *EFI Proceedings*. Klimo, E., Hager, H. & Jirí, K., European Forest Institute. Nr. 33, p. 11-26.
- Steckel, M., M. del Río, M. Heym, J. Aldea, K. Bielak, G. Brazaitis, J. Černý, L. Coll, C. Collet, M. Ehbrecht, A. Jansons, A. Nothdurft, M. Pach, M. Pardos, Q. Ponette, D. O. J. Reventlow, R. Sitko, M. Svoboda, P. Vallet, B. Wolff & H. Pretzsch (2020), Species mixing reduces drought susceptibility of Scots pine (*Pinus sylvestris* L.) and oak (*Quercus robur* L., *Quercus petraea* (Matt.) Liebl.) – Site water supply and fertility modify the mixing effect. *Forest Ecology and Management* Nr. 461, p. 117908, <https://doi.org/10.1016/j.foreco.2020.117908>.
- Sturrock, R. N., S. J. Frankel, A. V. Brown, P. E. Hennon, J. T. Kliejunas, K. J. Lewis, J. J. Worrall & A. J. Woods (2011), Climate change and forest diseases. *Plant Pathology* Nr. 60, p. 133-149.
- Thrippleton, T., F. Lüscher & H. Bugmann (2020), Climate change impacts across a large forest enterprise in the Northern Pre-Alps: dynamic forest modelling as a tool for decision support. *European Journal of Forest Research* Nr. 139, p. 483-498.
- Thurm, E. A., S. Brandl, H. Fischer, K. H. Mellert, T. Mette, B. Reger & W. Weis (2020), Nadelbäume im Trockenstress. *LWF-aktuell* Nr. 3, p. 24-27.
- Vacik, H. & M. J. Lexer (2014), Past, current and future drivers for the development of decision support systems in forest management. *Scandinavian Journal of Forest Research* Nr. 29(sup1), p. 2-19, [10.1080/02827581.2013.830768](https://doi.org/10.1080/02827581.2013.830768).
- Vivin, P., G. Aussenac & G. Levy (1993), Differences in drought resistance among 3 deciduous oak species grown in large boxes. *Annales des sciences forestières* Nr. 50(3), p. 221-233.
- Wang, F., D. Israel, J.-A. Ramírez-Valiente, D. Sánchez-Gómez, I. Aranda, P. J. Aphalo & T. M. Robson (2020), Seedlings from marginal and core populations of European beech (*Fagus sylvatica* L.) respond differently to imposed drought and shade. *Trees*, [10.1007/s00468-020-02011-9](https://doi.org/10.1007/s00468-020-02011-9).
- Weisse, W. (1880), *Ertragstabellen für die Kiefer*. Springer, Berlin, GER.
- ZAMG (2015), *Das Klima von Tirol – Südtirol – Belluno*. Zentralanstalt für Meteorologie und Geodynamik, Abteilung Brand- und Zivilschutz – Autonome Provinz Bozen, Agenzia Regionale per la Prevenzione e Protezione Ambientale del Vento (ARPAV).
- Ziegner, K. (2020), *Klimafitter Bergwald Tirol*. Innsbruck, AT, Department of Forest Planning.

Orchard Meadow Trees: Tree Detection Using Deep Learning in ArcGIS Pro

Sabine Hennig

Vienna University, Austria

Abstract

'Orchard meadows' refers to the combination of extensively managed fruit trees in combination with fields and pastures. In many regions, among others in Germany, Austria and Switzerland, they are a landscape-defining element and of particular ecological, economic and social importance. However, the numbers of orchard meadows and fruit trees have been decreasing for quite some time. Current and detailed data that allow for the identification of suitable countermeasures to maintain this cultural landscape element are often missing. Such data can be obtained through deep learning. Various deep learning frameworks can now be used in the context of ArcGIS Pro. But what exactly does the use of deep learning involve, in the context of ArcGIS Pro, to get an insight into the stocks of orchard meadow trees? What are the challenges? Initial analyses were carried out using selected areas in Franconian Switzerland (Northern Bavaria) as an example. The results confirm the potential of the approach, but also that training data, model and output data must be refined.

Keywords:

cultural landscape, machine learning, monitoring, landscape maintenance

1 Introduction and research question

Orchard meadows include half-standard (height $\leq 5\text{m}$) and standard fruit trees (height $> 5\text{m}$ and height $\leq 8\text{m}$), which stand individually, in rows or groups, in meadows, pastures or arable fields, or along paths or ditches, and are extensively cultivated. Depending on the location and cultivation tradition, pome fruits (e.g. apples, pears), stone fruits (e.g. cherries, plums) and shell fruits (walnuts, sweet chestnuts) are grown in orchard meadows. The distances between the individual trees are relatively large to enable the agricultural use of both the fruit trees and the areas under the trees (Haas & Treter, 1988; Kornprobst, 1994; Prinz et al., 2007).

Due to the occurrence of trees of different ages and different varieties, and the relatively large distances between the individual trees, orchard meadows are a cultural landscape element with high structural diversity. They not only contribute to the characteristic appearance of the corresponding landscape, but also support various aspects of sustainability (Degenbeck, 2004; Girstenbreu, 2006; Haas & Treter, 1988; Kilian, 2013; Kornprobst, 1994; Prinz et al., 2007). These aspects relate to (i) the natural space: e.g. soil erosion reduction, local climate regulation

(e.g., temperature, precipitation), supporting high biodiversity; (ii) economic issues: e.g. regional food products (e.g., juice, schnapps), nature-related tourism; (iii) societal aspects: e.g. contributing to nature experience and recreation, importance for education for sustainable development, supporting trends towards more regionality. Orchard meadows are therefore important elements of the cultural landscape. In terms of the functions they fulfil, they cannot be replaced, for example by the dense planting and intensive cultivation of low-growing fruit trees and spindle trees (i.e. by plantations of market fruits) (Haas & Treter, 1988; Kornprobst, 1994).

Although there are still substantial stocks of orchard meadows in Germany, Austria and Switzerland, their number and size have been in decline since the 1960s. Reasons are the designation of some of the land for building, land consolidation, and conversion into arable land or for large-scale production of market fruits. Tree care and replanting of young trees have often been neglected, so that orchard meadows are now often obsolete, and scrub and forest have encroached on them (Bocheneck, 2019; Degenbeck, 2004; Haas & Treter, 1988; Kornprobst, 1994; Prinz et al., 2007). In the German state of Bavaria, for example, the number of orchard meadow trees fell by an estimated 70% from 20 million in 1965 (250,000 ha) to around 5 million in 2013 (approximately 75,000 hectares) (Girstenbreu, 2006; Kilian, 2013). As a result, orchard meadows in Bavaria are now considered an endangered cultural landscape element (LfL, n.d.). Although knowledge of the current situation and the changes taking place are an important basis for the implementation of measures to maintain orchard meadows, there is a lack of detailed and current data regarding orchard meadows and their trees. In Bavaria, such data was last collected in 1965; in 1975, there was an update based on sample counting; later data refer to estimates (Bocheneck, 2019; Degenbeck, 2004; Kilian, 2013).

The collection of data on orchard meadow trees and their monitoring is usually based on on-site mapping (Prinz et al., 2007), but computer-based methods such as deep learning (DL) now offer the possibility of identifying and localizing objects, including trees, in remote sensing images. Moreover, different DL frameworks can also be used in a user-friendly manner in the context of ArcGIS Pro. Using the corresponding geoprocessing tools, which are well-supported by tutorials, the entire DL workflow can be performed: (i) prepare imagery training data; (ii) train an object detection model; (iii) produce results (Guirado et al., 2017; Paschke, 2020; Schüpferling, 2019). But what exactly does it involve to perform DL in the context of ArcGIS Pro in order to get an insight into the stocks of orchard meadow trees? What are the challenges? These questions were examined in Franconian Switzerland (Northern Bavaria, Germany), where three sites were selected for the provision of training and test data (Figure 1). In this part of the North Franconian Alb, fruit tree cultivation has a long tradition and orchard meadows are a significant part of the cultural landscape (Kornprobst, 1994; Rippel, 2003).

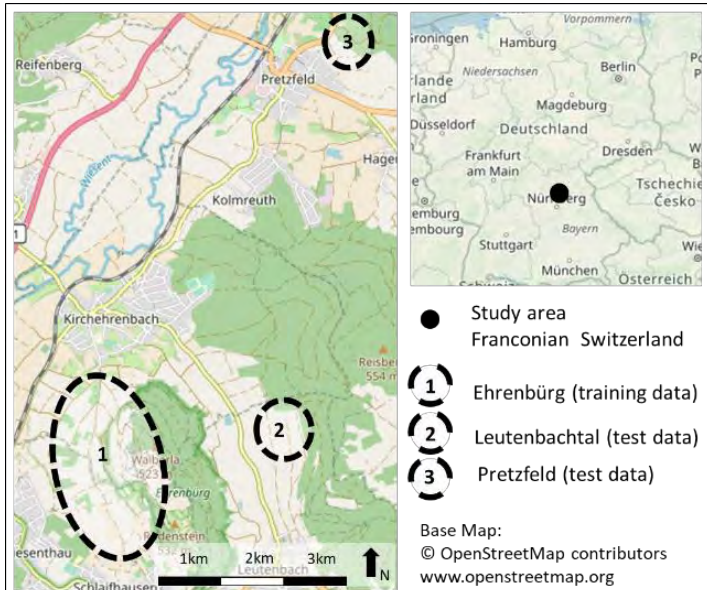


Figure 1: Study area and sites for the provision of training and test data

2 Workflow, methods and tools

Deep learning (DL) is a branch of machine learning (ML) and artificial intelligence (AI). It is used, among other things, for image classification and object detection. Using artificial neural networks (ANN) (i.e. models), DL strives to interpret images on the basis of pixel values and recurring patterns and textures, in a manner inspired by biological information processing and the human brain (Goodfellow et al.; 2016; Grekousis, 2019; Sanchez et al., 2020). Briefly, an ANN is a network of nodes arranged in layers (with weighted connections between them), which receive inputs and produce outputs. ANNs therefore consist of an input layer, an output layer, and one or more layers in between, the so-called hidden layers. ANNs are trained through an iterative process that takes the input data into account. The specific network criteria that are important for correct object detection are defined from the available data; the node connection weights to identify patterns and valuable information are then adjusted. Networks trained in this way can then also be applied to unknown data (Goodfellow et al., 2016; Grekousis, 2019; LeCun et al., 2015).

A special kind of ANN are Convolutional Neural Networks (CNN), introduced by LeCun et al. (1998). CNNs have brought about breakthroughs particularly in image classification and pattern recognition (Grekousis, 2019; LeCun et al., 2015). Their architecture comprises stacks of different operational blocks. The first stacks are convolutional layers. These layers consist of a set of filters (i.e. kernels) that perform scanning operations on the input data and deliver (i) a feature/activation map which keeps the important features, and (ii) pooling layers which, due to down-sampling operations (i.e. applying filters to intensify features), have reduced

image sizes. The other stacks refer to fully connected layers, i.e. hidden layers, exactly as in typical ANNs (Grekousis, 2019).

As already mentioned, various external DL frameworks can now be used in the context of ArcGIS Pro, with the ArcGIS Image Analyst extension using various geoprocessing tools. The workflow for identifying and locating orchard meadow trees comprises six steps: (i) input image provision; (ii) manual digitization of orchard meadow trees as a basis for the creation of training data, and as test data (i.e., ground truth features) for reviewing the results; (iii) generating training data; (iv) training the network, i.e. creating the model; (v) detecting objects, i.e. orchard meadow trees; (vi) reviewing the results, i.e. computing the accuracy for the orchard meadow trees detected, taking into account the ground truth features.

The work was carried out using ArcGIS Pro 2.7.0. For a visualization of the steps, and details of the geoprocessing tools including input parameters and values used, see Figure 2. As detailed in Figure 2 step 1, the basis for the DL process and all related work is ESRI's World Imagery (for Export) (ESRI, 2019), which (for the study area) was downloaded in ArcGIS Pro and pre-processed.

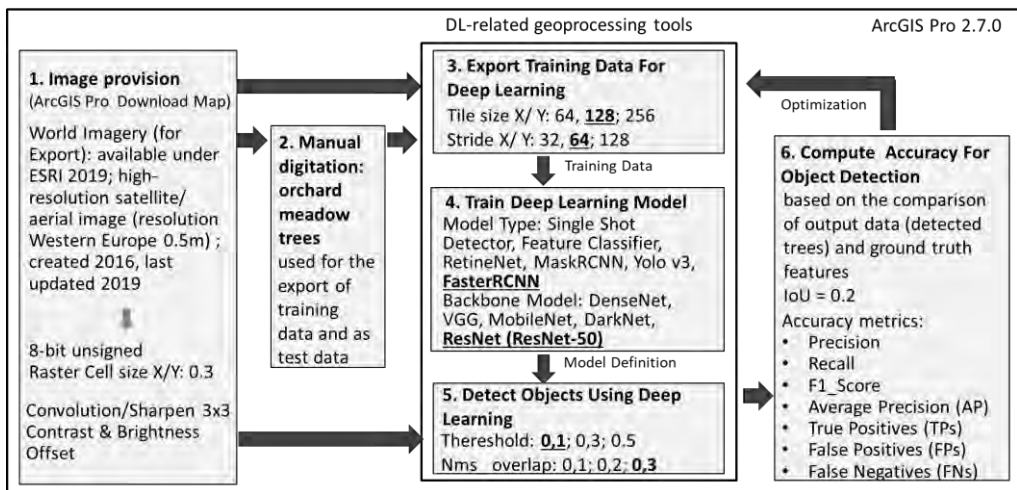


Figure 2: Workflow for the detection of orchard meadow trees using DL in the context of ArcGIS Pro. If no default values have been used, input parameters and values are mentioned. The values include those used for experimental comparison to decide the most suitable values. The values ultimately used, based on the available hardware resources (AMD RyzenTM 7 CPU, 16 GB RAM, 512 GB SSD, Graphics Radeon Vega 10 Mobile), are given in bold and underlined.

In step 2, the orchard meadow trees were digitized manually on-screen using the pre-processed image. This is possible because the distances between the trees are relatively large, and the trees are therefore usually recognizable as individual objects. As a basis for the export of the training data, orchard meadow trees located on the predominantly west-facing slopes of the Ehrenbürg mountain (near the villages of Kirchehrenbach and Schlaifhausen; Figure 1) were selected randomly then digitized (total 1,594 trees, with an average tree canopy base area of 42.2 m²). The sites selected as sources for the test data (i.e. trees used for ground truth features) are in

the Leutenbach valley (Leutenbachtal) and near the village of Pretzfeld (Figure 1). 677 trees (tree canopy base area average: 80.6 m²) and 524 trees (tree canopy base area average: 37.3 m²) from the Leutenbachtal and Pretzfeld test sites respectively were digitized. Since the ground truth features are used for reviewing and evaluating results (step 6), all trees in both areas were digitized. The manual on-screen digitization of the trees was supported by on-site inspections in autumn 2020.

The corresponding DL-related geoprocessing tools were used for steps 3, 4 and 5. Different input parameters can be selected. Choices for the corresponding values were based (in part) on experimental comparisons. Thus, different values were used for the input parameters (e.g., Tile Size X/Y, Stride X/Y, Threshold, NMS_Overlap) of the tools for Export Training Data For Deep Learning (step 3), and Detect Objects Using Deep Learning (step 5). The results were compared for accuracy (step 6). The values ultimately selected, because they gave the best results for the data used, are shown in Figure 2 (bold and underlined).

Findings from the literature were also taken into account in selecting input parameters and values. For Train Deep Learning Model (step 4), various model types (Single Shot Detector, Feature Classifier, RetineNet, MaskRCNN, Yolo v3, FasterRCNN) and backbone models (ResNet, DenseNet, VGG, MobileNet, DarkNet) can be used. They differ in aspects such as application domain, accuracy, computing time, processing capacities, and memory usage (see e.g. Arcos-García et al., 2018; Bianco et al., 2018; Bressen et al., 2018; Chowdhury et al., 2019; Krassimir et al., 2018; Nguyen et al., 2020; Reddy et al., 2018; Ren et al., 2015; Sanchez et al., 2020). Given the available hardware resources (AMD Ryzen™ 7 CPU, 16 GB RAM, 512 GB SSD, Graphics Radeon Vega 10 Mobile), using FasterRCNN and ResNet-50 was seen as expedient – a trade-off between accuracy, computing time etc. and the available hardware resources. This approach is in line with, for example, Bressen (2020), Krassimir (2018) and Reddy et al. (2018).

The review and evaluation of the results relied on the Accuracy Computing For Object Detection geoprocessing tool (step 6). Accuracy metrics were computed for:

- Precision (the ratio of the number of true positives to the total number of predictions);
- Recall (the ratio of the number of true positives to the total number of positive predictions);
- F1_Score (The weighted average, with values ranging from 0 to 1, of the precision and recall combined ; highest accuracy: 1);
- Average Precision (AP; the precision averaged across all recall values between 0 and 1);
- True Positives (TPs; the number of true positives generated by the model);
- False Positives (FP; the number of false positives generated by the model);
- False Negatives (FNs; the number of false negatives generated by the model).

The overlap of detected objects and ground truth features is evaluated using the value for Intersection over Union (IoU; Häger et al., 2018; Rezafighi et al., 2019). Instead of 0.5 as the typical IoU value used, 0.2 was used. This allows inaccuracies in manually digitized (and thus error-prone) ground truth features to be taken into account (Bochinski et al., 2016; Cai & Vasconcelos, 2018).

Since the digitized trees are represented by circles (corresponding to the tree canopy base area) but the FasterRCNN model represents detected trees by rectangular bounding boxes, three options for computing the accuracy of the detected trees were considered: (i) digitized trees (circles) and features referring to the largest circle within(?) a rectangular bounding box for the detected trees; (ii) bounding box features representing the manually digitized trees, and rectangular bounding boxes indicating the detected trees; (iii) digitized trees (circles) and rectangular bounding box features representing the detected trees.

3 Detected orchard meadow trees and their accuracy

Depending on the input parameter values used, the detected trees and the results of the accuracy metrics vary. The findings presented below are based on the input parameter values that were ultimately used in steps 3, 4 and 5 (Figure 2).

3.1 Accuracy metrics

While 524 ground truth features in the Pretzfeld test site were manually mapped, only 257 orchard meadow trees were detected. In the Leutenbachtal test site, 677 ground truth features were mapped and 553 orchard meadow trees were detected.

The accuracy metrics computed with respect to the different options (i.e. bounding boxes/circles) vary only slightly. For this reason, the numbers given in what follows refer to the accuracy metrics computed using bounding boxes for the detected objects, and circles for the ground truth features.

The figures reveal that many trees were not detected, and that some trees were incorrectly identified (Figure 3). For example, Precision is only 0.77 (Pretzfeld) and 0.76 (Leutenbachtal); Recall is 0.38 (Pretzfeld) and 0.62 (Leutenbachtal).

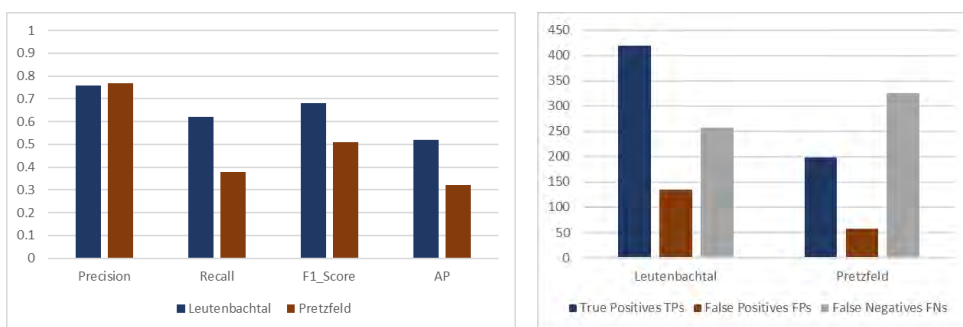


Figure 3: Accuracy metrics for the two test sites, Leutenbach and Pretzfeld (IoU=0.2)

The data shows that the trained model works to different degrees in the two test sites, with higher accuracy for Leutenbachtal than for Pretzfeld. In the Leutenbachtal test site, the share of correctly identified trees is 62% (421 true positive trees detected from 677 ground truth features); in the Pretzfeld site, 38% of trees were correctly identified (199 out of 525 trees). Of

the 533 trees in the Leutenbachtal site, 24% (134 trees) were incorrectly identified. For the Pretzfeld site, the corresponding figure was 23% (58 out of 257 trees).

3.2 Undetected and incorrectly detected orchard meadow trees

In general, orchard meadow trees with a below-average tree canopy base area (50 m^2 ; Kornprobst, 1994) were less well identified than those with a larger canopy base area ($\geq 50 \text{ m}^2$). In the Leutenbachtal test site, 49% of the manually digitized, small-canopy trees were detected, while 76% of the large-canopy trees were identified; in Pretzfeld, the figures were 36% of the small-canopy and 63% of the large-canopy trees (Figure 4). This difference between trees with small and large canopy base areas is also highlighted by the examples in Figure 5 (a, b).

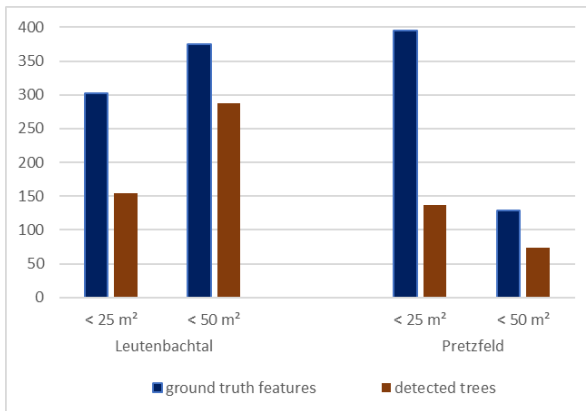
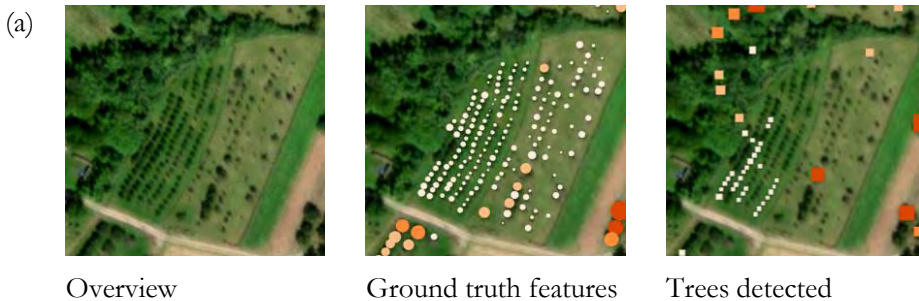


Figure 4: Comparison of ground truth features and orchard meadow trees detected, with regard to different tree canopy base areas, for both test sites



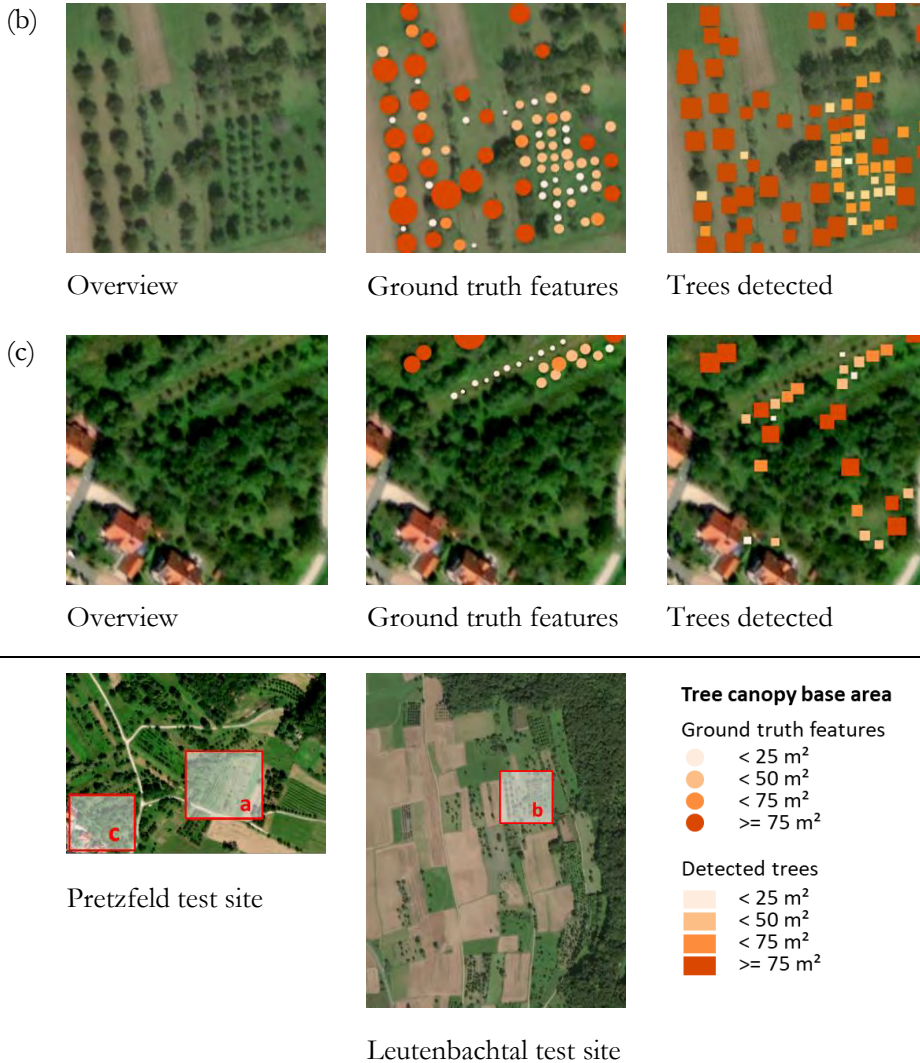


Figure 5: Comparison of trees detected and ground truth features: (a) focus on trees with small canopy base area; (b) focus on trees with large canopy base area; (c) focus on sites encroached by scrub and forest

The difference between small- and large-canopy trees also helps us to understand why in the Leutenbach site the TPs are higher and the FNs are lower than in the Pretzfeld site: the number and share of small-canopy trees in the Leutenbachtal site (45%) is considerably lower than in the Pretzfeld site (75%).

With regard to the incorrectly detected (FP) orchard meadow trees, the visual analysis shows that these are mainly solitary trees, trees in areas encroached by scrub and forest, or trees in obsolete stocks, at the forest edge or in settlement areas. In such cases, humans were less able to identify the trees when digitizing on-screen, but the trained model did do so (Figure 5 c).

4 Opportunities for result improvement

The results show that by using ArcGIS Pro DL-related geoprocessing tools for the workflow presented in Figure 2, a first general, but by no means complete, insight into the number and location of orchard meadow trees can be gained. There are several opportunities to improve the model and the results.

4.1 Training and test data

For effective model training, suitable and abundant data from which to create training data is required (Bochinski et al., 2016). Thus, the digitization of further orchard meadow trees from which further data are extracted would influence and/or improve the trained model. Moreover, additional on-site inspections would also improve the quality of the training data itself. This would counteract the problem of error, which makes its way into the training data when trees are digitized by humans on-screen (see, e.g., Bochinski et al., 2016). On-site inspections can also increase the quality of ground truth features, and thus have an impact on the accuracy metrics. This refers in particular to situations in which humans did not recognize trees on-screen, but the trained model did. This raises the question of whether trained models perform better than humans (in particular in the case of obsolete stocks of trees, scrub- and forest-encroached orchard meadows, solitary trees), as is also discussed in the literature (see, e.g., He et al., 2015). Related to this, it is essential to clarify whether and to what extent obsolete and scrub- and forest-encroached stocks of fruit trees as well as solitary trees should still be considered orchard meadow trees, taking into account their particular characteristics and multiple functions (as presented in Section 1).

4.2 Model training

The decisions on the model type and backbone model to use (FasterRCNN, ResNet-50) were influenced by the available computing power and the models' accuracy. A trade-off between the available hardware resources and the demands of the models in terms of the required computing power is widely accepted, as discussed by Arcos-García et al. (2018) and Sun (2017). Given that other model types and backbone models (e.g., Mask R-CNN; ResNet-101) will result in higher accuracy in object detection, the use of more powerful hardware resources should be considered (Reddy et al., 2018; Krassimir, 2018; Sanchez et al., 2020). In addition, other model configurations and combinations should be used in the context of further experimental comparisons. The creation of training data from other tree canopy base areas (smaller and/or larger) would also be useful.

4.3 Use of additional data

False positive objects found in areas that are not suitable for them can be excluded by taking into account data that identifies such areas (Robson et al. 2020). For example, in the mountainous and hilly landscapes of Franconian Switzerland, meadow orchards are located outside settlements, on forest-free, flatter, sun-exposed slopes of Dogger Sandstone (Kornprobst 1994; RvO, 2005). By considering data on land use (e.g. settlements and forest areas), geology, slope inclination and exposure, false positive trees can be excluded. While such

data is generally available as Open Governmental Data (OGD), for specific natural features crowdsourced data can be valuable in reviewing and/or enriching ground truth feature data and results. For instance, OpenStreetMap (OSM) contains (incomplete) data on features such as orchard meadows, hedges and single trees. To fill the data gaps, citizen science is a promising means of obtaining relevant data from local people and experts (Hennig, 2017; Hennig et al., 2021). Specifically, in the present case, citizen science could help to clarify (for example) whether stocks are obsolete, or if there has been encroachment by scrub and forest.

5 Conclusion and Outlook

Orchard meadows are extensively used meadows, pastures or arable land where standard and half-standard fruit trees grow. In many regions in Germany, Austria and Switzerland, they are an important but endangered element of the cultural landscape. Despite their ecological, economic and social importance, the number and extent of orchard meadows have declined in recent decades. For suitable countermeasures to be devised and implemented, current data on orchard meadow trees is needed. DL can be used to identify and locate trees in remote sensing images and fill in the missing data. The use of DL is made easier by the fact that DL frameworks can be used in the context of ArcGIS Pro.

DL-related geoprocessing tools were used to prepare imagery training data, train the object detection model, and produce results. Before and after these particular steps, other tasks had to be carried out using other ArcGIS Pro geoprocessing tools: the imagery had first to be procured, and the digitization of orchard meadow trees had to be carried out manually on-screen. The results also had to be reviewed. Although ArcGIS Pro geoprocessing tools open up a well-supported and user-friendly possibility for using DL, particular attention had to be paid to the different input parameters and their values. The example of orchard meadows in Franconian Switzerland (Germany) demonstrates that – on the basis of the available (somewhat limited) hardware resources, which require a trade-off with regard to computing time, processing capacities and accuracy – DL can provide an initial insight into the number and locations of orchard meadow trees. However, in the two test sites, there are significant numbers of false positives or false negatives for the orchard meadow trees detected. This is due to problems detecting trees with small canopy base areas, solitary trees, and trees located in obsolete orchard meadows or meadows encroached on by scrub and forest.

The results presented clearly show that further work is required. Several measures could be taken with the aim of obtaining better results: (i) providing more ground truth features, and supporting the manual on-screen digitization of trees through more on-site inspections; (ii) using other model types and backbone models as well as other input parameter values, even though this would require the availability of better hardware resources; (iii) taking into account data on typical location factors of orchard meadows (e.g. geology, slope, exposure), and relevant natural features (e.g. hedges, single non-fruit trees) to review and/or enrich the data on the digitized trees and the results.

In addition, training data from other areas should be integrated in order to provide an improved and more general model. The appropriately trained model could then be used

successfully in other regions and thus contribute to the maintenance of this endangered element of the cultural landscape.

References

- Arcos-García, Á., Álvarez-García & Soria-Morillo, L.M. (2018). Evaluation of deep neuronal networks for traffic sign detection. *Neurocomputing* 316(2018), 332-344. doi: 10.1016/j.neucom.2018.08.009
- Bianco, S., Cadéne, R., Celona, L. & Napoletano, P. (2018). Benchmark Analysis of Representative Deep Neural Network Architectures. *IEEE Access* 6. doi: 10.1109/ACCESS.2018.2877890
- Bocheneck, J. (2019). Abschlussbericht zum Projekt Inwertsetzung von Streuobstbeständen für eine Modellregion (Mittelfranken). Retrieved from https://www.dbu.de/OPAC/ab/DBU-Abschlussbericht-AZ-33535_01-Hauptbericht.pdf
- Bochinski, E., Eiselein, V. & Sikora, T. (2016). Training a convolutional neural network for multi-class object detection using solely virtual world data. 13th IEEE AVSS 2016, 278-285. doi: 10.1109/AVSS.2016.7738056.
- Bressem, K., Adams, L., Erxleben, C., Hamm, B., Niehues, S. & Vahldiek, J. (2020). Comparing different deep learning architectures for classification of chest radiographs. *Sci Rep* 10(13590). doi: 10.1038/s41598-020-70479-z
- Cai, Z. & Vasconcelos, N. (2018). Cascade R-CNN: Delving into High Quality Object Detection. *IEEE/CVF* 2018, 6154-6162, doi: 10.1109/CVPR.2018.00644.
- Chowdhury D.R., Garg P., More V.N. (2019) Pedestrian Intention Detection Using Faster RCNN and SSD. In M. Singh, P. Gupta, V. Tyagi, J. Flusser, T. Ören & R. Kashyap (Eds.), *Advances in Computing and Data Sciences. ICACDS 2019. Communications in Computer and Information Science*, 1046: Springer, Singapore
- Degenbeck, K. (2004). Zur Situation der Streuobstbestände in Bayern. Zustand - Probleme – Handlungsbedarf. In Bayer. Landesanstalt für Weinbau u. Gartenbau Abt. Landespflege (Eds.), *Veitshöchheimer Berichte aus der Landespflege* 79/2004.
- ESRI Environmental Systems Research Institute (2019). World Imagery (for Export). <https://www.arcgis.com/home/item.html?id=226d23f076da478bba4589e7eae95952>
- Girstenbreu, W. (2006). 5 Jahre Aktion Streuobst 2000 Plus. In Bayer. Landesanstalt für Landwirtschaft (Eds.), *Fachtagung Streuobst in der Kulturlandschaft*.
- Goodfellow, I., Bengio, Y. & Courville, A. (2016). *Deep Learning*. Retrieved from MIT <http://www.deeplearningbook.org>
- Grekousis, G. (2019). Artificial neural networks and deep learning in urban geography: A systematic review and meta-analysis. *Computers, Environment and Urban Systems* 74, 244-256. doi: 10.1016/j.compenvurbsys.2018.10.008
- Guirado, E., Tabik, S., Alcaraz-Segura, D., Cabello, J. & Herrera, F. (2017). Deep-learning Versus OBIA for Scattered Shrub Detection with Google Earth Imagery: *Ziziphus lotus* as Case Study. *Remote Sensing* 9(12) 1220. doi:10.3390/rs9121220
- Haas, D. & Treter, U. (1988). Die Bedeutung des Streuobstbaus für die Süddeutsche Kulturlandschaft am Beispiel von Wertheim/ Main. *FGG Mitteilungen* 35(n36), 273-334.
- Häger, G., Felsberg, M. & Khan, F. (2018). Countering bias in tracking evaluations. 13th International Joint Conference on Computer Vision, Imaging and Computer Graphics Theory and Applications - Volume 5: VISAPP, 581-587. doi: 10.5220/0006714805810587
- He, K, Zhang, X., Ren, S. & Sun, J. (2015). Delving Deep into Rectifiers: Surpassing Human-Level Performance on ImageNet Classification. *IEEE/ ICCV* 2015, 1026-1034. doi: 10.1109/ICCV.2015.123.

- Hennig, S. (2017). OpenStreetMap used in protected area management. The example of the recreational infrastructure in Berchtesgaden National Park. *eco.mont* 9(2), 30-41. doi: 10.1553/eco.mont-9-2s30
- Hennig, S., Abad, L., Hölbling, D. & Tiede, D. (2021). Implementing Geo Citizen Science Solutions: Experiences from the citizenMorph Project. *GI_Forum Journal* 8(1), 2-14. doi: 10.1553/giscience2020_01_s3
- Kilian, S. (2013). Bestands- und Bedarfssituation zum Streuobstbau in Bayern aus fachlicher Sicht. In Bayer. Landesanstalt für Landwirtschaft (Eds.), *Heimisches Streuobst ist wieder gefragt. Eine Chance für Landwirtschaft und Natur*. 11. Kulturlandschaftstag.
- Kornprobst, M. (1994). Lebensraumtyp Streuobst. *Landschaftspflegekonzept Bayern, Band II.5*. StMLU, ANL, München.
- Krassimir, V., Schumann, A., Sommer, L. & Beyerer, J. (2018). A Systematic Evaluation of Recent Deep Learning Architectures for Fine-Grained Vehicle Classification. *29th Pattern Recognition and Tracking (2018)*. doi: <https://doi.org/10.1117/12.2305062>
- LeCun, Y., Bottou, L., Bengio, Y., Hafner, P. (1998). Gradient-based Learning applied to document recognition. *IEEE* 86/1, 2278-2324.
- LeCun, Y., Bengio, Y. & Hinton, G. (2015). Deep Learning. *Nature* 521, 436-444.
- LfL Bayer. Landesanstalt für Landwirtschaft (n.d.). Neuanlage und Pflege einer Streuobstwiese. Retrieved from <https://www.lfl.bayern.de/iab/kulturlandschaft/142259/index.php>
- Nguyen, N.D., Do, T., Ngo, T.D. & Le, D.-D. (2020). An Evaluation of Deep Learning Methods for Small Object Detection. *Journal of Electrical and Computer Engineering* 20, 1-8. doi: <https://doi.org/10.1155/2020/3189691>
- Paschke, T. (2020). GeoAI: Deep Learning Integration in ArcGIS Pro für Imagery [Blog post] Retrieved from <https://arcgis.esri.de/geoai-deep-learning-integration-in-arcgis-pro-fuer-imagery/>
- Prinz, M., Renetzeder, C., Schmitzberger, I., Stocker-Kiss, A. & Wrбка, T. (2007). Obstbaumwiesen als Schlüsselemente zur Erhaltung und Förderung der natürlichen Vielfalt in österreichischen Agrikulturlandschaften. *Online-Fachzeitschrift des Bundesministeriums für Land- und Forstwirtschaft, Umwelt und Wasserwirtschaft* 2017.
- Reddy, N., Rattani, A. & Derakhshani, R. (2018), Comparison of Deep Learning Models for Biometric-based Mobile User Authentication. *IEEE BTAS 2018*. doi: 10.1109/BTAS.2018.8698586
- Ren, S., He, K., Girshick, R. & Sun, J. (2015). Faster R-CNN: Towards Real-Time Object Detection with Region Proposal Networks. *Computer Vision and Pattern Recognition 2015/1*. Retrieved from <https://arxiv.org/abs/1506.01497>
- Rezatofighi, H., Tsoi, N., Gwak, J.Y., Sadeghian, A., Reid, I. & Savarese, S. (2019). Generalized Intersection over Union: A Metric and A Loss for Bounding Box Regression. *IEEE/ CVPR 2019*. doi:10.1109/CVPR.2019.00075
- Rippel, R. (2003). Aktion „Streuobst 2000 Plus“ – Aus der Region für die Region. In Bayer. Landesanstalt für Landwirtschaft (Eds), *Streuobst in der Kulturlandschaft* 6/03.
- Robson, B.A., Bolch, T., MacDonell, S., Hölbling, D., Rastner, P. & Schaffer, N. (2020). Automated detection of rock glaciers using deep learning and object-based image analysis. *Remote Sensing of Environment* 120/2020. doi: <https://doi.org/10.1016/j.rse.2020.112033>
- RvO Regierung von Oberfranken (2005). *Landschaftsentwicklungskonzept Region Oberfranken-West, LEK 4*.
- Sanchez, S.A., Romero, H.J. & Morales, A.D. (2020). A review: Comparison of performance metrics of pretrained models for object detection using the TensorFlow framework. *IOP Conf. Ser.: Mater. Sci. Eng.* 844(2020) 012024. doi: 10.1088/1757-899X/844/1/012024
- Schüpferling, R. (2019). Deep Learning mit ArcGIS Pro [Blog post]. Retrieved from <https://arcgis.esri.de/deep-learning-mit-arcgis-pro/>
- Sun, L. (2017). ResNet on Tiny ImageNet. Retrieved from <http://cs231n.stanford.edu>

Examining Wildfire Spread Variables for Assessing Forest Burn Vulnerability

Victoria Chmarycz¹ and K. Wayne Forsythe¹

¹Ryerson University, Toronto, Canada

Abstract

The scale and danger of wildfires are a growing concern in Western Canada. The Northwest Fire Centre is one of six designated wildfire management districts in the Canadian Province of British Columbia. It covers 25 million hectares, or a quarter of the area of the province. The centre sees the greatest area burned from wildfire spread in the province although it experiences the lowest number of active wildfires annually. This study examined two Sentinel-2 images capturing the 'before' and 'after' of a major wildfire that took place in the Lutz Creek area within the Northwest Fire Centre in 2018. Higher-risk wildfire spread areas were identified by combining Normalized Difference Vegetation Index, Normalized Difference Water Index and slope gradient variables. When slope was included, the Moderately High and High burn vulnerability categories increased to ~54% of the area analysed, compared to ~33% when it was not included. Together, all three variables provide the basis for a more accurate assessment of forest burn spread and vulnerability.

Keywords:

wildfire, spread, Northwest Fire Centre, Sentinel-2, British Columbia

1 Introduction

In recent years (2017–2019), British Columbia (BC) reported that the Northwest Fire Centre (NFC) district had one of the lowest numbers of fires; yet, it had the greatest number of hectares burned due to wildfire spread. The NFC (one of six dedicated BC fire districts) is the largest wildfire response centre in the province, covering over 25 million hectares, equivalent to 25% of the province's land area. The Centre stretches from the Pacific coast to just west of the Town of Endako, and south from the Yukon border to Tweedsmuir Provincial Park (Government of British Columbia, 2020a) (Figure 1). The district encompasses part of the northern interior plateau as well as the Coastal Mountain range. The forests consist primarily of pine and spruce trees, with balsam found at higher elevations. Hemlock and red cedar become more prevalent along the coast (Government of British Columbia, 2020b).

Forest fires are one of the primary causes of changes in forest ecosystems throughout Canada (Weber & Flannigan, 1997; Kasischke & Turetsky, 2006; Schroeder et al., 2011; Forsythe & McCartney, 2014). Wildfires are a naturally occurring phenomenon during the summer months

in BC. They can reduce insect invasions, control the spread of disease, promote new vegetation growth, and in general help maintain a healthy forest, promoting the diversity of both plant and animal life (Coogan et al. 2019; Government of British Columbia, 2020a; USGS, 2020a). However, above-normal wildfire activity has occurred in BC over the last few decades. A history of effectively suppressing wildfire has led to a significant surplus of fuel (combustible forest materials), resulting in an increased risk of large wildfires, and as a side effect, decreased forest biodiversity (Podur & Wotton, 2010). With Western Canada showing above-average temperatures and less precipitation (according to the Environment and Climate Change Canada (ECCC) climate research program), BC may see above-normal numbers of wildfires during the wildfire season, resulting in potentially significant and devastating wildfires during the 21st century (Kirchmeier-Young et al., 2017; Government of Canada, 2020).

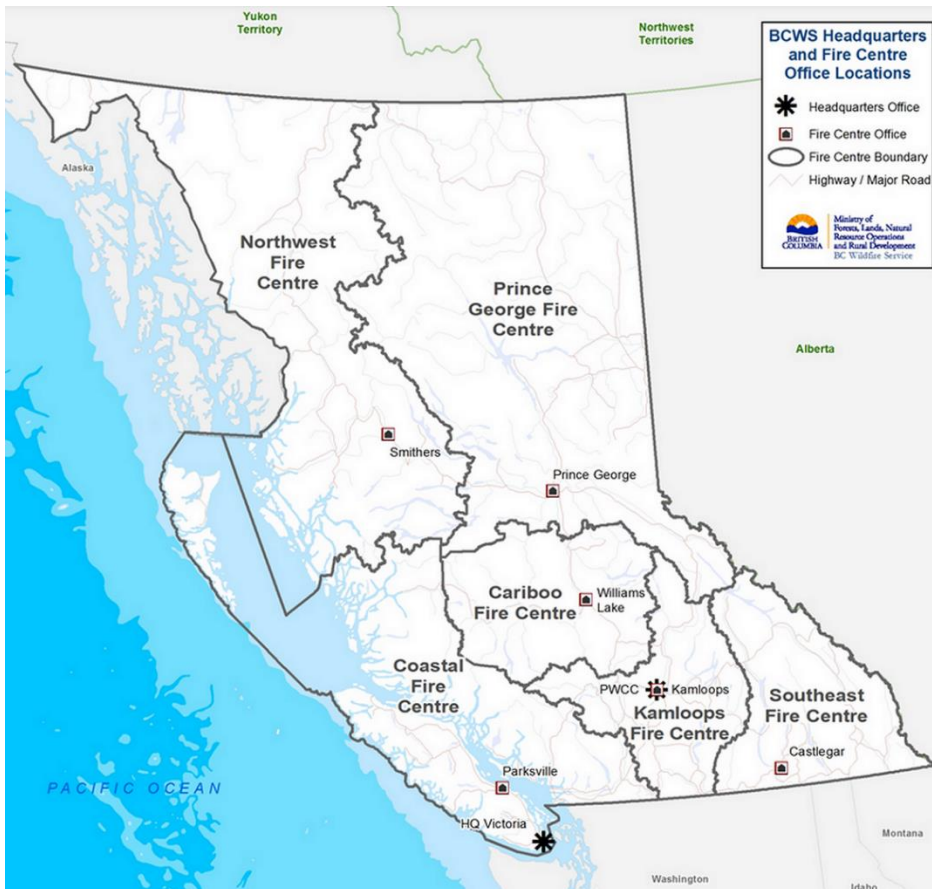


Figure 1: British Columbia's regional Fire Centre districts; (Source: Government of British Columbia. 2020b)

In addition to the density and quantity of fuels present, the moisture content (or dryness) of the materials necessary for a wildfire to thrive, spread and accelerate its burn rate is often influenced by slope gradient. Fire moves faster uphill on steeper slopes (the wind promoting

uphill spread), and falling debris contributes to downward slope spread (Weise & Biging, 1996; Government of Northwest Territories, 2020).

In a study of peat wildfires in Indonesia using Weighted Linear Combination (WLC) and regression techniques, the Normalized Difference Vegetation Index (NDVI) together with the Normalized Difference Water Index (NDWI) of pre-fire conditions resulted in a greater than 50% contribution to predicting land and forest vulnerability to wildfires. The study also revealed that although surface and air temperatures were able to partially explain forest vulnerability, they were less effective than vegetation and water indices in explaining wildfires in the region (Nurdiana & Risdiyanto, 2015). Similarly, Ferster et al. (2016) concluded that the traditional methods of observing wildfire vegetation loss through indicators such as fuel type, canopy coverage and dry conditions were universally applicable in predicting wildfires. Their recommendation for forest management was to take a holistic approach to wildfire activity to improve prediction models and enhance wildfire control practices.

The National Aeronautics and Space Administration's Moderate Resolution Imaging Spectroradiometer (MODIS), with channels specifically designed for fire detection, is the most commonly used satellite sensor for detecting fires over large regions (Natural Resources Canada, 2021). Wildfires spread either at a slow rate and low intensity, or at a fast rate and high intensity, but lengthening spread days increase the likelihood of considerable areas being burned regardless of a fire's intensity (Podur & Wotton, 2011). With the number of days conducive to the spread of fires increasing, it is important to study past wildfire spread activity to better prepare fire management teams in understanding where and how a wildfire will spread within an ecoregion. Throughout the fire season in BC, lightning strikes are responsible for approximately 60% of wildfires annually; the other 40% occur due to human negligence (Government of British Columbia, 2020a). Reducing the number of human-caused wildfires is achievable through awareness-raising initiatives, and area blockages/closures. However, lightning-caused wildfires are almost unavoidable and increasing (Wierchowski et al., 2002).

This study, through an analysis of fuel availability and fuel moisture conditions in combination with slope gradient, examines wildfire-conducive factors in the NFC. It aims to examine the conclusions of Nurdiana & Risdiyanto's (2015) study, where NDVI and NDWI provided a strong indication of the vulnerability of forest and land to wildfires; and NDVI and NDWI were shown to be stronger indicators than air and surface temperatures.

2 Data and Methods

The satellite images used in this study were acquired from the United States Geological Service (USGS) Earth Explorer data portal (USGS, 2020b). The cloud-free Sentinel 2A images were acquired on May 16, 2018 (pre-fire) and September 19, 2018 (post-fire). They were the highest-quality images available for this study when prevailing cloud cover and haze/smoke were considered during the 2018 fire season. They were also the closest in terms of date to the lightning-caused Lutz Creek fire that started on August 4, 2018 (Government of British Columbia, 2020a). The boundary file for the NFC was acquired from the Government of British Columbia's Data Catalogue (Government of British Columbia, 2020d).

Using the May imagery, the burnt area from the Lutz Creek fire was examined in terms of NDVI, NDWI and slope gradient characteristics to identify areas that are potentially vulnerable to wildfire spread. Pre-fire conditions were compared to post-wildfire vegetation loss. NDVI rather than the Normalized Burn Ratio (NBR) was utilized to show the burn scar, because while NBR shows fire severity, the aim was to identify surrounding vulnerable areas based on their NDVI values in combination with the other two variables.

The database that was created had all layers resampled to a 20m spatial resolution at 5,362 columns x 3,423 lines; the area measured $\sim 7,341.6504$ km² (734,165.04 hectares). The geoprocessing of the data was performed in ArcGIS Pro (ESRI, 2020), where the NFC border features were utilized for selection and extraction. For both the NDVI and NDWI images, the calculations were completed using the Spatial Analyst tool 'Raster Calculator'. The following equations were utilized:

$$\text{NDVI} [\text{float} (\text{Band } 8 - \text{Band } 4) / \text{float} (\text{Band } 8 + \text{Band } 4)] \quad (1)$$

$$\text{NDWI} [\text{float} (\text{Band } 11 - \text{Band } 8) / \text{float} (\text{Band } 11 + \text{Band } 8)] \quad (2)$$

The purpose of this process is to show the differences in healthy vegetation and moisture content pre- and post-wildfire. To better observe the pre-fire and post-fire conditions, the NDVI and NDWI results of the post-fire images were subtracted from pre-fire images by using the raster calculator. This revealed the total loss of vegetation, and allowed observation of the moisture conditions in May 2018 and September 2018. Slope gradient was calculated using the 'raster slope' function to predict burn spread vulnerability (ESRI, 2020). The Digital Elevation Model (DEM) data source was the ArcGIS online WorldElevation/Terrain dataset (ArcGIS Online, 2020).

Each of the NDVI, NDWI and slope gradient data layers were reclassified into five classes based on observations of each layer's characteristics in the Lutz Creek burn area. Quantiles that divide data layers into equal groups were utilized. All of the layers were then combined using raster join procedures. For the reclassification of the NDWI results, the class ranks were 'inverted' to combine and correctly represent the raster classes. As a result, the combined map shows the highest NDVI results, lowest NDWI results and steepest slope results. The following calculation was performed using the 'Raster Calculator':

$$\text{reclassified NDVI} + \text{reclassified NDWI} + \text{reclassified Slope} \quad (3)$$

All three input variables were weighted equally. The most common fire susceptibility method used to represent forest burn vulnerability is the natural breaks classification. This method creates classes of similar values and separates them at breakpoints to effectively categorize the data, showing the levels of vulnerability and allowing for easy interpretation (Ghorbanzadeh et al., 2019).

3 Results and Discussion

The change in NDVI between May and September shows the immense burnt area (Figure 2). For this study, the focus was on the large burnt area in the centre of the image (Lutz Creek fire). The burnt area shown further south was a separate wildfire that extended significantly into the neighbouring Prince George Fire Centre. A close look at the burnt area in the NFC reveals a few dense areas with extreme burn scars caused by high-intensity burning.

This study shows that three variables NDVI, NDWI and slope gradient can be utilized to predict locations that are potentially vulnerable to wildfires. In this paper, the definition of ‘vulnerability’ is “how easily damaged a particular area is to a fire of a given intensity” (CIFFC, 2017).

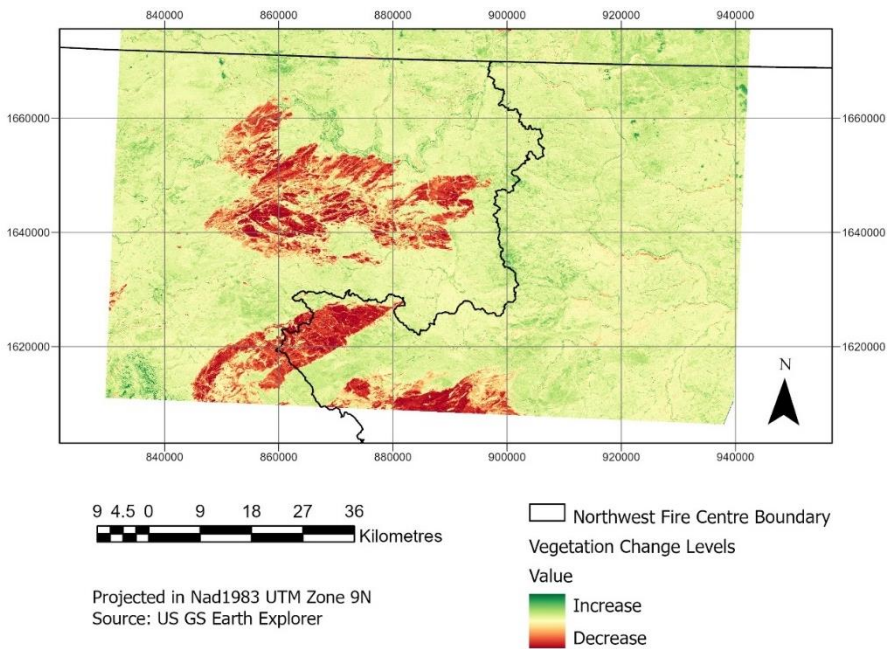


Figure 2: Lutz Creek Wildfire's Burnt Area (2018): The vegetation change difference between May and September

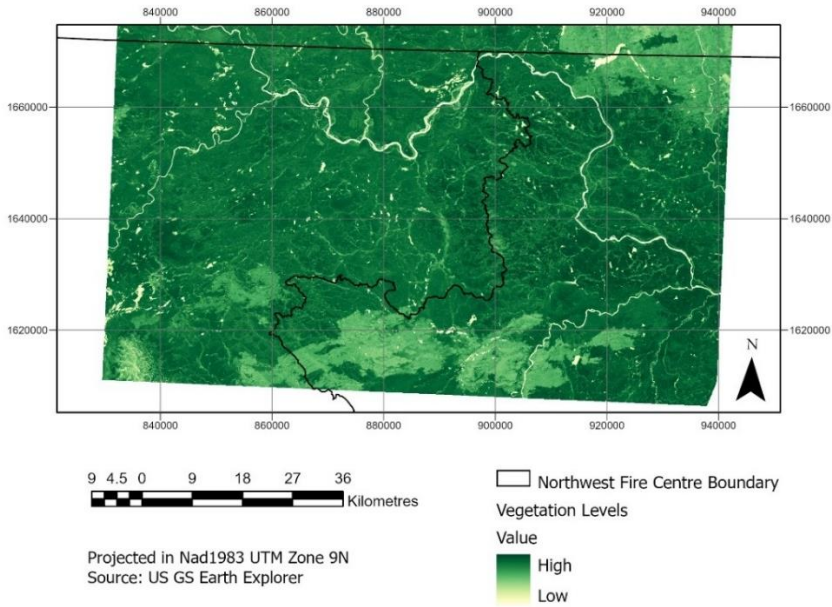


Figure 3: May NDVI Calculation Results pre-fire

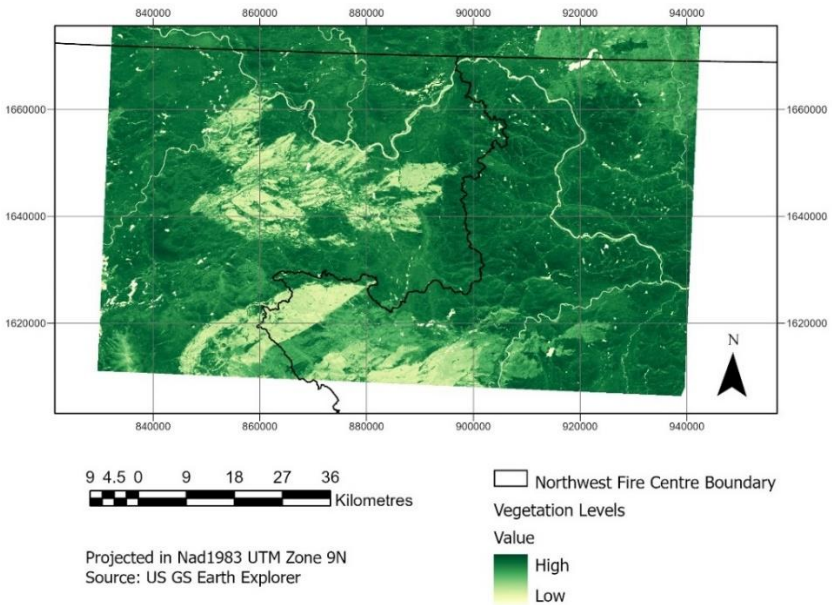


Figure 4: September NDVI Calculation Results post-fire

The NDWI for May and September (Figures 5 and 6), reveals a value range of between -1 and +1. Low NDWI results (below 0) show there are low to very low moisture levels. In Figure 6, the results show even lower NDWI levels, meaning drier conditions are present when

compared to Figure 5. Meteorological conditions may play a role here (hot, dry conditions), and it is possible that large wildfires could create their own (drier) weather conditions. Meteorological data were not part of the analyses, as there are no weather stations located in close proximity to Lutz Creek.

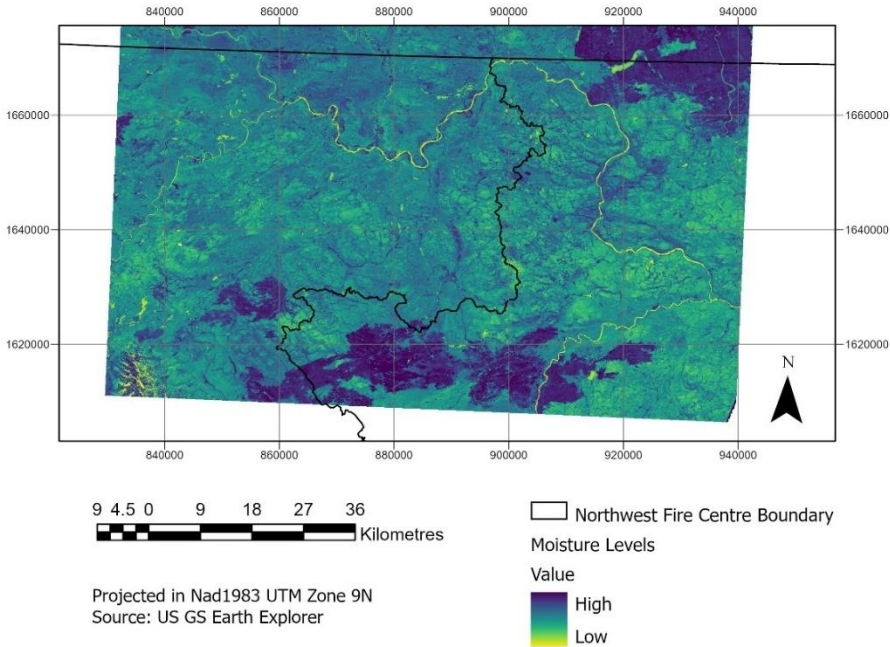


Figure 5: May NDWI Calculation Results pre-fire

A closer look at the changes from May to September (Figures 2 and 7) as well as the results in Table 1 reveals that in May the mean NDVI was 0.418, and the mean NDWI was -0.114. This shows that the vegetation is healthy but has a slightly low water content. For September, the mean NDVI was 0.460 and the mean NDWI was -0.230, showing that the vegetation was slightly healthier than in May, but that the region could have experienced low moisture levels in the interim period. The increase of 0.042 in mean NDVI between May and September can be attributed to the normal increases in vegetation growth during the summer months and warm temperatures, which promote healthier growth. Additionally, increased temperatures and lower precipitation during the summer months (as generally experienced in BC) may have resulted in drier vegetation conditions. Overall, the mean NDVI and mean NDWI from May and September show that there was increased fuel availability. Combined with generally lower moisture levels during the summer months, this provided ideal conditions for the wildfire that took place.

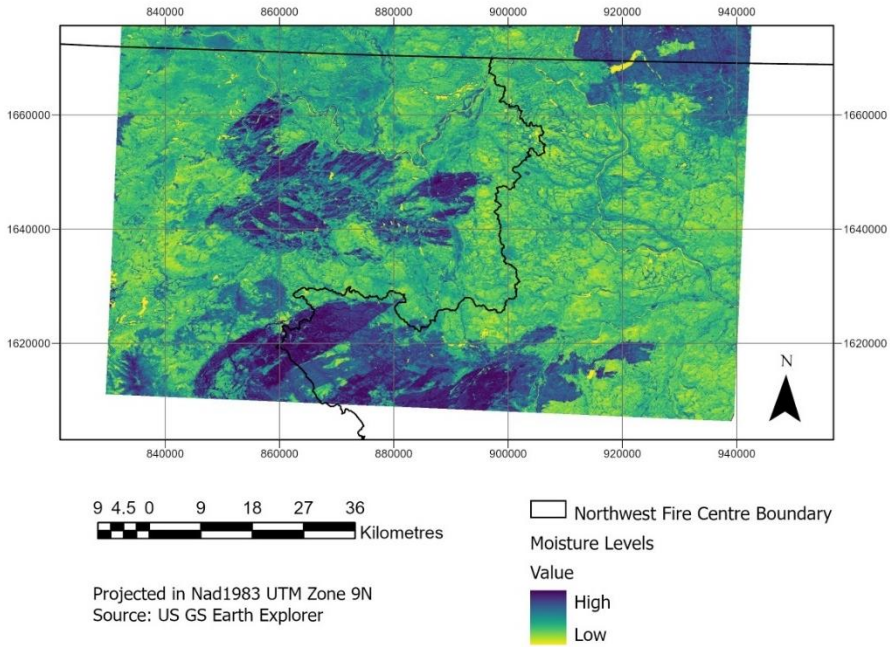


Figure 6: September NDWI Calculation Results post-fire

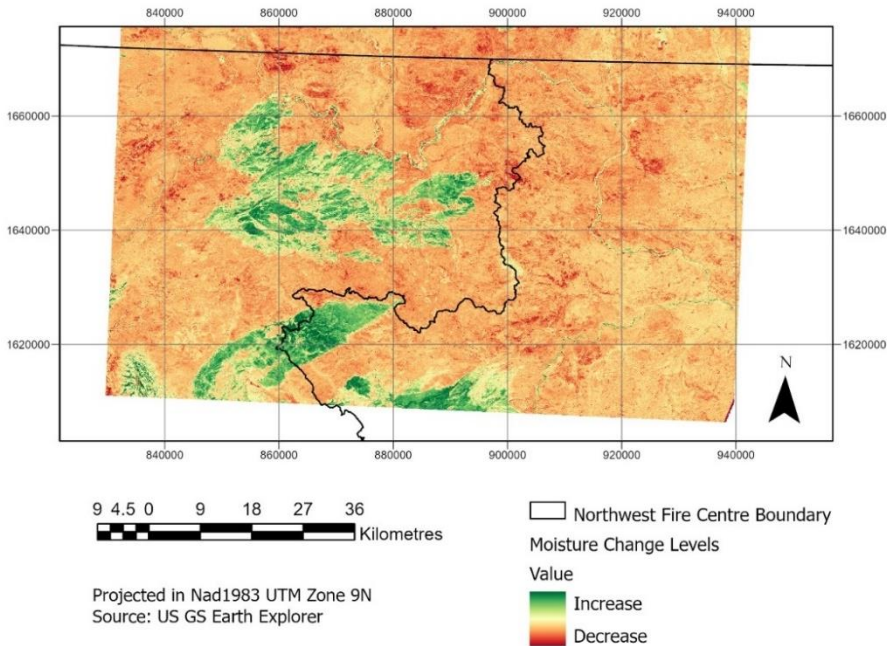


Figure 7: May-September NDWI Difference Results

Table 1: Mean Differences between May and September

Image	NDVI mean	NDWI mean
May	0.418	-0.114
September	0.460	-0.230
Change Difference	0.042	-0.116

The reclassified raster layers for NDVI and NDWI (Figure 8) reveal that there are quite a few clusters of high vulnerability where fire may thrive and spread. Most of the map shows moderately high vulnerability and provides a general picture of the locations where wildfire may spread.

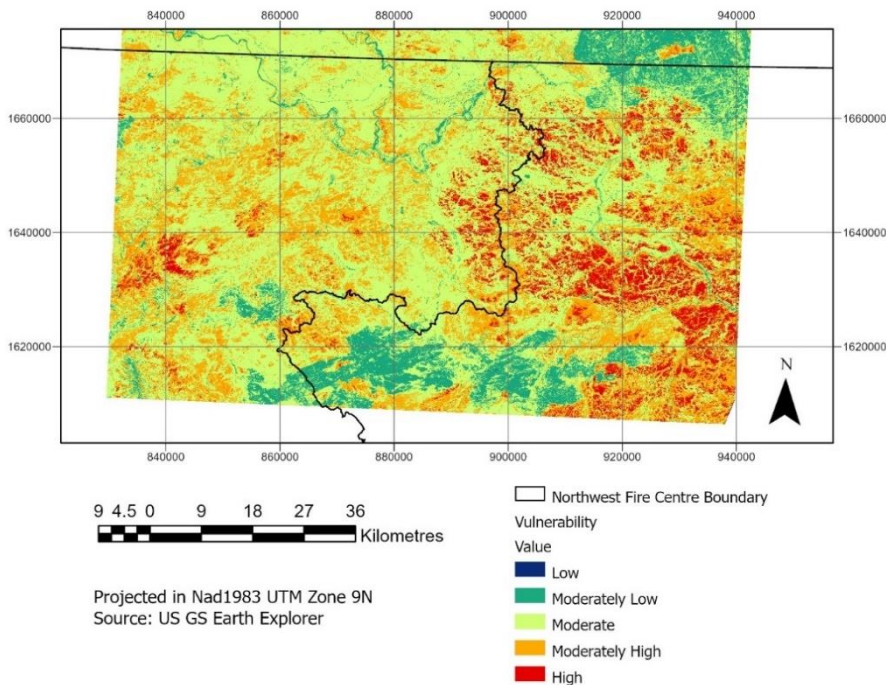


Figure 8: Land Vulnerability based on high NDVI and low NDWI results.

The reclassified raster results of NDVI, NDWI and slope gradient combined (Figure 9) reveal that more of the study area was identified as being vulnerable; locations of Moderately High to High vulnerability were found in the general area where the wildfire took place. The shape of the area where the fire burned can be observed. The results demonstrate that the area to the east, over the NFC district boundary, could be the next area to be affected by high fuel/burn spread.

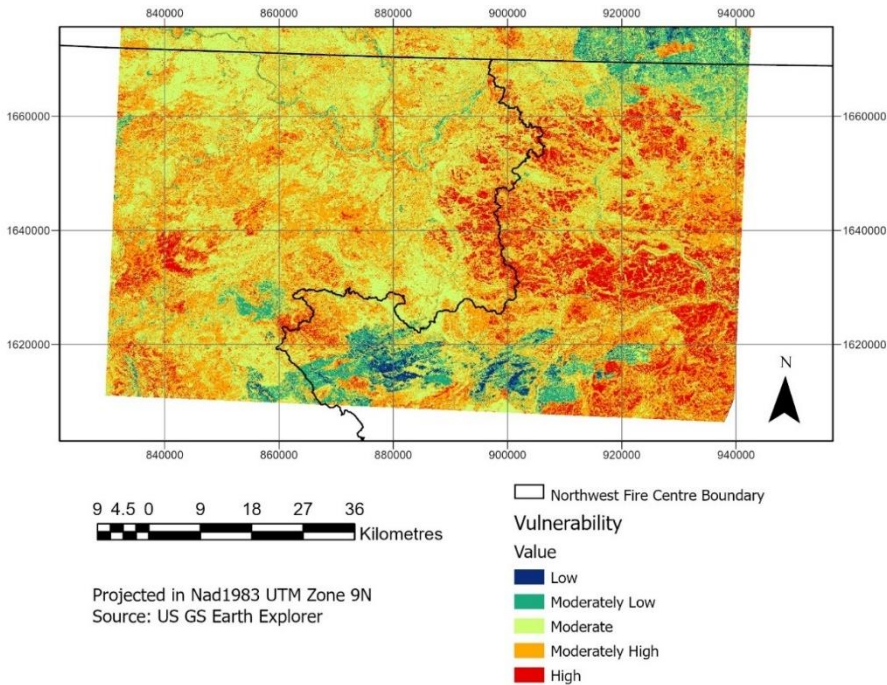


Figure 9: Land Vulnerability based on high NDVI, low NDWI and Slope Gradient results.

The NDVI and NDWI statistics for Figure 8 (that identify the five vulnerability categories) were extracted (Table 2). When the third variable, slope gradient, was added to the analysis (Table 3), the importance of including it becomes apparent.

Table 2: Burn Vulnerability Areas based on NDVI and NDWI

Category	Hectares	Square km	Percent
High	54,284.72	542.8472	7.3940
Moderately High	191,810.28	1,918.1028	26.1263
Moderate	410,662.24	4,106.6224	55.9360
Moderately Low	77,233.08	772.3308	10.5199
Low	164.04	1.6404	0.0223
No Data	10.68	0.1068	0.0015

Output classes that identify raster calculation results with values greater than seven (7) represent moderately vulnerable to highly vulnerable areas. Of note is that areas found to be of Moderately High to High vulnerability risk increased when the slope gradient variable was included (approximately 54% of the study area compared to approximately 33%). When slope was included, the Moderate vulnerability category decreased from approximately 56% to 37%, with most of the area being transferred to higher categories of fire-burn susceptibility.

Moderately Low and Low categories varied somewhat but accounted for just 10.5% (Figure 8 and Table 2) and 7.5% (Figure 9 and Table 3) of the study area.

Table 3: Burn Vulnerability Areas based on NDVI, NDWI, and Slope Gradient

Category	Hectares	Square km	Percent
High	95,916.48	959.1648	13.0647
Moderately High	307,317.52	3,073.1752	41.8595
Moderate	275,121.36	2,751.2136	37.4740
Moderately Low	55,780.88	557.8088	7.5979
Low	17.20	0.1720	0.0023
No Data	11.60	0.1160	0.0016

The main goal of this study was to determine whether Nurdiana & Risdiyanto's (2015) study showing NDVI and NDWI to be strong indicators of forest vulnerability to wildfires had relevance for the forests of British Columbia. The results illustrate that these factors can indeed be utilized to examine potential fuel loads for forest fires. When slope gradient was included as an additional variable, the calculations for wildfire vulnerability were improved. The combined variables of NDVI, NDWI and slope gradient could assist fire prevention efforts by helping to predict how a wildfire might spread. This particular combination of variables can also help identify how vulnerable land is to wildfire.

4 Conclusion

Using a major wildfire, in Lutz Creek (BC), from the Northwest Fire Centre district, this study assessed a combination of three variables – fuel availability (NDVI), fuel moisture (NDWI), and slope gradient - to ascertain whether they can be used to predict the vulnerability of land to wildfire spread. The NDVI variable was calculated to represent fuel availability as well as to observe wildfire spread/burned area. NDWI was utilized to observe general moisture levels in the study area. Slope gradient was calculated to determine where in the ecoregion wildfire spread is more likely. These three variables provide useful information for predicting land vulnerability to wildfire spread.

The results show that slope was a very important indicator for determining how a wildfire could spread. When slope gradient was included, larger areas were identified as being of Moderately High or High vulnerability. Although slope gradient by itself does not predict vulnerable areas for wildfire spread, when the three variables are combined, they present a good estimate of where/how a wildfire may spread.

This knowledge could potentially be applied to help fire management teams better predict, prepare for and monitor wildfire activity. Additionally, since wildfires are best left to run their course, fire management teams can predict the impact a wildfire may have, and decide at what point it will become appropriate to take mitigating action.

Finally, during particularly dry seasons, this prediction method could identify areas of land that are extremely vulnerable to wildfire spread; regions could thus take precautions, limiting human access to the areas identified. This would help prevent accidental fires caused by human negligence, which account for 40% of all BC wildfires (Government of British Columbia, 2020a). Since the data from studies similar to this one will in all probability show dispersed areas vulnerable to wildfire spread, Fire Centres would be unable to protect all identified vulnerable areas. Nonetheless, applying this approach could reduce the risk of very dangerous and large fires of human origin occurring in highly vulnerable areas.

References

- ArcGIS Online. (2020). WorldElevation/Terrain data set. Retrieved from <https://elevation.arcgis.com/arcgis/rest/services/WorldElevation/Terrain/ImageServer>
- Arellano-Pérez, S., Castedo-Dorado, F., López-Sánchez, C.A., González-Ferreiro, E., Yang, Z., Díaz-Varela, R.A., Álvarez-González, J.G., Vega, J.A., & Ruiz-González, A.D. (2018). Potential of Sentinel-2A Data to Model Surface and Canopy Fuel Characteristics in Relation to Crown Fire Hazard. *Remote Sensing*, 10(10), 1645. doi:10.3390/rs10101645
- Baker, W.L. (2015). Are high-severity fires burning at much higher rates recently than historically in dry-forest landscapes of the western USA? *PLoS One*, 10(9). <https://doi.org/10.1371/journal.pone.0136147>
- Canadian Interagency Forest Fire Centre (CIFFC) (2017). Canadian Wildland Fire Management Glossary. Retrieved from https://www.cifffc.ca/sites/default/files/2019-03/CIFFC_Canadian_Wildland_Fire_Mgmt_Glossary_2017_10_24.pdf
- Conny, J.M., & Slanter, J.F. (2002). Black carbon and organic carbon in aerosol particles from crown fires in the Canadian boreal forest. *Journal of Geophysical Research- Atmospheres*, 107(D11), 4116-AAC 4-12. doi: 10.1029/2001JD001528
- Coogan, S.C.P., Robinne, F-N, Jain, P., & Flannigan, M.D. (2019). Scientists' warning on wildfire — a Canadian perspective. *Canadian Journal of Forest Research*, 49(9): 1015-1023. doi:10.1139/cjfr-2019-0094
- Cruz, M.G., & Alexander, M.E. (2006). Evaluating a model for predicting active crown fire rate of spread using wildfire observations. *Canadian Journal of Forest Research*, 36(11), 3015-3028. doi:10.1139/x06-174
- Environmental Systems Research Institute (ESRI). (2020). Applying a z-factor. ArcGISPro Tool reference.
- Ferster, C-J., Eskelson, B.N.I., Andison, D.W., & LeMay, V.M. (2016). Vegetation mortality within natural wildfire events in the western Canadian boreal forest: What burns and why? *Forests*, 7(9), 187. doi:10.3390/f7090187
- Flannigan, M. (2017). Canadian Wildland Fire Smoke Newsletter. Retrieved from https://docs.wixstatic.com/ugd/90df79_bfcc500b532a4e38abaa78e1ecfdd26b.pdf
- Forsythe, K.W., & McCartney, G. (2014). Investigating Forest Disturbance Using Landsat Data in the Nagagamisis Central Plateau, Ontario, Canada. *ISPRS International Journal of Geo-Information*, 3(1), 254-273. doi:10.3390/ijgi3010254
- Ghorbanzadeh, O., Blaschke, T., Gholamnia, K., & Aryal, J. (2019). Forest Fire Susceptibility and Risk Mapping Using Social/Infrastructural Vulnerability and Environmental Variables. *Fire*, 2(3), 50. doi:10.3390/fire2030050
- Government of British Columbia (2020a). Wildfire History- Wildfire Season Summary and Statistics. Retrieved from <https://www2.gov.bc.ca/gov/content/safety/wildfire-status/about-bcws/wildfire-history/wildfire-season-summary>

- Government of British Columbia (2020b). Fire Centres. Retrieved from <https://www2.gov.bc.ca/gov/content/safety/wildfire-status/about-bcws/wildfire-response/fire-centres>
- Government of British Columbia (2020c). Wildfire Rank. Retrieved from <https://www2.gov.bc.ca/gov/content/safety/wildfire-status/about-bcws/wildfire-response/fire-characteristics/rank>
- Government of British Columbia (2020d). BC Wildfire Fire Centres. Retrieved from <https://governmentofbc.maps.arcgis.com/apps/MapSeries/index.html?appid=d70a0e9d100e4ac18c832988dabb3e51>
- Government of Canada (2020). Climate Trends and Variations Bulletin Winter. Retrieved from <https://www.canada.ca/en/environment-climate-change/services/climate-change/science-research-data/climate-trends-variability/trends-variations/winter-2020-bulletin.html>
- Government of Northwest Territories (2020). Environment and Natural Resources- Wildfire Operations- Fire Behaviour, Retrieved from <https://www.enr.gov.nt.ca/en/services/wildfire-operations/fire-behaviour>
- Government of Western Australia (2020). Prescribed Burning. Retrieved from <https://www.dpaw.wa.gov.au/management/fire/prescribed-burning#:~:text=Prescribed%20burning%20is%20the%20process,burns%20are%20the%20same%20thing>
- Kasischke, E.S., & Turetsky, M.R. (2006). Recent changes in the fire regime across the North American boreal region-Spatial and temporal patterns of burning across Canada and Alaska. *Geophysical Research Letters*, 33(9). doi:10.1029/2006GL025677
- Kirchmeier-Young, M.C., Zwiers, F.W., Gillett, N.P., & Cannon, A.J. (2017). Attributing extreme fire risk in Western Canada to human emissions. *Climate Change*, 144, 365-379. doi: 10.1007/s10584-017-2030-0.
- Mamuji, A.A., & Rozdilsky, J.L. (2019). Wildfire as an increasingly common natural disaster facing Canada: understanding the 2016 Fort McMurray wildfire. *Natural Hazards* 98, 163-180. doi:10.1007/s11069-018-3488-4
- Natural Resources Canada. (2021). Fire Monitoring, Mapping, and Modeling (Fire M3). Retrieved from <https://cwfis.cfs.nrcan.gc.ca/background/dsm/fm3>
- Nurdiana, A., & Risdiyanto, I. (2015). Indicator Determination of Forest and Land Fires Vulnerability using Landsat-5 TM Data (Case Study: Jambi Province). *Procedia Environmental Sciences*, 24, 141-151. doi:10.1016/j.proenv.2015.03.019.
- Penman, T.D., Collins, L., Syphard, A.D., Keeley, J.E., & Bradstock, R.A. (2014). Influence of fuels, weather, and the built environment on the exposure of property to wildfire. *PLoS One*, 9(10), e111414. doi:10.1371/journal.pone.0111414
- Podur, J., & Wotton, M. (2010). Will climate change overwhelm fire management capacity? *Ecological Modelling*, 221, 1301-1309. doi:10.1016/j.ecolmodel.2010.01.013
- Podur, J., & Wotton, M. (2011). Defining fire spread event days for fire-growth modelling. *International Journal of Wildland Fire*, 20, 497-507. doi:10.1071/WF09001
- Rodríguez-Veiga, J., Gómez-Costa, I., Ginzo-Villamayor, M., Casas-Méndez, B., & Sáiz-Díaz, J.L. (2018). Assignment problems in wildfire suppression: Models for optimization of aerial resource logistics. *Forest Science*, 64(5), 504-514. doi:10.1093/forsci/forxy012
- Schroeder, T.A., Wulder, M.A., Healey, S.P., & Miosen, G.G. (2011). Mapping wildfire and clear-cut harvest disturbances in boreal forest with Landsat time series data. *Remote Sensing of Environment*, 115, 1421-1433. doi:10.1016/j.rse.2011.01.022
- Stocks, B.J., & Martell, D.L. (2016). Forest fire management expenditures in Canada: 1970-2013. *The Forest Chronicle*, 92(3): 298-306. doi: 10.5558/tfc2016-056
- Thom, D., & Seidl, R. (2015). Natural disturbance impacts on ecosystem services and biodiversity in temperate and boreal forests. *Biological Reviews*, 91(3), 760-781. doi:10.1111/brv.12193.

- United States Geological Survey (USGS). (2020a). Wildfire Support from 438 Miles Above. Retrieved from <https://www.usgs.gov/news/wildfire-support-438-miles-above>
- United States Geological Survey (USGS). (2020b). Earth Explorer data portal. Retrieved from <https://earthexplorer.usgs.gov/>
- Wang, X., Parisien, M.A., Taylor, S.W., Candau, J.N., Stralberg, D., Marshall, G.A., Little, J.M., & Flannigan, M.D. (2017). Projected changes in daily fire spread across Canada over the next century. *Environmental Research Letters*, 12(2). doi:10.1088/1748-9326/aa5835
- Weber, M.G., & Flannigan, M.D. (1997). Canadian boreal forest ecosystem structure and function in a changing climate: Impact on fire regimes. *Environmental Reviews*, 5, 145-166. doi:10.1139/a97-008
- Weise, D.R., & Biging, G.S. (1996). Effects of wind velocity and slope on flame properties. *Canadian Journal of Forest Research*, 26(10), 1849-1858. doi:10.1139/x26-210
- Westerling, A.L., & Bryant, B.P. (2018). Climate change and wildfire in California. *Climatic Change*, 87, 231-249. doi:10.1007/s10584-007-9363-z
- Wierzchowski, J., Heathcott, M., & Flannigan, M.D. (2002). Lightning and lightning fire, central cordillera, Canada. *International Journal of Wildland Fire*, 11(1), 41-51. doi:10.1071/WF01048

Unpacking Layers of Space-Time Complexity in Land-Use Dynamics. A Case Study from the Olive Agrosystems of Sicily (Italy)

GI_Forum 2021, Issue 2

Page: 108 - 121

Full Paper

Corresponding Author:

vincenza.ferrara@arkeologi.uu.se

DOI: 10.1553/giscience2021_02_s108

Vincenza Ferrara^{1,2} and Anders Wästfelt²

¹Uppsala University, Sweden

²Stockholm University, Sweden

Abstract

The biocultural heritage of historical landscapes is an expression of intertwined ecological and socio-cultural dynamics at different temporal and spatial scales. Such a legacy is what confers high nature value on agricultural systems worldwide. Today there is an urgent need to develop approaches that may allow a more integrated study of biocultural heritage in order to better direct future endeavours for the sustainable management on such agricultural systems. Here, a methodological approach to unpack space-time complexity in the land-use dynamics of historic and current-day agrosystems is presented, based on the use of contextual and spatial-relational segmentation techniques within the research framework of historical ecology.

With reference to work done in a case study area in Sicily, the authors first extract geographic contextual configurations and develop a spatial-relational ontology for their semantic interpretation, before using these spatial objects as temporal proxies to disentangle the spatial and temporal dynamics of land use. The result is a cross-disciplinary approach in which perspectives from historical ecology can be used to achieve a deeper understanding of evidence extracted from remotely sensed images. At the same time, advanced spatial analysis techniques may provide a further interpretative tool for scientific inquiry into biocultural heritage.

Keywords:

historical ecology, contextual analysis, relational ontology, olive

1 Introduction

In the face of massive environmental, societal and cultural changes, research on historic agricultural landscapes and their biocultural heritage is crucial. Intercropping and agroforestry systems worldwide are all part of high nature value landscapes maintained through customary practices of management, protection and living heritage. These complex systems result from entwined dynamics occurring at different temporal and spatial scales. Thus cross-disciplinary approaches may allow a more integrated study of the systems' past, to direct future endeavours for their sustainable management (Manzano et al., 2020).

Here, a methodological approach to unpack space-time complexity in the land-use dynamics of historic agrosystems is presented. The approach is step-wise: (a) application of contextual and spatial-relational analysis to segment different land-use arrangements into spatial objects; (b) development of a spatial-relational ontology allowing a deeper semantic interpretation of the different spatial arrangements in terms of land-use strategies and human intentions; (c) the use of these spatial objects as temporal proxies to extract timescales of use dynamics.

With roots in archaeology and anthropology, historical ecology is a cross-disciplinary approach fostering the in-depth study of human-environmental heterarchical interactions happening at multiple spatial and temporal scales (Ray and Fernández-Götz, 2019). The use of remote sensing to analyse past human-nature systems (Pricope et al., 2019) and the application of object-based image analysis with geographic components (Hay and Castilla, 2008; Blaschke et al., 2014; Lang et al., 2019) in archaeology and related disciplines (Davis, 2019; Agapiou, 2020; Luo et al., 2019; Tapete, 2018) have focused so far on the semi-automatic digitalization of heritage maps (Gobbi et al., 2019), the extraction of information from remotely sensed data, mainly for feature detection (Sevara et al., 2016, Lasaponara and Masini, 2014), and the identification of surface and sub-surface remains (Lambers and Traviglia, 2016; Traviglia and Torsello, 2017). In many applications, a pre-defined ontology (Schuurman, 2006) of the image-objects detected is used as a tool to model real-world objects (Blaschke et al., 2014). In archaeology, in the course of the development of the GEOBIA ontology (Magnini and Bettineschi, 2019; Lombardo et al., 2020), the need to consider the spatial context and the temporal dimensions has been progressively highlighted (Calafiore et al., 2017; Sevara et al., 2016; Mathian and Sanders, 2015), accompanied by a call for attention to be paid to systems of related entities in the landscape, not single separate semantic objects (Traviglia and Torsello, 2017).

Thanks to its unique position in the Mediterranean, the island of Sicily has been a cross-roads of cultures for millennia, representing a special case of long-term human-nature inter-relationships and presenting high biological diversity of endemic species. The persistence of certain biocultural refugia in the landscape (Barthel et al., 2013) can be seen as the non-discursive result of a long-term cultural negotiation between humans and nature. In previous work (Ferrara et al., 2019), the authors demonstrated that the different spatial patterns resulting from the cultivation of *Olea Europea var. sativa* in the island (the olive tree, well known for its longevity) are related to a variety of land-use practices which differ over time. As such (spatial) biocultural continuities in the landscape are the expression of human–nature dynamics over time, contextual and spatial-relational analysis (Gurney and Townshend, 1983; Ahlqvist et al., 2012; Malmberg et al., 2014) can be applied to extract useful information. When integrated with other sources of evidence (i.e. from fieldwork), this information may allow a temporal categorization of the spatial patterns extracted. Such historical disentangling of landscape features may provide useful insights into centuries or even millennia of human–nature processes, allowing a better understanding of the foundational ecological and social dynamics underpinning biocultural heritage and present-day biodiversity (Crumley, 2019; Wästfelt, 2021).

The work presented here aims to contribute in this direction. The authors first describe in detail the methodology developed and the data used, with reference to work carried out in a case study area from 2016 onwards, and then present the results obtained. The results are

discussed, limitations pointed out, and the potential contributions of the approach for other disciplinary investigations in landscape and land-use studies are highlighted.

2 Study area and Methods

2.1 Study area

The study site, which had already been the subject of previous work (Ferrara et al., 2019), is located in the municipality of Villarosa, in central Sicily (Italy). The study area, a mosaic of olive orchards that are apparently homogeneous in terms of land cover and land use, covers an area 1,943 km² and rises to approximately 550 metres AMSL (Figure 1).



Figure 1: RGB orthophoto of the study area, Urbanistic and Environmental Department of the Sicilian Region, 2007, resolution 0.25 m.

2.2 Methods

The approach presented here is based on three steps:

- a. application of **contextual and spatial-relational analysis**, with the aim of segmenting into separate objects the different spatial cultivation arrangements of the olive trees present in the study area;

- b. development of a **spatial-relational ontology** allowing a deeper semantic interpretation and classification of the different spatial arrangements into classes, in terms of land-use strategies and human intentions;
- c. use of these spatial classes as **temporal proxies** from which to semantically extract temporal classes (as expressions of different time scales in the land-use dynamics).

Contextual and spatial-relational analysis

As a first step, a contextual and spatial-relational analysis was performed on an RGB orthophoto of the study area from 2007. With a spatial resolution of 0.25 metres, the image comes from the most recent freely available dataset provided by the Urbanistic and Environmental Department of the Sicilian Region.

The orthophoto was segmented and classified using a 3-step, semi-automated classification method developed by Malmberg et al. (2014) (Figure 2). This method uses both spectral and contextual relational criteria for the classification, allowing the user to decide a priori the number of classes to extract and the segmentation radius. In this case, the authors chose to use a segmentation radius of 55 pixels and to classify the image into 11 classes. The three steps of Malmberg et al.'s (2014) method are:

1. Initial classification using k-means clustering;
2. The calculation of the largest nearest-neighbour distance between each pixel and each pixel belonging to each class from step 1;
3. A second classification (again using k-means), performed on the basis of the largest nearest-neighbour distances calculated in step 2.

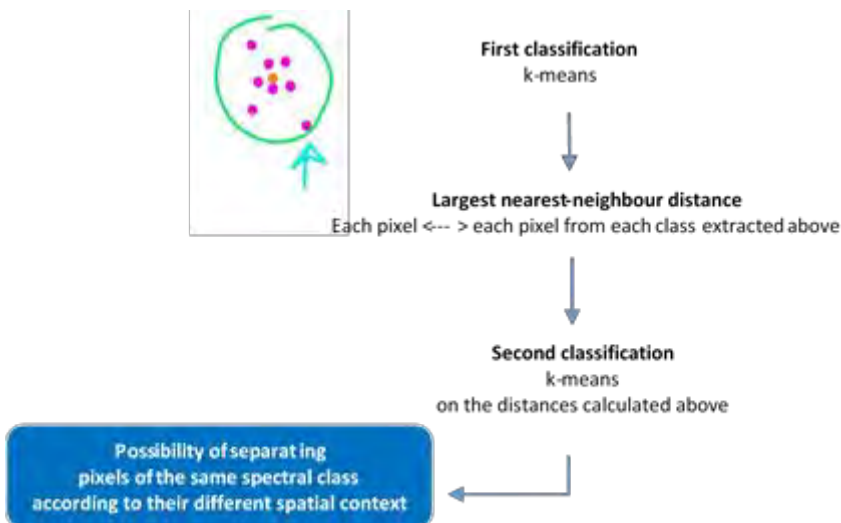


Figure 2: Workflow of the method developed by Malmberg et al. (2014) for semi-automatic classification of image information.

After these steps had been executed, a new composite image was obtained (Figure 3c). The use of the largest nearest-neighbour distance as a geometric criterion for the second classification allows the separation of pixels originally belonging to the same object and their classification into two or more different objects, depending on similarities identified in their spatial contexts (Figure 3b and 3d). From the visual interpretation of this processed image and its comparison with the initial raw orthophoto (Figure 3a), it emerged that the semi-automated classification method had been able to identify and group into objects a number of homogeneous areas. The local configurations of these areas correspond to specific spatial arrangements of their main vegetation features (olive trees) in relationship with other relevant features (i.e. vegetation, topographic and human-made elements) (Figure 3d). In other words, in the processed image, pixels were grouped into objects that should not be interpreted as representing the spectral reflectance of different items on the ground (vegetation, concrete, water, etc.), but rather as their geographical contextual configuration. The authors believe that this opens up a higher level of semantic abstraction in assigning meanings to these spatial objects.



Figure 3a: Initial raw RGB orthophoto. The red square indicates a section of the fieldwork area, detailed in Figures 3b and 3d.



Figure 3b: Spatial context of trees in part of the study site; view from the ground.

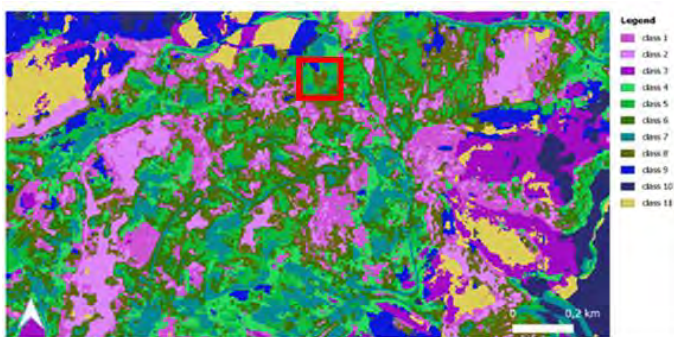


Figure 3c: New composite image showing the spatial objects extracted using the method developed by Malberg et al. (2014).



Figure 3d: Olive trees segmented and classified into spatial objects according to their spatial contexts. Section of the study site, view from above.

Development of ontology, in-field validation and classification of spatial objects

Seen from above, at first sight the study area appears to be a homogeneous landscape of olive orchards. Nonetheless, the different spatial objects extracted show that each is characterized by a unique contextual configuration of the image elements (pixels), corresponding to unique characteristics resulting from different spatial arrangements. These spatial arrangements are the expression of diverse human land-use strategies over time. The interpretation of these local configurations cannot be done directly from the images and requires expert knowledge of the local farming systems (Wästfelt, 2015).

To proceed with the interpretation of the objects extracted, the authors adopted abductive logic (Couclelis, 2009; Khazraee and Khoo, 2011), associating expert knowledge (Ferrara et al., 2019) with the low-level information obtained from the image objects by visual interpretation. It was thus possible to perceive these objects, conceptually, as being embedded within an (apparent) hierarchy of spatial complexity. Deconstructing this complexity level by level made it possible to uncover the meanings of the spatial arrangements that these land-use configurations represent.

The authors developed a spatial-relational ontology (Figure 4) which was used to semantically interpret these spatial objects. There followed field validation of the interpretation and the final classification (see Rajbhandari et al., 2017; Argyridis and Argialas, 2019). Methods combining spatial and thematic semantics have only recently started to be developed to address complex geospatial features (Blaschke et al., 2014). A spatial-relational ontology is an ontology that highlights the relational aspects of space (*sensu* Grauer, 2019; Kokla and Guilbert, 2020) and the human intentions in the use of space. Configurations of space are the expression of human–nature relationships, co-constituting themselves and creating the relational historical process, which unfolds in space, and has primacy over single discrete entities (Ferrara et al., forthcoming).

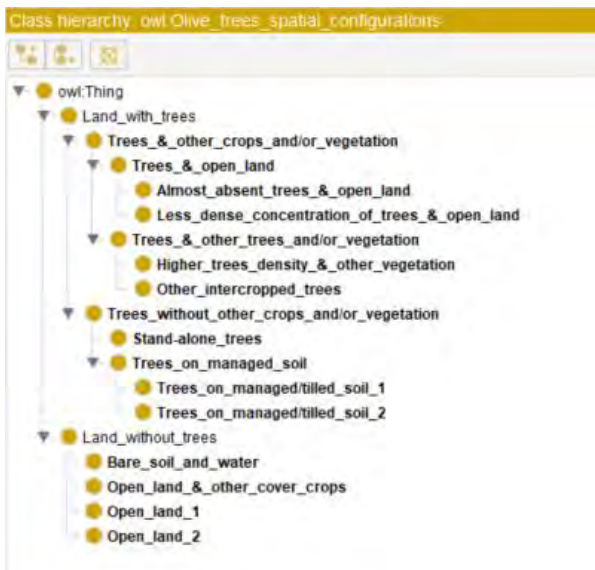


Figure 4: Spatial-relational ontology developed to interpret semantically the spatial objects extracted as described in the chapter "Development of ontology, in-field validation and classification of spatial objects".

In the spatial-relational ontology, on the first level of spatial complexity, a conceptual distinction is made according to the presence or absence of trees. The main classes are simply 'Land without trees' and 'Land with trees', which are super-objects in ontological terms (*sensu* Huang et al., 2017).

The two super-objects are then further classified, on a second level of spatial complexity, according to differences in each spatial arrangement of land-use:

- a) Within the super-object 'Land without trees', four different configurations can be distinguished:
 - 'Open land #1' (*open land type 1*)
 - 'Open land #2' (*open land type 2*)
 - 'Bare soil and water' (*bare soil, rocks, water*)
 - 'Open land & other cover crops'
- b) Within the super-object 'Land with trees', there are two different spatial configurations:
 - 'Trees & other crops and/or vegetation'
 - 'Trees without other crops and/or vegetation'

At a third, deeper, level of spatial complexity, the super-object 'Land with trees' can be further sub-divided.

Within the object 'Trees & other crops and/or vegetation', a distinction can be made between

- o Sub-object 'Trees and open land' (grassland) (trees intercropped with grasslands, pastures, etc.)
- and
- o Sub-object 'Trees & other trees and/or vegetation' (trees intercropped with other trees, cover crops and/or in plots where there are other significant vegetation features)

Within the object 'Trees without other crops and/or vegetation', a distinction can be made between

- o Sub-object 'Trees on managed soil' (trees on land which has been heavily worked by removing all vegetation apart from the trees)
- and
- o Sub-object 'Stand-alone trees' (trees scattered widely, or used as markers, or groups of trees used for fences).

At the final level of spatial complexity extracted, further divisions are made.

Within the object 'Trees & other crops and/or vegetation',

- o the sub-object 'Trees and open land' (grassland) is further distinguished according to the density of the trees into:
 - 'Less dense concentration of trees and open land'
 - 'Almost absent trees and open land'
- o the sub-object 'Trees & other trees and/or vegetation' is also further distinguished according to tree density into:
 - 'Higher tree density & other vegetation'

- ‘Other intercropped trees’

Within the object ‘Trees without other crops and/or vegetation’,

- the sub-object ‘Trees on managed soil’ is further distinguished into:
 - ‘Trees on managed/tilled soil #1’ (trees on land which has been heavily worked by removing all other vegetation and cover crops)
 - ‘Trees on managed/tilled soil #2’ (trees and bare soil, rock, concrete, etc.).

To cross-validate the semantic interpretation of the spatial objects extracted, fieldwork was carried out in the study site from June to November 2020. Three sampling units per class were taken (total: 33 samplings), in order to:

- 1) explore and confirm the local spatial configuration assigned to each class;
- 2) explore and confirm the content of each class in terms of vegetation composition and other existing relevant features;
- 3) collect further complementary data (e.g. size of tree trunks).

The spatial objects extracted from the orthophoto were classified according to the validated ontology; the resulting classes are shown in Figure 6.

Extraction of temporalities

In the final step of the methodology, the spatial classes extracted as described in chapter ‘Development of ontology, in-field validation and classification of spatial objects’ are used as temporal proxies to determine the different temporalities of the olive cultivation arrangements in the study site.

Spatial classes as temporal proxies

In the past, olive groves were mostly agro-forestry systems. The logic behind their spatial arrangements was to maximize the use of the empty spaces between the sparsely-planted trees by growing other crops (e.g. vegetables or fruit trees). Originally, local spatial configurations of olives are thought to have been scattered and sparse (Ruhl et al., 2011; Marchetti et al., 2002). Starting from this assumption, the authors referred to this configuration (sparse scattered olive trees) as T1 (time 1).

At a later stage, T2, more ‘structured’ orchards and groves began to appear, corresponding to intensified/optimized land use: instead of cultivating between widely spaced trees, land users preferred to focus on a single crop (the olive) and intensified its cultivation either by reducing the spaces between trees, or by removing competition from other crops (Ruhl et al., 2011; Barbera and Cullotta, 2016).

These temporal dynamics of land use and their intensification thus have spatial dimensions as well. These are *relational* in the sense that they are expressions of both cultural/social and natural/ecological processes.

Temporal interpretation, and re-classification of spatial classes as temporalities

Following these assumptions about changes in olive cultivation over time, the authors developed a temporal interpretation of the spatial classes extracted. The spatial classes were re-classified as temporalities:

- Within the Class ‘Trees & other crops and/or vegetation’, Class ‘Trees and open land’ is older than Class ‘Trees & other trees and/or vegetation’, since more widespread trees implies an older spatial arrangement for planting and land use.

With reference to the final class taxonomy described in chapter “Development of ontology, in-field validation and classification of spatial objects” (see Figure 6), the temporal progression is:

Class 2-1-1 (and relevant subclasses) = $T1_t\&v$ (time 1– trees and vegetation) > Class 2-1-2 (and relevant subclasses) = $T2_t\&v$ (time 2 – trees and vegetation) (see Table 1).

- Within the Class ‘Trees without other crops and/or vegetation’, a temporal distinction is possible at the 4th level of classification:

- Class ‘Trees on managed/tilled soil #1’ represents spatial patterns of trees that are older than Class ‘Trees on managed/tilled soil #2’ and Class ‘Stand-alone trees’, because it comprises widely-spaced and scattered trees, and because ‘Trees on managed/tilled soil #2’ also incorporates more recent objects, such as bare soil or concrete.

- Class ‘Stand-alone trees’ comprises trees which are scattered, and trees that in some cases look like borders, markers or fences. Such spatial configurations are probably older when found on worked land, but less old when associated with Class ‘Trees on managed/tilled soil #2’ (bare soil, concrete, road, etc.). The authors decided therefore that Class ‘Stand alone trees’ is less old than Class ‘Trees on managed/tilled soil #1’, but older than Class ‘Trees on managed/tilled soil #2’.

The temporal progression is thus: Class 2-2-1-1 = $T1_t\&ms$ (trees and managed soil) > 2-2-2-1 = $T2_t\&ms$ > 2-2-1-2 = $T3_t\&ms$ (Table 2).

Table 1: Temporal progression for Class ‘trees & vegetation’ (2-1).

	Time (t&v)	Class 2-1 (trees & vegetation)
Older	$T1_t\&v$	2-1-1
↓		
Younger	$T2_t\&v$	2-1-2

Table 2: Temporal progression for Class ‘trees & managed soil’ (2-2).

	Time (t&ms)	Class 2-2 (trees & managed soil)
Older	$T1_t\&ms$	2-2-1-1
↓		
	$T2_t\&ms$	2-2-2-1
↓		
Younger	$T3_t\&ms$	2-2-1-2

3 Results: Unpacked layers of space-time complexity

Thanks to the methodological approach developed and presented here, the authors were able to unpack the spatial and temporal complexity in the land-use dynamics of an apparently homogeneous area.

Through contextual and spatial-relational analysis, it was possible to extract spatial classes corresponding to different local configurations of olive trees (i.e. specific spatial arrangements of their cultivation, and spatial relationships with other vegetation and manmade features).

These classes are the expression of geographical contextual configurations, the result of strategies employed by people dwelling in the landscape, and adapting to it for land-use purposes: the classes correspond to different spatial logics in planting olive trees and, above all, increasing degrees of complexity in the spatial arrangements (Figure 5).

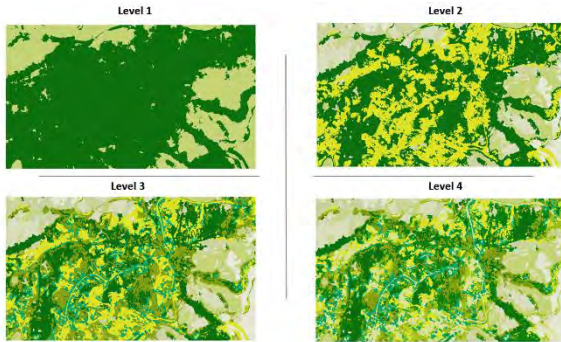


Figure 5: Different levels of relational complexity in the spatial arrangements of the land-use configurations extracted using the method devised by Malberg et al. (2014).

Supported by the development of a spatial-relational ontology, a higher level of semantic abstraction was reached in assigning a meaning to these classes, moving from purely geometric and spatial properties to the normative dimension of human land use. After validation in the field, the definitive classification of the spatial patterns extracted was finalized, as shown in Figure 6.

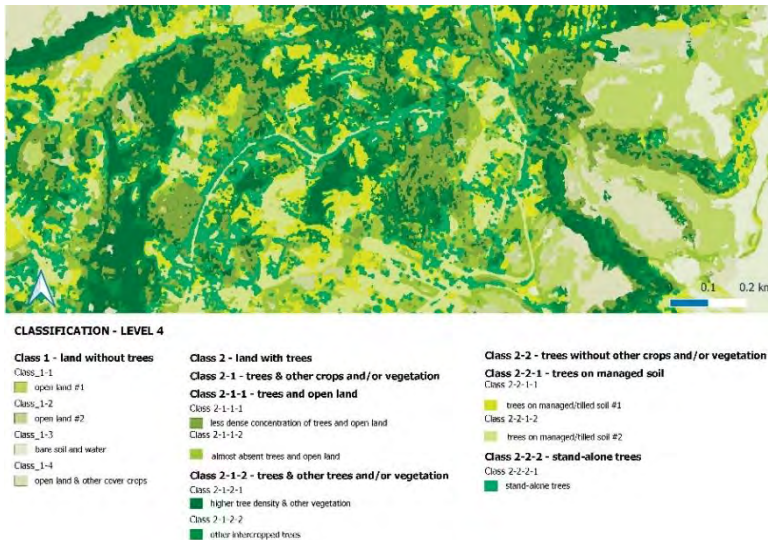


Figure 6: Final classification taxonomy.

In the last step of the approach (see chapter “Extraction of temporalities”), a trans-temporal representation of the geographical patterns of olive trees (Figure 7) was achieved, as the authors were able to extract different temporal dimensions from the local spatial configurations.

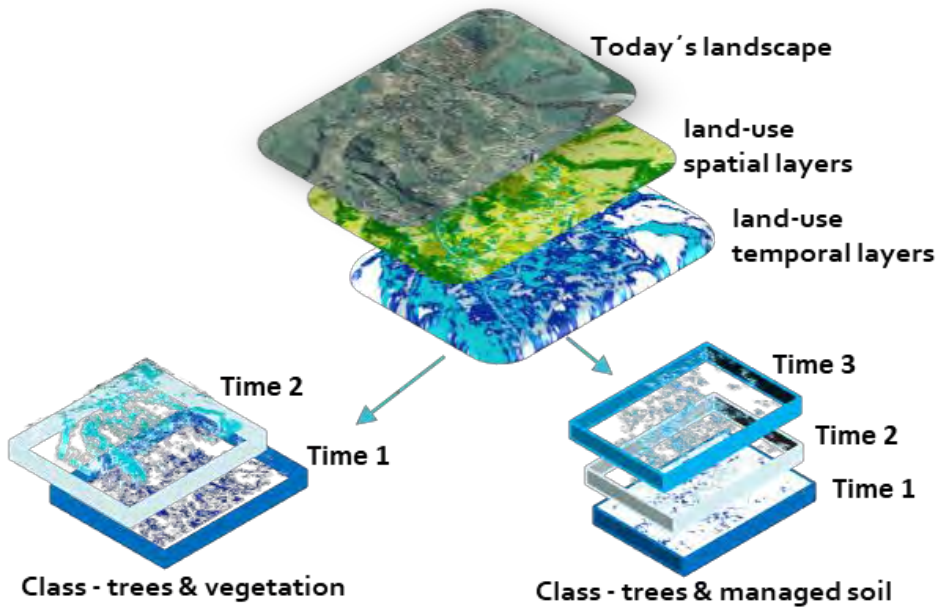


Figure 7: Different temporal dimensions of spatial configurations of olive trees extracted for Class 'trees & vegetation' and Class 'trees & managed soil'.

The overall result is very far from traditional land-cover or land-use maps, since here it is possible to visualize local contextual information corresponding to different human reasoning over time, which resulted in the different spatial configurations of the land-use practices.

4 Concluding discussion

Results obtained from the application of the approach presented here show that, by moving from the different reflectance levels of a remotely sensed image to meaningful categories of land use as composite, socially determined, spatio-temporal concepts (Wästfelt, 2015), it is possible to unpack the specific spatial configurations of land use during different periods.

By using evidence of biocultural heritage present in today's landscape as a 'bioindicator' of past land-use dynamics, and integrating methods from several different disciplines (historical ecology, archaeology, GIScience, philosophy, remote sensing), the authors developed a cross-disciplinary approach which is useful to inform analysis in deep time. Techniques for the extraction of spatial-relational data from remotely sensed images had not before been used to track land-use dynamics over the long term (i.e. over centuries or millennia) (Agapiou, 2020; Davis, 2019). Nor had the identification of contextual relations been used before to semantically uncover land-use categories and formally define them as conceptual spaces (Ahlqvist et al., 2012) correlated to different time periods. The methodology presented here may therefore be promising for transferability to, and applications in, human sciences and other disciplines studying landscape and land-use dynamics.

Of course, ground validation data must always substantiate the results from spatial analysis. One limitation of the work presented here is the lack of validation of the final temporal classification, which would require evidence provided by alternative dating methods (e.g. dendrochronology, or isotope analysis of plant and soil remains). Moreover, although described in a semi-formal notation, the spatial-relational ontology developed in this paper is still missing a true formalization according to the standards (e.g. OWL). The reason for this lies in the difficulties of developing formal ontologies when looking at landscape features in the context of human sciences and social interactions (Khazraee and Khoo, 2011; Janowicz et al., 2012). Nonetheless, perspectives found in the human sciences, such as historical ecology, can be used to achieve deeper interpretations of remotely sensed datasets. At the same time, advanced spatial analysis techniques may help as a further interpretative and directional tool. The integration of these different approaches could open up a dialogue across disciplinary boundaries and advance the scientific analysis of biocultural heritage.

Acknowledgements

This work was supported by Vetenskapsrådet (Swedish Research Council) as part of the research project ‘The Biocultural Heritage of Sicilian Olive Trees’, grant number 2020-02625.

The authors would like to thank the anonymous peer reviewers for their very helpful comments on this manuscript. Any errors are the responsibility of the authors.

References

- Agapiou, A. (2020). Evaluation of Landsat 8 OLI/TIRS Level-2 and Sentinel 2 Level-1C Fusion Techniques Intended for Image Segmentation of Archaeological Landscapes and Proxies. *Remote Sensing*, 12, 579.
- Ahlqvist, O., Wästfelt, A., Nielsen, M. (2012). Formalized interpretation of compound land use objects – Mapping historical summer farms from a single satellite image. *Journal of Land Use Science*, 7(1), 89-107.
- Argyridis, A., Argialas, D. (2019). Fuzzy ontology-based foreshore identification from digital terrain models and very high-resolution airborne imagery through GEOBIA multi-scale analysis. *International Journal of Geographical Information Science*, 33:11, 2153-2169.
- Barbera, G., Cullotta, S. (2016). The Traditional Mediterranean Polycultural Landscape as Cultural Heritage: Its Origin and Historical Importance, Its Agro-Silvo-Pastoral Complexity and the Necessity for Its Identification and Inventory (Part I, Chapter 1). In M. Agnoletti & F. Emanuelli (Eds.), *Biocultural Diversity in Europe*: Springer.
- Barthel, S., Crumley, C.L., Svedin, U. (2013). Biocultural refugia: combating the erosion of diversity in landscapes of food production. *Ecology and Society* 18(4), Article 71.
- Blaschke, T. (2010). Object based image analysis for remote sensing. *J. Photogramm. Remote Sens*, 50(1), 2-16.
- Blaschke, T., Hay, G.J., Kelly, M., Lang, S., Hofmann, P., et al. (2014). Geographic Object-based Image Analysis: A new paradigm in Remote Sensing and Geographic Information Science. *J. Photogramm. Remote Sens*, 87, 180–191.
- Calafiore, A., Boella, G., Borgo, S., Guarino, N. (2017). Urban Artefacts and Their Social Roles: Towards an Ontology of Social Practices. In E. Clementini, M. Donnelly, M. Yuan, C. Kray, P.

- Fogliaroni & A. Ballatore (Eds.) 13th International Conference on Spatial Information Theory (COSIT 2017), Article No. 6; pp. 6:1–6:13. Leibniz International Proceedings in Informatics. Schloss Dagstuhl – Leibniz-Zentrum für Informatik, Dagstuhl Publishing.
- Couclelis, H. (2009). The Abduction of Geographic Information Science: Transporting Spatial Reasoning to the Realm of Purpose and Design (Part VII, Chapter 1). In K.S. Hornsby, C. Claramunt, M. Denis & G. Ligozat (Eds.), *Spatial Information Theory. COSIT 2009. Lecture Notes in Computer Science*, vol 5756: Springer.
- Crumley, C. (2019). New Paths into the Anthropocene: Applying Historical Ecologies to the Human Future (Part I, Chapter 1). In C. Isendahl & D. Stump (Eds.), *The Oxford Handbook of Historical Ecology and Applied Archaeology*: Oxford University Press.
- Davis, D.S. (2019). Object-based image analysis: a review of developments and future directions of automated feature detection in landscape archaeology. *Archaeological Prospection*, 26: 155– 163.
- Ferrara, V., Ekblom, A., Wästfelt, A. (2019). Biocultural heritage in Sicilian olive groves; the importance of heterogeneous landscapes over the long term. In M.I. Goldstein & D.A. DellaSala (Eds.). 2020. *Encyclopedia of the World's Biomes*, Elsevier.
- Ferrara, V., Wästfelt, A., Ekblom, A. (forthcoming). From landscape as heritage to biocultural heritage in a landscape. The ecological and cultural legacy of millennial land use practices for future natures. In G. Pettenati (Ed). 2021. *Landscape as heritage: critical perspectives*. London, Routledge.
- Gobbi, S., Ciolli, M., La Porta, N., Rocchini, D., Tattoni, C., Zatelli, P. (2019). New Tools for the Classification and Filtering of Historical Maps. *ISPRS Int. J. Geo-Inf.*, 8, 455.
- Grauer, K.C. (2019). Active environments: Relational ontologies of landscape at the ancient Maya city of Aventura, Belize. *Journal of Social Archaeology*, 20(1), 74-94.
- Gurney, M.C., Townshend, J.R.G. (1983). The use of contextual information in the classification of remote sensed data. *Photogrammetric Engineering and Remote Sensing*, 49(1), 55-64.
- Hay, G.J., Castilla, G. (2008). Geographic Object-Based Image Analysis (GEOBIA): a new name for a new discipline. In: T. Blaschke, S. Lang, G. Hay (Eds.), *Object-Based Image Analysis*. Springer, Heidelberg, Berlin, New York, pp. 75–89.
- Huang, H., Chen, J., Li, Z., Gong, F., Chen, N. (2017). Ontology-Guided Image Interpretation for GEOBIA of High Spatial Resolution Remote Sense Imagery: A Coastal Area Case Study. *ISPRS Int. J. Geo-Inf.*, 6, 105.
- Janowicz, K., Scheider, S., Pehle, T., Hart, G. (2012). Geospatial semantics and linked spatiotemporal data – Past, present, and future. *Semantic Web* 3, 321–332. IOS Press.
- Khazraee, E., Khoo, M. (2011). Practice-Based Ontologies: A New Approach to Address the Challenges of Ontology and Knowledge Representation in History and Archaeology. In E. García-Barriocanal, Z. Cebeci, M.C. Okur, A. Öztürk (Eds.) *Metadata and Semantic Research. MTSR 2011. Communications in Computer and Information Science*, vol 240. Springer, Berlin, Heidelberg.
- Kokla, M., Guilbert, E. (2020). A Review of Geospatial Semantic Information Modeling and Elicitation Approaches. *ISPRS Int. J. Geo-Inf.*, 9, 146.
- Lambers, K., Traviglia, A. (2016). Automated detection in remote sensing archaeology: a reading list. *AARGnews* 53, 25-29.
- Lang, S., Hay, G.J., Baraldi, A., Tiede, D., Blaschke, T. (2019). GEOBIA Achievements and Spatial Opportunities in the Era of Big Earth Observation Data. *ISPRS Int. J. Geo-Inf.*, 8, 474.
- Lasaponara, R., Masini, N. (2014). Beyond modern landscape features: New insights in the archaeological area of Tiwanaku in Bolivia from satellite data. *International Journal of Applied Earth Observation and Geoinformation*, 26: 464-471.
- Lombardo, V., Damiano, R., Karatas, T., Mattutino, C. (2020). Linking Ontological Classes and Archaeological Forms. In: J. Z. Pan et al. (Eds.) *ISWC 2020, LNCS 12507*, pp. 700–715, Springer Nature Switzerland.

- Luo, L., Wang, X., Guo, H., Lasaponara, R., Zong, X., et al. (2019). Airborne and spaceborne remote sensing for archaeological and cultural heritage applications: A review of the century (1907–2017). *Remote Sensing of Environment*, 232, 111280.
- Magnini, L., Bettineschi, C. (2019). Theory and practice for an object-based approach in archaeological remote sensing. *Journal of Archaeological Science*, 107, 10-22.
- Malmberg, B., Nielsen, M., Wästfelt, A. (2014). Method for Performing Automatic Classification of Image Information. Patent No. 8,781,216. Washington, DC: U.S. Patent and Trademark Office.
- Manzano, S., Julier, A.C.M., Dirk, C.J., Razafimanantsoa, A.H.I., Samuels, I., et al. (2020). Using the past to manage the future: the role of palaeoecological and long-term data in ecological restoration. *Restor Ecol*, 28: 1335-1342.
- Marchetti, M., La Mantia, T., Messina, G., Barbera, G. (2002). Il significato dei popolamenti arborei ed arbustivi fuori foresta nel paesaggio agrario e la loro dinamica evolutiva in due aree campione della Sicilia. *L'Italia Forestale e Montana* 57(4), 369-389.
- Mathian, H., Sanders, L. (2015). *Spatio-temporal approaches: geographic objects and change process*. London; John Wiley & Sons.
- Pricope, N.G., Mapes, K.L., K.D. Woodward (2019). Remote Sensing of Human–Environment Interactions in Global Change Research: A Review of Advances, Challenges and Future Directions. *Remote Sens.*, 11, 2783.
- Rajbhandari, S., Aryal, J., Osborn, J., Musk, R., Lucieer, A. (2017). Benchmarking the Applicability of Ontology in Geographic Object-Based Image Analysis. *ISPRS Int. J. Geo-Inf.*, 6, 386.
- Ray, C., Fernández-Götz, M. (2019). *Historical Ecologies, Heterarchies and Transtemporal Landscapes*. London: Routledge.
- Ruhl, J., Caruso, T., Giucastro, M., La Mantia, T. (2011). Olive agroforestry systems in Sicily: Cultivated typologies and secondary succession processes after abandonment. *Plant Biosystems*, 145(1), 120–130.
- Schuurman, N. (2006). Formalization Matters: Critical GIS and Ontology Research. *Annals of the Association of American Geographers*, 96: 726-739.
- Sevara, C., Pregesbauer, M., Doneus, M., Verhoeven, G., Trinks, I. (2016). Pixel versus object — A comparison of strategies for the semi-automated mapping of archaeological features using airborne laser scanning data. *Journal of Archaeological Science: Reports*, 5: 485-498.
- Tapete, D. (2018). Remote Sensing and Geosciences for Archaeology. *Geosciences*, 8, 41.
- Traviglia, A., Torsello, A. (2017). Landscape Pattern Detection in Archaeological Remote Sensing. *Geosciences*, 7(4), 128.
- Wästfelt, A. (2015). Reclaiming Position: Using Local Context to Visualise Interpretations of Satellite Images in Humanities and Social Science. *Journal of Art History*, 84, 2, 108-122.
- Wästfelt, A. (2021). Landscape as filter - farm adaptation to changing contexts. *Journal of Land Use Science*, 1-17.

Automatic Detection of Driving-Lane Geometry Based on Aerial Images and Existing Spatial Data

Jakub Růžička and Lukáš Brůha
Charles University, Prague, Czechia

Abstract

Spatial data are a key element of geographic information systems (GIS). With the growing computational power of modern GIS, the demand for accurate and up-to-date high definition (HD) spatial data grows accordingly and increases the requirements of data acquisition. To simplify and automate the process of obtaining HD road data, several methods have been created with different approaches and stages of automation. A new method combining high resolution aerial images and existing linear road data is presented in this article. The method models roads in a vector environment at the level of single driving lanes. Object-based image analysis (OBIA) is used to identify road surface markings (RSMs) in aerial images; the geometry of RSM polygons is analysed (skeletonization, neighbourhood and context analysis, pattern recognition) in order to obtain a coherent network of driving lanes. The technique is able to distinguish automatically between solid and broken lines. The method proposed was tested and proven to satisfactorily model driving lanes, including in complex situations like junctions, roundabouts or over- or underpasses.

Keywords:

driving lanes, road surface markings, road geometry, aerial image analysis

1 Introduction

High definition (HD) spatial data are a prerequisite for sub-object-level analyses, such as identifying a location within a building, or determining the exact location of a car on a road, at the level of the specific lane on which it is travelling. Sub-object level of detail (road – object level; driving lane – sub-object level) is necessary for multiple purposes, especially within smart traffic management and autonomous driving. GPS tracks of vehicles (see e.g. Guo et al. 2007) or vehicles' on-board sensors (Gupta and Choudhary 2018) may be used to obtain HD road data. However, these mapping methods would be costly and ineffective for mapping large areas, and such mapping would not necessarily represent the car's position in a driving lane as marked on the road, but habitual lanes which drivers are accustomed to use (e.g. cutting sharp bends, or crossing lane separators in order to smooth their trajectory). A different approach is to use high resolution (aerial) imagery, where traffic lanes can be identified thanks to road surface markings (RSMs). Current segmentation and classification methods are able to identify

the different spectral values of markings and the surrounding road surface. Geometry analysis of identified RSM polygons would follow, to obtain a consistent network of driving lanes.

Extensive research has been done in identification and extraction of roads from satellite or aerial imagery; Wang et al. (2016) may serve as an overview. Most of the research, however, has been focused on identifying roads in satellite or aerial images rather than on identifying driving lanes within roads; therefore, only a limited amount of previous research is presented here.

Bakhtiari et al. (2017), Cheng et al. (2016), Hormese and Saravanan (2016), Leninisha and Vani (2015), Mátyus et al. (2017), Shahi et al. (2015), Xia et al. (2018), Yuan et al. (2009) and Zhang et al. (2018) describe the (semi-)automatic detection of road networks in airborne imagery. Their methods vary for identifying roads, and for overcoming the problems posed by road divisions at junctions, discontinuity in shadows, or misclassified areas. Jin, Feng and Li (2009) and Jin and Feng (2010) present two different methods for detecting driving lanes in aerial imagery. However, both studies end with identifying pixels of RSMs, and no geometry analysis of the network of driving lanes follows.

The pioneering work of Baumgartner and Hinz (2003) proposed extracting driving lanes from high-resolution aerial imagery in complex urban areas. Their results, however, have limited spatial accuracy and the resulting network has a lot of gaps and overlaps. Higher spatial accuracy was achieved by Jin et al. (2012) with their method of detecting RSMs in aerial imagery using Gabor filters. They did not carry out further geometry analysis of RSMs; nor did they address fading RSMs or long gaps in RSM lines. Seo (2012), on the other hand, combined aerial images with a rasterized representation of roads, and implemented a context analysis of single pixels and their iterative grouping to form driving lanes. However, computation in a raster environment is performance-intensive, and the use of topology and context rules is limited to a close neighbourhood of pixels. More recently, Fischer et al. (2018) combined OpenStreet Map (OSM) road data with aerial imagery and detected RSMs using the Random Forest classifier and Gabor Filtering. However, their method was tested only on highways, and the authors anticipated inadequate results for other types of roads, notably in urban environments.

The main objective of the method proposed in this paper is to create a vector representation of driving lanes using aerial imagery and vector road axes, like Fischer et al. (2018). However, the method is applicable to all types of road, including junctions, roundabouts, highway crossings and over-/underpasses. Similar to the method devised by Hormese and Saravanan (2016), in our approach object-based image analysis (OBIA) is used to identify polygons of RSMs in aerial images; the RSMs detected are further analysed to create a coherent network of driving lanes (similar to Baumgartner and Hinz's (2003)). The result is a linear network of driving-lane *borders* (in this, it is unlike the polygons of driving lanes in Baumgartner and Hinz (2003)). The method will be capable of modelling driving lanes in places where no RSMs are visible or detected. It uses road axes as a geometry source for the driving lanes leading to more accurate gap-bridging than in Jin et al. (2012). Unlike Seo (2012), the geometry analysis is carried out in a vector environment, which leads to better computational performance and the possibility of using topology rules. The proposed method distinguishes the pattern of RSM lines (broken or solid).

2 Materials and methods

The first step of the analysis is to detect RSMs in multispectral aerial images using OBIA. To extract RSM polygons, the pixel size must be smaller than or equal to the width of the narrowest RSM line, ideally at least as small as half the width. The parameters of RSM lines are defined by law or technical specification documents, and may vary from country to country. Using state-of-the-art aerial scanners, it is possible to obtain images with a spatial resolution of 2.5 cm (Holmes, 2012). The analysis described in this paper was carried out on multispectral (RGB) aerial imagery with a spatial resolution of 0.1 m (see details in Section 0).

2.1 Image classification

OBIA comprises two steps: image segmentation and segment classification. Various criteria can be used for segmentation, and it is possible to run the segmentation iteratively at multiple different scales. For identification of the RSMs, multi-resolution image segmentation with two iterations was used (scale factors 100 and 20), with a shape/colour ratio of 0.1/0.9 and a smoothness/compactness ratio of 0.5/0.5.

There are multiple parameters that can be used to classify segments (band values; geometrical, positional or textural characteristics; hierarchy; attributes, etc.); even segment-, scene- or region-related features can be used. RSMs are characterized by their colour, which leads to brightness being one of the most relevant criteria. To exclude other objects with similar brightness, geometry characteristics (width, and length:width ratio) are used, because RSMs consist of narrow lines with a specified width. As Fischer et al. (2018) suggest, roads (road axes) are used as buffers or limits to the area in which OBIA is applied, thus preventing misclassification of objects which are not located on roads. Nevertheless, redundant polygons such as cars, truck trailers, bright pavements or dust polygons (i.e. areas of dust, dirt or debris) can be misclassified and have to be removed during the geometry analysis. Polygons identified as RSMs (Figure 1) are used in the next step to detect RSM lines.

2.2 RSM geometry detection



Figure 1:
Classified RSM (red). Source: Author's visualization, aerial image IPR Prague

Classified RSMs consist of a vast number of small polygons, created during the segmentation. In order to create topologically correct RSM lines, these polygons are merged and further processed to remove geometrical inaccuracies (dangles, zigzags, irregular shapes etc.). The process of RSM geometry detection is illustrated step by step in Figure 2. Combining small neighbouring polygons into one polygon is the first step of the process. Next, agglomerates must have a main direction (i.e. a significant difference between height and length) in order to be skeletonized correctly in the following steps. Polygons which do not fulfil this condition represent a specific type of broken line and are processed separately. Agglomerates with evident main direction are thinned to the same degree (i.e. are given the same width) in order to reduce over/under-classification. Skeletonization of thinned polygons follows, and the resulting skeletons are simplified using the Douglas-Peucker algorithm (Douglas and Peucker, 1973) to prevent the resulting lines from zigzagging.

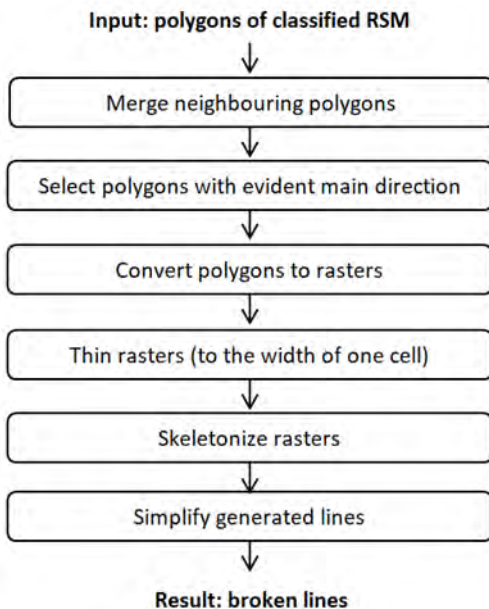


Figure 2: RSM geometry detection

2.3 Detection of driving lanes

RSM lines created in the previous step serve as the source of information about driving lanes, although one cannot fully rely on these as the only source. There may be cases where no RSM lines have been created (e.g. in shadows or on road patches) and additional data has to be taken into account. First, modelled RSM lines are analysed in order to create driving lanes (**Fehler! Verweisquelle konnte nicht gefunden werden.**); gaps (i.e. where there are no RSM lines) are then resolved.

Creating driving lanes can be simplified by interconnecting single RSM lines into continuous lines (borders of driving lanes); however, RSM line segments which are not borders of driving lanes (directional arrows, diagonal hatching, stop lines, etc.) have to be removed. This is done

by: (1) comparing the orientation of these particular segments with the closest road axis; the dataset of roads used for the purpose must therefore have appropriate scale, completeness and correctness; (2) calculating the distance to its nearest neighbour in the main direction of the line; when a line is too isolated (i.e. has no neighbour closer than a threshold value), it is not considered to be part of a driving lane border and is removed.

Interconnecting single RSM lines (bridging gaps between broken lines or short spaces between solid line segments) is performed using buffers. Two directions of buffer (of different sizes) are used: a small buffer in line segments with a transverse direction to eliminate small differences in orientation, and a larger buffer in line segments with a longitudinal direction to bridge gaps between neighbouring segments. (The size of the longitudinal buffer is a parameter that can vary under different RSM regulations.) Buffers of all segments are merged (in case they intersect) and skeletonized. Next, the dangles of skeletons are removed and the second criterion (distance to neighbour) is applied to remove the segments which are not driving-lane borders.

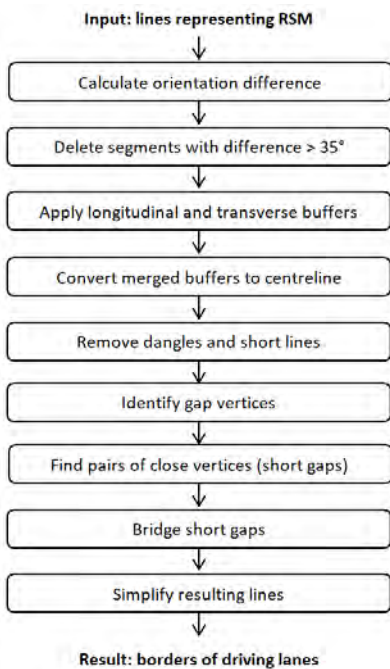


Figure 3: Driving lane detection

Two types of undesirable gap can occur in RSM borders: ‘short’ and ‘long’ ones. Gaps are identified as distances between the closest start/end vertices; the threshold distance between a short and a long gap is a numerical parameter whose value was determined experimentally as 3 metres. A short gap is created by misclassification of the aerial image (different brightness values in RSM lines, narrow shadows) or of real-life objects on the road surface (road patches, cars). Long gaps appear in places where RSM lines were not identified due to shadows (of trees or buildings), poor maintenance (fading lines), or where RSMs cannot be identified (e.g. under bridges or in tunnels). Their analysis is described in Section 0. To bridge short gaps, start/end

vertices are interconnected (i.e. a line is created between them), and the lines forming their connections are appended to the resulting dataset. After all vertex pairs are analysed, the resulting lines are simplified in order to remove potential zigzags and smooth the resulting line.

2.4 Bridging long gaps

In instances of long gaps without RSMs, the border between driving lanes has to follow the direction of the road; it cannot be simplified to a straight-line connection between its vertices. In other words, if the gap is located in a bend, the line created also has to have a curved shape. Therefore, the second input dataset (vector road dataset) is necessary in this step as the geometry source.

Long gaps have to be reviewed manually, and a decision has to be made about which gaps are to be bridged (in some cases, e.g. at junctions, a gap is correct). Next, a loop over gaps to be bridged starts the bridging process (one gap per iteration is bridged). Inside the bridging loop, the start point of a gap is identified, and a perpendicular projection vector of the start point on the corresponding road axis is calculated. A point is created for each vertex of the axis; an opposite vector to the perpendicular projection vector (a 'shift' vector) is added to the points created, thus 'shifting them back' on the missing RSM line. Once the projected point gets close enough to the endpoint of the gap, the gap has been bridged, the iteration is terminated, and the loop is repeated for the next gap until all gaps are bridged (see Figure 4 for details). In the final step, all bridging lines are appended to the driving-lane borders, and all the resulting lines are simplified to remove unwanted zigzags caused by combining locations from two different datasets (identified RSM lines and road axes).

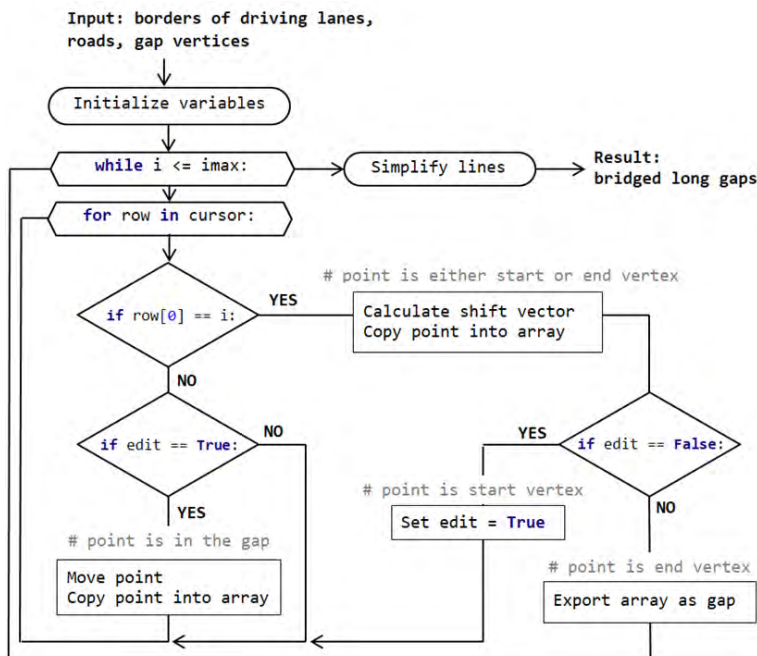


Figure 4: The loop for bridging long gaps

2.5 Identifying broken lines

The last step is based on the geometry analysis performed in the previous steps and adds attribute information about the line pattern to the resulting dataset. Broken lines excluded from the original process described in Section 0 may be analysed during this step or processed as a long gap (see Section 0).

The identification of broken lines (Figure 5) involves combining the geometry of the driving lanes modelled with the pattern information of the RSM lines created. The lengths of the broken line segments are standardized, and the resulting length serves as the criterion for selecting line segments in this step. The broken lines extracted may function as a stand-alone dataset, or the pattern information can be used as an attribute in the original dataset of driving lanes.

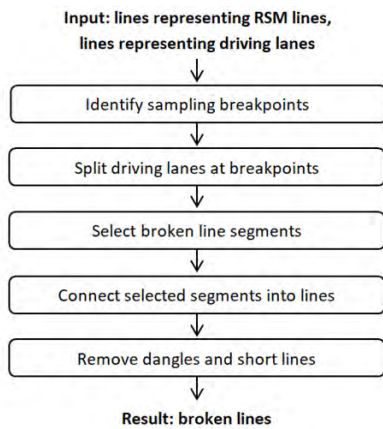


Figure 5: Identifying broken lines

3 Testing and results

The method was tested in a suburban area of Prague. Multiple small areas with an average size of 5,000 m² and various types of road infrastructure (including junctions, roundabouts, bends, multiple lanes in one direction, changes in the number of lanes, overpasses and underpasses) were chosen. The main goal of the test was to find out how the method coped with different types of road infrastructure rather than to evaluate its computational costs on a large amount of data.

Aerial imagery acquired during the non-vegetative season, provided by the Institute of Planning and Development of the capital city of Prague (IPR Prague), was used to minimize the influence of tree shadows. The imagery was recorded in the visible spectrum (RGB) using the digital sensor UltraCam Eagle Mark 3 from a flight height of approximately 2,500 m, with a spatial resolution of 0.1 m. Roads from OSM were used as the vector dataset of road axes.

Imagery was classified in e-Cognition Developer v9.5.0.; the geometry analysis was implemented in Python 3.6 using ArcPy library (ESRI 2020). The method was split into five

algorithms which were run consecutively in order to have better control over intermediate results.

This section is divided into two parts: first, modelled RSM lines (the first step of the analysis described in Section 0) are presented and discussed; second, the driving lanes modelled (the second step of the analysis described in Section 0) are discussed.

3.1 RSM lines

The first step of the geometry analysis and the first output dataset are lines representing RSMs (Figure 6). The positional accuracy of the lines created was assessed using root-mean-square error (RMSE) of more than 200 randomly assigned points. A line drawn on a road surface is technically a polygon, because the lines have a width – of 0.125 or 0.25 m, depending on type. Modelled RSM lines do not have width. The total RMSE of the modelled RSM lines is 0.126 metres.

The following shortcomings were identified, which would need to be taken into account if using this method on a large scale. However, solving these shortcomings is not within the scope of this paper.

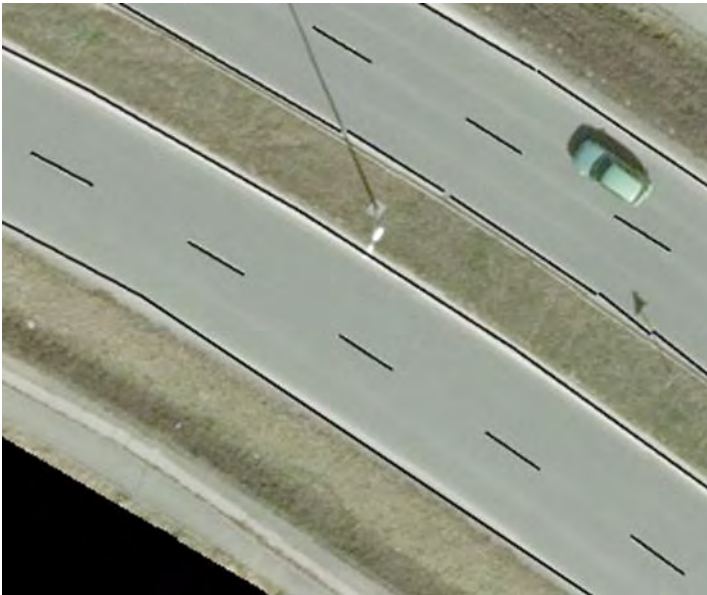


Figure 6: Modelled RSM lines (black). Source: Author's visualization, aerial image IPR Prague

Diagonal hatching

Diagonal hatching sometimes causes straight lines to oscillate (Figure 7). The oscillation was not removed during line simplification, because the lines of diagonal hatching intersect with the oscillating line. (The position of the intersection points remains unchanged.) A possible solution could be the elimination of diagonal hatching from the process at this stage. However,

the diagonal hatching lines are part of RSMs; therefore, their elimination would not always be an appropriate solution. For such cases, lines of diagonal hatching have to be removed from the process before the simplification, then added to and interconnected with the simplified lines after the simplification.



Figure 7: Oscillating line caused by diagonal hatching (on the left) and correctly created straight line (on the right). Source: Author's visualization, aerial image IPR Prague

Crash barriers, railings and other misclassified objects

Long and narrow objects with a similar brightness value are often misclassified as RSM lines during the classification, causing the RSM lines identified to be shifted closer to the edges of roads, or even away from roads. It is difficult to identify (and exclude) such objects during OBIA because their spatial and spectral characteristics are similar to those of RSMs. Consequently, such objects have to be excluded during the geometry analysis, possibly depending on the width of the driving lanes. However, this would require information about road width in the input road dataset.

Shadows

Shadows present in the original aerial image affect the brightness values of RSM lines and result in them being misclassified. Where narrow shadows are cast by streetlamps or traffic signs (see Figure 6 for examples), modelled RSM lines are broken into shorter segments or vanish completely when shaded by buildings or trees. The resulting gaps could be bridged using the same approach as for the gaps found when modelling driving lanes. However, this would require a manual review of cases to be bridged, as when bridging long gaps.

3.2 Driving lanes

Driving lanes (Figure 8) were modelled with a RMSE of 0.149 metres. The driving lanes created reflect the quality of the RSMs modelled; that is, they are influenced by the shortcomings of the modelling. The procedure includes steps to bridge gaps, leading to the complete elimination of undesired gaps.

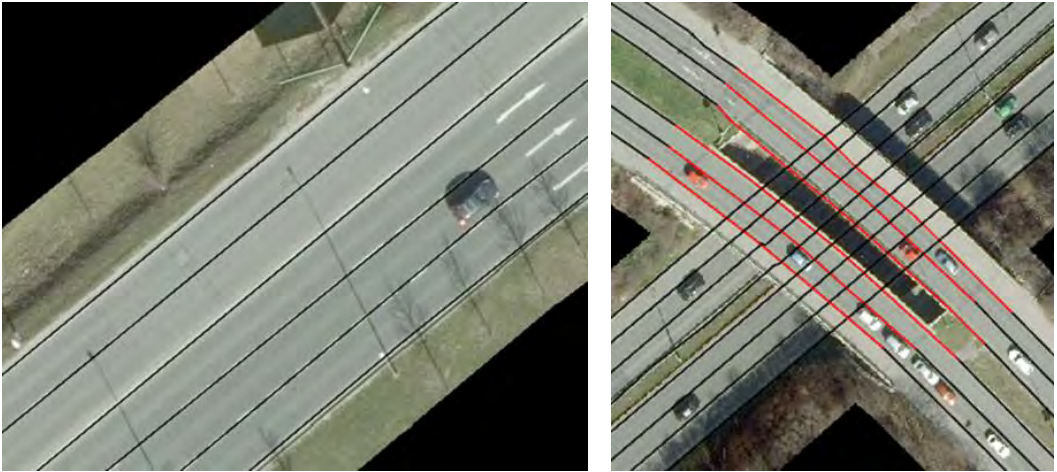


Figure 8: Modelled driving lanes, showing (on the right) an overpass with multiple levels (surface in black; bridge in red). Source: Author's visualization, aerial image IPR Prague

The problem of bridges and tunnels is solved in a semi-automated way – the location of a bridge or a tunnel has to be identified manually and is divided into multiple surface levels; each level is then analysed and modelled separately. The driving lanes created are merged into one dataset, with no differences between levels (see Figure 8, right), and with no splitting of the original dataset. It might be possible to automate the identification of the various levels, by splitting and merging processes, and through further querying of the input data in such a way as to show the locations of bridges and tunnels, either in another input layer, or as attributes of the road data being used.

Two phenomena causing inaccuracies in the resulting driving lanes were identified: undesired line oscillation, and incoherent geometry of input road lines.

Undesired line oscillation

The irregular shape of the driving lanes created is caused when an object is covering the original RSM line in the aerial image (e.g. a drainage cover and a shadow, in Figure 9 left and right respectively), resulting in a gap in the modelled RSM. In specific cases, road debris or dust polygons in the immediate vicinity of these gaps might be misclassified as RSMs and identified as the segment closest to both ends of the gaps. The misclassified objects then become incorporated into the network of drivinglanes, causing the resulting lines to oscillate.



Figure 9: Line oscillation caused by a drainage cover (left) and a shadow (right). Source: Author's visualization, aerial image IPR Prague

Incoherent geometry of input road lines

Lines created in order to bridge long gaps always copy the geometry of the input road dataset. An undesired shift of the resulting driving lanes can therefore appear when road lines with an inappropriately small scale are used (**Fehler! Verweisquelle konnte nicht gefunden werden.**). As mentioned in Section 0, the same distance from gap to road axis (shift vector) is used; consequently, the axis must retain the same distance from the missing RSM line throughout the whole gap. An abrupt change in the number of driving lanes at a junction can lead to a change of the shift vector and thus to incorrect results (see **Fehler! Verweisquelle konnte nicht gefunden werden.** for visualization).

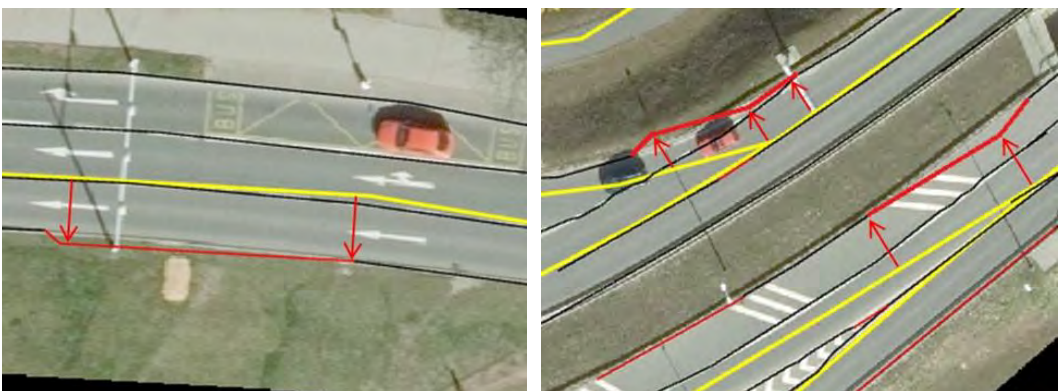


Figure 10: Bridged gaps (red) compared to input road lines (yellow); insufficient scale of input road line on the left and abrupt change of driving lanes at a junction on the right; red arrows symbolize the shift vectors. Source: Author's visualization, aerial image IPR Prague

4 Conclusion and outlook

A semi-automated method of identifying driving lanes in aerial images was developed, as presented in this article. The method requires two input data sources: high-resolution aerial images in the visible spectrum (RGB) with recognizable road surface marking, and polylines of road infrastructure (axes of roads). Furthermore, both datasets should depict the road network in a coherent manner (i.e., there should be no differences between the road geometries). The method is able to handle situations in which the road is blocked from view by bridges or in tunnels, and complex situations like junctions, roundabouts or a change in the number of driving lanes.

The first step is object-based image analysis to identify RSM polygons in the input aerial image. Next, the geometry of the classified RSM polygons is analysed in order to obtain a vector (linear) representation of RSMs, from which the vector (polyline) network of driving lanes is derived. Pattern analysis of the classified RSMs identifies broken lines, and the pattern information is appended as attributes.

The proposed method has been tested in multiple case study areas covering various types of road infrastructure, including junctions, main roads with multiple driving lanes, pedestrian crossings, over- and under passes. The positional accuracy of the results modelled was evaluated using RMSE, reaching 0.126 metres for RSM lines, and 0.149 metres for driving lanes. After taking into account the width of the RSM lines, which vary between 0.125 and 0.25 metres, and the spatial resolution of the input aerial imagery (0.1 metres), it can be stated that the positional accuracy is sufficient.

Several shortcomings were identified during the testing. Further research is needed to improve the method in order to obtain a full working solution for the detection of driving lanes. It is possible that increasing the resolution of the input aerial imagery or the classification itself could improve the quality of the results. Another way to achieve more accurate results would be to improve the maintenance of RSMs in the first place to avoid fading lines, lines being covered by debris, or other classification errors.

This research is innovative in modelling driving lanes from aerial imagery in a vector environment. We believe that using aerial imagery to detect driving lanes is more promising than analysing GPS traces or images from on-board cameras. However, more research is required to devise a method that is suitable for use on a larger scale.

Acknowledgements

This article is based on the research for a Master's thesis carried out in 2020 by Jakub Růžička under the supervision of Lukáš Brůha at the Department of Applied Geoinformatics and Cartography of the Faculty of Science, Charles University.

Input aerial imagery was provided by the Institute of Planning and Development of the Capital City of Prague (IPR Prague), licensed under CC BY-SA 4.0 [<http://creativecommons.org/licenses/by-sa/4.0/>]. The road centrelines used for the research originated in OpenStreet Map (OSM), licensed under CC-BY-SA 2.0 [<https://creativecommons.org/licenses/by-sa/2.0/>].

References

- Aeberhard, M., Rauch, S., Bahram, M., Tanzmeister, G., Thomas, J., Pilat, Y., Homm, F., Huber, W., Kaempchen, N. (2015): Experience, Results and Lessons Learned from Automated Driving on Germany's Highways. *IEEE Intelligent transportation systems magazine*, 7(1), 42–57. DOI: 10.1109/MITS.2014.2360306
- Bakhtiari, H. R. R., Abdollahi, A., Rezaeian, H. (2017): Semi-automatic road extraction from digital images. *The Egyptian Journal of Remote Sensing and Space Sciences*, 20, 117–123. DOI: 10.1016/j.ejrs.2017.03.001
- Baumgartner, A., Hinz, S. (2003): Automatic extraction of urban road networks from multi-view aerial imagery. *ISPRS Journal of Photogrammetry & Remote Sensing*, 58, 83–98. DOI: 10.1016/S0924-2716(03)00019-4
- Cheng, G., Zhu, F., Xiang, S., Wang, Y., Pan, Ch. (2016): Accurate urban road centerline extraction from VHR imagery via multiscale segmentation and tensor voting. *Neurocomputing*, 205, 407–420. DOI: 10.1016/j.neucom.2016.04.026
- Douglas, D. H., Peucker, T. K. (1973): Algorithms for the Reduction of the Number of Points Required to Represent a Digitized Line or Its Caricature. *The Canadian Cartographer*, 10(2), 112–122
- ESRI, Environmental Systems Research Institute (2020): ArcGIS Pro Python reference. Redlands, California. Retrieved from <https://pro.arcgis.com/en/pro-app/latest/arcpy/main/arcgis-pro-arcpy-reference.htm>
- Fischer, P., Azimi, S. M., Roschlaub, R., Krauß, T. (2018): Towards HD Maps from Aerial Imagery: Robust Lane Marking Segmentation Using Country-Scale Imagery. *ISPRS International Journal of Geo-Information*, 7 (458), 1-14. DOI: 10.3390/ijgi7120458
- Guo, T., Iwamura, K., Koga, M. (2007): Towards high accuracy road maps generation from massive GPS Traces data. 2007 IEEE International Geoscience and Remote Sensing Symposium – Conference Proceedings, 1, 667-670. DOI: 10.1109/IGARSS.2007.4422884
- Gupta, A., Choudhary, A. (2018): A Framework for Camera-Based Real-Time Lane and Road Surface Marking Detection and Recognition. *IEEE Transactions on Intelligent Vehicles*, 3(4), 476 – 485. DOI: 10.1109/TIV.2018.2873902
- Holmes, O. (2012): High Resolution Digital Aerial Imagery vs High Resolution Satellite Imagery – Part 1. Retrieved from <https://aerometrex.com.au/technical/high-resolution-digital-aerial-imagery-vs-high-resolution-satellite-imagery-part-1/>
- Hormese, J., Saravanan, C. (2016): Automated Road Extraction From High Resolution Satellite Images. *Procedia Technology*, 24, 1460– 1467. DOI: 10.1016/j.protcy.2016.05.180
- Jin, H., Feng, Y. (2010): Automated road pavement marking detection from high resolution aerial images based on multi-resolution image analysis and anisotropic Gaussian filtering. *Proceedings of the 2nd International Conference on Signal Processing Systems (ICSPS)*, 1, 337–341. DOI: 10.1109/ICSPS.2010.5555636
- Jin, H., Feng, Y., Li, Z. (2009): Extraction of road lanes from high-resolution stereo aerial imagery based on maximum likelihood segmentation and texture enhancement. *Digital Image Computing: Techniques and Applications. Conference proceedings*. 1, 271-276. DOI: 10.1109/DICTA.2009.52
- Jin, H., Miska, M., Chung, E., Li, M., Feng, Y. (2012): Road Feature Extraction from High Resolution Aerial Images Upon Rural Regions Based on Multi-Resolution Image Analysis and Gabor Filters. In Escalante, B.: *Remote Sensing – Advanced Techniques and Platforms*. China: InTech, Shanghai.
- Leninisha, S., Vani, K. (2015): Water flow based geometric active deformable model for road network. *ISPRS Journal of Photogrammetry and Remote Sensing*, 102, 140–147. DOI: 10.1016/j.isprsjprs.2015.01.013

- Máttyus, G., Luo, W., Urtasun, R. (2017): DeepRoadMapper: Extracting Road Topology from Aerial Images. 2017 IEEE International Conference on Computer Vision (ICCV) Proceedings, 3458–3466. DOI: 10.1109/ICCV.2017.372
- Seo, W.-Y. (2012): Augmenting Cartographic Resources and Assessing Roadway State for Vehicle Navigation. PhD Thesis, April 2012, The Robotics Institute, Carnegie Mellon University, Pittsburgh, PA 15213, USA.
- Shahi, K., Shafri, H. Z. M., Taherzadeh, E., Mansor, S., Muniandy, R. (2015): A novel spectral index to automatically extract road networks from WorldView-2 satellite imagery. *The Egyptian Journal of Remote Sensing and Space Sciences*, 18, 27–33. DOI: 10.1016/j.ejrs.2014.12.003
- Wang, W., Yang, N., Zhang, Y., Wang, F. (2016): A review of road extraction from remote sensing images. *Journal of Traffic and Transportation Engineering (English Edition)*, 3 (3), 271–282. DOI: 10.1016/j.jtte.2016.05.005
- Xia, W., Zhang, Y., Liu, J., Luo, L., Yang, K. (2018): Road Extraction from High Resolution Image with Deep Convolution Network – A Case Study of GF-2 Image. 2nd International Electronic Conference on Remote Sensing, Proceedings 2 (325). DOI: 10.3390/ecrs-2-05138
- Yuan, J., Wang, D., Wu, B., Yan, L., Li, R. (2009): Automatic Road Extraction from Satellite Imagery Using LEGION Networks. *Proceedings of International Joint Conference on Neural Networks*, 1, 3471–3476. DOI: 10.1109/IJCNN.2009.5178605
- Zhang, Z., Zhang, X Sun, Y., Zhang, P. (2018): Road Centreline Extraction from Very-High-Resolution Aerial Image and LiDAR Data Based on Road Connectivity. *Remote Sensing*, 10

Multidimensional Exploratory Spatial Data Analysis

Oliver Hennhöfer¹, Julian Bruns¹, Peter Ullrich¹, Andreas Heiß², Galibjon Sharipov²
and Dimitrios Paraforos²

¹Disy Informationssysteme GmbH, Germany

²University Hohenheim, Germany

Abstract

The assessment of spatial autocorrelation is one of the primary tasks in geographical data analysis. Identifying and examining deviations from the expected autocorrelation is key to gaining a thorough understanding of the phenomenon under investigation. Traditional measures of geospatial sciences focus on the detection of spatial clusters or spatial heteroscedasticity, often in low-dimensional data. However, phenomena are often multidimensional and interdependent – both with and without their spatial dependency – and the toolbox of geospatial sciences is not yet well developed in this regard. The present study aims to contribute to this toolbox for scientists and practitioners. The proposed approach focuses on the detection of spatial discontinuity, considering heteroscedasticity by spatially contrasting residuals from a fitted spatial error model (SEM). This *contrast-enhancing* technique identifies locations whose attributes differ significantly from those of the surrounding features, and with that the technique indicate spatial breaks. The approach is evaluated using agro-ecological field data to identify anomalies and was originally motivated for application in the context of precision farming. Our results enhance understanding of the underlying spatial processes of agricultural fields. The findings contribute to advanced, multidimensional, exploratory, spatial data analysis and present an alternative approach to conventional methods.

Keywords:

heteroscedasticity, heterogeneity, spatial autocorrelation, spatial discontinuity, spatial error model, spatial outlier detection, spatial regression

1 Introduction

Exploratory data analysis is the first step in any data-driven analysis. It allows researchers to pose the question of why something is happening and provides the foundation for formulating hypotheses and for deriving confirmatory analysis (Tukey, 1977). Typical approaches to detect phenomena of interest include outlier or clustering detection methods. Within the field of spatial analysis, we extend our questions: not only why is this happening, but why is this

happening here? Therefore, we are interested in the detection of spatial anomalies. In the context of this work, we differentiate between outliers in general and what we define as anomalies. The difference is that an anomalous observation of interest belongs to the underlying population, whereas the term ‘outlier’ covers anomalies as well as erroneous observations.

We will focus solely on what we will define as contextual anomalies. These appear exclusively when observations are contextualized using certain observations of other variables – for example, when an unusually high deviation from the observed relationship between two or more observations in one location can be determined. In this study, the presence of potentially prevalent heteroscedasticity will be taken into consideration. A simple example from precision farming can illustrate this. While traditional hotspot analysis may indicate where soils are particularly fertile, contextual anomaly detection can explain where observations were expected based on (known) environmental conditions, and where the actual observations made may indicate an anomaly, according to a predefined model. These are rarely the focus of new methods in the field of typical spatial exploratory analysis, and few methods are in common use. However, in agro-ecological research, we often find that the parameter of interest is (spatially) dependent on several different external factors. For example, the anticipated crop yield may be dependent on weather, different qualities of the soil, and the spatial distribution of fertilizer. As each parameter influences the yield, we would expect their impact to be spatially homoscedastic. However, deviations from this can lead to interesting new questions and insights, often associated with the identification of factors that had been omitted. As the number of parameters adds up, it becomes increasingly difficult to understand the respective models and to identify anomalies – even for trained geographers and experts in this particular domain.

We aim to provide an intuitive and easy-to-understand method for the detection and visualization of these phenomena without extensive input by the analyst. We call our approach the Contrast-Enhancing Spatial Error Model (CESEM).

2 Related Work

The detection of spatial anomalies and unusual spatial patterns in multivariate ecological datasets is a research area that has remained largely untouched. Where powerful machine-learning approaches fail in practice due to low data availability, more traditional statistical methods for outlier detection are not particularly suitable either, since spatial data often violate important underlying statistical assumptions.

Spatial statistics tries to bridge this gap by offering a wide range of tools that are adapted to the characteristics of spatial data, and able to take spatial autocorrelation into account. Two of the most popular methods using spatial statistics for outlier detection – specifically for detecting statistically-significant clusters of higher or lower values of a certain variable in geographic space – are Local Moran’s I (Anselin, 1995) and Getis-Ord G_i^* (Getis & Ord, 1992) (Ord & Getis, 1995). Several modifications exist for both (univariate) methods, allowing for bivariate or even temporal data analysis, namely the Local Bivariate Moran’s I (Anselin et al., 2002) and the Local Differential Moran’s I (Anselin et al., 2020). However, multivariate

data cannot be analysed appropriately this way, and demands for alternative approaches are still prevalent.

One common way to detect unusual data is regression analysis. This allows for the incorporation of several variables and, like most statistical methods, it can be adapted to a geographically weighted form that meets the requirements of spatial analysis and spatial data. One of the most popular spatial regression methods is Geographically Weighted Regression (GWR) (Brunsdon et al., 1996), which seeks to fit a local model to every feature in a dataset, taking into account locally varying relationships between observations in a study area, preferably for several dozen explanatory variables. This method is therefore able to handle spatially heteroscedastic relationships between the input variables. However, GWR comes with some drawbacks, as discussed by Bivand (2012) (Bivand, 2012) and Wheeler et al. (2005) (Wheeler et al., 2005). Some of these issues have been addressed by the Multiscale Geographically Weighted Regression (MGWR) (Fotheringham et al., 2017), whose developers allowed for each parameter to have a different spatial lag. MGWR learns the different lags dynamically through an iterative approach: after an initial distribution of spatial lags and then fixing all but one spatial lag, the optimal lag for this parameter is computed and then iterated for every parameter. After one overall iteration, a defined convergence criterion is checked for, and the process is repeated. This allows (M)GWR to be a powerful tool for the exploration of high-dimensional spatial datasets.

Other spatial regression approaches are commonly applied in econometrics and can model the data in a fashion similar to the non-spatial regression model (OLS) while considering the effects of spatial autocorrelation. These models extend the non-spatial linear regression model by three different spatial effects (Manski, 1993):

- Endogenous Effect: The behaviour of a spatial analysis unit in geographic space (regressand) depends on the behaviour of other spatial analysis units in proximity.¹
- Exogenous Effect: The behaviour of a spatial analysis unit in geographic space (regressand) depends on the behaviour of the independent explanatory variables (regressors) of other spatial analysis units in proximity.
- Correlated Effect: The behaviours of a spatial analysis unit in geographic space are alike because they ‘face similar institutional environments’ (Manski, 1993, S. 533), but they do not directly influence each other by their own behaviour.

The theoretical model that incorporates every spatial effect is called the Manski-Model. It can be restricted to a range of other models that incorporate different combinations of spatial effects, applicable for the different phenomena under investigation:

$$Y = \rho WY + X\beta + WX\theta + u$$

$$u = \lambda Wu + \epsilon$$

where:

- WY describes the endogenous effect of spatially lagged variable y on Y ,

¹ Cf. *peer pressure* in social contexts.

- ρ is the spatial autoregressive coefficient controlling the effect of the spatially lagged variable y ,
- $X\beta$ describes the exogenous effects,
- WX describes the exogenous interaction effect, or the effect of the spatially lagged variable X on Y ,
- θ controls the effect of the spatially lagged variable of all variables in X ,
- u and ϵ are error terms of unobservables,
- Wu describes the correlated effect or the effect of the spatially lagged variable of the unobservables²,
- λ controls the effect on Y of the spatially lagged variable of the residuals.

Many model selection procedures exist that help to determine which effects to exclude, as described in (Anselin et al., 1996), (LeSage et al., 2009), (Darmofal, 2015), (Floch et al., 2016) and (Elhorst, 2010), amongst others. Although those effects (and models) were established in more of a socio-economic context, they can be adapted to spatial data in other contexts.

In addition to the methods reviewed so far, which are comparatively well-known in spatial analytics, numerous algorithms exist that focus on spatial outlier detection. Some examples are described in the works of (Kou, Lu, & Chen, 2006), (Sun & Chawla, 2004), (Takeuchi & Yamanishi, 2006), (Liu, Ting, & Zhou, 2012) and (Chen, Lu, & Boedihardjo, 2010). Each suggests a different outlier detection algorithm, but each identifies outliers by the deviation from neighbouring points. While the outlier detection algorithm introduced in (Kou, Lu, & Chen, 2006) was applied to cleanse the yield data in our work, the approaches generally focus on spatial outlier detection as part of data preparation, rather than for actual spatial data exploration.

The findings in the literature suggest that the range of tools available for multivariate spatial data exploration is limited (the detection of potentially erroneous points aside). Furthermore, each method suitable for spatial anomaly detection is based on a different concept, making direct comparisons difficult. Thus, additional methods are needed for the identification of anomalous behaviour in spatial datasets.

² For example, in cases of spatial heteroscedasticity the residuals ϵ are autocorrelated.

3 Methodology

Data A spatial dataset containing one dependent variable and at least one independent variable. Spatial data from different observations should be interpolated in a common regular grid raster.

Result Statistical significance (z-scores) of the residuals from the fitted spatial error model.

```

define spillover-function;
    #weighting function for spatial
    neighbors
fit spatial error model;
    #direct neighborhood
calculate Global Moran's I and SOH;

while Global Moran's I  $\lesseqgtr$  0.6 & SOH  $\lesseqgtr$  0.9:

    increase neighborhood;
    #i.e., the spillover
    calculate G. Moran's I and SOH;

end
calculate residuals;
calculate residual significances;

```

It should be noted that for a spill-over function that puts exponentially more weight on direct neighbors than on more distant neighbors, both indicators will converge sooner towards their global maximum, as illustrated in Figure 3 (right).

Figure 1: Brief outline of the CESEM algorithm.

Our approach of multivariate spatial anomaly detection is based primarily on the application of spatial regression models and the assessment of the models' residuals. In short, residuals that deviate significantly from all other residuals will be identified as anomalous.

For the detection of multivariate spatial anomalies by means of spatial regression, we propose a contrast-enhancing technique based on the Spatial Error Model (SEM) (Anselin L. , 1988). The ordinary SEM extends the linear model³ by an error term $u = \lambda W u + \varepsilon$. This allows the residuals to spill over spatially, with $y = X\beta + u$. Usually, the error term in the SEM adjusts for local deviations from the non-spatial linear model (OLS) by incorporating the error term as an omitted or unobserved, but spatially autocorrelated, variable.

³ The SEM can in turn also be seen as a restriction of the *Manski-Model*.

The technique proposed here provides for an artificial increase⁴ of the number of neighbours affected for each observation, and with that for the expansion of the spill-over in the error term. In practice, this leads to overlapping spill-overs of errors from different points that are in proximity to each other. For similar points, this spill-over of errors does not greatly impact the predictions made by the model, which can adjust for slight deviations from the predictions. However, when points differ greatly, numerically speaking, from their surroundings, the model cannot adapt. This results in even higher model deviations for these points, since their predicted value further increases or decreases. Model deviations that are detected indicate spatial discontinuity and will subsequently be identified as anomalous, provided that the deviation of the residuals is statistically significant. Due to the locality of the error spill-overs, the method is not overly prone to heteroscedasticity if the change happens gradually (continuously) and not suddenly (discontinuously).

For purely predictive purposes (for which the SEM is usually applied), considering direct neighbourhood would most often lead to the highest model precision of the SEM, since the model can adapt readily to the most minute variation within a given area. By extending the spill-over, there is a trade-off: the SEM becomes practically impaired in exchange for more spatially autocorrelated residuals, without a complete generalization back to the non-spatial linear model (OLS).

In practice, increasing the area defined as a neighbourhood can be realized by two parameters: (i) modelling the spatial influence of the spill-over in the error term; (ii) the extent (distance) of the spill-over itself. As part of this work, an inverse distance function is defined that increases the impact of error spill-overs on immediate neighbours. The greater the impact of the error on more distant neighbours, the larger the spatial anomalies obtained may be. In the extreme case of every residual from every point spilling over to the rest of the points, the SEM could potentially become comparable to the non-spatial linear model.

A more detailed example of the effects of the CESEM is presented in Section 3.2.

3.1 Parametrization

For the parametrization of the CESEM, two measures were calculated for two different powers of the inverse distance function by gradually increasing neighbourhood radiuses: (i) the Global Moran's I (Moran, 1950) (Cliff & Ord, 1972) for the quantification of the global spatial autocorrelation of the residuals across the entire study area; (ii) the Stability of Hotspots (SOH) (Bruns & Simko, 2017) for the quantification of the magnitude of change between (significant) residuals obtained from the iteratively computed SEM.

⁴ *Artificial* in the sense that the predictive abilities of the fitted SEM would potentially be more accurate with a sparser spatial weights matrix (i.e., if a smaller neighbourhood was defined).

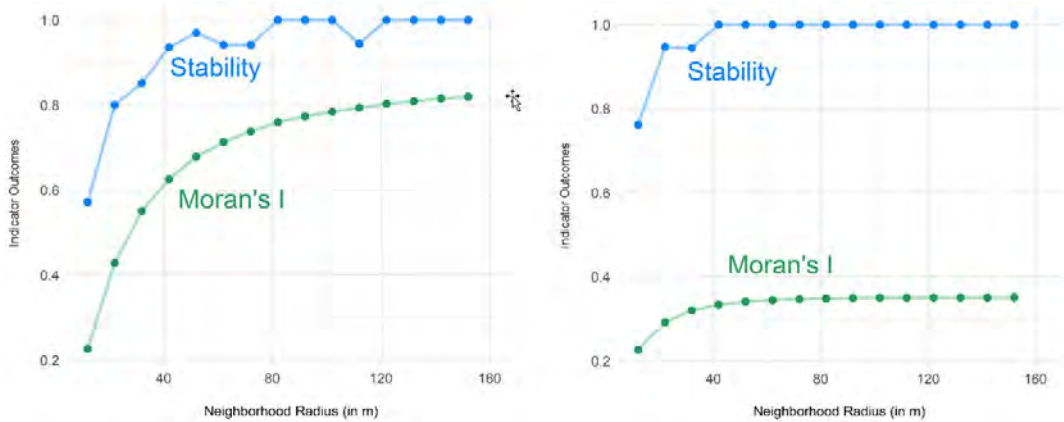


Figure 2: Stability of Hotspots and the Global Moran's I of significant residuals ($\alpha = 0.5$) of a SEM calculated for an increasing neighbourhood size of $\frac{1}{2}$ (left) and an inverse distance power of 4 (right). The effect of the neighbourhood radius for higher inverse distance powers is much smaller, since the impact of the error term peters out faster, with no meaningful impact whatsoever on more distant neighbours.

The calculation of the Global Moran's I gives information about the spatial autocorrelation of the residuals of the SEM. The smaller the defined neighbourhood, the less spatially autocorrelated the residuals will be. While precisely this outcome is usually intended when the calculation is applied in order to obtain the underlying SEM (for the sake of an accurate spatial prediction), it may be less useful for the detection of spatial anomalies, since the SEM adapts to the most minute spatial variations for these smaller neighbourhoods. On the other hand, the larger the neighbourhood, the more similar the model will be to the non-spatial linear model, since the errors will cancel each other out until the predictions resemble the regression mean.

The chief intention of the model parametrization here is to generalize the SEM by a spill-over expansion until the residuals start to cluster spatially. The main idea of the CESEM is that the residuals that start to cluster first are the ones that represent the most severe model deviations, which are particularly difficult to predict for the SEM due to their variable characteristics.⁵ The parametrization process seeks to determine for which parameter the SEM falls apart first, and which residuals first start to cluster spatially.

The SOH, on the other hand, gives information about the stability of the resulting hot- and coldspots. The measure compares the clusters for the smaller neighbourhood with those of the next-largest neighbourhood and quantifies the similarity between them (comparable to the computation of a difference map). For higher values of the SOH, the clusters of significant residuals remain stable for the next-largest neighbourhood. We aim for a convergence of the SOH values, which would indicate that the gradual extension of the spill-over has stopped. To date, we have not been able to find a fully standardized and automated approach for this

⁵ Here, defined by an [assumed] linear relationship between the input variables.

problem. However, plots like the ones in Figure 4 can serve as a reference for how to parametrize the CESEM.

In this example, the choice of an inverse distance power is driven mainly by the spaciousness of potential anomalies. Lower inverse distance powers, which are able to compensate for smaller irregularities, will result in more extensive trend-deviating (regional) clusters as the error term is propagated to more distant spatial neighbours. In turn, for higher inverse distance powers, the current spatial analysis unit is compared to spatially closer neighbours, resulting in the detection of spatially less extensive (local) clusters.

The spill-over itself can be modelled by practically any function and is required for the computation of the CESEM. The primary effect of the distance band for neighbourhood definition is that it increases computational performance, since for an inverse distance function the area of meaningful impacts by the error term is spatially restricted anyway.

Based on this initial approach, the CESEM was parametrized with a neighbourhood radius of 40 metres and an inverse distance power of $\frac{1}{2}$. From the corresponding plot based on this parametrization (see Figure 2a), it can be observed that at about 40 metres (1) the SOH starts to peak, and (2) the residuals are about to cluster spatially.

3.2 Contrast-Enhancing Effects

The following example illustrates the contrast-enhancing effects that can be achieved by extending the spill-over of an error term in a SEM.

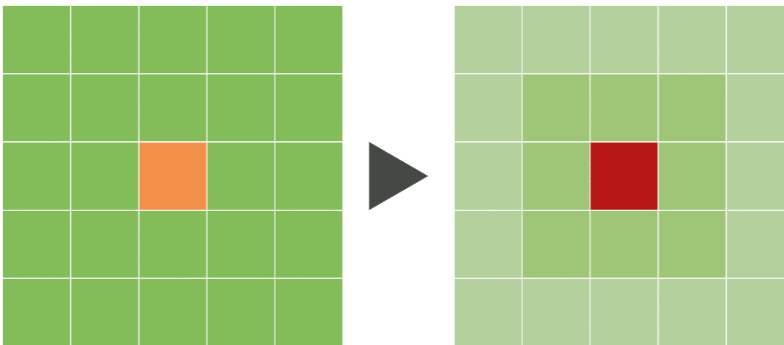


Figure 3: Visualization of the impacts of an extended (contrast-enhancing) spill-over effect of an error term from a SEM.

The visualization of residuals for an exemplary non-spatial linear regression (OLS) – as depicted in Figure 3 (left) – between a dependent variable and one or more explanatory variables shows an overestimated spot (orange; negative residual) in the centre of an exemplary geographic space, surrounded by underestimated spots (green; positive residual). The application of CESEM depicted in Figure 3 (right) now incorporates a spatially dependent error term spilling over to adjacent sections in geographic space. As a result, the overestimated spot in the centre becomes more significant, since the positive error terms spilling over from

the surrounding underestimated spots mean that this central spot deviates even more strongly from the predicted value of the SEM.

For the very same reason, underestimated spots now appear to be less significant, due to the compensation by overlapping (positive) errors adjusting for their collective underestimation. Since the spill-over has a greater effect on immediate neighbours (because of the impact modelled by an inverse distance function), the spots adjacent to the centre are in turn also affected by the negative error term of the centre counteracting (to some extent) the adjustment. As a result, the location of the highest spatial discontinuity (i.e. the centre and adjacent spatial analysis units) becomes more significant compared to the entirety of the residuals in the hypothetical area of study, which appear to be spatially continuous due to their similarity. The second consequence is that the central spot is penalized additionally since it is located between spatial units that appear to have strongly differing characteristics. The application of the CESEM, therefore, primarily penalizes spatial discontinuity based on a global and linear relationship between regressand and regressor(s).

Due to the focus exclusively on model residuals for anomaly detection, the SEM is predestined to be the foundation for CESEM, as it tries to adapt the model to the data by means of spatially autocorrelated residuals only. Another advantage is that the interpretations of model coefficients for the SEM and for the non-spatial linear model (OLS) correspond to each other. This stands in contrast to other spatial regression models: in other models, the interpretation of coefficients (and hence model comprehensibility) can become non-trivial because of the incorporation of spill-over effects for the dependent and/or independent variables.

However, for the sensitivity of the application of the CESEM, the theoretical requirements for the application of an ordinary SEM must be met and assessed by the relevant model selection processes, as stated in Section 2.

4 Evaluation

4.1 Dataset

The technique will be demonstrated for cleansed⁶ and interpolated⁷ yield data and apparent soil electrical conductivity measurements (ECa), both sets of data collected in an experimental field (Lammwirt⁸) at the Ihinger Hof research farm of the University of Hohenheim.

⁶ The unprocessed yield data were cleansed using the *Averaged Difference Algorithm* as proposed in (Kou, Lu, & Chen, 2006).

⁷ The processed yield data were interpolated using *Ordinary Kriging* (spherical variogram function considering the 50 nearest observations) and then converted onto a hexagonal grid with a resolution of 10 m.

⁸ Location: N48°44'50'', E8°54'33''.

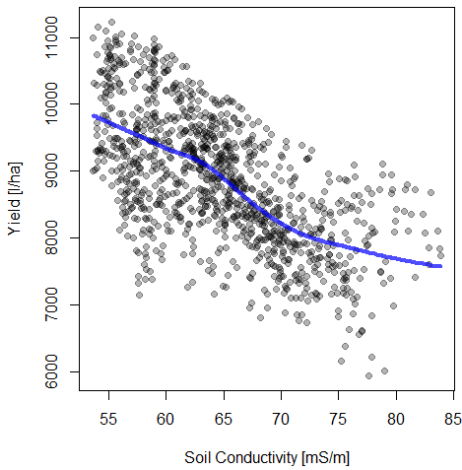


Figure 4:

Relationship between crop yield and electrical conductivity of soil. A locally weighted scatterplot to which smoothing (LOWESS) was added for the identification of potential structural breaks in the data.

The two variables studied exhibit a fairly strong negative correlation to each other (compare Figure 4 and Table 1), which will be examined in order to identify any anomalous field sections. In general, it can be stated that higher values for soil electrical conductivity typically correspond to soil characteristics that lead to an impaired crop yield (Kitchen, Sudduth, & Drummond, 2003). Examples of such soil characteristics may be waterlogging due to high clay content, or overly saline soil. Both high clay content and saline soil exhibit higher electrical conductivity.

Table 1: Correlation coefficients between soil conductivity and yield obtained for the non-spatial Pearson correlation coefficient (r_p), the Spearman's rank correlation coefficient (r_s), and for the two spatial correlation measures Moran's I and Lee's L (Lee, 2001). The global bivariate Moran's I is identical to the mean of the total of the local bivariate for Moran's I for an area.

Year	r_p	(r_s)	p	Moran's I global, bivariate	p	Lee's L	p
2007	-0.571	(-0.537)	<0.0001	-0.537	<0.0001	-0.530	<0.0001
2008	-0.504	(-0.515)	<0.0001	-0.455	<0.0001	-0.440	<0.0001
2010	-0.583	(-0.577)	<0.0001	-0.548	<0.0001	-0.541	<0.0001
2012	-0.493	(-0.505)	<0.0001	-0.483	<0.0001	-0.487	<0.0001
average	-0.630	(-0.635)	<0.0001	-0.595	<0.0001	-0.588	<0.0001

The data were interpolated upfront and converted onto a regular grid for data homogenization as an efficient way to define neighbourhoods. Regular hexagonal grids are particularly suitable for this purpose, since the neighbourhood definition becomes unambiguous.

4.2 Approach

In general, evaluating the results of the CESEM by using results from other approaches is difficult since no comparable approach is readily available. We compared our results to those for Local Bivariate Moran's I (LBMI) as the parametric and computational restrictions of this very method led to the conception of the approach of this paper. However, the CESEM is not intended to enhance the results obtained for the LBMI; rather it aims to provide an approach that complements the findings and tries to overcome some of the main (computational) limitations of the LBMI's detective abilities.

The LBMI represents a modification of the (univariate) Local Moran's I and allows for the incorporation of a dependent and an independent variable; it is based on the correlation of observations from one data layer and the spatially lagged observations of another data layer for identical locations.

$$I_{B,i} = x_i \sum_{j=1}^n w_{i,j} y_j$$

where:

- x_i is an original observation and y_j the corresponding spatially lagged observation of another variable
- $w_{i,j}$ are the weights assigned to the neighbour (row-standardized; $\sum w_{i,j} = 1$)

The cluster designations obtained using this calculation are comparable to those of the Local Moran's I. As already stated, the computational limitation of the LBMI lies in its great dependence on the (normalized) means of the respective variables of both layers, which results in a limited detective ability (see Figure 5). Consequently, while the method can detect clusters based on the correlation between an original observation and a spatially lagged observation of another variable, it is unable to differentiate between strong or moderate occurrences within such trends. The statistical significance is determined by a random permutation test for which merely pseudo z-scores can be obtained, which of course comes with certain drawbacks.

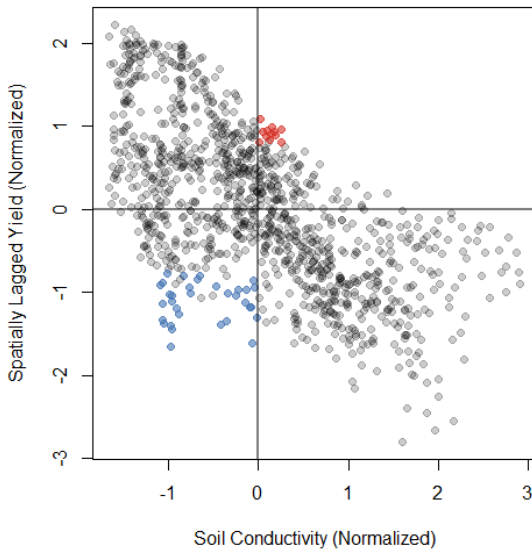


Figure 5:

Scatterplot showing the normalized input data and the coloured (pseudo-)significant data points. The strong break at the normalized means becomes evident.

Since the approaches are not directly comparable with each other, no difference maps or statistical comparisons were generated. Instead, the results will be compared visually, supplemented by expert knowledge of the locality itself (if available).

4.3 Results

What follows aims to demonstrate the operating principles of the CESEM, illustrated by a direct comparison of selected findings for both the CESEM and the LBMI.

One field section that could be identified a priori as a potential anomaly, according to domain experts, is the outer south-eastern corner of the field, the access point for any agricultural machinery used to till, fertilize, and eventually harvest the field. This area is characterized by overall lower plant productivity due to soil compaction from frequently being driven over, and mechanically-induced stress to the plants. The CESEM was able to identify a coldspot at this very location: the model prediction was significantly lower than the expected value, i.e. even after the automatic adjustment by the model to a lower value (spatial heteroscedasticity) to take into account the localized effects of the farm machinery. The LBMI does not indicate any anomalies for the same region.

For this example, the differences between the methods become evident. The CESEM identifies a suspiciously strong deviation from the modelled trend, despite local adjustments introduced by the error spill-over. The LBMI, on the other hand, is able to identify field sections that oppose the modelled trend directly. However, it is computationally incapable of identifying suspicious deviations within such trends. In this case, both the yield and the soil conductivity are below average (see Figure 5), but this does not constitute a violation of the (modelled) underlying trend. This example demonstrates how the CESEM can be applied to supplement and complement the findings of the LBMI.

The next example demonstrates the limitations of the CESEM which should be considered at the outset, before any interpretation of its findings. In this case, the notable accumulation of coldspots in the centre of the research field are examined more closely.

In the visualization of the average crop yields (Figure 6, upper right), an area of lower productivity can be identified. The LBMI identifies two cold spots for this region. Again, this can be explained by a positive correlation between crop yield and soil conductivity, a correlation which goes against the general trend. The very same areas can be identified when the CESEM is applied, although the geographical extent appears to be smaller. Additionally, the CESEM yields a third coldspot, one which protrudes into an area of increased conductivity and thus actually fits the model. Here, the effects of the spill-over become apparent. This third coldspot obtained by the CESEM does not conflict with the underlying model, but solely because it is surrounded by field sections of above-average productivity, especially towards the west. As a result, the expected yield value is much higher than the actual yield. Therefore, it should be kept in mind that the CESEM is not only a reverse correlation between variables but also a spatial discontinuity, even though the observations fit

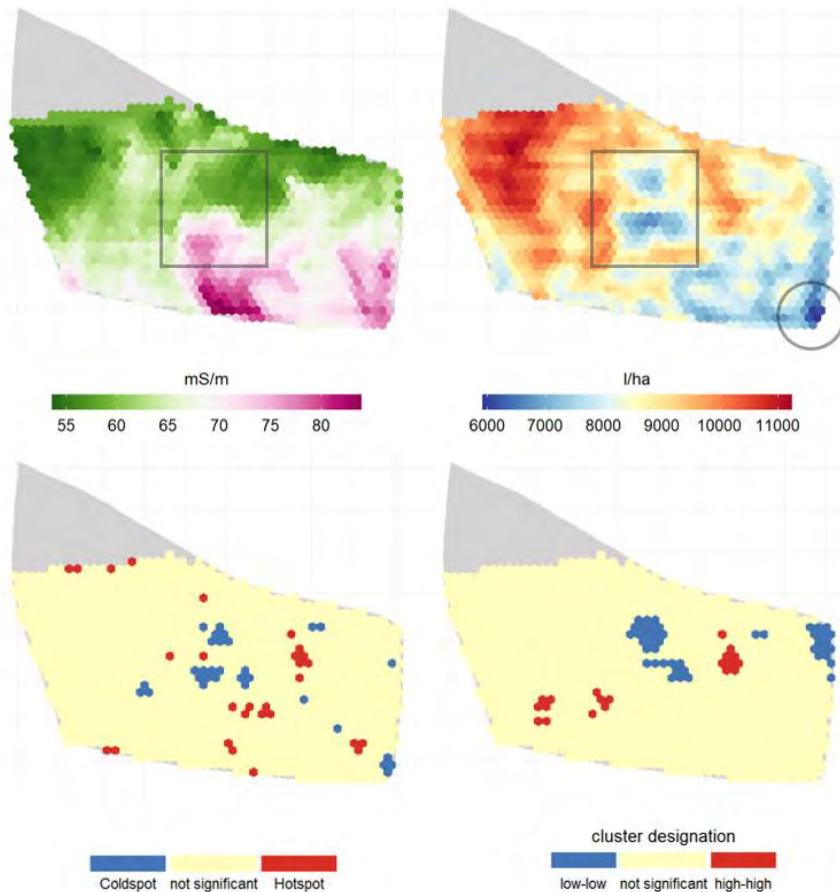


Figure 6: Input data consisting of the soil conductivity (upper left) and crop yield (upper right) and the respective results for the CESEM (lower left) and the LBMI (lower right).

The next example demonstrates the limitations of the CESEM which should be considered at the outset, before any interpretation of its findings. In this case, the notable accumulation of coldspots in the centre of the research field are examined more closely.

In the visualization of the average crop yields (Figure 6, upper right), an area of lower productivity can be identified. The LBMI identifies two cold spots for this region. Again, this can be explained by a positive correlation between crop yield and soil conductivity, a correlation which goes against the general trend. The very same areas can be identified when the CESEM is applied, although the geographical extent appears to be smaller. Additionally, the CESEM yields a third coldspot, one which protrudes into an area of increased conductivity and thus actually fits the model. Here, the effects of the spill-over become apparent. This third coldspot obtained by the CESEM does not conflict with the underlying model, but solely because it is surrounded by field sections of above-average productivity, especially towards the west. As a result, the expected yield value is much higher than the actual yield. Therefore, it should be kept in mind that the CESEM is not only a reverse correlation between variables but also a spatial discontinuity, even though the observations fit the underlying model.

In practice, these findings could now be used to identify other omitted or unknown ecological variables that might explain plant behaviour, and the CESEM could be applied in conjunction with other methods such as the LBMI, (M)GWR etc.

5 Discussion and Conclusion

Here, we have presented the CESEM as a new technique for the application of Spatial Error Models to identify multidimensional spatial hot- and coldspots, not only under the consideration of spatial autocorrelation but also spatial heteroscedasticity. The model compares neighbouring areas by applying the model correction of a SEM for one area to that of an adjacent area, in order to detect any sudden spatial breaks within a defined (linear) model and its inherent trend. Due to the spatially limited range of the comparisons that the technique allows, the technique is not overly prone to heteroscedasticity unless there are sudden changes (discontinuity) in the observed variances.

Our method is based on the combination of classical hotspot analysis and spatial regression analysis. By focusing more on the spatial discontinuity between the interaction of different dimensions and increasing the comparable neighbourhood, the CESEM contrasts the spatial residuals and resulting hot- and coldspots. It performs well in comparison to other approaches. We evaluated our method with real-world agricultural field data and demonstrated that the method provides advantages in the exploration of existing spatial phenomena. Discussion with agricultural experts allowed the results to be verified and explained. The approach improves visual detection of anomalies and therefore also improves time-efficiency for their analysis. An implementation of the method is already available as a webservice within the project iFAROS.

However, there are several limitations which need to be considered. First, the evaluation of methods for exploratory data analysis is quite difficult (see e.g. (Ben-David & Ackermann, 2008)). While (Bruns & Simko, 2017) provide an approach using SOH, it was evaluated only for one-dimensional spatial data. Second, while the results were discussed with experts for the

specific use-case, a broader evaluation in other contexts, using datasets from different scientific fields, would enable a more general evaluation of the method and its applicability. Finally, we compared the approach solely to the Local Bivariate Moran's I. During our literature research, we did not find any comparable approaches for the challenge we are aiming to meet, namely improving precision agriculture. An in-depth comparison with other spatial regression approaches, and analysis of variants of kriging or multi-stage hotspot approaches could be of interest. However, this is beyond the scope of the present study. Our focus is on providing a simple, intuitive approach for computation and visualization by researchers and practitioners, who often do not have the means to carry out the alternative approaches discussed here.

In the future, we aim to remedy the limitations to which we have pointed. A more in-depth evaluation using more datasets and different approaches would be highly interesting to the authors, as would testing the CESEM using more variables, which were reduced in number for the present study in favour of comparability to the Local Bivariate Moran's I. Classic ecological topics such as water or air pollution, or more human-centred ones such as mobility or irregularities in complex supply chains, are interesting fields that could generate numerous use-cases for future studies. These are areas that require urgent investigation, but also specialist knowledge to understand and evaluate the results. In addition to evaluating the method's reliability on real-world data, the use of synthetic datasets, for an even more reliable assessment is also planned.

Acknowledgements

We would like to thank Erik Haas for his valuable inputs and interesting discussions during the development of the CESEM method.

This work has been partially funded by the German Federal Ministry of Food and Agriculture (Bundesministerium für Ernährung und Landwirtschaft, BMEL) through the ICT-AGRI ERA NET project iFAROS (Decision Support for Optimized Site-Specific Fertilization based on Multi-Source Data and Standardized Tools, grant # 2817ERA11H), <https://www.ifaros-ictagri.com/>.

References

- Anselin, L. (1988). *Spatial Econometrics: Methods and Model*. Dordrecht: Kluwer.
- Anselin, L. (1995, April). Local Indicators of Spatial Association. *Geographical Analysis* 27 (2), pp. 93-115.
- Anselin, L. (2020, 10 10). geodacenter. Retrieved from Local Autocorrelation (2): https://geodacenter.github.io/workbook/6b_local_adv/lab6b.html#differential-local-moran
- Anselin, L., Bera, A., Florax, R., & Yoon, M. (1996). Simple Diagnostic Tests for Spatial Dependence. *Regional Science and Urban Economics*, pp. 77-104.
- Anselin, L., Syabri, I., & Smirnov, O. (2002). Visualizing Multivariate Spatial Correlation with Dynamically Linked Windows.

- Ben-David, S., & Ackermann, M. (2008). Measures of Clustering Quality: A Working Set of Axioms for Clustering. In D. Koller, S. Dale, B. Yoshua, & B. Léon, *Advances in Neural Information Processing System 21* (pp. 121-128). Vancouver, British Columbia, Canada: Curran Associates, Inc.
- Bivand, R. (2012, February 16th). *r-sig-geo*. Retrieved from a question about *gwr.morantest* pvalue: <http://r-sig-geo.2731867.n2.nabble.com/A-question-about-gwr-morantest-pvalue-td7292670.html>
- Bruns, J., & Simko, V. (2017). Stable Hotspot Analysis for Intra-Urban Heat Islands. *GI_Forum Journal* (pp. 79-92). Salzburg: Austrian Academy of Sciences Press.
- Brunsdon, C., Fotheringham, A., & Charlton, M. (1996, October). Geographically Weighted Regression: A Method for exploring Spatial Nonstationarity. *Geographical Analysis* 28 (4), pp. 281-298.
- Chen, F., Lu, C.-T., & Boedihardjo, A. (2010). GLS-SOD: A Generalized Local Statistical Approach for Spatial Outlier Detection. *Proceedings of the 16th ACM SIGKDD International Conference on Knowledge Discovery and Data Mining* (p. 1069). New York: ACM.
- Cliff, A., & Ord, K. (1972). Testing for Spatial Autocorrelation among Regression Residuals. *Geographical Analysis*, pp. 267-284.
- Darmofal, D. (2015). *Analytical Methods for Spatial Research*. New York: Cambridge University Press.
- Elhorst, J. (2010). Applied Spatial Econometrics: Raising the Bar. *Spatial Economic Analysis*, pp. 9-28.
- Floch, J.-M., & Le Saout, R. (2016). *Econométrie Spatiale: Une Introduction Pratique*. Paris, France: Institut National de la Statistique et des Études Économiques.
- Fotheringham, A., Yang, W., & Kang, W. (2017). Multiscale Geographically Weighted Regression. *Annals of the American Association of Geographers* 107 (6), pp. 1247-1265.
- Getis, A., & Ord, J. (1992, July). The Analysis of Spatial Association by use of Distance Statistics. *Geographical Analysis* 24 (3), pp. 189-206.
- Kitchen, N., Sudduth, K., & Drummond, S. (2003, 5). Soil Electrical Conductivity and Topography Related to Yield for Three. *Agronomy Journal*, pp. 483-494.
- Kou, Y., Lu, C.-T., & Chen, D. (2006). *Spatial Weighted Outlier Detection*. Philadelphia: Society for Industrial and Applied Mathematics.
- Lee, S.-I. (2001). Developing a Bivariate Spatial Association Measure: An Integration of Pearson's R and Moran's I. *Journal of Geographical Systems*, pp. 369-385.
- LeSage, J., & Pace, R. (2009). *Introduction of Spatial Econometrics*. Statistics, Textbooks and Monographs.
- Liu, F., Ting, K., & Zhou, Z.-H. (2012). Isolation-Based Anomaly Detection. *ACM Transactions on Knowledge Discovery from Data*, pp. 1-39.
- Manski, C. (1993). Identification of Endogenous Social Effects: The Reflection Problem. *The Review of Economic Studies*, p. 531.
- Moran, P. (1950). Notes on Continuous Stochastic Phenomena. *Biometrika*.
- Ord, J., & Getis, A. (1995). Local Spatial Autocorrelation Statistics: Distributional Issues and an Application. *Geographical Analysis*, 286-306.
- Sun, P., & Chawla, S. (2004). On Local Spatial Outliers. *Proceedings / Forth IEEE International Conference on Data Mining* (pp. 209-216). Los Alamitos, California: IEEE Computer Society.
- Takeuchi, J., & Yamanishi, K. (2006). A Unifying Framework for detecting Outliers and Change Points from Time Series. *IEEE Transaction on Knowledge and Data Engineering* (pp. 482-492). IEEE Computer Society.
- Tukey, J. W. (1977). *Exploratory data analysis*. Pearson.
- Wheeler, D., & Tiefelsdorf, M. (2005). Multicollinearity and Correlation among Local Regression Coefficients in Geographically Weighted Regression. *Journal of Geographical Systems*, 7(2), pp. 161-187.

A Comparison of Convolutional Neural Network Architectures for Automated Detection and Identification of Waterfowl in Complex Environments

Mohammad Mustafa Sa'doun¹, Christopher D. Lippitt², Gernot Paulus¹ and Karl-Heinrich Anders¹

¹Carinthia University of Applied Sciences, Villach, Austria

²University of New Mexico, Albuquerque, USA

Abstract

Waterfowl monitoring is an important task for understanding waterfowl distribution and habitats. Surveying approaches using hyper-spatial airborne imagery, collected by small unoccupied aerial systems (sUAS), hold potential to overcome the limitations of traditional methods while improving count efficiency and reliability. Difficulties obtaining waterfowl counts, particularly in complex image scenes, from the high quantity of imagery required hinders deployment of large-scale surveys. In this paper, we test Convolutional Neural Networks (CNNs) to understand their potential and how they behave across different versions of our waterfowl dataset. Three CNN architectures (YOLO, Retinanet and Faster R-CNN) were trained on 3 hierarchical levels: waterfowl detection (True / False), waterfowl type (3 classes), and waterfowl species (8 classes). The architectures generally performed well, and results indicate that automated waterfowl detection in complex environments, and therefore enumeration, is feasible using current technology. Waterfowl identification in complex environments was not successful using the available training data, but we propose steps that might enhance the results.

Keywords:

waterfowl surveying, YOLO, Retinanet, Faster R-CNN, sUAS, deep learning

1 Introduction

Waterfowl population recognition and classification have traditionally been undertaken by a combination of ground-based and manned aircraft surveys. Manned aircraft enable the surveying of large areas, but they are expensive and can cause stress to wildlife (Wilson et al., 1991). Small unoccupied aerial systems (sUAS) have been used successfully to survey a variety of bird species worldwide, with much lower costs and risks (Linchant et al., 2015). One factor hindering the adoption of surveys using sUAS is the work required to manually identify targets in the imagery compared with counts in the field (Linchant et al., 2015). Numerous automated techniques have been used for waterfowl recognition, with accuracy comparable to manual

image counts, including spectral thresholding (Laliberte & Ripple, 2003), supervised classification (Grenzdörffer, 2013), and template matching (Abd-Elrahman et al., 2005). However, these methods are limited in that they require animals to be highly distinct spectrally from their surroundings. This hinders applications in heterogeneous environments for the study of species with cryptic colouration, or with image sets of varying brightness due to camera performance or weather conditions (Linchant et al., 2015; Chabot & Francis 2016). Some machine learning (ML) approaches, such as convolutional neural networks (CNNs), have the potential to enable efficient detection and classification in complex scenes (Chen et al., 2012). Compared to other ML techniques such as the use of support vector machines and Key Nearest Neighbour, CNNs produce high detection and classification accuracies owing to their non-linearity, ability to increase model complexity (adding convolutional layers for deeper feature extraction), and implicit segmentation capabilities (Ghorbanzadeh et al., 2019; Wang & Raj, 2017). The latest CNNs can be used in many automated processes in various application domains, for example in crowd counting, object detection, face-attribute recognition, and geo-localization (Howard et al., 2017; Girshick et al., 2014; van Gemert et al., 2014; Chen et al., 2012).

CNNs were applied to three hierarchical levels of increasing difficulty, namely waterfowl detection, identification of waterfowl type, and identification of waterfowl species. The selected CNN architectures were trained and validated using a set of labelled sUAS-acquired images of waterfowl to enable comparisons of the architectures' abilities to recognize and classify waterfowl species. The primary aim of this empirical research project was to identify the CNN architecture that can produce the most accurate classifications and counts (relative to the ground truth) as part of an effort to develop a prototype sUAS-based waterfowl survey programme for the United States Fish and Wildlife Service (USFWS).

2 Deep learning and CNNs

Deep Learning (DL) is a sub-category of ML that mimics how the human brain works (Krogh, 2008). It uses Artificial Neural Networks (ANNs) consisting of many layers, each containing neurons (or nodes) connected to form a web-like structure. CNNs are a special type of ANNs, the main difference being that in a CNN a deeper neuron layer is connected only to a subset of neurons in the previous layer (Albawi et al., 2017). Figure 1 shows the basic architecture of a CNN. Many frameworks are available for DL, of which Google's TensorFlow (Abadi et al., 2016) is the latest. The Tensorflow API, which is publicly available, can be used to distribute load between multiple nodes (CPUs or GPUs). Keras is a fast-growing deep learning framework. This open-source library written in Python can run on top of TensorFlow or Theano. Theano is an open-source Python library for numerical computations; it simplifies the process of writing DL models. Caffe, developed by the Berkeley Vision and Learning Centre, has many worked examples of deep learning, written in Python. Giving more importance to GPUs is the Torch framework, which has an underlying C/CUDA implementation and is widely used for DL, as is MATLAB's *matconvnet*.

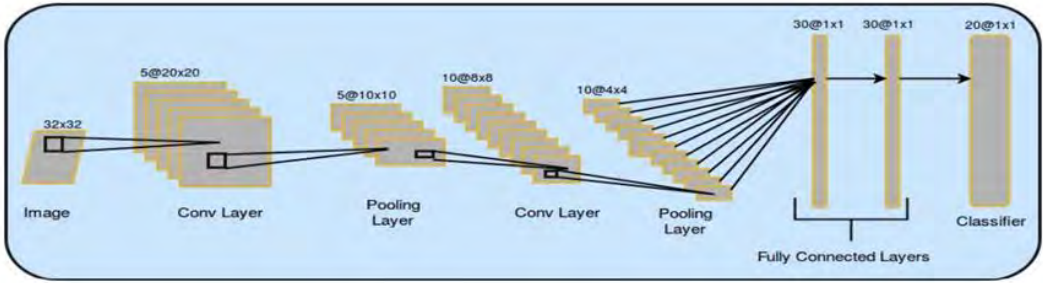


Figure 1: Basic CNN architecture (Aloysius and Geetha, 2017)

Various CNN architectures, such as CifarNet, MobilNets, AlexNet, GoogLeNet or YOLO (Howard et al., 2017; Zha et al., 2015), have accomplished significantly improved performance in many application domains, including object labelling and classification, event detection for safety systems, obstacle avoidance in autonomous driving, and identity checking (Zha et al., 2015). Each architecture differs in the number of intermediary layers, number and size of kernels used, error calculation methods, and activation functions. A feature common to all CNNs, however, is the need for robust training sets that contain both the desired input and the desired output (questions and right answers). The CNN then performs error calculations for its predictions, and runs through further iterations in order to improve predictions.

2.1 Related work using CNNs for bird detection

In a recent study carried out in Korea (Hong et al., 2019), five different CNN architectures were employed for bird detection, namely Faster R-CNN, R-FCN, SSD, Retinanet and YOLO, and were evaluated by comparing their speed and accuracy. The accuracy of the detection was measured using the Intersection over Union (IoU), defined as the ratio of intersection between the predicted box and the ground truth box. A threshold of 0.3 and 0.5 of IoU to determine the acceptability of the detection and the CNNs' performance was measured for both thresholds. The training data comprised 25,864 sUAS images that include 137,486 birds. Although Hong et al. (2019) stated that a 0.3 IoU threshold was sufficient, a threshold of IoU of 0.5 was used in our study. This was because a relatively small number of training samples (not hundreds or tens of thousands) were fed into the CNNs, and a 0.3 IoU led to the CNN twice as many non-waterfowl labels relative as the 0.5 IoU threshold.

2.2 Choice of CNN

A Weighted Linear Combination (WLC) operation was applied to rank the CNNs used by Hong et al. (2019); the three best, based on accuracy defined as an IoU score of 0.3, were selected. It should be noted that not all the CNNs in Table1 were taken into consideration. R-FCN with Resnet 101 was not selected, as this model performed in a manner very similar to Faster R-CNN, with slightly less accuracy but better time. Another reason to suppress R-FCN was that it contains the same feature extractor as Faster R-CNN (Resnet 101) as the core model for detection. Only the IoU of 0.3 was considered because it was sufficient to detect all bird

objects. YOLOv2 was also suppressed, because YOLOv3 was developed to obtain better accuracy, which is the prime focus in this study.

First, normalization of the speed and accuracy for each option was performed using equation (1) to obtain values between 0 and 1 for each field.

$$Z_i = \frac{X_i - \min(X)}{\max(X) - \min(X)} \quad (1)$$

where Z represents the normalized value (Normalized IoU:0.3 in Table 1) and X represents the IoU value of 0.3.

Table 1: Accuracy measurements based on IoU 0.3 and performance ranking

CNN	IoU:0.3	Normalized IoU:0.3	Rank
Faster R-CNN with Resnet 101	95.44	1	1
Mobilenet v.1	85.01	0	5
Retinanet with Resnet 50	91.94	0.621	3
SSD with Mobilenet v.2	85.9	0.085	4
YOLOv3 with Darknet-53	91.8	0.65	2

3 Data

The training set was collected using a crowdsourced image-labelling service called LabelBox and consists of 13 images of 5,472 x 3,648 pixels each; the total label count was 18,469. The survey mission took place in November 2018 in Bosque del Apache Wildlife Refuge, New Mexico (see Figure 2) using a DJI Mavic sUAS equipped with a Hasselblad L1D-20c RGB sensor operated at a flight altitude of 40 m. There were 13 species classes in the dataset: American wigeon, mallard, northern pintail, other, Canada goose, teal, sandhill crane, gadwall northern shoveller, ring-necked duck, redhead, ruddy and snow goose. However, the gadwall northern shoveller, ring-necked duck, redhead, ruddy and snow goose had fewer than 200 labels each. They were therefore not representative and, compared to other larger classes, had little chance of being detected. They would have been a source of uncertainty to the CNN. The remaining 8 species were aggregated to 3 waterfowl types: duck, goose and crane.

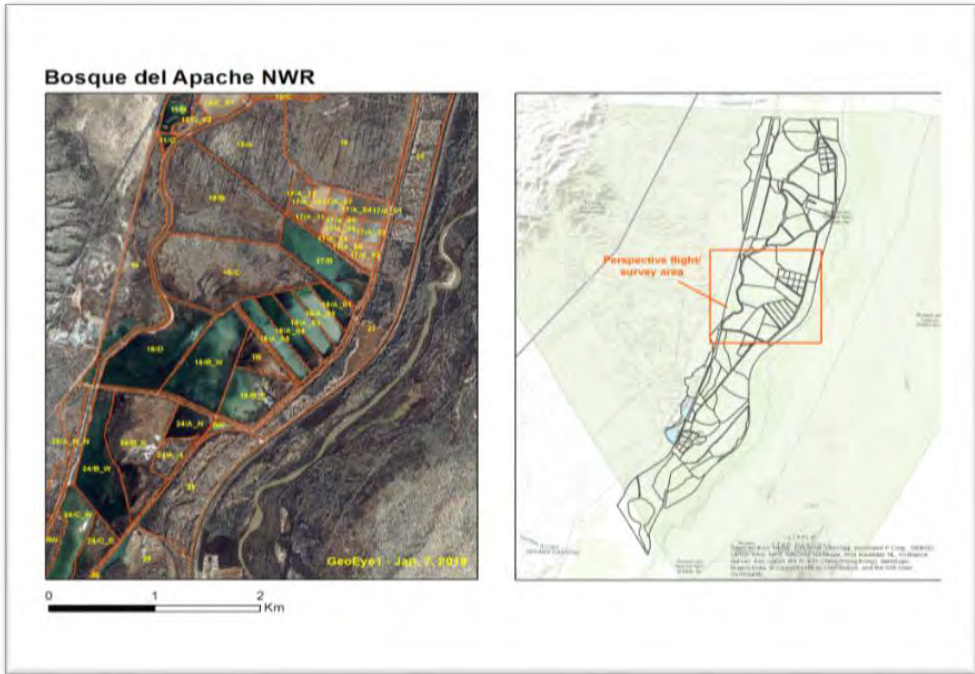


Figure 2: Location of Bosque del Apache Wildlife Refuge

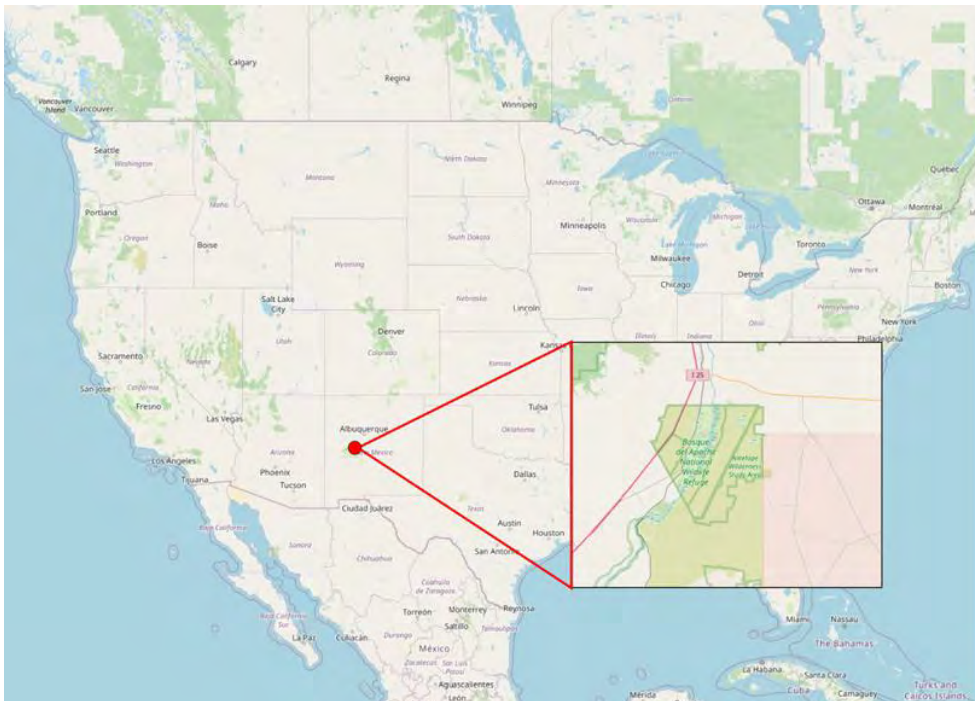


Figure 3: Location of Bosque del Apache Wildlife Refuge

4 Pre-processing

Pre-processing comprises the following steps:

- Convert LabelBox JSON Annotations to format accepted by each CNN.
- Split each image to a group of sub-images for the object to be easily identified.
- Remove multiple labels so that each target object has only one label.
- Construct a validation set (images not fed to the CNN in the training process).

The data are then segmented into three parts, namely training, testing and evaluation. The conversion process resulted in 18,469 labels for the 8 classes. However, as the dataset was labelled by 13 experts, redundant labels for each object had to be removed. If there were two or more labels with an IoU of more than 50%, the label with the larger area was removed (Figure 4).



Figure 4: Removing multiple labels from the training set

Each image has 5,472 x 3,648 pixels and the average label size is 52 x 54 pixels, occupying 0.014% of the total image area. This small percentage limits the ability of YOLOv3 to detect desired objects, causing the CNNs to perform very poorly on the original images (<3% accuracy of count). It was necessary to crop to multiple sub-images in order to enlarge the ratio of the area covered by the label in the image. Each image was therefore tiled to 56 sub-images (7 rows, 8 columns) of 684 x 521 pixels, increasing the average percentage of the area covered by a single label to 0.78%. Figure 4 shows how a bird is enlarged by the cropping procedure.



Figure 5: Image of the same bird shown before and after cropping

5 Model training and evaluation process

Table 2 presents the training parameters of the CNNs.

Table 2: Training Parameters for the CNNs

Training Parameter	YOLOv3	Retinanet	Faster R-CNN
Number of training samples	2908	2908	2908
Epochs (species/fowl type/detection)	16/12/11	3/2/2	118/92/87
Training time (sec./epoch)	212	1340	2280

Accuracy measurement is divided into accuracy of *detection* and accuracy of *identification*. The accuracy of detection is defined by how close the number of successful predictions is to the actual number of birds in the test data. The identification accuracy refers to how close the number of successful class predictions is to the actual number of class occurrences in the test dataset. Nevertheless, manual evaluation of the results (looking at each individual image result) is necessary to understand why an error has occurred in the detections. The most common method of representing prediction results is to build a confusion matrix. A cross-validation process was implemented by taking the ground truth labels (10% of the dataset that contains all waterfowl classes and different background conditions) as a reference, where the difference between the IoU of each label in the ground truth and prediction labels was calculated. The prediction label with the highest IoU was then assigned to the ground truth label. A successful count is defined as a prediction label that intersects a labelled object with the same class in the

ground truth. This assessment was carried out for all levels (detection, fowl type and species) to explore the effect of increasing the number of classes on the general counting performance.

6 Results

The results of CNN for waterfowl detection, waterfowl-type identification and species identification were evaluated by performing a cross-validation, where each prediction label is compared to the corresponding ground truth label. Finally, the results were summarized in a confusion matrix.

6.1 Detection

Figure 6 shows the detection performance in relation to the 3 hierarchical levels for the 3 CNN implementations. The x-axis represents implementation levels for each CNN (1: detection; 3: waterfowl type; 8: species); the y-axis represents the detection performance of the predictions broken down into three categories: detected waterfowl; undetected waterfowl; detection of non-waterfowl objects as waterfowl. Increasing the number of classes to be detected limits the ability of CNNs to detect waterfowl, and increases the number of undetected waterfowl (omission errors) and the number of non-waterfowl species detected (commission errors).

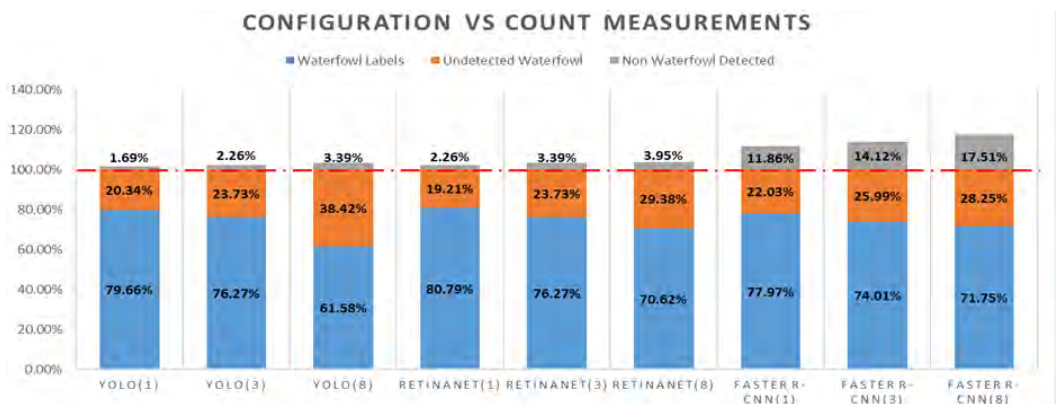


Figure 6: Detection Performance (Detection levels)

6.2 Waterfowl Type

The second assessment concerned the detection and identification accuracy of the CNNs on 3 classes of waterfowl (Duck, Goose and Crane); the confusion matrices in Tables 3–5 document the detection accuracies. The grey cells indicate successful classification (true-positive prediction); the rows represent the reference or the ground truth; and the columns present the measurement modelled.

Table 3: YOLO confusion matrix for fowl type (true-positives in grey)

Class	Duck	Goose	Crane	undetected	Grand Truth Total	Non-WF
Duck	95	14	0	34	143	3
Goose	1	21	0	7	29	1
Crane	0	0	4	1	5	0
Detection Total	96	35	4	42	177	4

Table 4: Retinanet confusion matrix for fowl type (true-positives in grey)

Class	Duck	Goose	Crane	undetected	Grand Truth Total	Non-WF
Duck	106	4	0	33	143	6
Goose	4	17	1	7	29	0
Crane	0	0	3	2	5	0
Detection Total	110	21	4	42	177	6

Table 5: Faster R-CNN confusion matrix for fowl type (true-positives in grey)

Class	Duck	Goose	Crane	undetected	Grand Truth Total	Non-WF
Duck	106	3	0	34	143	25
Goose	8	10	0	11	29	0
Crane	1	0	3	1	5	0
Detection Total	115	13	3	46	177	25

Duck was confused with Goose but not Crane by all CNNs, probably as a result of the very different size and coloration of cranes compared to ducks and geese.

6.3 Species level

The third assessment was for accuracy of species detection and identification. The confusion matrices (Tables 7–9) reveal how the CNNs behaved at species level. The grey cells represent successful classification (true-positive predictions). As the dataset contains six out of the eight classes belonging to fowl-type 'duck', it is no surprise that the classes belonging to this fowl-type were very frequently confused with each other (unlike what happened for the classes Canada Goose and Sandhill Crane).

Table 6: YOLO confusion matrix for species (true-positives in grey)

Class	American wigeon	Canada goose	Gadwall	Mallard	Northern pintail	Other	Sandhill crane	Teal	Undetected	GT total	Non-WF
American wigeon	0	1	0	0	2	1	0	0	4	8	0
Canada goose	0	28	0	0	0	0	1	0	0	29	4
Gadwall	0	2	0	0	1	0	0	1	2	6	0
Mallard	0	8	0	13	23	4	0	1	46	95	0
Northern pintail	0	2	0	1	2	0	1	1	2	9	1
Other	0	3	0	0	5	0	0	0	10	18	0
Sandhill crane	0	1	0	0	0	0	4	0	0	5	1
Teal	0	0	0	0	3	0	0	0	4	7	0
Detection Total	0	45	0	14	36	5	6	3	68	177	6

Table 7: Retinanet confusion matrix for species (true-positive in grey)

Class	American wigeon	Canada goose	Gadwall	Mallard	Northern pintail	Other	Sandhill crane	Teal	Undetected	GT total	Non-WF
American wigeon	2	0	2	0	0	0	0	2	2	8	3
Canada goose	0	20	1	0	0	1	1	1	5	29	1
Gadwall	2	0	0	0	0	1	0	1	2	6	1
Mallard	24	0	14	10	5	1	0	13	28	95	0
Northern pintail	3	0	0	0	1	2	0	0	3	9	0
Other	4	0	1	2	0	1	0	3	7	18	0
Sandhill crane	0	0	0	0	0	0	3	0	2	5	0
Teal	1	0	3	0	0	0	0	0	3	7	2
Detection Total	36	20	21	12	6	6	4	20	52	177	7

Table 8: Faster R-CNN confusion matrix for species (true-positives in grey)

Class	American wigeon	Canada goose	Gadwall	Mallard	Northern pintail	Other	Sandhill crane	Teal	Undetected	GT total	Non-WF
American wigeon	0	0	1	3	3	0	0	1	0	8	13
Canada goose	2	12	1	0	0	4	0	4	6	29	0
Gadwall	0	0	1	1	0	2	0	1	1	6	2
Mallard	4	1	2	13	25	10	0	12	28	95	0
Northern pintail	0	0	0	1	0	4	0	1	3	9	1
Other	1	0	0	1	0	5	0	1	10	18	15
Sandhill crane	1	0	0	0	0	0	3	0	1	5	0
Teal	0	0	0	0	3	2	0	1	1	7	0
Detection Total	8	13	5	19	31	27	3	21	50	177	31

7 Discussion

The first observation on the results is that the number of waterfowl detected decreased as we increased the number of classes for detection (waterfowl level to sub-species level). This is probably due to the decrement in the number of training examples per waterfowl type as we segregated waterfowl species. At species and fowl-type levels, the CNN tries to capture class-specific patterns using fewer training samples, defining each class independently. The second observation is that the result images often include individual waterfowl that are labelled multiple times (see Figure 3). This is probably due to the limited ability of the CNN to distinguish between different waterfowl species. This limitation can be most directly addressed by including more samples for each class. The third insight is the effect of surroundings and population density on performance. It was clear that better performance is achieved in low population densities and clear surroundings (no shadows, shrubs etc.), suggesting that there will be a sample bias based on the landscape composition being observed.

The confusion matrices shown above have a non-traditional setup; the number of detected objects does not match the number of objects in the ground truth. Some objects were not detected, and others were detected that did not represent waterfowl. This forced us to add undetected and non-waterfowl classes which have no ground truth reference. Our results were therefore reported in terms of correct/incorrect classification, undetected waterfowl, and non-waterfowl detection.

8 Conclusion and Future work

The results of this research show that CNNs have the potential to automate the process of waterfowl detection and identification. Across all CNN architectures, using a higher number of classes to train the network resulted in lower waterfowl detection accuracy, increasing both omission and commission errors. Increasing the number of classes to be detected reduced the number of labels generated by YOLO and Retinanet, but not Faster R-CNN.

Our experience suggests that this potential depends on the volume, quality, and structural and textual composition of training data in terms of image resolution and labelling correctness. We discovered that hyperspatial image data of waterfowl captured by a sUAS have special characteristics when compared to many other CNN applications: target objects are small while species morphology is often relatively similar. These characteristics need to be taken into consideration for adequate pre-processing.

In this project, valuable insights were collected on the performance and applicability of several freely accessible CNNs to waterfowl detection and identification using hyperspatial airborne imagery. One of the most important steps in future research will be to investigate how a much larger waterfowl training dataset (hundreds of thousands of training samples) will affect the results and behaviour of the CNNs. The findings presented here suggest that a phased approach should be explored, whereby a single-class 'waterfowl' detector is followed by a waterfowl-labelling step using a CNN trained on all classes. Finally, the class imbalance between species and fowl types is likely to be a persistent issue even as the number of labels available for training increases. Given the performance with respect to rare classes of the

models evaluated here, and the potential importance of rare classes in a wildlife survey context, data augmentation techniques with the potential to magnify the training samples of those rare classes warrant investigation.

From a practical perspective, the possibility of entering aerial images of waterfowl to the CNN in their original size also warrants further research. Keeping images in their original size would reduce the pre-processing tasks, making the model more efficient, but the computational feasibility of doing this needs to be investigated. For example, what would the memory requirements be? Could the computations be achieved through modifying state-of-the-art CNNs? Or would a CNN architecture have to be built from scratch, allowing the design of the hyperparameters to be oriented towards this specific application?

References

- Abadi, M., Barham, P., Chen, J., Chen, Z., Davis, A., Dean, J., ... & Zheng, X. (2016). Tensorflow: A system for large-scale machine learning. In 12th {USENIX} symposium on operating systems design and implementation ({OSDI} 16) (pp. 265-283).
- Abd-Elrahman, A., Pearlstine, L., & Percival, F. (2005). Development of pattern recognition algorithm for automatic bird detection from unmanned aerial vehicle imagery. *Surveying and Land Information Science*, 65(1), 37.
- Albawi, S., Mohammed, T. A., & Al-Zawi, S. (2017, August). Understanding of a convolutional neural network. In 2017 International Conference on Engineering and Technology (ICET) (pp. 1-6). Ieee.
- Aloysius, N., & Geetha, M. (2017, April). A review on deep convolutional neural networks. In 2017 International Conference on Communication and Signal Processing (ICCSP) (pp. 0588-0592). IEEE.
- Chabot, D., & Francis, C. M. (2016). Computer-automated bird detection and counts in high-resolution aerial images: A review. *Journal of Field Ornithology*, 87(4), 343-359.
- Chen, K., Loy, C. C., Gong, S., & Xiang, T. (2012, September). Feature mining for localised crowd counting. In *BMVC* (Vol. 1, No. 2, p. 3).
- Ghorbanzadeh, O., Blaschke, T., Gholamnia, K., Meena, S. R., Tiede, D., & Aryal, J. (2019). Evaluation of different machine learning methods and deep-learning convolutional neural networks for landslide detection. *Remote Sensing*, 11(2), 196.
- Girshick, R., Donahue, J., Darrell, T., & Malik, J. (2014). Rich feature hierarchies for accurate object detection and semantic segmentation. In *Proceedings of the IEEE conference on computer vision and pattern recognition* (pp. 580-587).
- Grenzdörffer, G. J. (2013). sUAS-based automatic bird count of a common gull colony. *International archives of the photogrammetry, Remote sensing and spatial information sciences*, 1, W2.
- Hong, S. J., Han, Y., Kim, S. Y., Lee, A. Y., & Kim, G. (2019). Application of deep-learning methods to bird detection using unmanned aerial vehicle imagery. *Sensors*, 19(7), 1651.
- Howard, A. G., Zhu, M., Chen, B., Kalenichenko, D., Wang, W., Weyand, T., ... & Adam, H. (2017). Mobilenets: Efficient convolutional neural networks for mobile vision applications. *arXiv preprint arXiv:1704.04861*.
- Krogh, A. (2008). What are artificial neural networks?. *Nature biotechnology*, 26(2), 195-197.
- Laliberte, A. S., & Ripple, W. J. (2003). Automated wildlife counts from remotely sensed imagery. *Wildlife Society Bulletin*, 362-371.

- Linchant, J., Lisein, J., Semeki, J., Lejeune, P., & Vermeulen, C. (2015). Are unmanned aircraft systems (UAS s) the future of wildlife monitoring? A review of accomplishments and challenges. *Mammal Review*, 45(4), 239-252.
- van Gemert, J. C., Verschoor, C. R., Mettes, P., Epema, K., Koh, L. P., & Wich, S. (2014). Nature conservation drones for automatic localization and counting of animals. In *European Conference on Computer Vision* (pp. 255-270). Springer, Cham.
- Wang, H., & Raj, B. (2017). On the origin of deep learning. *arXiv preprint arXiv:1702.07800*.
- Wilson, R. P., Culik, B., Danfeld, R., & Adelung, D. (1991). People in Antarctica—how much do Adélie Penguins *Pygoscelis adeliae* care?. *Polar biology*, 11(6), 363-370.
- Zha, S., Luisier, F., Andrews, W., Srivastava, N., & Salakhutdinov, R. (2015). Exploiting image-trained CNN architectures for unconstrained video classification. *arXiv preprint arXiv:1503.04144*.

Extracting and Geocoding Locations in Social Media Posts: A Comparative Analysis

Helen Ngonidzashe Serere, Bernd Resch, Clemens Rudolf Havas and Andreas Petutschnig

University of Salzburg, Austria

Abstract

Geo-social media have become an established data source for spatial analysis of geographic and social processes in various fields. However, only a small share of geo-social media data are explicitly georeferenced, which often compromises the reliability of the analysis results by excluding large volumes of data from the analysis. To increase the number of georeferenced tweets, inferred locations can be extracted from the texts of social media posts. We propose a customized workflow for location extraction from tweets and subsequent geocoding. We compare the results of two methods: DBpedia Spotlight (using linked Wikipedia entities), and spaCy combined with the geocoding methods of OpenStreetMap Nominatim. The results suggest that the workflow using spaCy and Nominatim identifies more locations than DBpedia Spotlight. For 50,616 tweets posted within California, USA, the granularity of the extracted locations is reasonable. However, several directions for future research were identified, including improved semantic analysis, the creation of a cascading workflow, and the need to integrate different data sources in order to increase reliability and spatial accuracy.

Keywords:

location extraction, geocoding, Twitter, DBpedia Spotlight, spaCy

1 Introduction

‘Geo-social media data’ refers to social media posts that have a geospatial reference. This geospatial reference may be explicit or implicit. Explicit references include geographic coordinates measured by a smartphone’s built-in location capabilities, for example by accessing a Global Navigation Satellite System (GNSS) sensor or nearby Wi-Fi access points. Alternatively, an explicit place tag can be added by the user. Implicit references include a place or location name that a user mentions in their post. Most geo-social media analysis approaches use explicitly georeferenced data with a GNSS reference, because of their high accuracy, technical accessibility and lack of ambiguity. However, only a small share of social media posts (roughly 2–10%) are explicitly georeferenced (Cheng et al., 2010; Laylavi et al., 2016). The low number of georeferenced posts reduces the sample size used for analysis, thereby compromising the reliability of the results.

Although some research efforts have been made over recent years to identify precise user locations in social media posts, challenges still remain in extracting and geocoding places with high recall and fine spatial granularity. This paper addresses these shortcomings through a customized workflow for inferred place extraction from tweets, and compares two different geocoding methods: DBpedia Spotlight (DBpedia) and a tailored workflow using spaCy, for location extraction; OpenStreetMap (OSM) Nominatim, for geocoding locations extracted by spaCy.

2 Related Work

Although Twitter offers an extensive data source, the relatively small number of explicitly georeferenced tweets poses a challenge in validating the authenticity of a tweet text. Over the years, research has been conducted to increase the percentage of geotagged tweets by extracting and geocoding implicit locations within posted tweets. For example, Das & Purves (2019) geocoded inferred locations in tweets to detect traffic events; Yaqub et al. (2018) used geocoding of inferred locations of tweets to map user sentiments during the 2016 US presidential elections. Although both studies showed high percentages of extracted locations, their results did not include a validation of the geocoded places.

Lee et al. (2014) extracted and geocoded locations from tweet posts linked to Foursquare. Their results found that 34% of the extracted locations were within a 250 m radius of the GNSS position provided. Whilst this result seemed highly satisfactory, the increase in georeferenced locations found by Lee et al. is biased towards Foursquare users and is not representative of the population of social media users as a whole. Another closely related study was conducted by (Laylavi et al., 2016), who geocoded tweet locations by giving priority to the finest-grained locations from textual content, or from users' profile locations, or from place-labelled locations. Their approach returned an accuracy of 60% of predicted locations within a 10 km radius, surpassing most state-of-the-art extractions. However, their results were obtained from a final sample of just 2,409 tweets out of ~90k tweets. In this research, we attempt to return a high accuracy of geocoded locations with a minimal loss of tweet sample size.

3 Methodology

The primary focus of this research is on extracting and geocoding inferred locations from tweets to increase the number of georeferenced social media posts for geospatial analysis. Our study uses two established tools for named entity recognition, namely DBpedia (Mendes et al., 2011) and spaCy's pre-trained 'en_core_web_trf' model.¹ We used both DBpedia and spaCy in order to better assess the performances of the two models for future studies.

DBpedia Spotlight builds upon Wikipedia data and provides links to DBpedia resources following a four-stage process of entity extraction, outlined in (Mendes et al., 2011). spaCy, on

¹ <https://spacy.io/>

the other hand, extracts entities based on the context of a word’s use and is hence not limited to a list of entities within a gazetteer, as is the case with DBpedia. However, unlike DBpedia which can perform both extraction and geocoding, spaCy does not have a built-in geocoding service. We therefore used OSM’s Nominatim to geocode entities extracted using spaCy; DBpedia performed both tasks itself. Figure 1 shows our general workflow. Detailed steps in chronological order will be found in section 3.1.

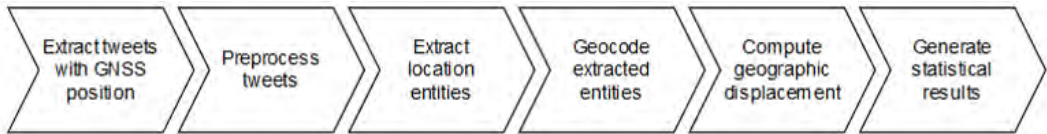


Figure 1: General Workflow.

3.1 Detailed workflow

Data: To enable the validation of our method’s performance, we based our analysis exclusively on tweets containing a GNSS position; the performance is measured through the displacement distance between the geocoded location and the tweet’s given GNSS position. We used a random subset of 56,052 tweets posted within the San Francisco Bay Area in California, USA, between April 2013 and May 2019. After pre-processing this dataset, we ended up with 50,616 tweets.

Pre-processing: Tweets are short, unstructured and noisy. The nature of the unstructured text makes pre-processing necessary to allow applicability of natural language processing methods. We performed text pre-processing in five stages.

First, we removed non-English tweets to simplify our analysis. Second, we substituted @ characters with the word ‘at’ to avoid false negatives in entity extraction due to non-matching words to be looked up in the DBpedia gazetteer, and ambiguous syntax for spaCy entity prediction. Third, we removed emojis, web addresses and hash-tag signs as we could not extract any locational information from these characters. We then discarded empty cells that resulted from the preceding step. Since our analysis was greatly interested in extracting the user’s current location, as a final pre-processing step, using keyword filtering, we eliminated tweets with either future or past locational reference, and automatically-generated tweets such as weather, news or marketing messages.

Location extraction: DBpedia’s performance in entity extraction is based on values assigned to the parameters ‘confidence’ (range between 0 and 1) and ‘support’ (integer values starting from 1) (Mendes et al., 2011). While high-confidence values increase accuracy, they risk omitting valuable entities. Likewise, higher support values discard all entities with Wikipedia in-links of less than the defined support value. Since we did not have an annotated dataset, we manually checked 100 tweets for the best support and confidence value pairs. A confidence level of 0.4 with a support value of 10 gave a more acceptable balance for both accuracy and recall.

The spaCy pre-trained model has locational entities divided into four classes: Geopolitical Entities (GPE), Facilities (FAC), Organisations (ORG) and Locations (LOC). GPEs are administrative units such as countries, states and cities. FACs include buildings, airports, highways, bridges etc., while the class ORG includes companies, agencies and institutions. LOC defines remaining location entities like street names, mountains, lakes or rivers. Using spaCy’s pre-trained ‘en_core_web_trf’ model, we first extracted all four types of location entity separately. We then paired LOC, FAC and ORG to the corresponding GPE entity (when available) in order to reduce locational ambiguity between common entities such as building names.

Displacement computations: To assess the geocoding accuracy, we computed the displacements as geodesic distances between Twitter’s GNSS points and the coordinates that resulted from using either DBpedia or Nominatim.

Generating statistical results: We computed the frequency distributions of displacement values for DBpedia and spaCy. We then evaluated various groupings of spaCy entities to find an entity grouping that gave higher accuracy and recall in predicting the user’s location. We gave higher priority to precise locations (i.e. FAC, ORG and LOC linked to a corresponding GPE entity) than to individual location entities such as ORG or LOC. It should be noted that a geocoded tweet was counted only once in the grouping regardless of possibly having more than one geocoded entity. That is, a tweet with FAC and GPE was counted once in the group of FAC_GPE and discarded from both FAC and GPE individually.

4 Results

Figure 2 presents an overview of the number of tweets with an extracted location, and the percentage of geocoded locations. Overall, spaCy returns a higher number of entities (18,448) in comparison to DBpedia (11,701). However, DBpedia shows a higher percentage (96.0%) of geocoded entities than Nominatim (91.8%) for combined spaCy entities. When analysing spaCy entities separately, our results show lower geocoded percentages, especially for the precise locations. LOC_GPE returned approximately 68.0% geocoded locations, while ORG_GPE and FAC_GPE returned fewer than 50% geocoded locations. The FAC and ORG entities also showed relatively lower percentages of geocoded locations (70.9% and 58.9% respectively).

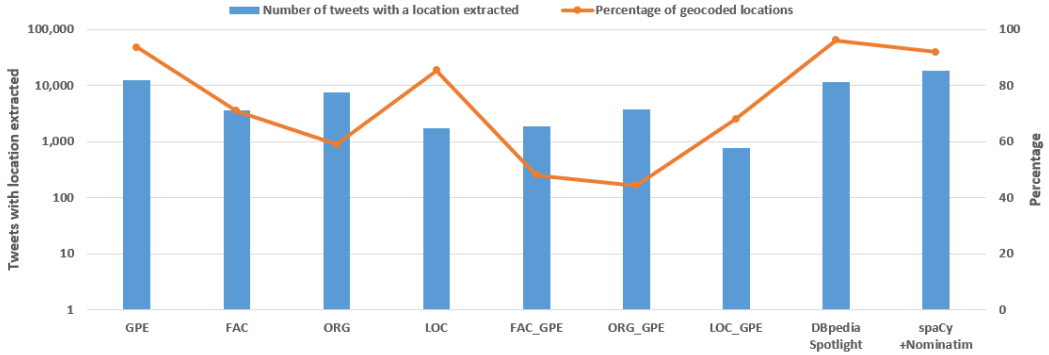


Figure 2: Number of tweets with location entity extracted (log scaled); and percentage of geocoded entities for DBpedia, and spaCy with Nominatim.

The statistical results of the computed displacements for spaCy’s geocoded entities are shown in Table 1. Overall, the precise locations, FAC_GPE, ORG_GPE and LOC_GPE, show higher cumulative percentages for lower displacements (81.9%–87.4% within 10 km radius) in comparison to the individual location entities (28.2%–74.2% within a 10 km radius). On the other hand, the individual locations returned higher absolute numbers (1,493–11,426) compared to the precise locations (530–1,676).

Table 1: Displacement statistics for spaCy geocoded locations.

Displacement	Cumulative frequency					Displacements	Cumulative percentage				
	1km	5km	10km	50km	>50km		1km	5km	10km	50km	>50km
GPE	2,816	7,209	8,482	9,437	11,426	GPE	24.6	63.1	74.2	82.6	100.0
FAC	911	1,085	1,118	1,167	2,535	FAC	35.9	42.8	44.1	46.0	100.0
ORG	1,041	1,203	1,250	1,451	4,431	ORG	23.5	27.1	28.2	32.7	100.0
LOC	485	609	666	777	1,493	LOC	32.5	40.8	44.6	52.0	100.0
FAC_GPE	601	737	767	817	878	FAC_GPE	68.5	83.9	87.4	93.1	100.0
ORG_GPE	940	1,246	1,393	1,481	1,676	ORG_GPE	56.1	74.3	83.1	88.4	100.0
LOC_GPE	318	411	434	469	530	LOC_GPE	60.0	77.5	81.9	88.5	100.0

spaCy geocoded entities were grouped starting with precise locations (Group A), with further groups being created as follows:

- Group A* = FAC_GPE + LOC_GPE + ORG_GPE.
- Group B* = *Group A* + GPE.
- Group C* = *Group B* + FAC.
- Group D* = *Group C* + LOC.
- Group E* = *Group D* + ORG.

Priority was given to entities with the highest cumulative percentage within a 5 km radius (see Table 1). Table 2 shows the displacement results of the DBpedia and spaCy entity groupings: there is an inverse relationship between the cumulative frequency and percentage of each displacement class. DBpedia showed a lower overall cumulative percentage within a 5 km

displacement compared to spaCy’s groupings, and the lowest cumulative frequency of geocoded entities apart from Group A.

Table 2: Displacement statistics for groupings of spaCy geocoded locations and DBpedia

Cumulative frequency						Cumulative percentage					
Displacement	1km	5km	10km	50km	>50km	Displacement	1km	5km	10km	50km	>50km
Group A	1,823	2,343	2,541	2,712	3,017	Group A	60.4	77.7	84.2	89.9	100.0
Group B	4,401	8,752	10,021	11,078	13,108	Group B	33.6	66.8	76.4	84.5	100.0
Group C	4,866	9,301	10,583	11,662	14,373	Group C	33.9	64.7	73.6	81.1	100.0
Group D	5,076	9,584	10,902	12,044	15,171	Group D	33.5	63.2	71.9	79.4	100.0
Group E	5,516	10,081	11,417	12,610	16,936	Group E	32.6	59.5	67.4	74.5	100.0
DBpedia	3,294	6,172	7,947	9,012	11,235	DBpedia	29.3	54.9	70.7	80.2	100.0

5 Discussion and Conclusion

This study set out with the aim of proposing a workflow for extracting locational information from tweets. Using tweets with GNSS positions, we extracted and geocoded location mentions in tweet texts and compared these locations with the tweets’ GNSS positions. We presented two sets of results: (1) locations extracted and geocoded by DBpedia Spotlight; (2) locations extracted by spaCy and geocoded using Nominatim.

We note that our location extraction and geocoding methods will have great potential to yield finer results, once a more detailed and comprehensive analysis has been carried out. Our groupings using spaCy (Table 2) showed remarkable results, with 84.2% being within a 10 km radius of the actual user location. This result surpasses that of (Laylavi et al., 2016), who returned only 60% for the same radius and sample size of tweets. Although these results seemed satisfactory, the high percentages were achieved at the expense of sample size. Hence, we present as our main results spaCy’s Group B, which retained a high sample size (10,021), with 76.4% of the retained tweet locations within a 10 km radius. DBpedia retained a rather lower sample size (7,924), with 70.7% within a 10 km radius.

Multiple reasons help explain our failure to obtain 100% accuracy. First, although keyword filtering was used to remove location mentions that were not the user’s actual location, we admit that this method was not robust. Undesired tweets were likely to have been left in the sample due to mismatches or ambiguous sentence structures leading to errors in geocoding the users’ actual locations. Second, the presence of ambiguous place names leads to obtaining wrong locations. Organisation entities such as ‘McDonalds’ were all geocoded to the headquarters, leading to large displacement values. When combined with a GPE entity, the displacement was reduced but also geocoded to the main store/location, despite there being potentially multiple locations in one city.

Our next set of steps for a complete analysis will hence be to increase the grammatical filtering of place mentions, and to combine tweets from single users to disambiguate mentioned locations based on locational trend analysis. In terms of geocoding with Nominatim, our results have shown that although Nominatim is well capable of geocoding locations down to street level, it fails to geocode place names written in a different syntax. This concurs with the

finding of (Di Rocco et al., 2016). We take note of this limitation and make two proposals for a more comprehensive assessment. First, we consider additional pre-processing steps before geocoding extracted locations. Second, we propose linking Nominatim OSM to other geocoding services.

References

- Cheng, Z., Caverlee, J., & Lee, K. (2010). You are where you tweet: A content-based approach to geolocating Twitter users. *International Conference on Information and Knowledge Management, Proceedings*, June, 759–768. <https://doi.org/10.1145/1871437.1871535>
- Das, R. D., & Purves, R. S. (2019). Exploring the Potential of Twitter to Understand Traffic Events and Their Locations in Greater Mumbai, India. *IEEE Transactions on Intelligent Transportation Systems*, 21(12), 5213–5222.
- Di Rocco, L., Bertolotto, M., Catania, B., Guerrini, G., & Cosso, T. (2016). Extracting fine-grained implicit georeferencing information from microblogs exploiting crowdsourced gazetteers and social interactions. *AGILE International Conference on Geographic Information Science*.
- Laylavi, F., Rajabifard, A., & Kalantari, M. (2016). A multi-element approach to location inference of Twitter: A case for emergency response. *ISPRS International Journal of Geo-Information*, 5(5), 1–16. <https://doi.org/10.3390/ijgi5050056>
- Lee, K., Ganti, R. K., Srivatsa, M., & Liu, L. (2014). When twitter meets foursquare: Tweet location prediction using foursquare. *MobiQuitous 2014 - 11th International Conference on Mobile and Ubiquitous Systems: Computing, Networking and Services*, 198–207. <https://doi.org/10.4108/icst.mobiquitous.2014.258092>
- Mendes, P. N., Jakob, M., García-Silva, A., & Bizer, C. (2011). DBpedia spotlight: shedding light on the web of documents. *Proceedings of the 7th International Conference on Semantic Systems*, 1–8.
- Yaqub, U., Sharma, N., Pabreja, R., Chun, S. A., Atluri, V., & Vaidya, J. (2018). Analysis and visualization of subjectivity and polarity of Twitter location data. *Proceedings of the 19th Annual International Conference on Digital Government Research: Governance in the Data Age*, 1–10.
- Yu, M., Bambacus, M., Cervone, G., Clarke, K., Duffy, D., Huang, Q., Li, J., Li, W., Li, Z., Liu, Q., Resch, B., Yang, J., & Yang, C. (2020). Spatiotemporal event detection: a review. *International Journal of Digital Earth*, 13(12), 1339–1365. <https://doi.org/10.1080/17538947.2020.1738569>

Design of an Experiment to Evaluate Modes of Value Generalization in Animated Choropleth Maps

Christoph Traun, Gudrun Wallentin and Manuela Larissa Schreyer
Salzburg University, Austria

Abstract

In this research, we discuss five design parameters found in cognitive studies related to animated choropleth maps and compare existing studies accordingly. With reference to these parameters, we present the design of an experiment to assess how different forms of value generalization in choropleth map animation affect the perception of overall trends and local deviations therefrom. The mixed study design of the experiment allowed a direct comparison of within-subject and between-subject designs. Using repeated subsampling of our empirical data, the greater statistical power of the within-subject design was proven, even when correcting for differences in the number of data elements analysed.

Keywords:

cartography, empirical study design, choropleth map animation

1 Introduction

In these times of the COVID-19 pandemic, informational dashboards are mushrooming around the globe. Many of them contain temporal animations of choropleth maps, showing the development of such things as the number of infections per 100,000 people over time. Whether or not choropleth map animation is the best choice for such an endeavour, it is at least a popular way to depict time-series data aggregated to enumeration units, as it shows the dynamics of spatial processes in a direct fashion (Campbell & Egbert, 1990; Multimäki, 2016) and is technically straightforward to implement (Butler, 2016).

As animated maps pose a heavy processing workload on the human brain (Harrower, 2007a), generalization is expected to help in the pattern recognition process (Harrower, 2003; Monmonier, 1996). Thus, we conducted an experiment to investigate the effect of value generalization ('smoothing of values/colours') on the perception of choropleth map animations. In order to design this experiment, we surveyed the literature on cognitive studies on animated choropleth maps. Despite the popularity of map animation, related empirical research is relatively sparse and results are difficult to judge and compare due to the great variety of study setups used. This sparked our interest and we identified several fundamental design criteria connected to this type of empirical cartographic research, namely

- the type of data used for stimulus design,
- the number of frames per stimulus,
- frame duration,
- the number of stimuli exposures per person, and
- the (statistical) design of the study

While all the studies reviewed comment on one or other of these criteria and decisions on the respective parameters, there are several instances where important choices are barely justified or are seemingly made for the sake of convenience or pragmatism. As the interpretation of data from experiments involving humans depends greatly on the design of the test instruments being used (Olson, 2009), we consider it worth shedding light on this important aspect of cognitive cartographic research in general and as it relates to choropleth map animation in particular.

In the following section, we briefly discuss the criteria mentioned in the context of the empirical studies identified. To exemplify the rationales associated with the choice of particular parameters, we present the design of an experiment that aims to assess the impact of value generalization in time, in space, and in a combination of space and time, on a person's ability to determine global trends as well as to detect local outliers from them.

While the discussion from a cognitive perspective of the data acquired is outside the scope of this paper, a mixed within-subject and between-subject design allows us to perform a comparative power analysis of those study designs that are widely used in empirical cognitive (cartography) research –something that we had not encountered in our domain.

2 Design criteria for empirical studies on the cognition of animated choropleth maps

From among the numerous empirical studies involving map animation (see Lobben (2008) for a taxonomy of evaluation-based approaches in the map animation literature), we surveyed studies focussing on cognitive effects related to variation of properties (data structure, map design) of animated choropleth maps. In Table 1, we list all such studies that we are aware of, and compare them by design criteria that we consider worthy of discussion.

Table 1: Cognitive studies on animated choropleth maps

Author and year	Aim of the study	Type of data used	# of frames per stimulus	Frame duration in ms	# of stimulus exposures per person	(Statistical) study design
(A. L. Griffin, MacEachren, Hardisty, Steiner, & Li, 2006)	Identification of moving clusters in animated maps and small multiples	Synthetic data - regular array of 756 hexagons	6	250 350 450 550	26	Within-subject design - 24 students
(Harrower, 2007b)	Comparison of classed and unclassed choropleth map animation	Unemployment rates for >3100 US counties	34	125	2	Within-subject design - 55 students
(McCabe, 2009)	Map reading task performance between raw, temporally averaged, and temporally aggregated data	Measles infection rates for 35 different-sized districts in Niger	52 (26 in aggregated version)	400	15	Between-subject design - 96 students in 3 groups
(Fish, Goldsberry, & Battersby, 2011)	Influence of the design of scene transitions on change-detection abilities	Unemployment rates for 64 counties in Georgia	2	2000	108	Within-subject design - 78 students
(DuBois, 2013)	Effects of cluster intensity, number of simultaneous clusters, and cluster position on change cluster detection	Synthetic data - 1541 (relatively similar-sized) polygons	2	2000	39	Within-subject design - 84 students
(Moon, Kim, & Hwang, 2014)	Effects of magnitude of change and spatial distribution on gross change-detection	Synthetic data - 42 (relatively similar-sized) polygons	2	1000 2000 3000	108	Within-subject design - 18 students
(Cybulski & Medyńska-Gulij, 2018)	Effects of increasing polygon border width on the identification of extreme values.	(Fictional) unemployment rates for 14 different-sized districts in Saudi Arabia	10	3000	1	Between-subject design - 60 students in 2 groups
(Cybulski & Krassanakis, 2021)	Effects of different magnitude of change conditions on correct detection of non-changing polygons	Data of unclear origin - 3 maps of 7, 24 and 54 very different-sized polygons	2	unlimited (user controlled)	3	Between-subject design - 45 students in 3 groups

2.1 Type of data

Map stimuli for empirical tests can be made from real-world geospatial data, synthetic data, or combinations of the two, like real geometries and synthetic attributes. While real-world data have the benefit of being realistic by default, synthetic data have the following advantages:

- Good control over data and therefore stimulus properties like the degree of spatial and temporal autocorrelation,
- prevention of unwanted confounding effects due to familiarity with the geographic region or topic,
- avoidance of large area-differences of enumeration units.

Referring to the latter, McCabe (2009) self-critically notes that the high visual salience of large but sparsely populated districts in Niger probably distorts the results of his study. Being aware of the problem that changes in large counties ‘visually overpower other locations’, Harrower (2007b) limited his questions to several, highlighted US areas containing counties of similar size. As the generation of dynamic geospatial data with the desired properties is itself challenging (A. L. Griffin et al., 2006), there might be pragmatic reasons for only three out of eight studies using artificially generated data, and except for the study by A. L. Griffin et al. (2006), even those use stimuli comprising just two frames and disregard temporal autocorrelation.

2.2 Number of frames per stimulus

Half of the studies reviewed use stimuli limited to two animation frames. This seems valid for the assessment of human ability to detect change between two map scenes while focusing on individual enumeration units (Cybulski & Krassanakis, 2021; Fish et al., 2011), clusters of units (DuBois, 2013), or the gross change for the whole map (Moon et al., 2014). From our perspective, however, the question remains open as to whether the task of viewing and understanding a map animation (portraying the fluid development of a spatial process) is cognitively equivalent to evaluating a considerable number of concatenated before/after changes within a map scene.

2.3 Animation speed

Although studies are not fully consistent (Moon et al. (2014), for example, did not find differences in correctness of response in relation to animation speed), the viewing time per frame is considered to be positively correlated to change-detection capabilities (McCabe, 2009; Multimäki & Ahonen-Rainio, 2015). Conversely, the slower an animation gets, the more it loses its potential to create an illusion of motion due to coordinated colour changes of adjacent polygons. To give an example, the outbreak of an infectious disease might lead to the impression of an expanding figure of high infection rates around its origin. If the frame rate is too low, the apparent motion of the expanding boundary cannot be established by our visual system (A. L. Griffin et al., 2006). The studies reviewed vary a lot in animation pace, from a slideshow-like 3 seconds per frame up to a speed 24 times greater, of 8 frames per second.

2.4 Number of stimulus exposures per person

The overall number of stimuli to which each participant is exposed during an empirical test depends on several criteria:

- The number of independent variables (factors) to test, e.g. effect of animation speed and generalization type.
- The number of levels for each factor, e.g. three different animation speeds.
- The number of tasks being tested, e.g. reading out values, focussing on global trends, comparing two regions.
- The risk that some unnoticed yet special configuration in one particular map stimulus acts as a confounding factor and thus leads to ‘untypical’ results. Thus it is wise to take such erratic behaviour into account through the redundant use of several different base stimuli.
- The overall test design, namely whether each person has to see every condition or only a subset thereof.

The range of the numbers of stimulus trials in the studies reviewed is enormous. Cybulski and Medyńska-Gulij (2018), for example, test three different map types, including a choropleth map, using just one base stimulus for each. The two levels (unmodified/enhanced borders) of the choropleth map stimulus were presented to different respondents. Harrower (2007b) circumvents the problem of having just one large stimulus map by concentrating on several subdivisions – which could be seen as redundant stimuli themselves. Conversely, Fish et al. (2011) and Moon et al. (2014) had their respondents work through 108 stimuli – and put their patience and concentration to the test.

2.5 Study design

In behavioural and cognitive sciences, there are two basic study designs: between-subject and within-subject testing (Charness, Gneezy, & Kuhn, 2012; Keren, 2014). In a typical within-subject design, each participant is exposed to different versions of the same (base) stimulus, modified by the independent variable(s). Since only relative performance differences within each person are analysed, a within-subject design controls for heterogeneity between participants and potentially different testing environments. Thus, within-subject testing is often associated with higher statistical power and smaller sample sizes. Disadvantages are decreasing motivation due to longer tests and the danger of carry-over effects. If, for example, participants remember a stimulus they have already seen, their reaction is altered and the experiment is flawed. Although attempts are made to minimize this risk by temporally separating and concealing variants of the same stimulus-maps (e.g. through rotating or mirroring the variants), between-subject designs are safe in this respect as each person – randomly assigned to one condition – is exposed to each stimulus only once. Due to increased variance caused by personal differences and the division of participants into several groups, between-subject testing requires a larger sample size. In section 4 of this article, we compare the performance of both test designs by using empirical data from our mixed (within- and between-subject) study design on generalization of animated choropleth maps, which is outlined below.

3 An experiment on value generalization in animated maps

In this section, we address some rationales of cognitive cartographic experimental design using a real-world example. The experiment was applied in a full-scale empirical study (Traun, Schreyer, & Wallentin, 2021), aiming to examine whether and how different forms of value generalization of unclassed choropleth map animations affect the ability of users to detect general trends and local outliers thereof. The experiment was in two parts. In the first part, participants are exposed to short sequences of animated map frames, with each animation ('stimulus') consisting of a general trend and two local outliers. These local outliers are polygons with values that differ greatly from the mean value of their neighbours in space AND from the mean value of their neighbours in time (for the definition of neighbourhood, see Figure 2). Immediately after each animation, the stimulus disappears and participants have to select the correct outliers from a set of outlier candidates. In the second part, the same stimuli are shown again, but now test subjects are told to focus on the overall trend and to choose the correct trend response item after the stimulus disappears. Using differently generalized versions of the animations (non-generalized reference, temporally-, spatially- and spatiotemporally generalized versions), we investigate the effect of the generalization mode on the ability of users to correctly detect local outliers and overall trends. The following subsections describe the development of the animated maps used as test stimuli (3.1), the response items participants have to choose from (3.2), the study design and implementation (3.3), and finally the dataset acquired (3.4).

3.1 Test stimuli

Each of our stimuli comprises 14 animation frames showing unclassed attribute/colour changes of an artificial basemap. The basemap consists of 85 irregular enumeration units of roughly similar size to prevent visual dominance of large polygons while preserving the familiar 'choropleth map look' (Figure 1).

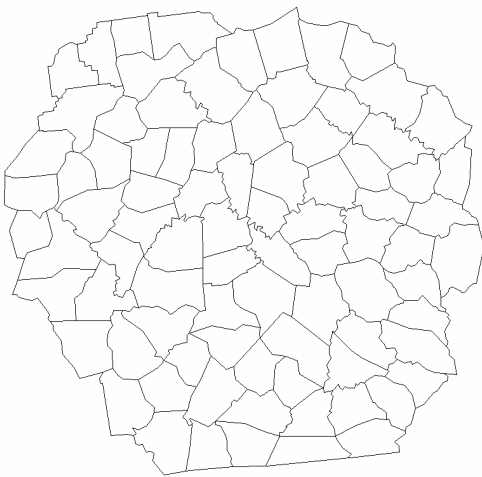


Figure 1: Basemap used for synthetic time-series data

To construct the basemap, we clipped a roughly circular subset of Counties from the US State of Kentucky and merged, split or freely changed several County geometries to approximate their areas. According to Traun and Mayrhofer (2018), choropleth map animation of time-series data seems useful only for data that exhibits a high level of autocorrelation in space and time, as this will lead to a continuous development of patterns throughout the animation. In turn, weakly autocorrelated data result in uncoordinated flicker, hampering perception, and thus calling into question the use of map animation generally. For generating such highly autocorrelated synthetic data, we developed a model using the GAMA agent-based simulation environment (<https://gama-platform.github.io>). The model produces moving clusters embedded in a global trend and allows for parameterizing spatial autocorrelation, temporal autocorrelation, the weight of the overall trend and clustering, and the probability of local outliers in space and time. After determining suitable parameter settings (significant clustering, high autocorrelation, rare appearance of local outliers), a large number of test stimulus candidates was simulated. From these, we chose five time-series stimuli containing exactly two local outlier polygons in space and time in order to ensure comparability between stimuli when analysing outlier detection performance. In addition, we selected only stimuli in which the two outlier polygons

- were separated by at least 0.6 seconds, in order to avoid attentional blink phenomena (Raymond, Shapiro, & Arnell, 1992), and where
- local outlier polygons were not located at the beginning or the end of the 14-frame time-series sequence.

Local outliers were determined by a high value-difference in relation to their first-order neighbourhood in space and time. To define thresholds, we used the heuristic of Traun and Mayrhofer (2018) that evaluates local differences in the context of global autocorrelation. It is based on the rationale that a certain local difference might qualify as a local outlier in a smoothly changing, highly autocorrelated dataset, but not in a less autocorrelated, ‘rougher surface’ (see Traun & Mayrhofer, 2018 for further detail). The explicit generation of a few (the probability of a polygon being a local outlier was set to = 0.002) but highly deviating local values within the otherwise relatively ‘smooth’ data from the GAMA model allowed a fairly clear separation of local outliers from ‘regular’ polygons.

Because of our interest in different types of generalization, we derived three differently generalized versions for each of the test stimuli by smoothing the polygon values that we generated by their

- spatial neighbours
- spatiotemporal neighbours
- temporal neighbours (Figure 2).

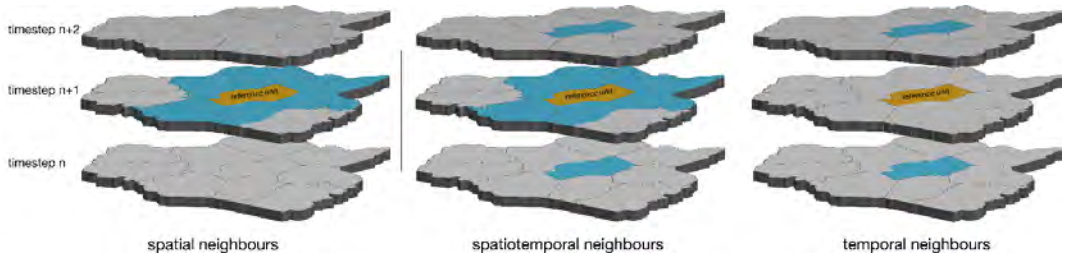


Figure 2: The three definitions of neighbourhood (blue) shown for a single reference unit (orange).

Using the methods and software provided by Traun and Mayrhofer (2018), the amount of smoothing adapts to the degree of autocorrelation in the data. Since all stimuli result from the same model parameters, spatiotemporal autocorrelation is similarly high, with Moran's I_s (Moran, 1950) being between 0.84 and 0.93. Consequently, the strength of the value generalization is fairly similar for all stimuli. It is important to note that the values of the two local outlier polygons in each stimulus were excluded from these generalization processes.

As we wanted to avoid potential visual artefacts introduced by cartographic classification, we opted for unclassified animated choropleth maps (Harrower, 2007b) and linearly applied a sequential yellow-to-dark-brown continuous colour scheme to the data values. While the two local outliers preserve their colour throughout all variants of each stimulus, generalization shifts the colour of other polygons slightly towards the mean value of their spatial, temporal or spatiotemporal neighbours, leading to smoother overall changes within the respective dimension (Figure 3).

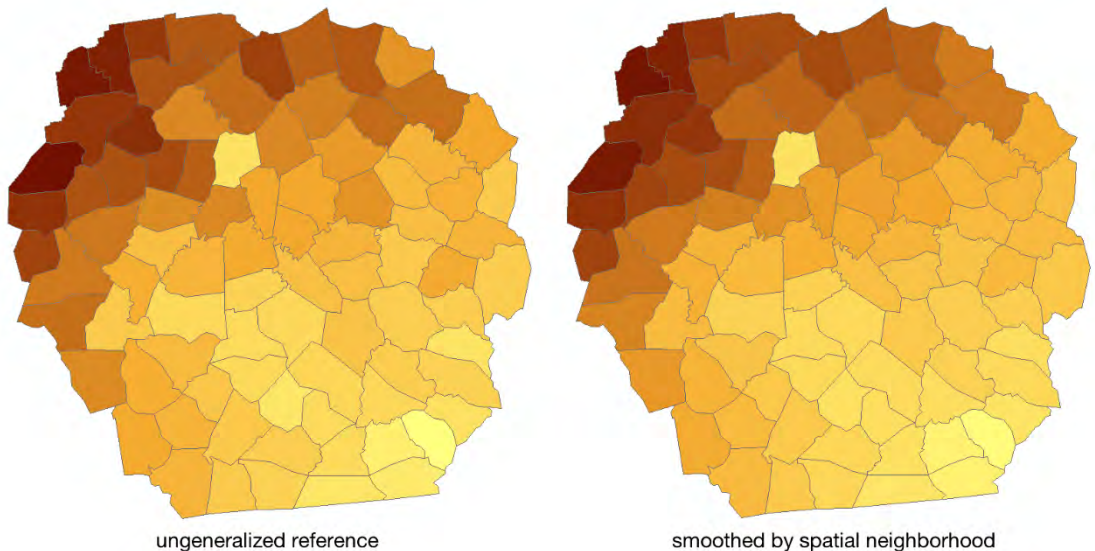


Figure 3: Subtle reduction of local contrast in the spatially generalized version (right) of a frame from Stimulus 1. The colour of a local outlier polygon (light-coloured polygon in the upper-left from centre) is not altered by generalization. Source: Traun et al. (2021)

All test stimuli, measuring 512 by 512 px, were shown at a rate of 5 frames per second and without tweening (Battersby & Goldsberry, 2010; Fish et al., 2011). The resulting 200 ms per frame are within the ‘appropriate’ speed range of 100 to 400 ms found by McCabe (2009), while still being both fast enough to get a passable impression of animation and slow enough to discern individual map frames (Harrower & Fabrikant, 2008). Each stimulus animation was preceded by a leader showing the empty basemap polygons superimposed by a three-second countdown text ‘Start in [3, 2, 1] seconds’. While one of the five stimuli was used as a trial stimulus to familiarize participants with the experiment, four stimuli (referred to in what follows as Stimulus 1, 2, 3 and 4) were used to collect data.

3.2 Response items

Immediately after a stimulus was shown, it was replaced by a set of response items on local outliers (first part of the experiment) or global trends (second part) for participants to choose from.

Local outlier response items

Six randomly arranged basemaps, highlighting one outlier candidate each, contain the two correct outliers from the stimulus and four wrong outlier candidates (Figure 4).

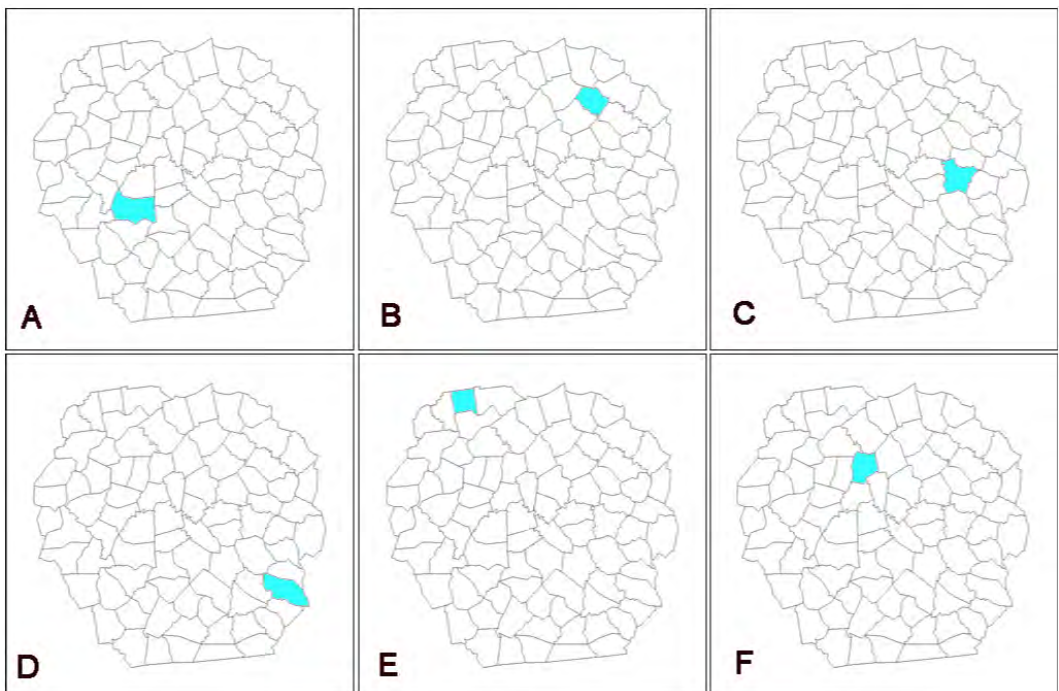


Figure 4: Local outlier response items for Stimulus 1. Compare the options A to F to the local outlier shown in Figure 3. Source: Traun et al. (2021)

For the incorrect candidates, we did not randomly choose non-outlier polygons from the basemap but founded our selection on two criteria:

- Throughout the animation, incorrect outlier candidates should have a low value difference to their spatiotemporal neighbourhood. Thus, polygons were ordered according to their maximum absolute value difference during the whole animation sequence, and incorrect outlier candidates were chosen from the lowest third of the resulting distribution (with the two real outliers being at the top of the distribution). This ensures that participants cannot choose medium local contrast polygons from the non-generalized reference animations, misinterpreting them as local outliers.
- Only polygons not adjacent to other outlier candidates (regardless of whether they were correct or incorrect) qualified as outlier candidates. Spatial dispersion of outlier candidates across the basemap was preferred to prevent participants being confused by similar location. For example, if the correct local outlier is located in the upper left of the animation, there should be just a single outlier candidate within this region.

Giving a clear separation of correct and incorrect outlier candidates both in local brightness contrast and in location, we aimed to prevent accidental misclassification. We thus increased the discriminatory power of the experiment in terms of measuring perception differences between different modes of generalization.

Global trend response items

Compared to the measurement of outlier detection capability, the development of a test for global trend detection was challenging. We soon decided against the use of verbal descriptions of the patterns seen, as this would require further abstraction, including a transformation from visual to verbal cognitive modes. In a pre-test, we tried to assess the perception of pattern-change by using blurred still-images of the first, the seventh and the last frame of the stimulus animation (true candidate), and two other animations (false-trend candidates) (Figure 5). Low success rates, at times close to a random choice, indicated that participants had great difficulties relating the correct, 3-frame, small multiple to the animation stimulus that they had seen.

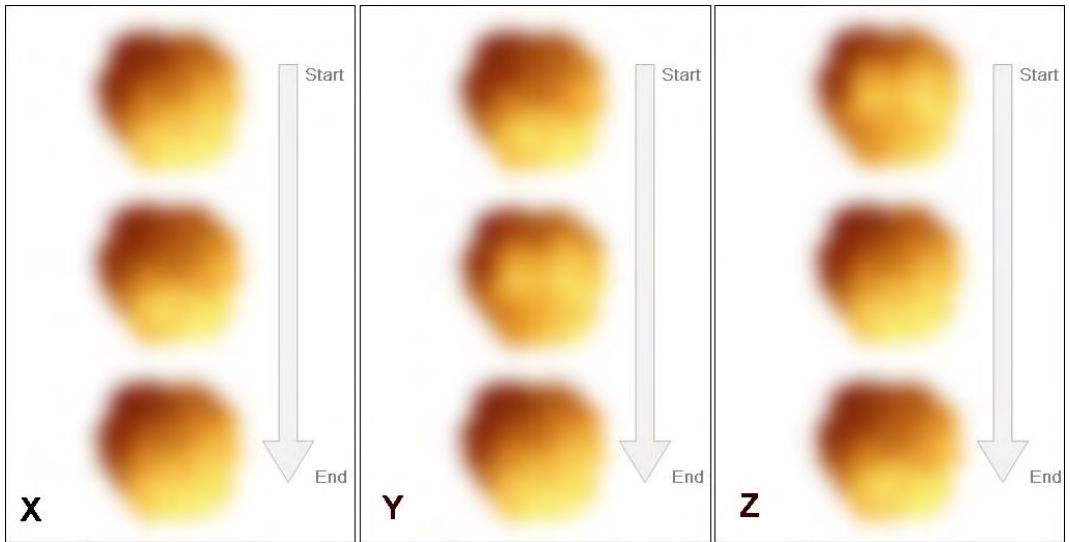


Figure 5: Rejected attempt using static response items for trend detection. Participants in this pre-test had to choose the correct item out of three trend candidates (X, Y, Z)

Thus, we decided to keep presentation mode and temporal granularity, and produced animated response items from downscaled and blurred versions of the actual stimuli and unused test stimulus candidates. While rescaling was necessary to fit response items beside each other on the screen, blurring removed local detail while preserving the overall trend. To ensure that the correct response items were actually determined by their changing global pattern rather than by visually salient outliers, we first removed the two local outliers by assigning them the mean colour of their neighbourhood. Then we downscaled the animations to 160 x 160px and applied a 15px blur (lowpass) filter. Three such global trend response animations (one of which was derived from the actual stimulus animation) were randomly placed next to each other (Figure 6). Each is started by a mouse click and could be replayed as often as desired.

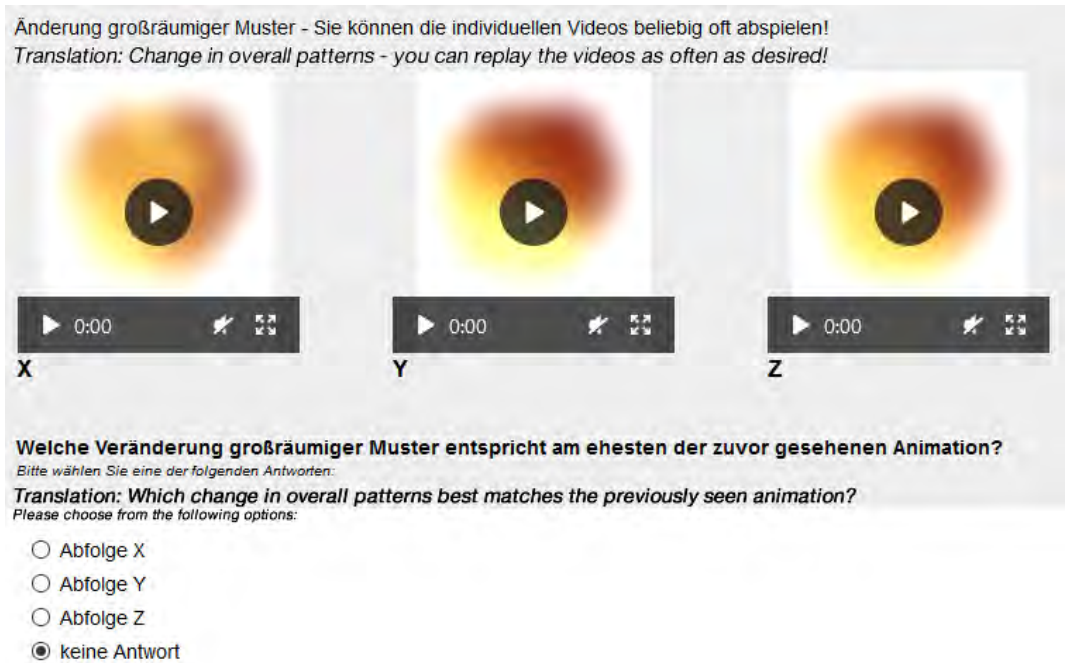


Figure 6: Global trend response item animations. (Original response items did not include English translations.)

3.3 Study design

Despite losing the more closely controlled environment of a laboratory, we chose an online study mode in anticipation of a higher sample size, especially under the current COVID-19 restrictions. We primarily used a four-group between-subject testing design, with the addition of within-subject testing of one stimulus. We did this for two reasons:

1. The anticipated higher power of a within-subject design can act as a ‘backup’ in case of a very small effect size of generalization, not detectable by between-subject testing.
2. If an effect is detected by the between-subject design (which was the case), we planned to empirically compare both design options in terms of their statistical power by using a repeated subsampling approach.

The results of an extensive pilot study led us to assume that generalization in space might have the largest effects on perception. Therefore, a spatially generalized version and the non-generalized reference of Stimulus 1 were shown to each participant in both parts of the experiment. While half of the participants saw the spatially generalized version first, the other half started with the reference version. To reduce the chance of carry-over effects, these stimulus variants were placed at the beginning (Stimulus 1.1) and the end (Stimulus 1.2) of each of the two test sequences, rotated differently and flipped in a balanced fashion (see Figure 7). In case of (unlikely) carry-over effects, a between-subject comparison of Stimulus 1.1 provides another backup level, thanks to a doubled group size.

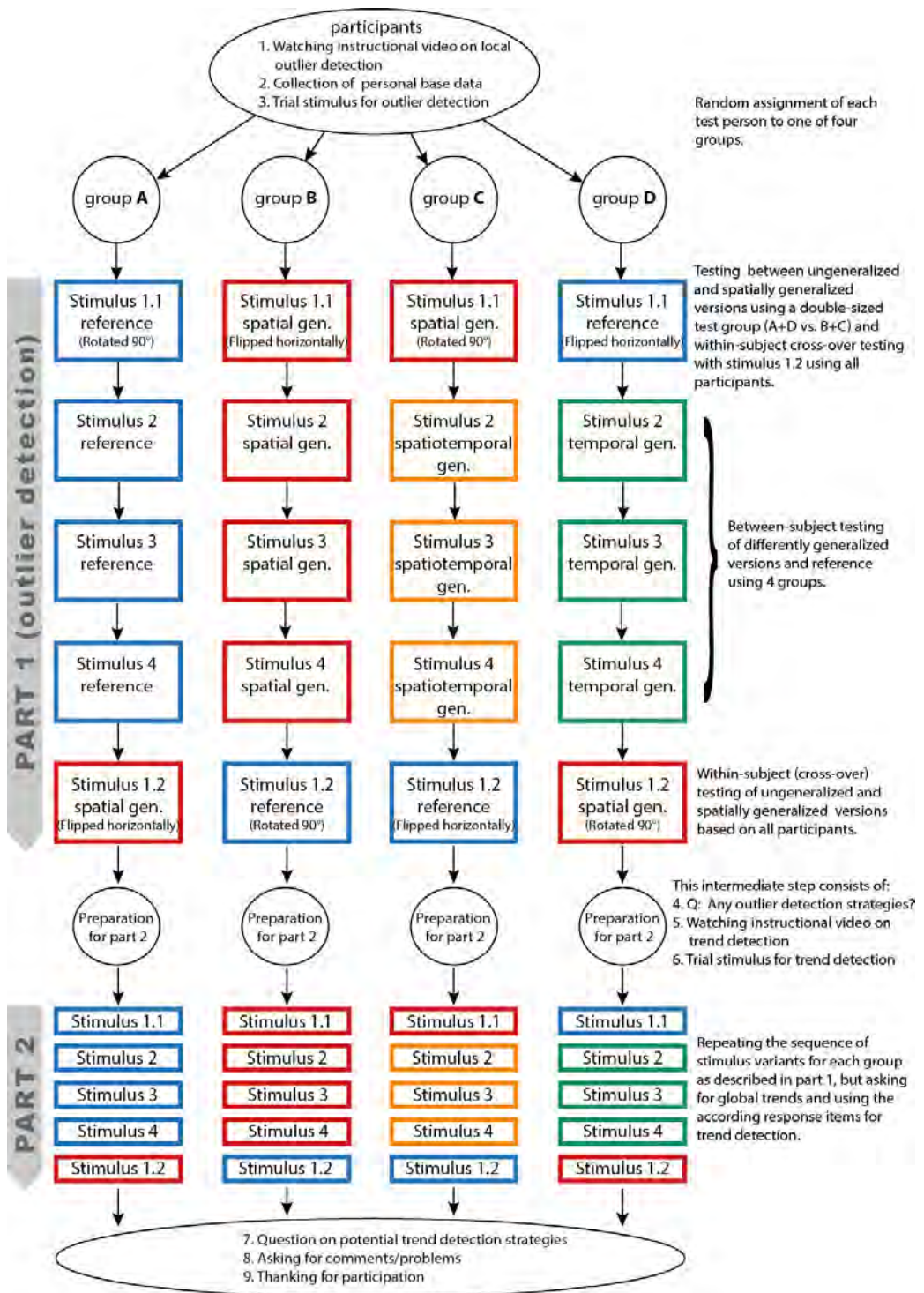


Figure 7: Study design. Source: Traun et al. (2021)

The experiment was implemented as an online study on our university's limesurvey (www.limesurvey.org) instance. To avoid tiny stimuli on small screens and to prevent distraction during participation, we prevented the experiment from running on mobile operating systems and clearly communicated this fact. Forced preloading of stimulus animations in the web-client ensured smooth playback, even in cases of slow internet connection. (Please refer to Figure 7 for the detailed steps in the study procedure.)

3.4 Participants and data

The study was conducted in December 2020 and led – after data cleaning – to a total of 440 responses for analysis, which were distributed equally between the four groups and both genders. Thus, each group (A, B, C, D) provided data from 55 male and 55 female respondents with similar age distributions. (See Traun et al. (2021) for further details on the recruitment of participants and characteristics of the sample.) As in most online studies, participation was motivated primarily by curiosity and personal interest. Such self-selected participation requires critical evaluation as it can bias study results. In our case, we did not see any problem, for two reasons:

1. The study is not related to any personal opinion, but tests basal perceptual abilities. In contrast, participation in a study on personal impacts of the covid-19 crisis might be more attractive to more affected persons. Thus, the aggregated results would potentially be biased by predominant opinions and experiences of a non-representative sample.
2. We assessed potentially confounding factors like cartographic competence, educational level and computer gaming affinity; we did not find any significant effect of these variables on the ability to detect local outliers and global trends.

While analysis and discussion of the data from a cognitive perspective are outside the scope of this paper (see Traun et al. (2021)), the data allowed us to empirically analyse and compare the statistical power of the within-subject and the between-subject designs, as outlined in the following section.

4 Comparing within-subject and between-subject testing

Thanks to our mixed study design, we were able to directly compare both design approaches. For this purpose, we used data on local outlier detection from Stimulus 1. As can be seen in Figure 7, each of the 440 participants saw both variants (ungeneralized reference and spatial generalization) of this stimulus. Half of them (groups A + D) saw the reference version first, while the other half (groups B + C) first saw the spatially generalized version. For each stimulus instance, the number of correctly detected outliers (0, 1 or 2) was recorded.

4.1 Within-subject testing

In the within-subject testing approach, for each participant we calculated the difference in the number of correctly detected outliers between the reference and the spatially generalized versions. For the resulting distribution (Table 2), the 95%-bootstrap-confidence interval (Efron, 1992) for the mean is given by [-0.640, -0.493] and the null hypothesis (mean is equal to 0/there is no difference between spatially generalized and reference variants) is rejected.

Table 2: Differences in correctly identified outliers between reference and spatially generalized animations of Stimulus 1.

Reference - Spatial Variant # of correct outliers	-2	-1	0	1	2
Frequency	42	206	154	36	2

4.2 Between-subject testing

For between-subject testing, we pooled the data from groups A + D (reference in Stimulus 1.1, 220 persons) and tested them against the pooled data from B + C (spatially generalized variant in Stimulus 1.1, 220 persons) using the nonparametric ANOVA-type test statistic from the R package *npmv* (see Ellis, Burchett, Harrar, & Bathke, 2017 for further details). The difference is highly significant ($p < 0.001$) and the null hypothesis is rejected. A repetition of this approach using the second instance (Stimulus 1.2) yields the same result. In this type of nonparametric analysis, effect size can be expressed as the probability of achieving a higher response (here: detect more outliers) when belonging to a certain group. With effect sizes of 0.24 (reference) and 0.76 (spatial generalization) for Stimulus 1.1, and of 0.32 and 0.68 for Stimulus 1.2 respectively, the effect of generalization is rather large.

4.3 Comparative analysis

Both design approaches provide evidence that there is a significant difference in outlier detection between the spatially generalized and ungeneralized versions of Stimulus 1 when using our large sample of 440 respondents. But what might have happened if there had been fewer participants (or smaller effect sizes)?

To answer this question, we used repeated subsampling and testing. From each of the eight instances (Stim1.1/group A, Stim1.1/B, Stim1.1/C, Stim1.1/D; Stim1.2/A, Stim1.2/B, Stim1.2/C, Stim1.2/D), we randomly drew the same number of persons while ensuring that nobody was selected twice. This led to subsample sizes of multiples of eight. The within-subject testing was done using the whole subsample, while for the between-subject testing we used only the personal results from the instance a person was drawn from: for example, the correct number of outliers seen in Stim 1.2 group B, if the person was drawn from that instance. These results were pooled into the corresponding spatially generalized group (Stim1.1/B, Stim1.1/C, Stim1.2/A, Stim1.2/D) and reference group (Stim1.1/A, Stim1.1/D, Stim1.2/B, Stim1.2/C), and tested in a between-subject fashion. Note: the inclusion of the second instance of Stimulus 1 was necessary to obtain an unbiased subsample in terms of

evolving learning strategies, as these might play a role in the within-subject case. This subsampling and testing procedure was repeated 500 times for each subsample size (n), each time recording whether the null hypothesis was rejected or not at a given alpha level (we tested at $\alpha = 0.05$ and $\alpha = 0.01$) for both design/testing approaches. The results (Figure 8) show large differences between the within-subject and the 2-group between-subject designs with regard to the total number of participants needed in order to obtain reliable results.

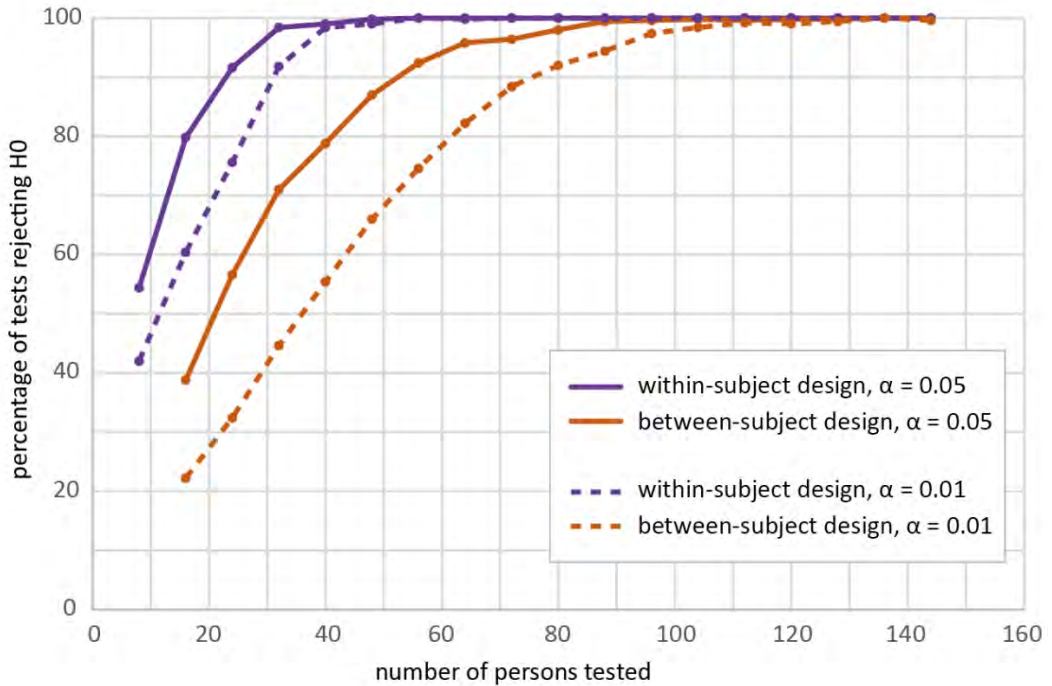


Figure 8: Percentage of the correct detection of significant differences between the spatially generalized and the ungeneralized variant of Stimulus 1 for different sample sizes/numbers of persons tested when using typical within-subject or between-subject approaches. Each data point is based on 500 subsamples/tests. For the between-subject design, 16 individuals (8 per stimulus variant) is the minimum number to achieve test results; for within-subject testing, 8 participants (each generating two data elements to compare) are sufficient for calculations.

Assuming that there is a difference between the spatially generalized and the reference variants, one can see from the simulation results that for an alpha level of 0.05, sample sizes of at least 24 respondents (within-subject testing) and 56 (between-subject testing) are needed for this particular stimulus to reject H0 in 90% of the cases. When more than two groups are to be compared, the total number of participants needed rises accordingly for the between-subject approach. However, having tested 110 persons per group in the remaining Stimuli 2, 3 and 4, we are safe in this respect, while one or the other empirical studies in this field (Table 1) might have been borderline.

To illustrate the difference between within- and between-subject testing (apart from the obvious increase of total persons needed in the latter, explained by a simple multiplication by

the number of groups), normalized results are shown in Figure 9. The total number of test subjects along the x-axis is replaced by the number of (compared) data elements, whereas each within-subject test person is represented by two data elements (Stim 1.1 and 1.2) and each between-subject test person provides just one data element.

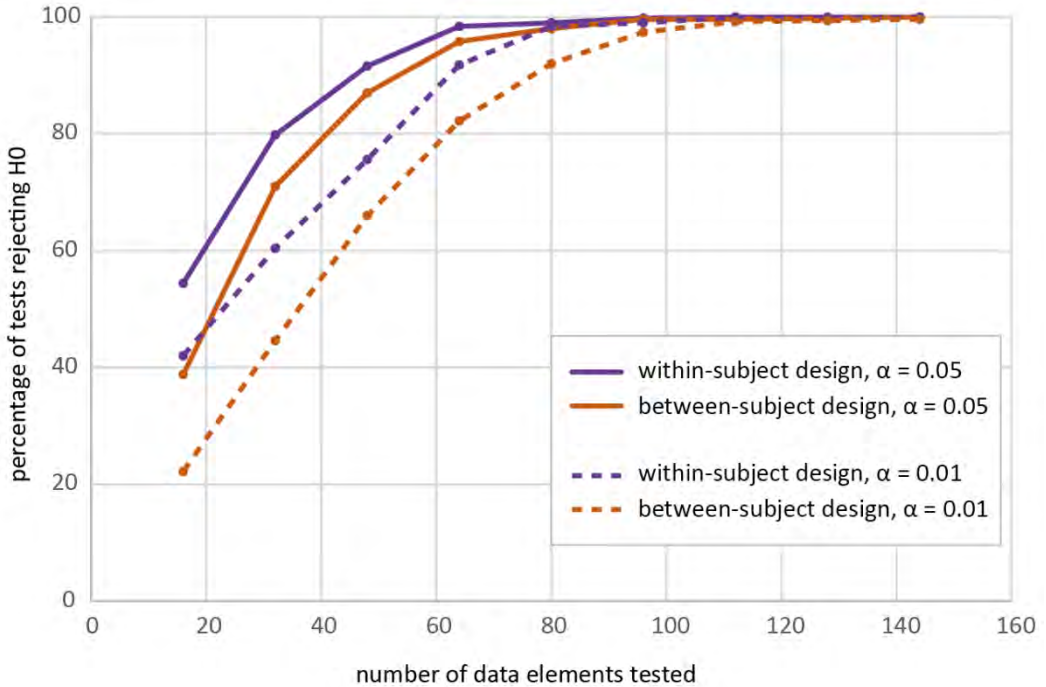


Figure 9: Percentage of tests rejecting H0 by comparing the number of data elements.

The smaller but still systematic difference can foremost be attributed to a better control of confounding variables, such as individual differences in visual perception, motivational level, screen resolution and contrast etc. in the within-subject design, as those variables are largely kept constant. However, the slightly different statistical power of the (nonparametric) bootstrapping approach and the nonparametric ANOVA-type test might also contribute to a difference in either direction.

5 Lessons learned and conclusion

Reviewing the literature, doing pre-testing and running an extensive pilot study provided valuable insights that contributed to the final study design presented here. To give an example, combining outlier and trend detection tasks while viewing the stimuli (although the stimuli were repeated) proved to be a weak point of an early conception used in the pilot study. Having to report on both tasks after the stimulus disappeared added confounding cognitive variables, like divided attention or short-term memory abilities, which diluted data on actual task

performance. Thus, a clear split of the study into two parts was necessary. Although participants still need to recall the outliers (part 1) and trends (part 2) seen in the chosen study setup, we assume the loss of perceived information due to memory imperfections to be invariant under different conditions of generalization, and so not affecting the general perceptive differences we wanted to explore. Study designs allowing for a more direct assessment of perception (like eye tracking) or directly indicating the appearance of an outlier (e.g. verbally or by pressing a button) are superior in this respect, as they are not affected by imperfect recall of information. In our case, however, the cognitive bottleneck is clearly in the perception, as remembering two outlier positions for a few seconds is certainly not a demanding task.

With this paper, we hope to emphasize the diversity of considerations associated with empirical cartographic experiments, notably in the domain of animation, as time adds a level of complexity. The careful design of map stimuli and study architecture play a pivotal role when robust results and transferable insights are the overall goal. Under the advantageous condition of a large effect size in the data we used for power analysis, around 30 participants in a within-subject and around 60 participants in a two-group between-subject design are the minimum to be relatively (around 95%) safe in avoiding type-II errors at the usual alpha level of .05. For smaller effect sizes, higher demands in type-II error prevention and/or smaller alpha levels, larger samples are needed. Apart from cartographic stimulus design in the narrow sense, good question design (Olson, 2009) and counterbalancing (A. Griffin, 2015) are also worth critical consideration when designing cartographic experiments.

Acknowledgements

The first author would like to thank Prof. Dr. Wolfgang Trutschnig for discussing the study design, as well as the anonymous reviewers for their valuable inputs.

References

- Battersby, S. E., & Goldsberry, K. P. (2010). Considerations in Design of Transition Behaviors for Dynamic Thematic Maps. *Cartographic Perspectives*(65), 16-32.
- Butler, P. (2016). Mapping Temporal Datasets with D3. *Cartographic Perspectives*(81), 44-48.
- Campbell, C. S., & Egbert, S. L. (1990). Animated cartography/Thirty years of scratching the surface. *Cartographica: The International Journal for Geographic Information and Geovisualization*, 27(2), 24-46.
- Charness, G., Gneezy, U., & Kuhn, M. A. (2012). Experimental methods: Between-subject and within-subject design. *Journal of Economic Behavior & Organization*, 81(1), 1-8.
doi:<https://doi.org/10.1016/j.jebo.2011.08.009>
- Cybulski, P., & Krassanakis, V. (2021). The Role of the Magnitude of Change in Detecting Fixed Enumeration Units on Dynamic Choropleth Maps. *The Cartographic Journal*, 1-17.
doi:10.1080/00087041.2020.1842146
- Cybulski, P., & Medyńska-Gulij, B. (2018). Cartographic redundancy in reducing change blindness in detecting extreme values in spatio-temporal maps. *ISPRS International Journal of Geo-Information*, 7(1), 8.

- DuBois, M. (2013). Complexity and Saliency: Evaluating the Inter-Scene Variability of Animated Choropleth Maps. (Master Thesis), University of South Carolina,
- Efron, B. (1992). Bootstrap methods: another look at the jackknife. In *Breakthroughs in statistics* (pp. 569-593): Springer.
- Ellis, A. R., Burchett, W. W., Harrar, S. W., & Bathke, A. C. (2017). Nonparametric inference for multivariate data: the R package nrmv. *Journal of Statistical Software*, 76(4), 1-18.
- Fish, C., Goldsberry, K. P., & Battersby, S. (2011). Change blindness in animated choropleth maps: an empirical study. *Cartography and Geographic Information Science*, 38(4), 350-362.
- Griffin, A. (2015). Designing your user study or experiment. Paper presented at the ICC 2015, Curitiba, Brazil.
- Griffin, A. L., MacEachren, A. M., Hardisty, F., Steiner, E., & Li, B. (2006). A comparison of animated maps with static small-multiple maps for visually identifying space-time clusters. *Annals of the Association of American Geographers*, 96(4), 740-753.
- Harrower, M. (2003). Tips for designing effective animated maps. *Cartographic Perspectives*(44), 63-65.
- Harrower, M. (2007a). The Cognitive Limits of Animated Maps. *Cartographica*, 42(4), 349-357. doi:10.3138/carto.42.4.349
- Harrower, M. (2007b). Unclassed animated choropleth maps. *The Cartographic Journal*, 44(4), 313-320.
- Harrower, M., & Fabrikant, S. I. (2008). The role of map animation for geographic visualization. In M. Dodge, M. M. Derby, & M. Turner (Eds.), *Geographic Visualization. Concepts, Tools and Applications* (pp. 49-65). Chichester.
- Keren, G. (2014). Between-or within-subjects design: A methodological dilemma. *A Handbook for Data Analysis in the Behavioral Sciences*, 1, 257-272.
- Lobben, A. (2008). Influence of data properties on animated maps. *Annals of the Association of American Geographers*, 98(3), 583-603.
- McCabe, C. A. (2009). Effects of Data Complexity and Map Abstraction on the Perception of Patterns in Infectious Disease Animations. (Master of Science Master Thesis), The Pennsylvania State University, University Park, Pennsylvania.
- Monmonier, M. (1996). Temporal generalization for dynamic maps. *Cartography and Geographic Information Systems*, 23(2), 96-98.
- Moon, S., Kim, E.-K., & Hwang, C.-S. (2014). Effects of Spatial Distribution on Change Detection in Animated Choropleth Maps. *The Journal of the Korean Society of Surveying, Geodesy, Photogrammetry and Cartography*, 32(6), 571-580.
- Moran, P. A. P. (1950). Note on Continuous Stochastic Phenomena. *Biometrika*, 37(1), 17-23.
- Multimäki, S. (2016). Reducing the information load in map animations as a tool for exploratory analysis. (Dissertation), Aalto University,
- Multimäki, S., & Ahonen-Rainio, P. (2015). Temporally Transformed Map Animation for Visual Data Analysis. *GEOProcessing 2015*, 34.
- Olson, J. M. (2009). Issues in human subject testing in cartography and GIS. Paper presented at the Proceedings of the International Cartographic Conference 2009.
- Raymond, J. E., Shapiro, K. L., & Arnell, K. M. (1992). Temporary suppression of visual processing in an RSVP task: An attentional blink? *Journal of experimental psychology: Human perception and performance*, 18(3), 849.
- Traun, C., & Mayrhofer, C. (2018). Complexity reduction in choropleth map animations by autocorrelation weighted generalization of time-series data. *Cartography and Geographic Information Science*, 45(3), 221-237. doi:10.1080/15230406.2017.1308836
- Traun, C., Schreyer, M. L., & Wallentin, G. (2021). Empirical Insights from a Study on Outlier Preserving Value Generalization in Animated Choropleth Maps. *ISPRS International Journal of Geo-Information*, 10(4), 208.

Towards Dynamic Isochrone Mapping Accounting for Uncertainty

David Li, Matthias Budde and Julian Bruns
Disy Informationssysteme GmbH, Germany

Abstract

Isochrone Mapping has been used since the late 19th century as a planning and visualization tool in various domains, such as transport planning and hydrology. In the past, isochrone calculation was based mainly on static properties and therefore also yielded static maps. This resulted in a potentially significant — and at the same time unquantifiable — degree of uncertainty. Today however, advances both in information technology and in the availability of input data allow much more nuanced views on the subject.

This paper gives an overview of work on dynamic factors that contribute to uncertainty in isochrone calculation and mapping. Various application scenarios and their constraints are discussed, and open research challenges and possibilities identified. Finally, we present preliminary results from a practical approach to quantifying uncertainties in isochrone calculation for motorized individual transport based on Monte Carlo simulations and data from open routing APIs.

Keywords:

accessibility analysis, isochrone map, travel time, uncertainty, transport science

1 Introduction

An isochrone (Greek: iso = equal, chronos = time) is a line or area on a map that denotes events with equal duration, or events taking place at the same time as each other. Isochrones are often used to visualize the accessibility of certain spatial entities, such as travel times from a certain point of origin. The first cartographer to draw such a map was Francis Galton 1881 (Bielecka and Bober 2013; Dovey, Woodcock and Pike 2017). His Isochronic Passage Chart for Travellers displayed how many days it took to travel to any place in the world from London without incurring unreasonable cost. However the quality of the data and its spatial coverage were naturally rather low, so the map could only be considered a rough estimate.

While data quality has increased greatly since then, uncertainty is often inadequately considered in isochrone calculation and mapping. The goal of this work is to address this issue and develop a method to measure and present the uncertainty of isochrone maps. Such an uncertainty metric may contribute to better decision making in urban and transport planning.

2 Isochrone Mapping

Following Galton's work, geographers, and transport and urban planners started to use isochrone maps as a tool to analyze and visualize the relationship between movement and time (Dovey, Woodcock and Pike 2017; Bielecka and Bober 2013). In particular, the map's strength lies in visualizing the accessibility of localities (Doling 1979; Berg et al. 2018). In recent years, through better computing power and faster routing algorithms (Baum et al. 2015), isochrone map generation has become much easier. Still, due to the high complexity and uncertainties involved, it is common to reduce the number of elements for consideration to just a handful for any one use-case. According to Dovey, Woodcock and Pike 2017, there are three primary uses for isochrone maps:

1. Comparing the accessibility of any given location at a given time for different modes of transport. For example: Allen 2018 linked travel times to network edges and compared the reachable edges by travel mode (e.g. bicycle and public transport). O'Sullivan, Morrison & Shearer 2000 used timetable and street network data to generate isochrones for travel by public transport.
2. Comparing the accessibility of locations for different time constraints – visualizing inequities of access. Such maps are developed yearly by the German Federal Institute for Research on Building, Urban Affairs and Spatial Development to show spatial transport-related accessibility in Germany (Schwarze et al. 2019).
3. Visualizing the effect of potential changes to help urban and transport planners. For instance, Berg et al. 2018; Efentakis et al. 2013 used isochrones with dynamic traffic and demographic data to look at what proportion of a population was unable to access a certain location within a given travel time.

As decisions and constraints vary according to individual demands, there is no single type of accessibility and isochrone map (Schwarze et al. 2019; Strubelt & Wegener 2001; Handy & Niemeier 1997). Instead, we must consider various factors and the spectrum of possible applications for isochrone maps. These factors were categorized into four accessibility components by Geurs & Van Wee (2004):

1. The land-use component considers "amount, quality and spatial distribution" of opportunities (e.g. jobs, shops, health, social facilities) and their demand.
2. The transportation component characterizes the individual (monetary or temporal) effort to cover the distance between the point of departure and the destination by one or more means of transport.
3. The temporal component describes the temporal availability of opportunities (e.g. opening times of shops) or individuals to engage in certain activities and their dynamic variability (weather, traffic load).
4. The individual component reflects the needs, abilities and opportunities of individuals. These factors depend on various attributes of the individual (e.g. age, income, physical condition or educational level).

These accessibility components can also be regarded as sources of uncertainty and thus reflect the factors that need to be considered when creating isochrone maps. Our goal is to explore how this can be approached effectively and efficiently.

3 Dynamic Isochrone Mapping and Uncertainty

In order to generate isochrone accessibility maps accurately, ideally all factors according to Geurs & Van Wee 2004 need to be taken into account (see Fig. 1).

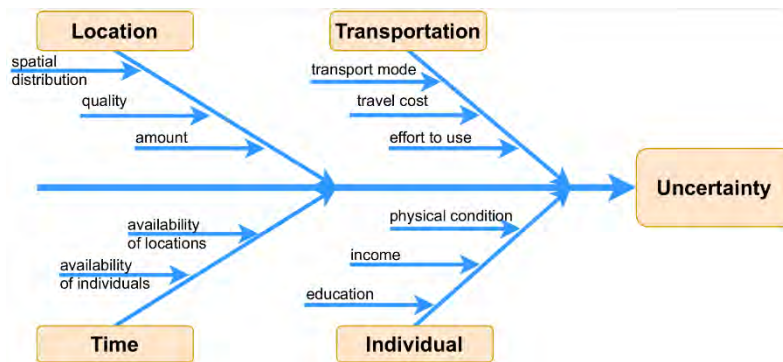


Figure 1: Accessibility components as sources of uncertainty in isochrone mapping.

In addition to understanding where uncertainty may stem from in isochrone mapping, there is another important aspect to consider: the degree of uncertainty that is acceptable from a user's point of view, which strongly depends on the application scenario, as do the constraints for each of the four components above. For instance, when planning a vacation, a higher degree of uncertainty concerning the travel time is likely to be acceptable, and the choice of mode of transportation may to some extent be flexible, whereas financial constraints will probably be more rigid.

However, there are other application scenarios that are completely different. If we were to apply isochrone mapping to determine which areas of a city can be reached by emergency response services (police, firefighters, ambulance), the time taken to arrive at the scene is (in some countries) constrained by law and too large an uncertainty is unacceptable. On the other hand, there are practically no individual components in this scenario.

In law enforcement, projecting which way a fugitive may have fled and what locations they could have reached can provide crucial information for apprehending criminals quickly. In such scenarios, the predominant source of uncertainty are individual factors.

Although there are a lot of studies which have used and developed isochrone maps to visualize specific forms of accessibility (Marciuska & Gamper 2010; Dovey, Woodcock & Pike 2017), few of them have included dynamic factors in their isochrone calculations (Efentakis et al.

2013; Berg et al. 2018). While there exists a lot of research about uncertainties in point-to-point vehicle routing, the level of uncertainty in isochrone mapping remains quite unclear.

Open routing APIs like Valhalla or GraphHopper (which are growing in importance) allow us to incorporate information on the dynamics of traffic into isochrone mapping and leverage this for decision making processes, which is a clear need, especially for emergency response services (Hu et al. 2020; Green et al. 2014).

4 Practical Isochrone Mapping Based on Open APIs

In this preliminary work, we take into account the three components location (coordinates of isochrone origins), time (start and range) and transport (mode) in a Monte Carlo simulation with the goal of reaching an uncertainty measure for isochrones. Due to its high complexity and the lack of available data, we disregard the individual component.

Data and Methodology

The general approach is to construct both static isochrones (i.e. ones that do not take dynamic factors into account) and dynamic isochrones, which incorporate the relevant traffic information for time and place in the accessibility mapping (see Figure 2). The degree of uncertainty can then be expressed by comparing the areas of reachability as determined by the two different types of isochrone.

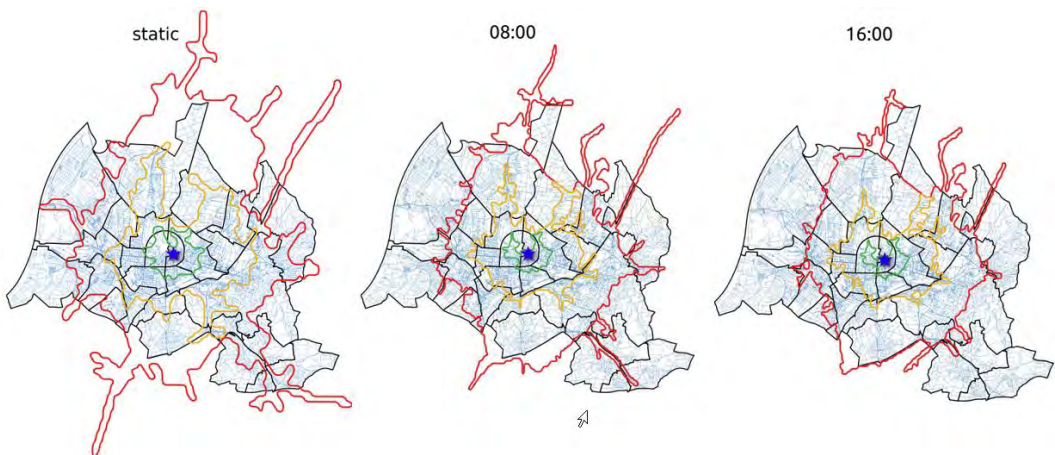


Figure 2: Map visualization of calculated isochrones. The static isochrone (left) does not take the traffic situation into account, whereas the dynamic ones do. The reduced reachability ranges, which differ depending on the time of day, show up clearly.

For this, we find that data from the HERE Routing API is fit for our purpose. The calculations of the isochrones are based on the passenger car as transport mode and road network data, for instance speed and turn restrictions.

HERE Routing is a cloud service for in-car navigation systems found in over 150 million vehicles, or 80% of road vehicle navigation systems in North America and Europe (Morlock et al. 2019; HERE Technologies n.d.). We can therefore assume that HERE Technologies provides data that is of sufficient quality for our purposes. Routing services exist for various modes of transport (car, pedestrian, public transport, truck and bicycle) as well as any combinations of these. Results are either a simple (temporal or distance) shortest path between two points or a matrix for a set of shortest paths between multiple points, such as the isochrone mapping. Furthermore, live or historical traffic data can be taken into account, so we can compare temporally different routing results. Access to HERE Technologies' data is possible via a simple REST API.

First, we generated evenly distributed isochrone start points within the City of Karlsruhe, Germany, which were map matched to car accessible roads; for each of these points, we calculated isochrones with a range of 15 minutes. Afterwards, we divided the results into two different categories: (1) static isochrones, which do not consider any dynamic factors; (2) dynamic isochrones, which utilize HERE Technologies' dynamic traffic model for calculation. For the latter category, we chose January 13th, 2020 – a Monday – as the investigation date, so that the traffic situation was not distorted due to the COVID-19 pandemic. Furthermore we investigated the changes of the isochrones over the day, by calculating them at each full hour.

In the next step, we calculated the area ratio between the dynamic isochrones and the static isochrones, and used histograms to visualize the distribution of the area difference ratio over the day. Finally we investigated the course of the mean and variance values of the area differences.

Preliminary Results and Discussion

The 24 histograms – one for each full hour of our investigation date – revealed the distribution of the area difference ratio of these isochrones. For the illustrative purposes, we have selected six representative histograms, as shown in Figure 3, for January 13th, 2020, with the timestamps: 5:00, 7:00, 11:00, 16:00, 18:00 and 22:00. The x-axis represents the ratio of the isochrone area differences and the y-axis represents the relative frequency. Each histogram shows the ratio distribution of a certain timeframe. The results show that nearly all dynamic and static isochrones have similar area size (the ratio approaches 1) during the night, between 22:00 and 05:00. This means that during the night there is nearly no dynamic isochrone uncertainty. This is to be expected, since during the night there is very little traffic on the roads. Between 5:00 and 7:00, a trend of increasing dispersion and a shift of the mean ratio value is identifiable – showing the first traffic peak in the morning. As the day progresses, the distribution skews towards the left due to the decreasing of the ratio value, which reaches its minimum at about 16:00. We may assume that this is caused by the evening traffic peak, following which the distribution starts to skew back towards the right until 22:00, when there is again nearly no difference between the dynamic and static isochrones.

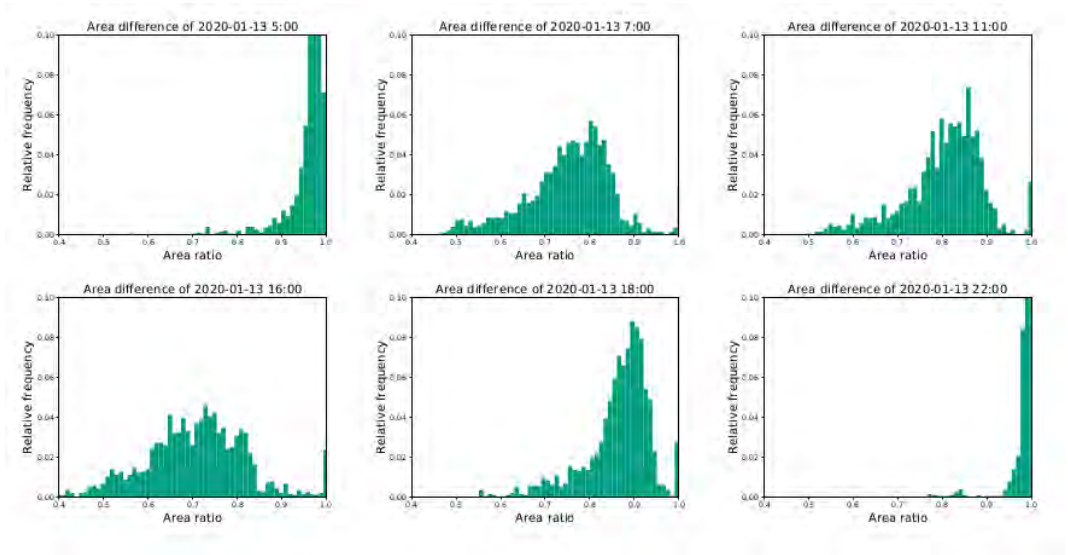


Figure 3: Selected histograms of the case study: The x-axis represents the area difference ratio between dynamic and static isochrones, and the y-axis represents the relative frequency. The area ratio varies over the time. In extreme cases in the daytime, there is an area overlap of only 40%.

Figure 4 shows the variance and the mean values of isochrone differences over the day. It should be noted that the y-axis of the means graph is reversed to allow a better visual comparison with the variance graph. When we look at Figure 4, we can see two big changes in the course of the curves. The first jump can be seen between 5:00 and 7:00. Between those two timestamps, the mean value has dropped significantly; simultaneously, the variance of the distribution has increased very significantly. This indicates that (1) the dynamic and static isochrones are quickly becoming different in size; (2) the variability of this difference is growing rapidly. Between 7:00 and 13:00, the curve remains relatively constant for both values, showing only small changes, or even small decreases of the traffic volume, at noon. From about 13:00, the traffic volume starts to increase until it reaches its peak at 16:00, when the mean area difference between both types of isochrone is the greatest. Finally, in the last major change of both values, the variance declines rapidly between 16:00 and 21:00, while the mean ratio increases towards 1, showing the declining traffic volume during the evening. There is another interesting result to be seen in Figure 4: a similarity between the daily courses of mean and variance. We interpret this as a positive correlation between the average uncertainty and the spatial uncertainty distribution.

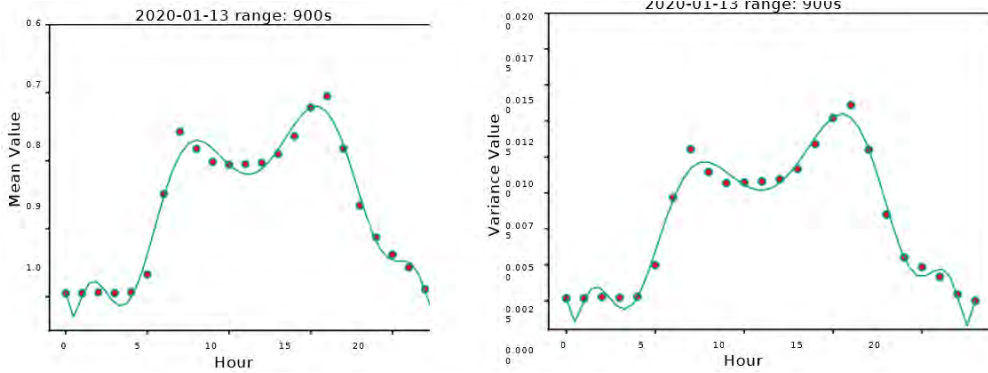


Figure 4: Uncertainty mean and variance over the day. The y-axis of the mean figure is reversed to allow a better visual comparison. A clear similarity between the courses of the mean and of the variance can be seen.

To summarize, we can say that there is a significant difference between the dynamic and the static isochrones during the daytime, between about 6:00 and 21:00. At the same time, there is also a high variance of the distribution. During the night, we have a low variance value and almost no difference between the static and dynamic isochrones, a result which we can interpret as follows: during the day there is significantly more traffic, and its distribution is more dispersed than during the night. In addition, there is a possible link between the traffic distribution (variance) and the total amount of traffic (mean difference ratio). The extent of the dynamic uncertainty should therefore be taken into account when a static isochrone map is used to support decision making.

5 Conclusion and Future Work

This work provides an overview of the scope of isochrone mapping and its application scenarios, factors that contribute to uncertainty, and the state of the art and current limitations — especially in handling dynamic factors.

Based on this theoretical background, we developed a practical approach that uses a Monte Carlo simulation to estimate the distribution of uncertainties in formerly static isochrone maps. Our preliminary results show the variability of the distribution over a single day and clearly highlight the need for more nuanced approaches in isochrone generation.

In future work, we plan to expand our Monte Carlo simulation by taking other uncertainty parameters into account. Firstly, we intend to investigate the impact of spatial variability on isochrone mapping. Secondly, we will address other open research challenges, such as adequate visualization of dynamic information uncertainties (MacEachren et al. 2005).

Acknowledgement

This work was partially funded as part of project OPENER-next, funded by the German Federal Ministry of Transportation and Digital Infrastructure (BMVI), funding measure mFUND, under grant no. 19F2147D.

References

- Allen, Jeff. 2018. Using Network Segments in the Visualization of Urban Isochrones. *Carto- graphica: The Int. Journal for Geographic Information and Geovisualization* 53 (4).
- Baum, Moritz, Valentin Buchhold, Julian Dibbelt and Dorothea Wagner. 2015. Fast Computation of Isochrones in Road Networks. arXiv preprint arXiv:1512.09090.
- Berg, Joris van den, Barend Köbben, Sander van der Drift and Luc Wismans. 2018. Towards a dynamic isochrone map: Adding spatiotemporal traffic and population data. Paper presented at the LBS 2018: 14th International Conference on Location Based Services, 195–209.
- Bielecka, Elzbieta, and Anna Bober. 2013. Reliability Analysis of Interpolation Methods in Travel Time Maps—The Case of Warsaw. *Geodetski vestnik* 57 (2).
- Doling, John. 1979. Accessibility and strategic planning. Research Memo 75 Monograph. Dovey, Kim, Ian Woodcock and Lucinda Pike. 2017. Isochrone Mapping of Urban Transport: Car-dependency, Mode-choice and Design Research. *Planning Practice & Research* 32 (4):402–416.
- Efentakis, Alexandros, Nikos Grivas, George Lamprianidis, Georg Magschab and Dieter Pfoser. 2013. Isochrones, traffic and DEMOgraphics. Paper presented at the Proceedings of the 21st ACM SIGSPATIAL International Conference on Advances in Geographic Information Systems, 548–551.
- Galton, Francis. 1881. On the construction of isochronic passage-charts. Paper presented at the Proceedings of the Royal Geographical Society and Monthly Record of Geography, 3:657–658. 11. JSTOR.
- Geurs, Karst T, and Bert Van Wee. 2004. Accessibility evaluation of land-use and transport strategies: review and research directions. *Journal of Transport geography* 12 (2):127–140. <https://doi.org/10.1016/j.jtrangeo.2003.10.005>.
- Green, Chéri, Gerbrand Mans, Peter Schmitz, David McKelly and Mark Te Water. 2014. Planning for emergency services using GIS-based geographic accessibility analysis. *Town and Regional Planning* 64:53–64.
- Handy, Susan L, and Debbie A Niemeier. 1997. Measuring accessibility: an exploration of issues and alternatives. *Environment and planning A* 29 (7):1175–1194.
- HERE Technologies. <https://developer.here.com>. Accessed on 28. Jan 2021.
- Hu, Wenyan, Jinkai Tan, Mengya Li, Jun Wang and Fahui Wang. 2020. Impact of traffic on the spatiotemporal variations of spatial accessibility of emergency medical services in inner-city Shanghai. *Environment and Planning B: Urban Analytics and City Science* 47 (5):841–854.
- MacEachren, Alan M, Anthony Robinson, Susan Hopper, Steven Gardner, Robert Murray, Mark Gahegan and Elisabeth Hertzler. 2005. Visualizing geospatial information uncertainty: What we know and what we need to know. *Cartography and Geographic Information Science* 32 (3):139–160.
- Marcuska, Sarunas, and Johann Gamper. 2010. Determining objects within isochrones in spatial network databases. Paper presented at the East European Conference on Advances in Databases and Information Systems, 392–405. Springer.

- Morlock, Florian, Bernhard Rolle, Michel Bauer and Oliver Sawodny. 2019. Forecasts of electric vehicle energy consumption based on characteristic speed profiles and real-time traffic data. *IEEE Transactions on Vehicular Technology* 69 (2):1404–1418.
- O’Sullivan, David, Alastair Morrison and John Shearer. 2000. Using desktop GIS for the investigation of accessibility by public transport: an isochrone approach. *International Journal of Geographical Information Science* 14 (1):85–104.
- Schwarze, B, K Spiekermann, T Holthaus, B Leerkamp and J Scheiner. 2019. Methodische Weiterentwicklungen der Erreichbarkeitsanalysen des BBSR. BBSR-Online-Publikation 9:2019.
- Strubelt, W., and M. Wegener. 2001. Kriterien für die räumliche Differenzierung des EU-Territoriums: Geographische Lage: Studienprogramm zur europäischen Raumplanung. Bundesamt für Bauwesen und Raumordnung. Bundesamt für Bauwesen und Raumordnung. ISBN: 9783879944323.

Application of Land Surface Temperature Analysis in Urban Green Spaces: Case Studies from South Asia

Gulam Mohiuddin and Jan-Peter Mund

Eberswalde University for Sustainable Development, Germany

Abstract

This paper demonstrates the use of remote sensing in planning urban green spaces (UGSs). UGSs emerged as a popular solution to combat the effects of Urban Heat Island, especially in tropical cities. UGS projects often need to identify priority implementation areas due to limited funding for UGSs. This study includes two Asian cities, namely Phnom Penh (Cambodia) and Chittagong (Bangladesh). It is not comparative, but it has identified priority administrative areas for future UGSs in both cities. We used Landsat 8 data and the remote sensing technique Land Surface Temperature (LST) analysis using radiance, temperature brightness and emissivity. LST data were then intersected with the administrative boundaries of the study areas. The identification of priority administrative areas for UGS considered both the area coverage and the percentage of coverage in terms of maximum LST within the administrative units' boundaries. The result found 8 and 10 administrative units to be hotspots for UGSs, for Phnom Penh and Chittagong respectively. The proposed method will be useful to both government and non-government organizations alike, especially in tropical countries.

Keywords:

Land Surface Temperature (LST), urban green spaces (UGS), remote sensing

1 Introduction

In the modern world, urbanization is an inevitable phenomenon. More than half of the global population currently lives in urban areas, with a projection of reaching 68% by 2050, an increase that will be seen especially in Asia (UN DESA | United Nations Department of Economic and Social Affairs, 2018). Urbanization influences various environmental factors, and it has noticeable effects on the local weather and regional climate (Souza et al., 2016). Urban areas have to cope with higher temperatures (both land surface and air temperatures) compared to adjacent rural settings due to the phenomenon known as the urban heat island (UHI) (Arya, 2001).

UHIs have multifaceted negative impacts on both the urban environment and residents. The most common effect is that they contribute to producing excessive heat in urban areas. Different economic classes deal differently with this excessive heat. Relatively poor

neighbourhoods in the urban areas of developing countries often do not have the physical resources (e.g. air conditioning) to cope with extreme heat (Harlan et al., 2007). While the comparatively richer classes can afford to use such resources, this produces more anthropogenic waste heat, contributing to the increase of the UHI effect itself (Oke, 1982).

UHIs also contribute to extreme weather phenomena such as heatwaves (Tan et al., 2010). Heatwaves affect health, making older people, the chronically ill and pregnant women especially more vulnerable (Hiemstra et al., 2017). There is also a positive correlation between UHIs and increased atmospheric pollution in urban areas where there is intense human activity (Sarrat et al., 2006). In large agglomerations, the effects of UHIs are likely to become exacerbated in the near future due to the increase in global warming (Santamouris, 2014).

A popular mitigation technique for the effects of UHIs is to increase evapotranspiration (Hiemstra et al., 2017) through increasing green spaces and water bodies within cities (Heaviside et al., 2017). The concept of urban green spaces (UGSs) has emerged as one of the most prevalent ideas in this regard (Gillet et al., 2007). UGSs can be defined as open areas reserved for different types of green space, including areas of vegetation and water features (WHO, 2017); UGSs may be gardens, parks, other recreational venues, bodies of water, and the vegetated areas themselves can be planned or unplanned (Gupta et al., 2012). Increased vegetation in dense built-up areas can reduce the temperature of an urban area by influencing its microclimate (Givoni, 1991), providing thermal comfort to citizens that can contribute to their wellbeing and mental health (ASHRAE, 2004). The increase of UGSs can also be useful to combat air and noise pollution (Dimoudi & Nikolopoulou, 2003).

There are challenges related to UGSs, especially in developing countries. In many Asian countries, most UGS efforts are grant-based, or existing green spaces are historical, inherited from royal or colonial eras. There are always resource constraints for the maintenance and enlargement of UGSs, not least because public bodies often have limited funding for UGS-related activities (Tian et al., 2012). Hence the prioritization of areas for investment is of utmost importance (Coutts et al., 2016). Funding in a city is often based on smaller administrative units. Prioritization based on these smaller administrative boundaries can therefore be helpful for decision-makers.

Remote sensing can be a useful tool for prioritization in terms of effectiveness and efficiency. Recording ground-based temperatures at many reference points is both time-consuming and costly, especially when it has to be carried out frequently and over time in order to understand temperature changes. Remote sensing analysis using satellite imagery provides repeatability and synoptic coverage that address these challenges by taking less time and using fewer resources.

Remote sensing uses the land surface temperature (LST) to understand UHIs through analysing spatial patterns (temperature) and identifying 'hotspots' where UGS could combat these. Here, 'hotspot' refers to an area with comparatively higher LST within a city. LST is the radiative emission of the surface estimated from the top-of-brightness temperature using the infrared spectral channel of a satellite (Copernicus, 2013). In simpler terms, it can be defined as the 'skin temperature' of the ground (Rajeshwari & Mani, 2014). LST is widely used to understand and monitor UHIs (Keramitsoglou et al., 2011). There are studies in cities across the world investigating UHIs using LST. These locations include Changchun in China (Yang et al., 2020), Cairo in Egypt (El-Hattab et al., 2018), Noida City in India (Kikon et al., 2016),

Ulaanbaatar in Mongolia (Gantumur et al., 2019), Erbil in Iraqi Kurdistan (Rasul et al., 2015), Bishan East and Serangoon Central in Singapore (Nichol, 1996), and Melbourne in Australia (Algretawee et al., 2019).

It is essential to distinguish between LST and air temperature: they are different physical phenomena and are measured differently. Air temperature is measured at a height of about 1.2 m above the ground, and so is different from the land surface temperature. However, using LST to identify hotspots or priority areas in terms of temperature depends on the assumption that higher LST coincides with higher air temperature (Aniello et al., 1995). One study suggests that air temperature and LST patterns can be substituted for each other (Saaroni et al., 2000). This assumption was tested in a later study, which found that compared to air temperature, LST provides higher local variability (Nichol et al., 2009). Moreover, measuring air temperature provides temperature data at a definite point or transect, whereas LST gives a continuous picture of temperature that is more useful for understanding temperature patterns (Saaroni et al., 2000).

Against this backdrop, this study aims to identify priority areas for UGSs according to their administrative boundaries, by the spatial mapping of LST, in two Asian cities.

2 Study area

The first empirical example used in this study is in the capital of Cambodia, Phnom Penh, adjacent to the Basāk, Sab and Mekong river system ('Phnom Penh | national capital, Cambodia', 2021). Phnom Penh has an area of about 680 sq km (<https://www.citiesabc.com/city/page/2 2020>) and a population of more than 2 million. The population has seen a steep growth rate, increasing by more than 1.5 million in the last 70 years (Phnom Penh Population 2020 (Demographics, Maps, Graphs), 2021). For administrative purposes, Phnom Penh is divided into City Districts (also known as *Khans*), which are themselves subdivided into *Sangkats*. Of the total number of 105 *Sangkats* (Kang et al., 2021), for this study we considered 80 *Sangkats* within the Phnom Penh Metropolitan Area. Each *Sangkat* was allocated a number from 1 to 80, randomly, for identification.

The second case study is in a rapidly growing urban centre, Chittagong (official name: Chattogram) in Bangladesh. The city is located on the South-East coast of Bangladesh, sharing a boundary with the Bay of Bengal. The city's Corporation (i.e. total administrative area) is about 161 square km, comprises 41 administrative units (wards), and is home to more than 2 million residents (Palit, 2001); the area is highly susceptible to different forms of pollution (Hossen & Hoque, 2018).

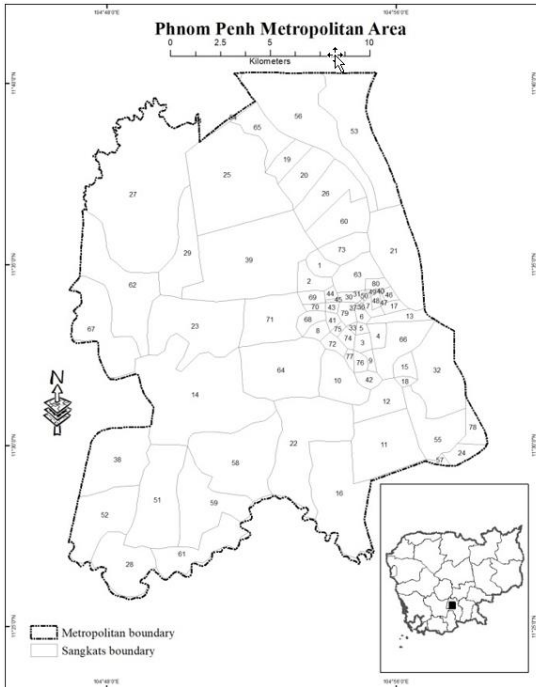


Figure 1: Phnom Penh Metropolitan Area

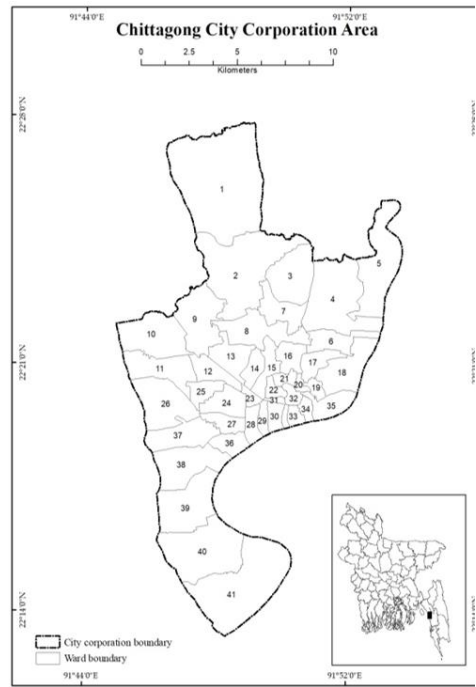


Figure 2: Chittagong City Corporation

3 Materials and Method

3.1 Data and data collection

The identification of patterns in LST requires coarser spatial resolution (ideally > 30 m) to pinpoint the hotspots for UGS (Coutts et al., 2016). Landsat data is suitable for this purpose in local municipalities (Keramitsoglou et al., 2012) because the resolution of Landsat 8’s thermal bands is 100 m, which allows LST patterns to be identified, but the data is not too coarse to allow patterns to be extracted at a local scale. The necessary data for this study (Landsat 8 OLI/TIRS C1 Level-1) was downloaded from the USGS website (<https://earthexplorer.usgs.gov/>) (see Table 1); the areas of interest were defined by the boundaries of the two metropolitan areas. Less than 10% cloud cover in the image frame was used as the criterion for selecting images. The city boundaries were then carefully checked to ensure they were cloud-free, because cloud cover can affect the LST estimation (Wang et al., 2019).

Table 1: The data

	Phnom Penh	Chittagong
LANDSAT_SCENE_ID	LC81260522020013LGN00	LC81360452020019LGN00
WRS_PATH	126	136
WRS_ROW	52	45
NADIR_OFFNADIR	NADIR	NADIR
DATE_ACQUIRED	1/13/2020	1/19/2020
SCENE_CENTER_TIME	03:20:12.5437870Z	04:19:11.9031299Z
CLOUD_COVER	10.22	3.55
CLOUD_COVER_LAND	10.22	4.85

3.2 Image processing and estimation of LST

Various algorithms have been used in different studies to estimate LST (Rajeshwari & Mani, 2014). In this study, LST was estimated using one thermal infrared (TIR) band (band 10), and three operational land imager (OLI) bands (bands 3, 4, 5) of Landsat 8. The equations used in estimating LST were taken from Avdan & Jovanovska (2016). As per the suggestion from the USGS (6 January 2014) in order to avoid greater calibration uncertainty, TIR band 11 was not included.

Preprocessing of LANDSAT data is required to reduce the solar, atmospheric and topographic effects, including distortion due to the sensor. LANDSAT Level-1 products are geometrically corrected (Young et al., 2017). Conversion to radiance (Equation 1) and thermal calibration (Equation 2) were done as part of preprocessing.

$$\text{Radiance} = R = ML * Q_{cal} + AL \quad (\text{eqn 1})$$

where ML and AL are band-specific multiplicative rescaling factors, and Q_{cal} is the thermal band of Landsat 8 (band 10) used in this study.

$$\text{Top-of-atmosphere brightness temp.} = TB = (K2 / \ln(K1 / R + 1) - 273.15 \quad (\text{eqn 2})$$

where, ' is the top-of-atmosphere spectral radiance, and K1 and K2 are band-specific thermal conversion constants.

The Normalized Difference Vegetation Index (NDVI) (Equation 3) and proportion of vegetation (Equation 4) were calculated to estimate emissivity (Equation 5).

$$NDVI = (NIR - Red) / (NDVI + Red) \quad (\text{eqn 3})$$

$$\text{Prop. of vegetation} = P_v = ((NDVI - NDVI_{min}) / (NDVI_{max} - NDVI_{min}))^2 \quad (\text{eqn 4})$$

$$\text{Emissivity} = E = 0.004 * P_v + 0.986 \quad (\text{eqn 5})$$

The LST was then estimated using the temperature brightness, radiance, Planck's constant, velocity of light and emissivity:

$$LST = TB / [1 + (R * TB / (h * c/s)) * \ln(\epsilon)] \quad (\text{eqn 6})$$

where TB is the top-of-atmosphere brightness temperature, R is the wavelength of the emitted radiance, h is Planck's constant, c/s is the velocity of light per second, and ϵ stands for emissivity.

3.3 Determining the analysis threshold

The LST observed in Phnom Penh ranges from 22.96°C to 36.64°C, and for Chittagong from 17.42°C to 31.82°C. The different amplitudes of the LST ranges do not allow any direct physical or climatological comparison of the cities. Hence, the spatial appearance of LST and the priority areas are shown separately, and the temperature categories (Table 2) are subjectively created, based on the temperature range of each city. In both cities, locations in category 5 are considered hotspots because they show the highest LST range for each city individually.

Table 2: LST thresholds of the two cities

Category	Phnom Penh	Chittagong
1	Up to 25.5°C	Up to 18.5°C
2	25.5°C to 27.5°C	18.5°C to 20.5°C
3	27.5°C to 29.5°C	20.5°C to 22.5°C
4	29.5°C to 30.5°C	22.5°C to 24.5°C
5	Above 30.5°C	Above 24.5°C

3.4 Criteria for selecting priority administrative areas

Category 5 LST locations (hotspots) were intersected with the administrative boundaries to identify priority administrative units (i.e. *Sangkats* and wards). Two criteria were considered in order to identify priority units:

- 1: What is the area of an administrative unit covered by hotspots? The top five administrative units in terms of area covered by hotspots are considered priority units.
- 2: What percentage of a particular administrative unit is covered by hotspots? The top five administrative units in terms of percentage coverage are selected as priority units.

4 Results

In Phnom Penh, the highest LST areas on 13 January 2020 were observed predominantly in the western part of the city (Figure 3). Specifically, there is a concentration of hotspots (category 5 LST) in the southwest of the city. The water bodies in the eastern and northern parts show lower LST.

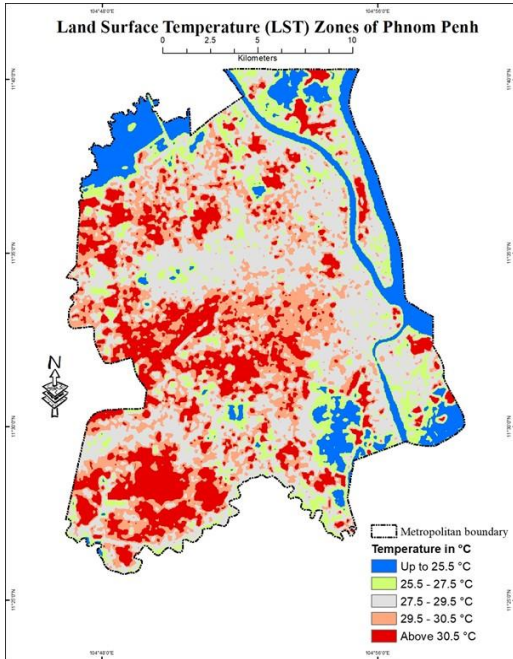


Figure 3: LST distribution of Phnom Penh

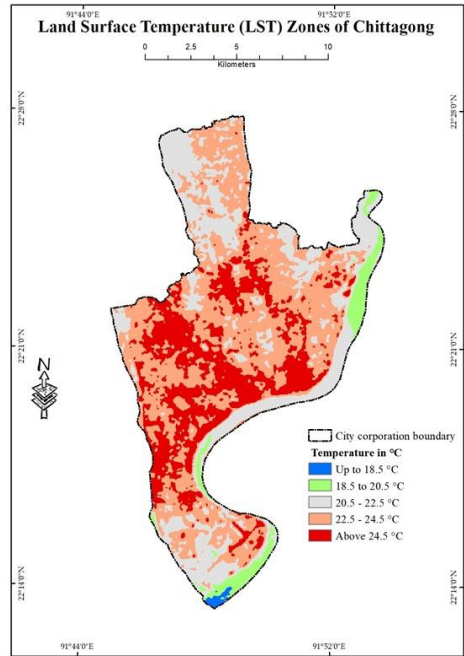


Figure 4: LST of Chittagong

For Chittagong (19 January 2020), most hotspots were scattered in the central area of the city, and lower LST was found within or close to open water bodies (Figure 4).

Figures 5–8 illustrate which administrative units fulfil the criteria for selection as priority areas.

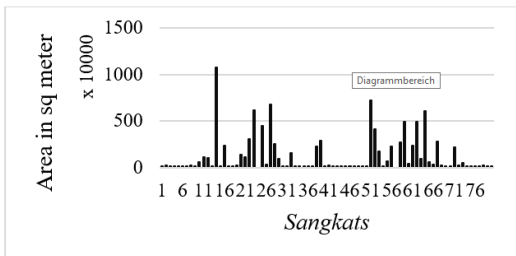


Figure 5: Area coverage of the hotspots (Phnom Penh)

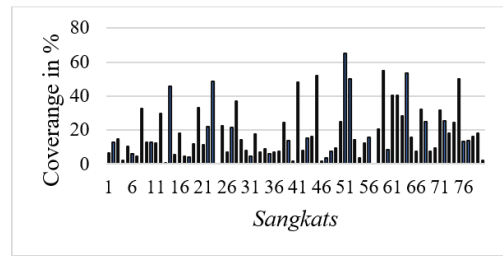


Figure 6: Percentage of coverage of hotspots (Phnom Penh)

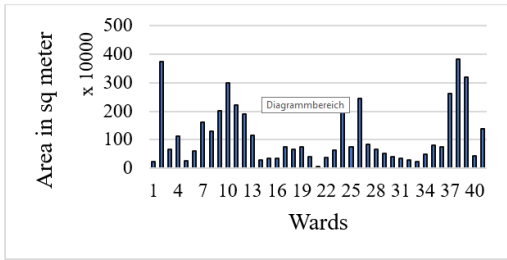


Figure 7: Area coverage of hotspots (Chittagong)

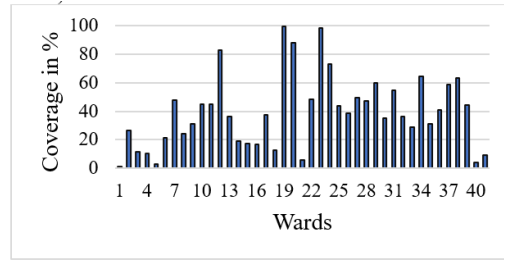


Figure 8: Percentage of coverage of hotspots (Chittagong)

The top five administrative units for both criteria and for each city (i.e. a total of 10 for each city) are presented in Tables 3 and 4. In Phnom Penh, two *Sangkats* (Pong Tuek and Stueng Mean Chey) figure among the top 5 for both criteria; for Chittagong, there is no such overlapping between the wards. Hence, eight *Sangkats* from Phnom Penh and ten wards from Chittagong were selected as priority administrative units for urban green spaces (Figures 11 and 12).

Table 3: Top five administrative units in terms of area coverage

<i>Area covered by the highest LST zone</i>				
Rank	Phnom Penh		Chittagong	
	Sangkat	Coverage (Area in sq m)	Ward no.	Coverage (Area in sq m)
1	Chaom Chau	10,749,123	38	3,820,428
2	Pong Tuek	7,210,586	2	3,743,287
3	Kouk Roka	6,812,670	39	3,187,357
4	Kakab	6,164,877	10	3,001,345
5	Stueng Mean Chey	6,065,042	37	2,610,842

Table 4: Top five administrative units in terms of coverage percentage

<i>Percentage of unit coverage in the highest LST zone</i>				
Rank	Phnom Penh		Chittagong	
	Sangkat	Coverage (%)	Ward no	Coverage (%)
1	Pong Tuek	65.15	19	99.86
2	Prey Veang	55.04	23	98.34
3	Stueng Mean Chey	53.72	20	88.40
4	Phsar Depou Ti Pir	52.10	12	82.92
5	Tuol Svay Prey Ti Pir	50.08	24	72.94

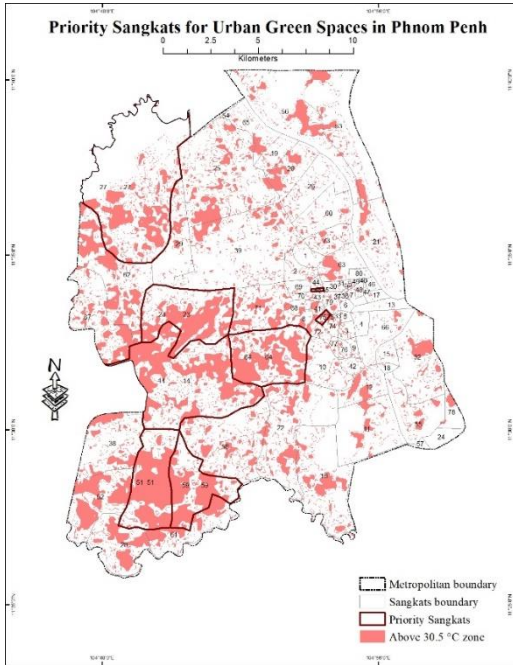


Figure 9: Priority areas of Phnom Penh

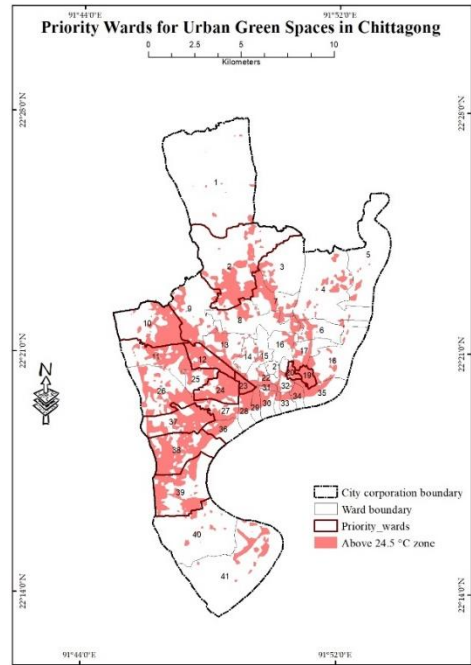


Figure 10: Priority areas of Chittagong

5 Discussion

This study has shown the LST distribution in two Asian cities in January 2020, the dry season in both areas. But it is important to remember that UHIs can vary significantly, over space and time (Grimmond et. al., 1993). Hence, the temperature ranges the study provided cannot be generalized over the year or to other cities.

The study identified the priority administrative units for urban green spaces, but it does not specify what types of UGS should be prioritized (parks, water bodies etc.). One study suggests that trees are more efficient and beneficial from an ecological point of view (Hiemstra et al., 2017), but this needs to be investigated further through studies comparing different types of UGS. In addition, social factors need to be taken into account in deciding the type of UGS to be established. For example, a park is appreciated differently by elderly and by young people (Gupta et. al., 2012).

The approach presented here of understanding the LST patterns in an urban area is a good substitute for recording ground-based temperature, considering resources, time, effort and repeatability (for change analysis). Presenting the results based on administrative units makes the method more user-friendly for urban decision-makers, who often need ready and accessible products to help them (Coutts et al., 2016).

The study identified eight *Sangkats* and ten wards as priority areas for Phnom Penh and Chittagong respectively. The overlap that happened in Phnom Penh cannot be explained

without further investigation, but it indicates that these two *Sangkats* require more attention in terms of UGS. However, LST should not be the only consideration in prioritizing areas for UGS. There are other important factors, such as the density of built-up areas, building heights and types (Schöpfer et al., 2005), existing vegetation and open spaces, that need to be considered in the planning and implementation of UGS.

The LST estimation for this study was done using existing images, so a real-time ground validation of LST was not possible. However, because the study's objective was to identify hotspots based on the highest LST (regardless of the absolute temperature ranges), the analysis is still valid for identifying the comparatively higher LST areas. For the same reason, seasonal variation was not considered. Future studies that use absolute air (1.2 m) and surface temperature for analysis would need to conduct ground validation.

The study has shown the distribution of LST in two cities at a particular time, but it does not explain the change scenario or the causes behind the distribution that was found. Further research is required to understand the different distributions of LST within the cities. It would also be useful, in order to understand the cause of change and distribution patterns, to triangulate LST and land-use change using very high resolution (VHR) TIR data (Kottmeier et al., 2007).

6 Conclusion

While estimating LST can be useful for UGSs, it does not lessen the importance of the urban climate model using air temperature. The approaches can complement each other and encourage collaboration between spatial planners and climate scientists. Although an increase of UGS can help combat the negative effects of UHIs, more than one type of action is required to combat them efficiently. Using reflective or 'cool' building materials and surfaces is another helpful approach. In addition, changing people's behaviour, so that less anthropogenic heat is emitted, could also make a significant contribution (Heaviside et al., 2017).

The present study will be particularly useful for urban planners, city authorities and organizations involved with UGS. However, the use of LST is not limited to the planning phase. It can also be an effective and efficient way to monitor and evaluate UGSs. LST can be a key indicator of negative UHI effects and a key consideration in UGS-related efforts.

It is important to understand the different spatial patterns that exist in urban areas. UGSs can act as a network that will help transform a city's green infrastructure more broadly. This transformation towards a green infrastructure is needed to combat UHIs and atmospheric pollution, while also contributing to an urban population's quality of life by helping with both physical and mental health.

References

- Algetawee, H., Rayburg, S., & Neave, M. (2019). Estimating the effect of park proximity to the central of Melbourne city on Urban Heat Island (UHI) relative to Land Surface Temperature (LST). *Ecological Engineering*, 138, 374-390.
- Aniello, C., Morgan, K., Busbey, A., Newland, L. (1995). Mapping Micro-Urban Heat Islands Using Landsat TM and a GIS. *Computers & Geosciences*, 21, 965-969.
- Arya, S. P. (2001). Introduction to micrometeorology (2nd ed.). This is volume 79 in the International geophysics series. San Diego: Academic Press.
- ASHRAE (2004). Thermal Environmental Conditions for Human Occupancy. (55), 2-25.
- Avdan, U., & Jovanovska, G. (2016). Algorithm for Automated Mapping of Land Surface Temperature Using LANDSAT 8 Satellite Data. *Journal of Sensors*, 2016, 1-8. <https://doi.org/10.1155/2016/1480307>
- Copernicus. (2013). Land Surface Temperature. Retrieved 11 July 2021, from <https://land.copernicus.eu/global/products/lst>
- Coutts, A. M., Harris, R. J., Phan, T., Livesley, S. J., Williams, N. S.G., & Tapper, N. J. (2016). Thermal infrared remote sensing of urban heat: Hotspots, vegetation, and an assessment of techniques for use in urban planning. *Remote Sensing of Environment*, 186, 637-651. <https://doi.org/10.1016/j.rse.2016.09.007>
- Dimoudi, A., Nikolopoulou, M. (2003). Vegetation in the urban environment: microclimatic analysis and benefits. *Energy and Buildings*, 35, 69-76.
- El-Hattab, M., Amany, S. M., & Lamia, G. E. (2018). Monitoring and assessment of urban heat islands over the Southern region of Cairo Governorate, Egypt. *The Egyptian Journal of Remote Sensing and Space Science*, 21(3), 311-323.
- Gantumur, B., Wu, F., Vandansambuu, B., Dalaibaatar, E., Tumursukh, B., Munkhsukh, U., & Zhao, Y. (2019, October). Implication of urban heat island (UHI) related to human activities: a case study in Mongolia. In *Remote Sensing Technologies and Applications in Urban Environments IV* (Vol. 11157, p. 111570V). International Society for Optics and Photonics.
- Gill, S.E., Handley, J.F., Ennos, A.R., & Pauleit, S. (2007). Adapting Cities for Climate Change: The Role of the Green Infrastructure. *Built Environment*, 33(1), 115-133. <https://doi.org/10.2148/benv.33.1.115>
- Grimmond, Christine & Oke, T. & Cleugh, Helen (1993). The role of 'rural' in comparison of observed suburban-rural flux differences. *Proceedings of the Yokohama Symposium*, 212, 165-174.
- Gupta, K., Kumar, P., Pathan, S. K., & Sharma, K. P. (2012). Urban Neighborhood Green Index – A measure of green spaces in urban areas. *Landscape and Urban Planning*, 105(3), 325-335. <https://doi.org/10.1016/j.landurbplan.2012.01.003>
- Givoni, B. (1991). Impact of planted areas on urban environmental quality: A review. *Atmospheric Environment*, 25B(3), 289-299.
- Harlan, S. L., Brazel, A. J., Jenerette, G. D., Jones, N. S., Larsen, L., Prashad, L., & Stefanov, W. L. (2007). In the shade of affluence: the inequitable distribution of the urban heat island. In *Research in Social Problems and Public Policy. Equity and the Environment* (Vol. 15, pp. 173-202). Bingley: Emerald (MCB UP). [https://doi.org/10.1016/S0196-1152\(07\)15005-5](https://doi.org/10.1016/S0196-1152(07)15005-5)
- Heaviside, C., Macintyre, H., & Vardoulakis, S. (2017). The Urban Heat Island: Implications for Health in a Changing Environment. *Current Environmental Health Reports*, 4(3), 296-305. <https://doi.org/10.1007/s40572-017-0150-3>
- Hiemstra, J. A., Saaroni, H., & Amorim, J. H. (2017). The Urban Heat Island: Thermal Comfort and the Role of Urban Greening. In D. Pearlmutter, C. Calafapietra, R. Samson, L. O'Brien, S. Krajter Ostoić, G. Sanesi, & R. Alonso del Amo (Eds.), *Future City. The Urban Forest* (Vol. 7, pp. 7-19). Cham: Springer International Publishing. https://doi.org/10.1007/978-3-319-50280-9_2

- Hossen, M. A., Hoque, A. (2018). Variation of Ambient air Quality Scenario in Chittagong City: A Case Study of Air Pollution. *Journal of Civil, Construction and Environmental Engineering*, 3(1), 10. <https://doi.org/10.11648/j.jccee.20180301.13>
- Kang, B., Bei, B., 𐄂, 𐄃., Muoy, B., 𐄄, 𐄅., & Pir, B. et al. (2021). Cambodia: Phnom Penh (City Districts and Communes) - Population Statistics, Charts and Map. Retrieved 27 June 2021, from <https://www.citypopulation.de/en/cambodia/phnompenh/admin/>
- Keramitsoglou, I., Daglis, I. A., Amiridis, V., Chrysoulakis, N., Ceriola, G., Manunta, P, Paganini, M. (2012). Evaluation of satellite-derived products for the characterization of the urban thermal environment. *Journal of Applied Remote Sensing*, 6(1), 61704. <https://doi.org/10.1117/1.JRS.6.061704>
- Keramitsoglou, I., Kiranoudis, C. T., Ceriola, G., Weng, Q., & Rajasekar, U. (2011). Identification and analysis of urban surface temperature patterns in Greater Athens, Greece, using MODIS imagery. *Remote Sensing of Environment*, 115(12), 3080-3090.
- Kikon, N., Singh, P., Singh, S. K., & Vyas, A. (2016). Assessment of urban heat islands (UHI) of Noida City, India using multi-temporal satellite data. *Sustainable Cities and Society*, 22, 19-28.
- Kottmeier, C, Biegert, Corsmeier, a., & U (2007). Effects of Urban Land Use on Surface Temperature in Berlin: Case Study. *Journal of Urban Planning and Development*, 133(2).
- Nichol, J. E. (1996). High-resolution surface temperature patterns related to urban morphology in a tropical city: a satellite-based study. *Journal of Applied Meteorology and Climatology*, 35(1), 135-146.
- Nichol, J. E., Fung, W. Y., Lam, K.-s., & Wong, M. S. (2009). Urban heat island diagnosis using ASTER satellite images and 'in situ' air temperature. *Atmospheric Research*, 94(2), 276–284. <https://doi.org/10.1016/j.atmosres.2009.06.011>
- Oke, T.R (1982). The energetic basis of the urban heat island. *Quarterly Journal of the Royal Meteorological Society*, 108, 1–24. <https://doi.org/10.1002/qj.49710845502>
- Palit, T. (2001). Chittagong City Corporation. In *National Encyclopedia of Bangladesh*. Dhaka: Government of People's Republic of Bangladesh.
- Phnom Penh Population 2020 (Demographics, Maps, Graphs). (2021). Retrieved 27 June 2021, from <https://worldpopulationreview.com/world-cities/phnom-penh-population>
- Phnom Penh | national capital, Cambodia. (2021). Retrieved 27 June 2021, from <https://www.britannica.com/place/Phnom-Penh>
- Gao, B. (1996). NDWI—A normalized difference water index for remote sensing of vegetation liquid water from space. *Remote Sensing of Environment*, 58(3), 257-266. doi: 10.1016/s0034-4257(96)00067-3
- Rajeshwari A, Mani N. D. (2014). Estimation of Land Surface Temperature of Dindigul District using Landsat 8 Data. *IJRET: International Journal of Research in Engineering and Technology*, 3(5), 122–126.
- Rasul, A., Balzter, H., & Smith, C. (2015). Spatial variation of the daytime Surface Urban Cool Island during the dry season in Erbil, Iraqi Kurdistan, from Landsat 8. *Urban climate*, 14, 176-186.
- Saaroni, H., Ben-Dor, E., Bitan, A., Potchter, O. (2000). Spatial distribution and microscale characteristics of the urban heat island in Tel-Aviv, Israel. *Landscape and Urban Planning*, 48, 1–18.
- Santamouris, M. (2014). On the energy impact of urban heat island and global warming on buildings. *Energy and Buildings*, 82, 100–113. <https://doi.org/10.1016/j.enbuild.2014.07.022>
- Sarrat, C., Lemonsu, A., Masson, V., & Guedalia, D. (2006). Impact of urban heat island on regional atmospheric pollution. *Atmospheric Environment*, 40(10), 1743–1758. <https://doi.org/10.1016/j.atmosenv.2005.11.037>
- Souza, D. O. de, Alvalá, R. C. d. S., & Nascimento, M. G. d. (2016). Urbanization effects on the microclimate of Manaus: A modeling study. *Atmospheric Research*, 167, 237–248. <https://doi.org/10.1016/j.atmosres.2015.08.016>

- Schöpfer, E., Lang, S., Blaschke, T. (2005). A “Green Index” Incorporating Remote Sensing and Citizen’s Perception of Green Space.
- Tan, J., Zheng, Y., Tang, X., Guo, C., Li, L., Song, G., . . . Li, F. (2010). The urban heat island and its impact on heat waves and human health in Shanghai. *International Journal of Biometeorology*, 54(1), 75–84. <https://doi.org/10.1007/s00484-009-0256-x>
- Tian, Y., Jim, C. Y., & Tao, Y. (2012). Challenges and Strategies for Greening the Compact City of Hong Kong. *Journal of Urban Planning and Development*, 138(2), 101–109. [https://doi.org/10.1061/\(ASCE\)UP.1943-5444.0000076](https://doi.org/10.1061/(ASCE)UP.1943-5444.0000076)
- UN DESA. (2018). 68% of the world population projected to live in urban areas by 2050, says UN | UN DESA | United Nations Department of Economic and Social Affairs. Retrieved 11 February 2021, from <https://www.un.org/development/desa/en/news/population/2018-revision-of-world-urbanization-prospects.html>
- WHO. (2017). Urban green spaces: a brief for action (p. 2). Copenhagen: World Health Organization, Regional Office for Europe. Retrieved from https://www.euro.who.int/__data/assets/pdf_file/0010/342289/Urban-Green-Spaces_EN_WHO_web3.pdf
- Wang, T., Shi, J., Ma, Y., Husi, L., Comyn-Platt, E., Ji, D., . . . Xiong, C. (2019). Recovering Land Surface Temperature Under Cloudy Skies Considering the Solar-Cloud-Satellite Geometry: Application to MODIS and Landsat-8 Data. *Journal of Geophysical Research: Atmospheres*, 124(6), 3401–3416. <https://doi.org/10.1029/2018JD028976>
- Yang, C., Yan, F., & Zhang, S. (2020). Comparison of land surface and air temperatures for quantifying summer and winter urban heat island in a snow climate city. *Journal of environmental management*, 265, 110563
- Young, N. E., Anderson, R. S., Chignell, S. M., Vorster, A. G., Lawrence R., Evangelista, P. H. (2017). A survival guide to Landsat preprocessing. *Ecology*, 98(4), 920–932.

A Web Application for Simulating Future Settlement Development

Yingwen Deng¹, Wolfgang Spitzer¹, Sabine Gadocha¹ and Thomas Prinz^{1,2}

¹Research Studios Austria Forschungsgesellschaft mbH - Studio iSPACE, Salzburg

²Salzburg University

Abstract

With the growing residential development of urban areas and their hinterlands in the Alpine region, urban sprawl is a major concern. It is therefore essential for decision-making authorities and urban planners to monitor the demand for, and consumption of, the limited reserve of land zoned for residential buildings and the development of future settlements. Data such as demographic statistics, population forecasts, and geospatial data of the land reserve are required for this purpose. However, due to the variety of these data, tools for exploring them in an integrated and intuitive manner are rarely available.

This paper introduces a web application designed to facilitate this task, a map-based strategical dashboard that was developed within the Alpine Building Centre project (Zentrum Alpines Bauen, www.alpinesbauen.at). The paper describes the application's design goals, data preparation, architecture and user interface. With a use case in Oberndorf bei Salzburg, we demonstrate how the application visualizes the predicted future settlement situation based on existing housing patterns and population development forecasts. The use case also shows how the application allows simulation and evaluation of various scenarios for housing demand and zoned residential land use, thus assisting decision makers to devise spatial development concepts for balancing housing sufficiency and reducing urban sprawl. This paper aims to present the application as an approach of using an interactive map-based dashboard to present and utilize multidimensional data in the field of residential land use for the purposes of urban planning.

Keywords:

web map, dashboard, residential land use, spatial planning, settlement development

1 Introduction

Demographic change, trends towards smaller household sizes, rising housing demand and costs, and urban sprawl are current challenges for the development of settlements in Salzburg state. To cope with these challenges, as the guidelines for the 'spatial development concept' (*Räumliches Entwicklungskonzept*) for municipalities in Salzburg state mentions, it is essential to link the development of settlements and population with each other (Land Salzburg, 2019). Therefore, a tool for monitoring the demand for, and consumption of, the limited reserve of

land zoned for residential building and the development of future settlements is needed. In earlier studies and projects, several tools designed to help with settlement planning were developed. For example, the Flächenmanagement Datenbank is available to municipalities in Bavaria to record and manage internal development potentials (Bayerisches Landesamt für Umwelt, 2018). It can estimate housing demand based on statistical parameters. RAUM + Monitor was developed as an online survey platform to inspect and maintain settlement area reserves, with particular attention being paid to the demand for new building land (Rheinland-Pfalz, 2015). However, interactive visualization techniques were barely used in these tools.

A map-based dashboard, as an innovative geo-visualization tool, is widely used for interactively visualizing and mining georeferenced information (Jing, Du, Li & Liu, 2019). For example, the Dublin Dashboard (McArdle & Kitchin, 2016) embeds maps in different modules which allow users to monitor the city of Dublin from environmental and transport perspectives. The map element in the City of Sydney Dashboard (Pettit, Lieske & Jamal, 2017) focuses on providing real-time monitoring of different types of transportation. The Galway dashboard ('Visualising the Social and Cultural Infrastructure in Galway City and County', 2015) combines maps with interactive charts to describe the commuting, housing and cultural infrastructures in Galway City and County, Ireland.

While a dashboard, as a visualization method, answers the 'what?' questions, visual analytics exploits dynamic, iterative processes to help people answer 'why?' questions. It combines the computational power of modern computers with human background knowledge and perceptions to solve complex problems (Andrienko et al., 2010; Keim, Mansmann & Thomas, 2010). Visual analytics methods are utilized by decision makers to drive the optimization of city services, mobility, sustainability, economy and citizen engagement (De Amicis et al., 2009; Karduni et al., 2017; Li, Bao, Sellis, Yan & Zhang, 2018; Senaratne et al., 2018). To answer the 'what' and 'why' questions within one application, several studies integrated visual analytics approaches with dashboards to explore individual aspects of a city. Würstle, Santhanavanich, Padsala, and Coors (2020) presented a concept for an urban energy dashboard integrated with 3D city models to compare the computed (projected) energy demand with the actual measured demand in different usage scenarios. Zuo, Ding, and Meng (2020) proposed an analytical dashboard to present and explore the spatio-temporal patterns of multidimensional economic factors in synchronized maps and bar charts.

In this paper, we also propose a web application, a map-based strategical dashboard, to explore the settlement development in Salzburg state and its municipalities. Through a visual analytics approach, the user is able to simulate future settlement development based on existing housing patterns and various land-use scenarios that the user creates. The application provides a platform for decision-making authorities and urban planners to interact with the datasets of existing residential buildings, the stocks of land zoned for residential buildings, and future demands based on population forecasts. It aims to help planning authorities understand the housing potential and the development of the housing demand at both state and municipal scales; it assists them in formulating targeted spatial development concepts for individual municipalities, and thus supports the strategic planning of settlement development.

2 Design goals

In the Alpine Building Centre, RSA FG Research Studio iSPACE develops indicators and interactive web tools to optimize the decision-making process for sustainable spatial development. The application described in this paper is an innovative visualization tool focused on residential land use and settlement development.

The tool is designed for decision-making authorities (here, municipalities in Salzburg state) and their urban planners. According to the guidelines for the spatial development concept (Land Salzburg, 2019), it is vital for them to present the inventory and structure of existing settlements, to analyse earlier developments, and to derive spatial development goals and measures based on the estimated demand for residential building land. Additionally, for an appropriate response to city development and urban planning, analysis of the past, present and future situations is indispensable (Phdungsilp, 2011). The goals of the application therefore focus not only on the simulation of the future settlement development but also on the current residential building structure.

We aim to help users answer the following questions:

- What does the current residential building structure look like in Salzburg state and its municipalities?
- What is the spatio-temporal trend of the development of the reserves of land zoned for residential building in Salzburg state and its municipalities?
- Within land zoned for residential building, is the housing potential sufficient for different building categories? If not, when will the municipalities run out of residential building land?
- If the housing potential is not sufficient to fulfil the forecast demand, what adjustments could be made (e.g. use residential building plots more efficiently by building blocks of flats rather than detached houses) to improve the supply-and-demand situation for housing while avoiding designating more land for residential purposes?

3 Test Data

The source data are stored in a file geodatabase. They were processed and structured into a multidimensional data repository as part of the Alpine Building Centre project:

- Future housing demand (2018–2043)
- Existing residential buildings (2018)
- Vacant residential building plots (2018)

The data were converted, using the number of households as a unit, to support the calculation of housing demands, potential and supplies in the pre-set scenario, and in user-defined scenarios, for housing demand and land use (Figure 1).

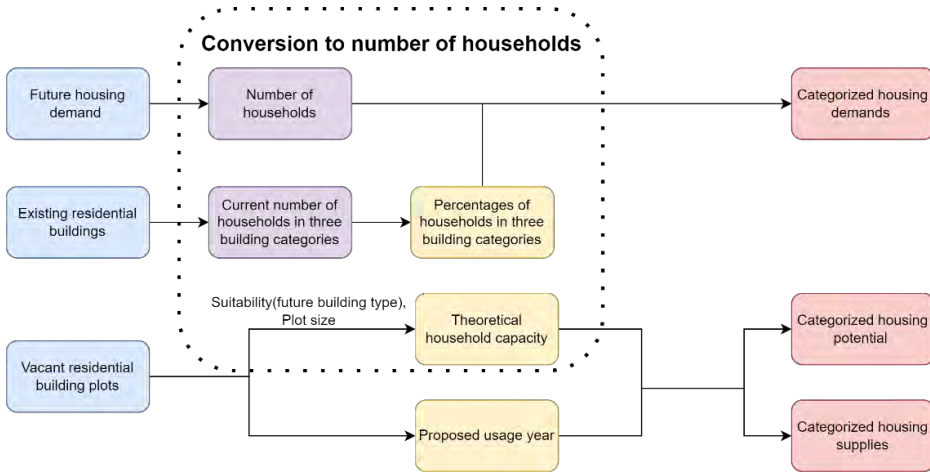


Figure 1: Data usage in the application

In the test dataset, the future housing demand in each municipality is assumed to be equal to the annual changes in the number of households. To calculate the change in the number of households, two factors need to be taken into consideration: (1) population size, and (2) household size (i.e. how many people live in a household). The annual change in the number of households caused by population development is estimated at municipality level, based on the total population number from the statistical data in 2018 and using annual population-change factors. These factors are calculated from the population forecasts that are available only at district (i.e. supra-municipal) level. As it is common for the population development to vary significantly between municipalities within the same district, the factors are calibrated according to the variability of the population development, from 2002 to 2020, within each district (Figure 2a). The annual changes of household *numbers* resulting from changes in household *size* are extrapolated from the number of households at municipality level given in the 2018 data (see Figure 2b). The future yearly housing demand used in this application is the sum of the changes in numbers of households caused by population development + the changes in number of households caused by household size development.

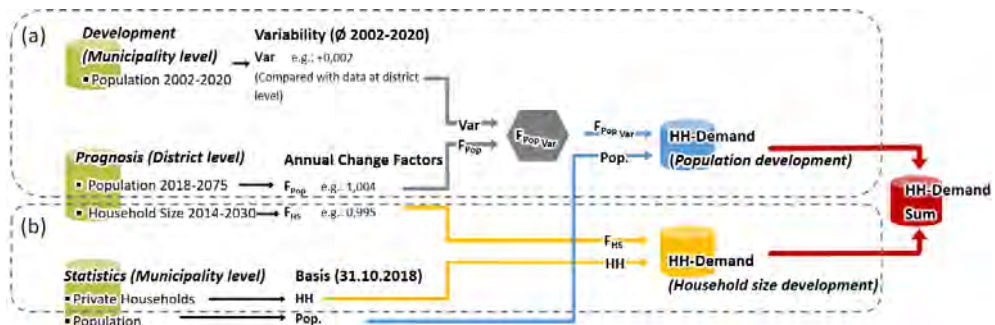


Figure 2: Future housing demand calculation: (a) the calculation of housing demand resulting from changes in size of population; (b) the calculation of housing demand resulting from changes in household size.

The existing residential buildings are classified into three categories (i.e. housing types): detached houses (Freistehendes Haus), compact low-rise buildings (Verdichteter Flachbau), and blocks of flats (Geschoßwohnbau) (Figure 3). Therefore, in this application, housing demands, potential and supplies are also assigned to these categories. The current household numbers in the building categories are calculated, and their percentages are used to estimate the future demands for different types of housing in the pre-set view. The overarching aim is to represent the projected development of settlement within the context of the overall townscape of municipalities in Salzburg state.

For the vacant zoned residential building land, each building plot is assigned a theoretical household capacity, based on its suitability (optimal future building type) and size. Vacant building plots are aggregated by their suitability and proposed usage year (given in the dataset) to calculate the yearly housing potential and supply for each building category.



Figure 3: Existing residential buildings classified into three categories: detached houses (blue), compact low-rise buildings (orange), and blocks of flats (red) (Salzburg Maxglan)

4 Application Architecture

There are four key elements for the development of the application: feature layers, map, widgets and dashboard. To fulfil the design goals mentioned in Section 2, the application was developed using JavaScript, HTML and CSS, and designed with Calcite Maps, in combination with ArcGIS API for JavaScript, ChartJS and JQuery (Figure 4).

The visualized data are stored as server-side data sources in ArcGIS online, a cloud-based, collaborative content-management system for maps, apps, data and other geographic content (ESRI, 2018). The data are integrated as feature layers in the map. These layers are referenced with unique portal item IDs, and loaded from a REST API service hosted on ArcGIS Online.

We used ArcGIS API for JavaScript (ESRI, 2019) to embed the map and tasks in the web application. Users can interact with the visualized data via the widgets offered in the application to perform several tasks. For example, a municipality selector is integrated to apply a spatial filter to all visualized data; a time slider is embedded to apply a time filter to the land reserve data; an editor widget is used to alter attributes of the vacant building plots. The time slider and the building plot editor were developed from the ready-to-use widgets provided by the ArcGIS API for JavaScript. The municipality selector applies filters to the visualized data by executing query tasks with a 'where' clause applied to the feature layers. In order to visualize

the results of these operations instantly, we linked these three widgets with the map and the dashboard.

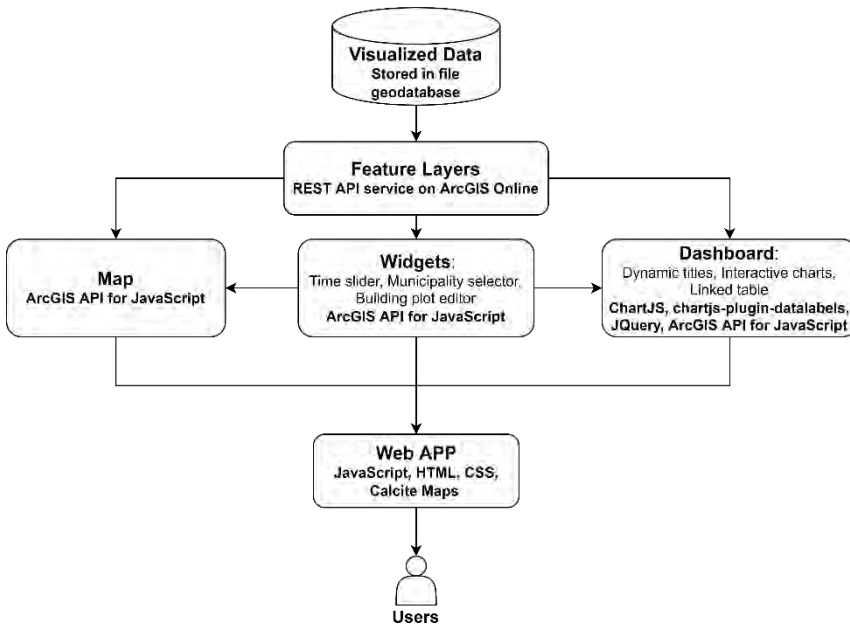


Figure 4: The architecture and libraries used to develop the application features.

Dashboard contents include dynamic titles, interactive charts and a linked table. Their input data are the results of queries on the feature layers. Three types of queries are supported by ArcGIS API for JavaScript: attribute, spatial and statistic queries (ESRI, 2016b). We used attribute queries to fetch attributes (e.g., future demands), and statistic queries to return statistics for fields (e.g., housing potential/supplies by summing up the household capacity of vacant building plots). We used ChartJS (ChartJS, 2016) and chartjs-plugin-datalabels (ChartJS, 2017) to create interactive charts in the dashboard. In addition to tooltips on data points and dataset filters, ChartJS also allows updates on the charts when the visualized dataset is modified. With this capability and JQuery (JQuery, 2008), the dashboard is able to provide instant visual feedback on the user's interactions with the application.

The application is built with JavaScript, HTML and CSS, and users have access to it via web browsers. Calcite map is a theme for Bootstrap (Bootstrap, n.d.) for designing, styling and creating modern map apps (ESRI, 2016a). We used it to design the layout of the application, and the layout adapts to the size of the device screen.

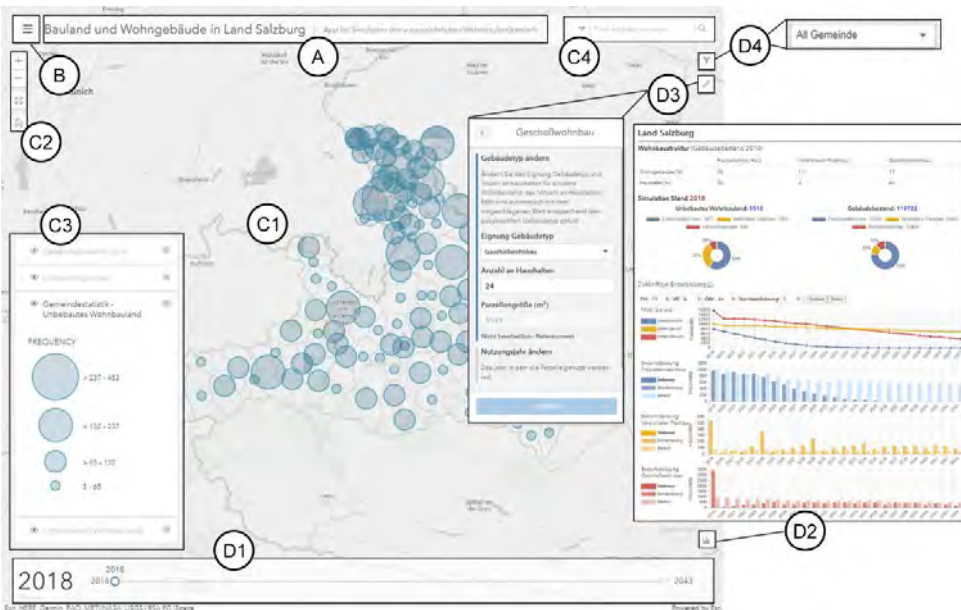
5 Results

This section introduces the application's user interface and a use case in Oberndorf bei Salzburg. The use case demonstrates how the questions which we mentioned in the design goals (Section 2) can be answered through user interactions with the application.

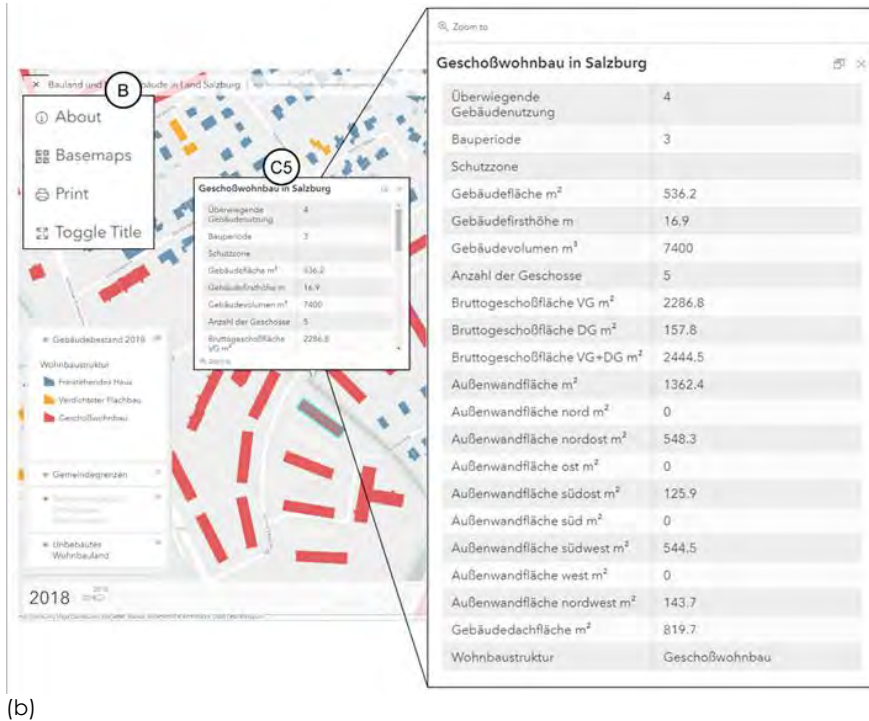
5.1 User Interface

The application follows the ‘Visual Information Seeking Mantra – Overview first, zoom and filter, then details-on-demand’ (Shneiderman, 1996). Users are able to access information at state, municipality, individual building and building plot levels. Figures 5a and 5b provide overviews of the application’s prototypical user interface and its components at two map scales. The user interface has the following components: header, dropdown menu, basic interactive map elements, and task-oriented features.

The header (Figure 5a - A) shows the title of the application, followed by a slogan which briefly explains the application’s purpose. The dropdown menu (Figure 5b - B) contains an ‘about us’ page, basemap gallery, map print service, and toggle to hide the header. Basic interactive map elements include a main map view (Figure 5a - C1), map controls (Figure 5a - C2), layer list (Figure 5a - C3), search window (Figure 5a - C4), and pop-up window (Figure 5b - C5). The map view is the background of the user interface. Map controls include zoom control, home button for resetting the map extent, and full-screen control. The layer list indicates the map layers that are visible, and adapts automatically according to the map scale selected by the user. It has an integrated foldable map legend. Users can also display or hide layers manually with the ‘eye-shaped’ toggle (as seen in Figure 3). When a larger scale is applied to the map, users are able to view attributes of the building or building plot selected, which appear in a pop-up window. Task-oriented features include a time slider (Figure 5a - D1), dashboard (Figure 5a - D2), building plot editor (Figure 5a - D3), and municipality selector (Figure 5a - D4). To ensure the user interface is not overcrowded, the latter three features are wrapped in collapsible elements. The application therefore stays uncluttered and clear for users, who need to view only the current and projected settlement development.



(a)



(b)

Figure 5: User Interface. (a) At state scale: header (A), dropdown menu (B), basic interactive map elements (C1–C4), and task-oriented features (D1–D4). (b) At building scale, the map shows three types of existing residential building; expanded dropdown menu (B), pop-up window of a selected block of flats (C5).

5.2 Use Case – Oberndorf bei Salzburg

Oberndorf bei Salzburg is a municipality in the north of Salzburg state. The use case allows us to answer the questions listed in the design goals (see Section 2).

After selecting Oberndorf using the municipality selector, the municipality border of Oberndorf and the spatial distribution of its vacant reserves of zoned residential building land in 2018 are shown on the map (Figure 6a). The spatial extent of the dataset visualized is limited to Oberndorf. This allows users to explore the settlement development of individual municipalities separately. As the housing supply and demand situations in each municipality differ greatly from each other, an overview of the settlement situation at the level of the state is inadequate. To support optimal decision-making, it is essential to provide users with views at both state and municipality level.

The table in the dashboard shows the proportions of buildings and numbers of households in the three building categories (Figure 6b). It allows users to see at a glance the current residential building structure in Oberndorf. We can see that the majority of the present residential buildings there are detached houses. These account for 69% of all residential buildings. Nevertheless, almost the same number of households reside in detached houses as in blocks of flats, which account for just 10% of the buildings.

Using the time slider, we can see how the zoned residential land reserve may evolve numerically and spatially over the next 25 years. The dynamic pie charts and their legends help users monitor the consumption of each type of land reserve and how this affects the building stock (Figure 6c). From the pie chart on the left, we can see that at the beginning of 2018, most vacant, zoned, residential building land was suitable for detached houses, while plots suited for compact low-rise buildings came second. In the map view, land reserves that are likely to be used in the near future are greyed out as users interact with the time slider. Figures 6d and 6e show the spatial distribution of the vacant residential building plots in northern Oberndorf in 2018 and 2030. This provides users with a clear image of how the land reserved for residential building evolves spatially over time.

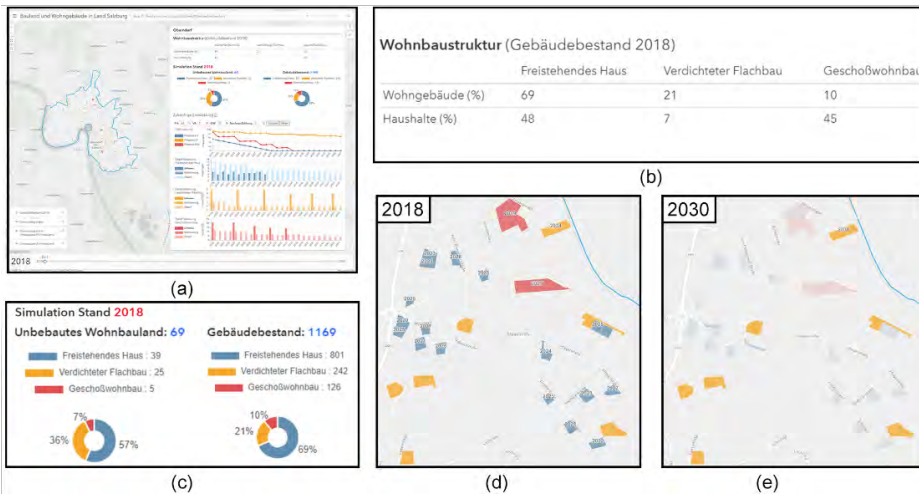


Figure 6: Use case in Oberndorf bei Salzburg. (a) Application with the expanded dashboard. It describes the residential buildings and building land reserve for settlement in 2018. (b) Table in the dashboard for types of housing. (c) Pie charts in the dashboard for vacant residential building land (left) and existing residential buildings (right) in 2018. (d) Vacant residential building land in 2018. (e) Vacant residential building land in 2030.

The serial charts in the dashboard (Figure 6a) show the projected yearly housing potential, demand and supply in terms of number of households. These help users to evaluate the projected future settlement situation. The pie chart in the dashboard (Figure 6c, left) shows that most vacant building plots are suitable for detached houses. However, based on the demands and proposed usage forecast for each year and for each vacant building plot, the potential for building detached houses is insufficient and will be the first to run out (in 2030) (Figure 7 - A). Compared to the demands forecast, building land in this category is insufficient (Figure 7 - B1). The graph in Figure 7 - B2 shows the cumulative difference between the projected housing demands and supplies. We can see that in the default scenario, due to the continuous gap between demand and supply, the total difference keeps increasing. For example, by 2030 there is a total housing shortfall of 57 housing units, yet most land reserve suited for compact low-rise buildings is unused. At the beginning of 2030, there is still the potential to build compact low-rise buildings that would provide 79 households with housing (Figure 7 - A).

As the serial charts depict, the housing potential is apparently insufficient for some building categories (as just described for detached houses). The web map therefore offers the possibility of creating user-defined scenarios: in the input fields, users can adapt the proportions of the demand, for example lowering the demand for detached houses while increasing that for compact low-rise buildings (Figure 7 - C). Users can also increase the re-densification index (Figure 7 - D) to reduce the demand for building land and fulfil more of the housing demand by densifying the existing building stock. Furthermore, users can adjust the use of individual building plots (e.g., change future building type, increase theoretical household capacity, adjust usage year) via the building plot editor (Figure 8). With one building type selected, a new theoretical household capacity is calculated automatically based on the building type and building plot size. Housing potential, supply and demand are immediately recalculated based on the modified parameters and visualized by the charts in the dashboard. Using also their human perception, decision makers can evaluate their alternative scenarios for housing demand and residential land use intuitively. These simulations can help users to test measures that could improve the imbalance between the supply and demand of housing, while avoiding re-designating for residential buildings land that has already been zoned for other purposes (e.g. as green spaces). Ultimately, the application can help municipalities and planners to identify the potential shortfall of housing at a fine-gained scale, and to formulate the optimal land-use concept customized for their own area.

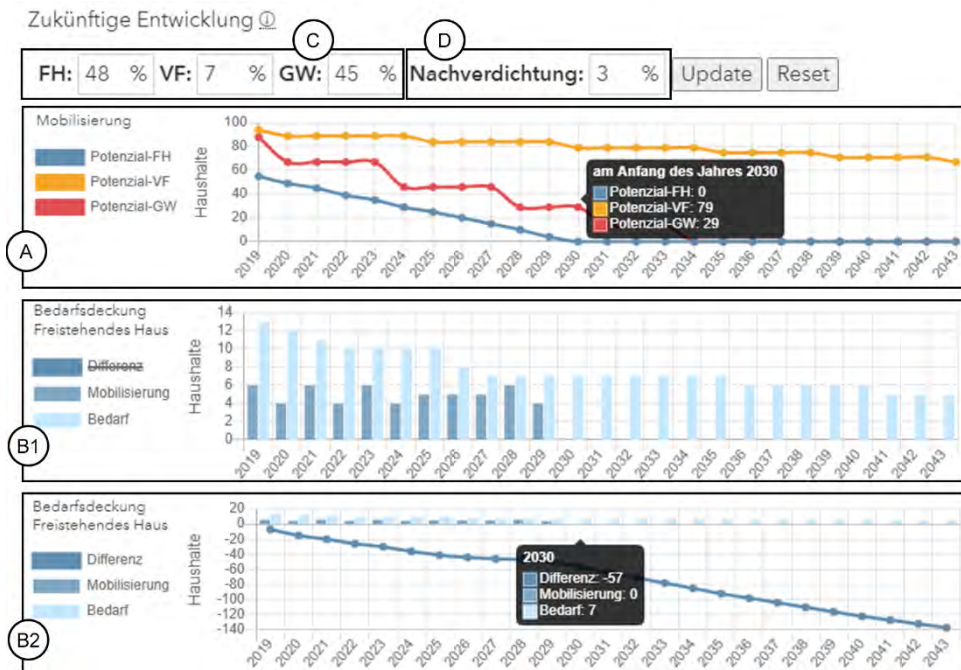


Figure 7: Use case in Oberndorf bei Salzburg. Serial charts: (A) yearly housing potential of three building categories; (B1) yearly housing supply and demand for detached houses, without cumulative difference line; (B2) yearly housing supply and demand for detached houses with cumulative difference line. All values are calculated as number of households. Input fields (top): (C) proportions of demands for each building category; (D) re-densification index.

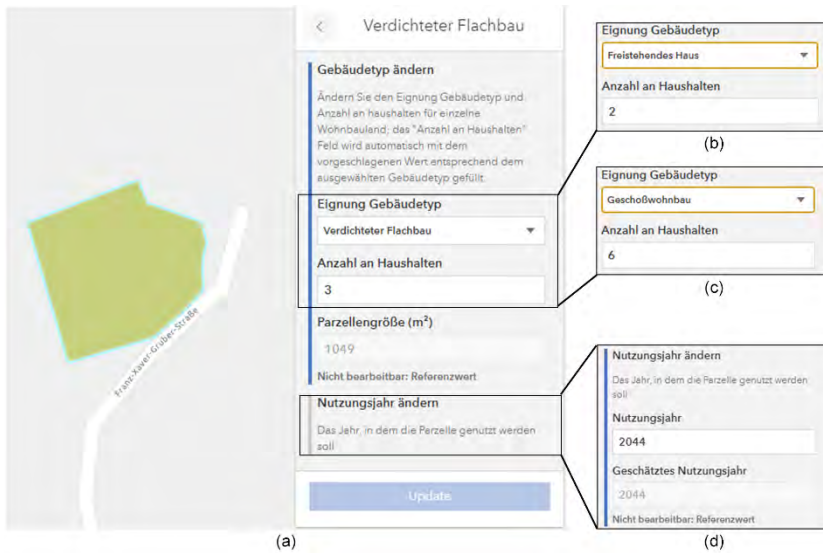


Figure 8: Using building plot editor: (a) expanded panel for editing building type and household capacity; (b) building type 'Detached house' selected; (c) building type 'Block of flats' selected; (d) expanded panel for editing usage year.

6 Conclusion and Outlook

In this paper, we introduced the prototype of a web application developed within the framework of the Alpine Building Centre (Zentrum Alpines Bauen). The application is a map-based strategical dashboard for the exploration of the settlement development in Salzburg state and its municipalities. The paper describes the design goals, data preparation, architecture and user interface of the application. With the use case in Oberndorf bei Salzburg, we demonstrated how the prototype fulfils its design goals: for Salzburg state and its municipalities, it visualizes the current spatial distribution and structure of residential buildings and zoned residential building land reserve using maps, tables and pie charts in the dashboard. With the time slider, the application is able to describe the forecast settlement and changes in the land reserve dynamically. By quantifying the land reserve with reference to household capacity and linking it with future demands that are calculated using forecasts for population and household sizes, users can explore, with the help of serial charts, whether land reserves are sufficient. Furthermore, using a visual analytic approach, users are able to simulate and evaluate various hypothetical scenarios for housing demand and residential land use. The application helps decision makers to follow the guidelines for the spatial development concept (Land Salzburg, 2019) for municipalities in Salzburg state, by offering them a platform to reflect on existing housing patterns and to experiment with alternative land-use scenarios. Information derived from this application can be used as a basis to formulate spatial development concepts for individual municipalities in Salzburg state, with the aim of improving future housing supply in the current reserves of land zoned for residential buildings, according to the various municipalities' individual trends in the development of population and household size. This paper presents the application as an approach that uses an interactive

map-based dashboard to present and utilize multi-dimensional data in the field of residential land use in urban planning. The application can be easily adapted for other municipalities or states.

The development of the web application is still in progress. We have presented it to a number of municipalities and urban planners in Salzburg state for initial feedback. Feedback for the concepts used has been positive, and planners and municipalities have shown interest in the prototype. Other feedback includes a suggestion to integrate the application with spatial data for re-densification potential, adding indicators that represent the actual availability of vacant zoned lands, and increasing the time interval used on the time slider and the serial charts. The current one-year interval is too short and thus not suitable for residential land-use planning. In future work within the Alpine Building Centre project, we will modify the application to take these suggestions into account. In addition, an evaluative study of the interactive map-based design of the dashboard is necessary to justify the design. With a view to improving the application, we therefore plan to conduct a usability study to evaluate the application with urban planners and decision-making authorities from pilot municipalities.

Acknowledgements

The web application for simulating the development of future settlement was developed by Research Studio iSPACE at the Alpine Building Centre (Zentrum Alpines Bauen) in the key research area ‘simulation of settlement systems’. The Alpine Building Centre is a cooperation between the RSA FG Research Studio iSPACE and Salzburg University of Applied Sciences. It is funded by Salzburg state and IWB EFRE.

Thomas Prinz (co-author) would like to thank University of Salzburg (PLUS) – IDA Lab (20204-WISS/225/197-2019 and 0102-F1901166-KZP) for their support.

References

- Andrienko, G., Andrienko, N., Demsar, U., Dransch, D., Dykes, J., Fabrikant, S. I., . . . Tominski, C. (2010). Space, time and visual analytics. *International Journal of Geographical Information Science*, 24(10), 1577-1600. doi:10.1080/13658816.2010.508043
- Bayerisches Landesamt für Umwelt. (2018). Flächenmanagement-Datenbank: praktische Hilfe für Kommunen. Retrieved from <https://www.lfu.bayern.de/umweltkommunal/flaechenmanagement/fmndb/index.htm>
- Bootstrap. (n.d.). Build fast, responsive sites with Bootstrap. Retrieved from <https://getbootstrap.com/>
- ChartJS. (2016). Chart.js: Open source HTML 5 Charts for your website. Retrieved from <https://www.chartjs.org>
- ChartJS. (2017). chartjs-plugin-datalabels: Display labels on data for any type of charts. Retrieved from <https://chartjs-plugin-datalabels.netlify.app>
- De Amicis, R., Conti, G., Simões, B., Lattuca, R., Tosi, N., Piffer, S., & Pellitteri, G. (2009). Geo-visual analytics for urban design in the context of future internet. *International Journal on Interactive Design and Manufacturing (IJIDeM)*, 3(2), 55-63. doi:10.1007/s12008-009-0060-1
- ESRI. (2016a). Calcite Maps. Retrieved from <https://esri.github.io/calcite-maps/samples/index.html>

- ESRI. (2016b). Query. Retrieved from <https://developers.arcgis.com/javascript/latest/api-reference/esri-tasks-support-Query.html#>
- ESRI. (2018). Working with the ArcGIS Platform. Retrieved from <https://developers.arcgis.com/javascript/latest/guide/working-with-platform/>
- ESRI. (2019). ArcGIS API for JavaScript. Retrieved from <https://developers.arcgis.com/javascript/>
- Jing, C., Du, M., Li, S., & Liu, S. (2019). Geospatial Dashboards for Monitoring Smart City Performance. *Sustainability*, 11(20), 5648. doi:10.3390/su11205648
- JQuery. (2008). JQuery: The Write Less, Do More, JavaScript Library. Retrieved from <https://jquery.com/>
- Karduni, A., Cho, I., Wessel, G., Ribarsky, W., Sauda, E., & Dou, W. (2017). Urban Space Explorer: A Visual Analytics System for Urban Planning. *IEEE Computer Graphics and Applications*, 37(5), 50-60. doi:10.1109/mcg.2017.3621223
- Keim, D. A., Mansmann, F., & Thomas, J. (2010). Visual analytics: how much visualization and how much analytics? *ACM SIGKDD Explorations Newsletter*, 11(2), 5-8.
- Land Salzburg. (2019). Leitfaden: Räumliches Entwicklungskonzept. Retrieved from https://www.salzburg.gv.at/bauenwohnen_/Documents/2019_11_06_REK-Leitfaden.pdf
- Li, M., Bao, Z., Sellis, T., Yan, S., & Zhang, R. (2018). HomeSeeker: A visual analytics system of real estate data. *Journal of Visual Languages & Computing*, 45, 1-16.
- McArdle, G., & Kitchin, R. (2016). The Dublin Dashboard: Design and development of a real-time analytical urban dashboard., III-4/W1, 19-25. doi:10.5194/isprs-annals-iii-4-w1-19-2016
- Pettit, C., Lieske, S. N., & Jamal, M. (2017). CityDash: Visualising a Changing City Using Open Data. In (pp. 337-353): Springer International Publishing.
- Phdungsilp, A. (2011). Futures studies' backcasting method used for strategic sustainable city planning. *Futures*, 43(7), 707-714.
- Rheinland-Pfalz. (2015). RAUM+Monitor. Retrieved from <https://mdi.rlp.de/de/unsere-themen/landesplanung/raum-monitor/>
- Senaratne, H., Mueller, M., Behrisch, M., Lalanne, F., Bustos-Jimenez, J., Schneidewind, J., . . . Schreck, T. (2018). Urban Mobility Analysis With Mobile Network Data: A Visual Analytics Approach. *IEEE Transactions on Intelligent Transportation Systems*, 19(5), 1537-1546. doi:10.1109/tits.2017.2727281
- Shneiderman, B. (1996, 3-6 Sept. 1996). The eyes have it: a task by data type taxonomy for information visualizations. Paper presented at the Proceedings 1996 IEEE Symposium on Visual Languages.
- Visualising the Social and Cultural Infrastructure in Galway City and County. (2015). Retrieved from <http://galwaydashboard.ie/social>
- Würstle, P., Santhanavanich, T., Padsala, R., & Coors, V. (2020). The Conception of an Urban Energy Dashboard using 3D City Models. Paper presented at the Proceedings of the Eleventh ACM International Conference on Future Energy Systems.
- Zuo, C., Ding, L., & Meng, L. (2020). A Feasibility Study of Map-Based Dashboard for Spatiotemporal Knowledge Acquisition and Analysis. *ISPRS International Journal of Geo-Information*, 9(11), 636. doi:10.3390/ijgi9110636

Towards Sustainable Urban Car-Parking Solutions: Exploring Effects of Parking Policies Using Spatial Regression Analysis

Meng-Chin Tsai, Stephan van Gassel and Tzu-Chin Lin
National Chengchi University, Taipei, Taiwan

Abstract

In urban policy development and transport planning, car parking has become a crucial topic, as an ill-designed system could lead to traffic congestion, safety problems, increased air pollution and other challenges, particularly in densely populated urban areas. Adjusting parking fees has been deemed the most effective tool to control parking behaviour for selected locations, in order to attract or repel drivers. However, in order to select target areas efficiently, and before any recommendation for fee adjustment is made, an analysis of the current parking situation and the identification of variables influencing parking behaviour are needed.

We present a spatial analysis targeted at parking demand and supply data gathered via road surveys by local authorities in Taipei City. The spatial analysis is complemented by a regression analysis to identify variables that influence parking behaviour.

Our approach examines the relationship between potential controlling and contributing factors, and we show the influence of variables in a specific example. Our aim is to provide a starting point for future policy development and pricing adjustment at a local level. This initial framework might provide a conceptual core for wider discussion and a tool for integrating other different scenarios in the future.

Keywords:

car parking policy, urban sustainability, spatial analysis, Geographically Weighted Regression (GWR)

1 Introduction

In urban transportation management, an effective parking policy is essential as increasing demand for mobility and denser traffic on the one hand need to be balanced with modern sustainable urban development concepts on the other (see e.g. Clements, 2019). The understanding is that parking behaviour can be controlled through effective price policies, which can control the overall traffic situation, and the attractiveness and safety of the neighbourhood or community in which the policy has been implemented.

Other variables (in addition to parking fees) that describe and influence parking behaviour are factors such as cruising time spent for locating free parking spaces, travel time to final destination, and the purpose of the parking (Brooke et al., 2014; Brooke, 2016; Ma et al., 2013; Yun et al., 2009). Of these factors, parking fees are considered the most influential, as it has been shown that lower-priced parking generally results in higher occupancy levels of parking spaces. Free on-road parking, as one extreme, could lead to traffic congestion and thus longer journey times, and result in an overloaded parking system. Moreover, if all parking spaces are free of charge, society has to bear the cost, which might ultimately lead to a deterioration of the quality of the available parking and of the service provision (e.g., Shoup, 1997; 2020). While it may be straightforward to charge for car parking homogeneously across a city, a more detailed fee policy has the potential to help adjust local situations and to create a better balance across the city.

This very discussion took place in Taipei City (see Figures 1a and 1b), and in 2015 fees were introduced for on-street parking. Before the policy was implemented, people used to park on the streets, leaving their cars there for long periods (up to several months) without moving them at all). According to the Taipei City Parking Management and Development Office, the main goal of this policy is to increase the turnover of kerb-side parking spaces to improve parking efficiency. Pricing for car parking was developed according to the Taipei City Public Parking Lot Rate Autonomy Act, which stated that the management agency responsible for the parking spaces would set varying rates according to the region, traffic flow and time of day. In spite of the requirement to set parking fees, the city government's approach to investigating parking behaviour is based on traffic zones (see Figure 1b), which do not coincide with the pricing scheme of charged road segments. While the effects of car-parking policies have been studied in great detail over the years (e.g., Young, 1988; Feeney, 1989; Barter, 2012, 2015, 2018; Marsden, 2014; Biswas et al., 2017), the effect of this policy implementation has not so far been investigated in detail. It seems timely to carry out a preliminary analysis of the situation before and after the policy was implemented, using the available statistics and metrics.

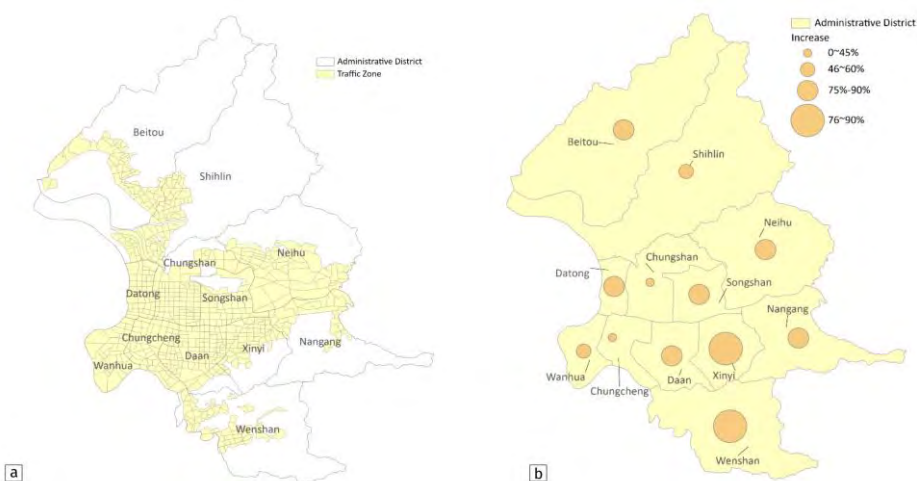


Figure 1: (a) Geographic distribution of urban districts and traffic zones in Taipei City; (b) districts with increased parking fees (city-wide car-parking policy introduced in 2015).

The city of Taipei proper is home to approximately 2.65 million inhabitants, with over 7 million people in the Greater-Taipei metropolitan area, which comprises Taipei City, New Taipei and Keelung (MOI, 2021). Taipei City has an average population density of about 9,900 people per square kilometre. To put this into perspective, most capitals in Europe are home to about 3,000–5,000 inhabitants per square kilometre; Asian capitals vary considerably, with Seoul being relatively high, with 16,000 inhabitants per square kilometre.

As in many Asian capital cities, the car parking situation in Taipei is tense, with high demand and limited supply at all times (see Barter, 2012), and comparably high parking fees charged by private providers of car-parking spaces. According to a recent report, Taipei City (like Beijing) follows a ‘moderate path’ with ‘modest parking standards’ and the development of multi-objective parking management policies. These policies are aimed at ‘serving wider urban and transport policy goals’ rather than optimizing demand and supply, as in more conventional approaches (ADB, 2011).

Taipei City’s government introduced fees for on-road parking in order to reduce lengthy stays in particular parking spaces, especially in residential areas. The aims were to improve the traffic situation and to contribute to a more sustainable living environment using local indicators and developments in the field of smart parking and neighbourhood traffic improvements (Chan, 2019; UN, 2015). A complementary aim of the city government has been to improve the demand to supply ratio of parking spaces. The new policy has addressed only part of Taipei’s parking situation, and it is difficult to ascertain whether changes in parking behaviour are due simply to the introduction of parking fees.

Management decisions in relation to parking policy have often been criticized for not integrating various transportation variables (e.g., Young et al., 1991). There exists only limited research showing the picture before and after a parking policy has been introduced. As parking policies can have a number of effects also on local businesses, a broader understanding is needed before recommendations are made (Chaturvedi, 2012).

The driving question in this investigation is whether the change of policy has changed overall parking behaviour significantly, as parking behaviour is known to be influenced by a number of factors but predominantly by charge adjustments. Along with this question comes the challenge of identifying (1) factors or variables that influence the behaviour, and (2) metrics recorded before and after the policy implementation, which may provide clues. In summary, our aims were:

1. Identifying changes before and after policy implementation in 2015;
2. Identifying variables that influence parking behaviour;
3. Promoting discussions on metrics to be collected in the future, which might allow for a detailed assessment of the challenges faced.

In the following section, we discuss the methodological approach taken to address these aims and summarize the available statistical data that was used in this investigation (Section 2). In Section 3, we discuss results from an exploratory statistical analysis, and those of a spatial regression model that was used to identify contribution variables. Finally, we end with a summary, conclusion and a brief outlook.

2 Methods and Data

In order to address the first aim, namely to identify changes before and after policy implementation in 2015, the first part of this work covers a spatial analysis that uses a set of conventional tools to identify local clustering, and the significance of any clusters and hot-/coldspots that might appear.

The second part of our research focuses on dependencies between a set of variables and a regression analysis to study the effects of these variables. This approach will provide insights into the second aim of the investigation, namely the identification of variables that influence parking behaviour; behavioural changes after the policy implementation might not be controlled by changes to parking charges alone. Both parts will highlight a number of challenges in response to the third aim, to identify open issues that need to be addressed further in subsequent work.

The basis of our investigation is data from the Parking Demand and Supply Surveys conducted between 2013 and 2017 for each traffic zone and road segment in Taipei City. The traffic zones in each administrative district were investigated for demand, supply, illegal parking, and both on- and off-road parking. There are 684 traffic zones in 12 administrative districts, supplying over 18,000 kerb-side parking places; half of these parking spaces require parking fees to be paid since the parking policy came into effect in 2015 (see Figures 1a and 1b).

The data from the Parking Demand and Supply Surveys include locational information and information about parking charges, in addition to the demand and supply data as represented by occupancy figures for both on- and off-road parking. All data were provided by the Taipei Parking Management and Development Office. In addition, demographic statistics were obtained from the Social and Economic Statistic Database of the Social and Economic Statistics Department, Ministry of the Interior, Taiwan. These data are complemented by data on urban zoning and land-use types, obtained from the Land Use Investigation for Taiwan, which was conducted by the National Survey Center in 2014. Additional data were derived during the spatial analysis using ESRI's commercial ArcGIS platform (Figure 2).

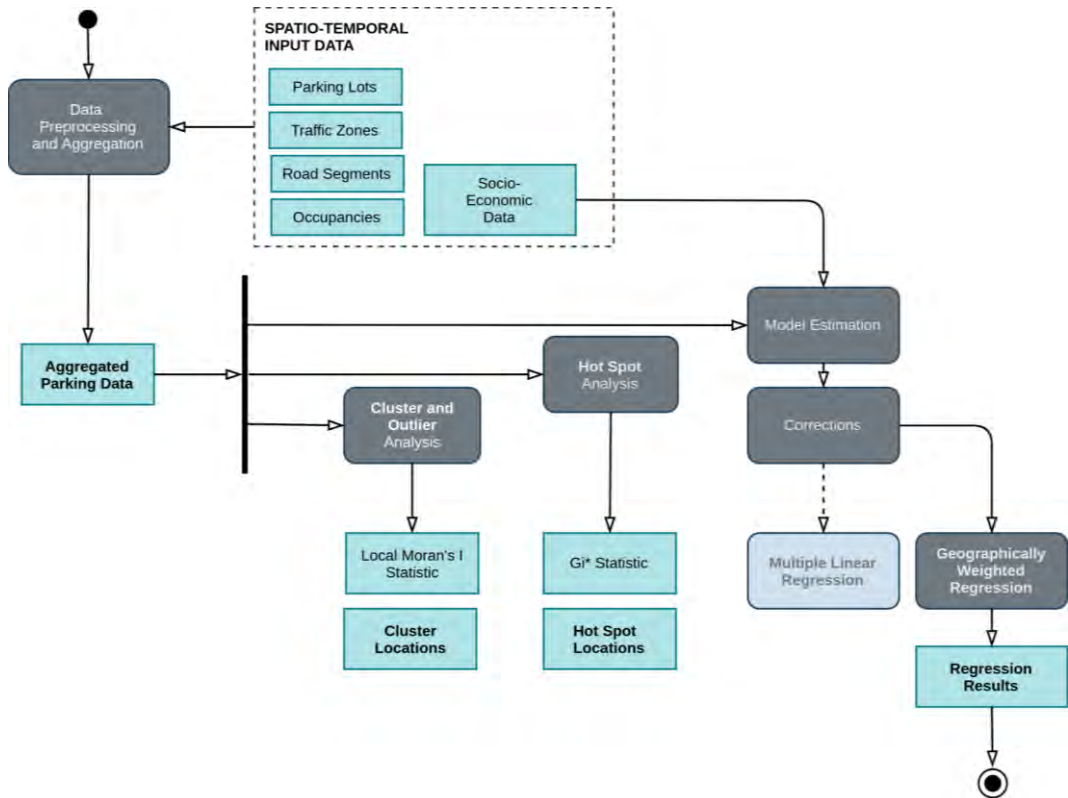


Figure 2: Data processing and analyses workflow as conducted in this investigation

Data pre-processing involves the aggregation of data from the street level to the level of the traffic zone, as street-level data are too granular to be merged with socio-economic variables. As most previous research has focused on data from a non-spatial perspective, we introduce a set of spatial analyses to obtain a better view of the data and the effects of policy on behaviour. Clustering is our first choice when it comes to identifying areas that could reveal significant effects after the policy implementation. Both Hot-Spot analysis (Getis & Ord, 1992; Ord & Getis, 1995) as well as Cluster and Outlier analyses (Anselin, 1995) were performed to identify correlations between pricing and location, both before and after policy implementation. More specifically, the Getis-Ord G^* statistic was expected to reveal spatial clustering of higher and lower parking charges, while the Moran's I was calculated to reveal significant spatial autocorrelation (see Figure 2). We expected the combination of both sets of statistics to provide further quantifiable insights into the results of the policy implementation. This approach to better characterize the parking situation by identifying potential patterns with respect to charges and location is of an exploratory nature.

The main purpose of this study was to obtain insights into the relationships between variables that might influence parking behaviour, from external variables (such as socio-economic factors), to location-dependent variables (such as proximity of alternative parking spaces and amount of parking space in a neighborhood). These relationships are explored using (1) a

Multiple Linear Regression (MLR) approach in the first step; they are further expanded upon using (2) a Geographically Weighted Regression (GWR) (Figure 2). Both MLR and GWR build on socio-economic variables that had been collected and integrated for each traffic zone area. They incorporated alternatives, such as the availability of off-road parking, which could potentially affect parking decisions.

In this study we collected, variables based on discussions in the research literature, and performed analyses to see whether parking behaviour is significantly affected by these variables. In order to obtain reliable results from the MLR, a number of tests and adjustments are required, including linearization of dependent and independent variables, and testing for multicollinearity and for homoscedasticity of error variances (Osborne and Waters, 2002; Uyanik and Güler, 2013) using the Breusch-Pagan test. For estimation of variables, the variables need to be tested for their relevance, using R-square values for comparing predicted and actual values. Finally, the significance of regression results is tested using an F-test over the mean-square regressions and the mean-square error. From the first results of the spatial regression analysis, it could be observed that parking patterns were distributed heterogeneously, showing that error variance is not uniform. This heteroscedasticity causes problems in the regression. This led us to select a more appropriate regression model (see Figure 2). The Geographically Weighted Regression (GWR), as an extension to the MLR, renders the original model more sophisticated by allowing relationships between the independent and dependent variables to vary by locality (Brunsdon et al., 1996). The spatial weights of observations are collected based on the distances between each location. GWR-estimated parameters are allowed to vary over space, which can be more suitable for analysis than arbitrarily-sized areas. It is known that GWR-estimated parameters have a better fit and offer better prediction in a scenario showing significant spatial heterogeneity (Brunsdon, et al., 1996; Fotheringham et al, 1999; Fotheringham et al, 2002).

The ratio of parking demand to supply is used as a descriptive index in this work. This ratio is the number of spaces occupied by cars (the demand) to the total number of off- and on-road parking spaces available in each traffic zone (supply). A small ratio indicates that the parking spaces are not being used efficiently, which means that the parking situation is relaxed but that there is an oversupply of parking space. Ratios in 2014 and 2015 were classified into five different categories to describe in detail the availability of parking spaces in each traffic zone. Ratios close to 1 reflect balanced demand and supply. Ratios between 1 and 1.25 indicate saturated supplies, and drivers may spend time cruising in search of a parking space or have to endure long waiting times. If the ratios are over 1.25, the parking system should be adjusted to avoid problems for the transport system as a whole.

3 Results and Discussion

In order to address our first aim, we mapped the classified demand-to-supply ratio (see Figure 3) and the distribution of charges (Figure 4) before and after policy implementation. In addition, we performed cluster and hotspot analyses to identify distribution characteristics that required further investigation.

In Figure 3, it can be seen that the overall situation after the introduction of the policy shifted towards a higher demand in a number of traffic zones, which puts more strain on available parking, but also helps optimize land use. Overall, the distribution shows subtle changes, with a number of potential clusters of higher ratios of demand to supply.

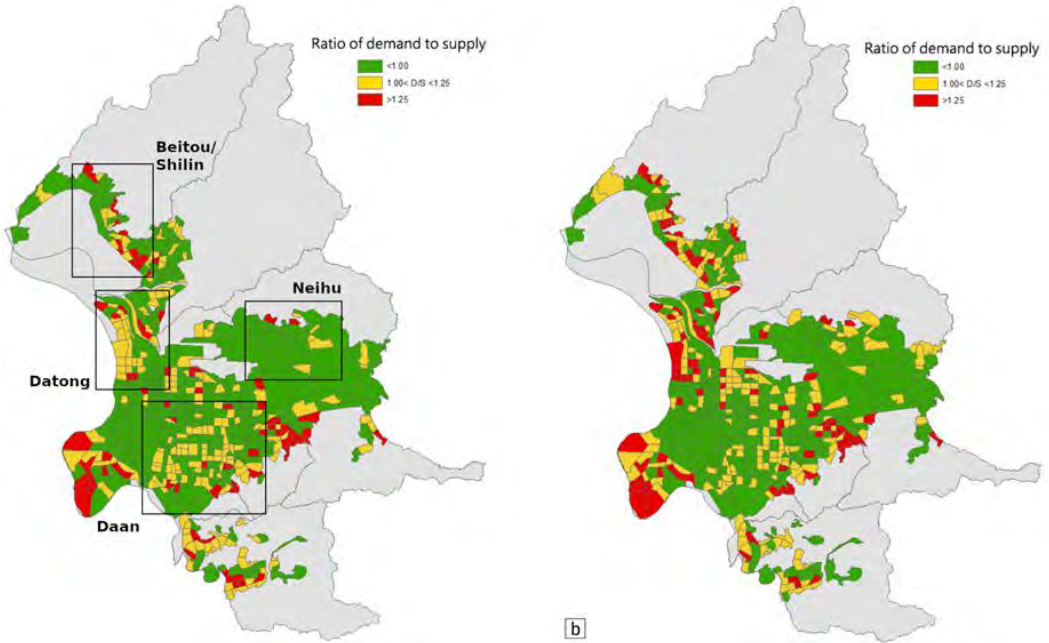


Figure 3: Demand to Supply Ratio for traffic zones in Taipei City (a) before parking-policy implementation in 2015, and (b) after implementation. Black boxes indicate (named) areas where there was significant change between the two periods (see also Figure 1 for reference)

The spatial distribution of fees (Figure 3) shows a significant change towards charging for parking throughout the city area, and towards lowering the parking charges. High charges remain within the city centre, while the second-highest charges are seen mainly in the northern and southern fringes, which are increasingly popular residential areas.

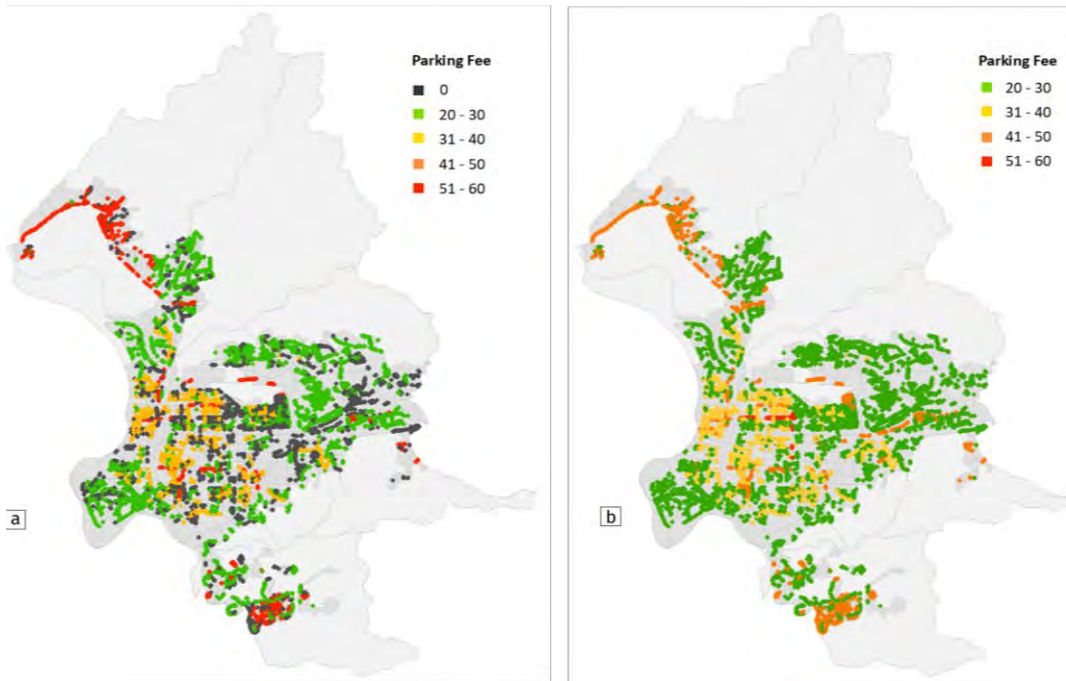


Figure 4: Distribution of kerb-side parking fees across districts and traffic zones in Taipei City, (a) before and (b) after policy implementation. (Fees in New Taiwan Dollars; 1 NTD = 0.03 EUR at the time of writing.)

The Cluster and Outlier analysis (Figure 5a) shows clear outliers in four districts where parking fees are higher. A small number of parking spaces are charged at a higher rate compared to surrounding ones (red areas in Figure 5a); in other traffic zones, some kerb-side parking spaces are charged less than in the surroundings (blue areas in Figure 5a). Both groups represent outliers. The effects of policy adjustments are well represented in these heterogeneous patterns indicating outliers. The distribution of outliers provides valuable information about location and direction of price adjustment.

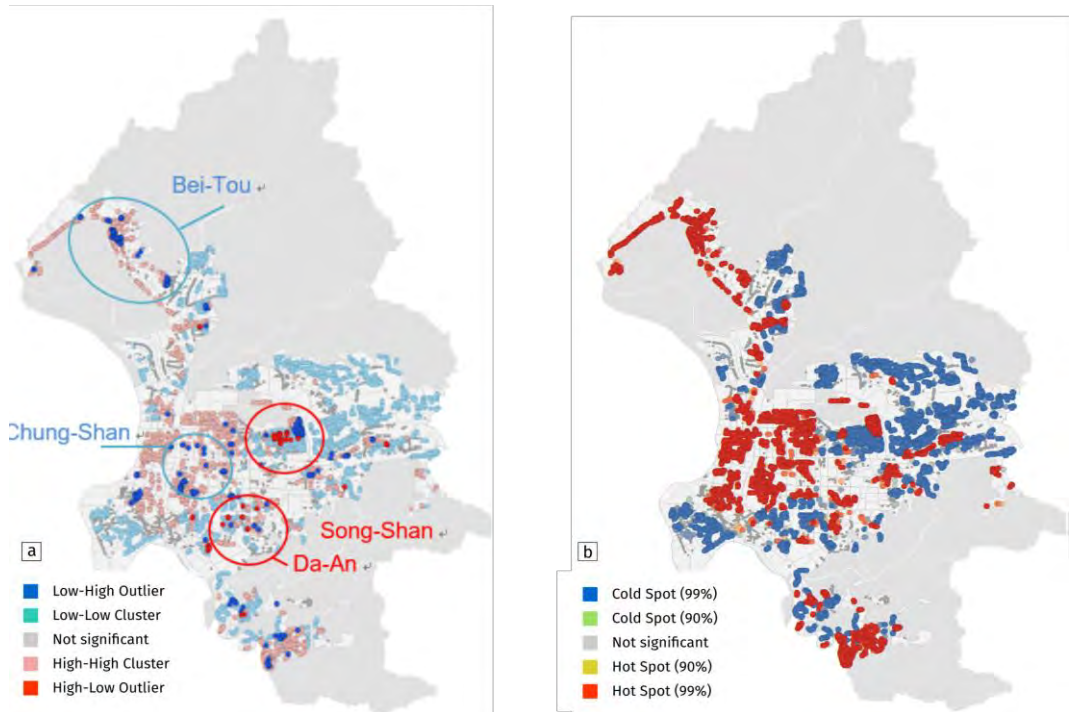


Figure 5: Distribution of (a) parking fee clusters and outliers, and (b) cold- and hotspots at traffic-zone level in Taipei City

In Figure 5b, kerb-side spaces charging higher fees appear as hotspots (in red) within areas of generally lower fees. The hotspots are predominantly in the western and central areas of the city. In contrast, outliers marked in Figure 5a are coldspots within their higher-charge environments. We can only speculate as to the reasons for these changes. While the local effect is likely to be to draw parking behaviour towards coldspots, the change might also increase pressure in the already tense inner-city traffic situation.

A secondary aim of our research was to assess the external (i.e. non-policy related) variables that were recorded along with on-street assessment of parking behaviour, in order to identify (a) the impact of these external variables on behaviour, and (b) their suitability as potential indicators in future assessments. In order to better understand dependencies, an initial Multi-Linear Regression analysis was performed using spatial and non-spatial socio-economic variables (e.g., household statistics).

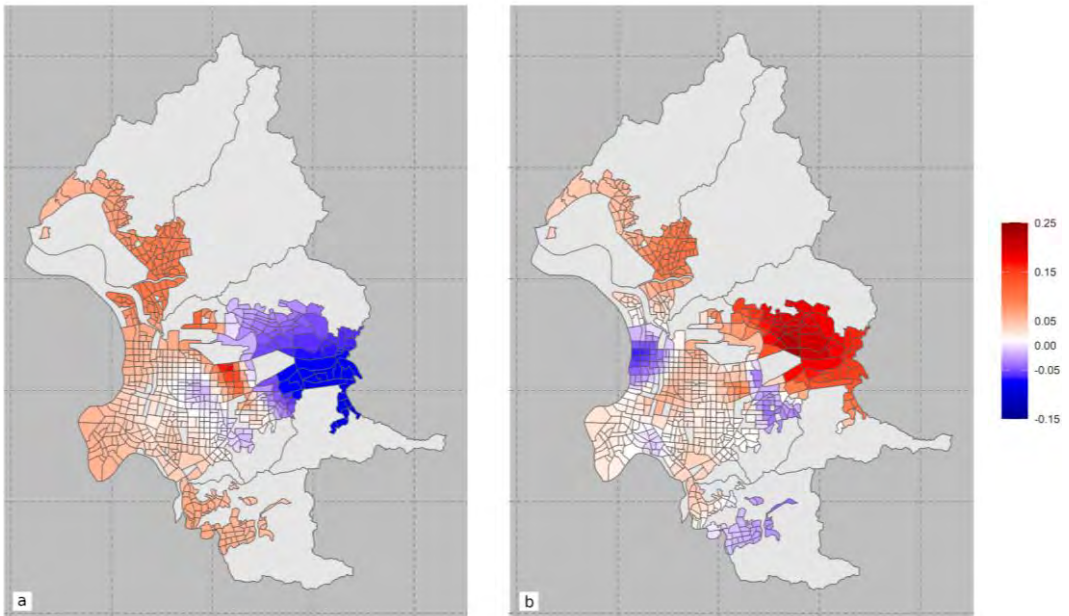


Figure 6: Coefficient results for the Geographically-Weighted Regression for the variable 'illegal parking (of cars)', (a) before and (b) after implementation of the new policy

Two approximate models were compared to determine which of them shows a larger effect with respect to parking-space occupancy. In the first model, numbers of on-road and off-road parking spaces were considered, accompanied by factors including land-use characteristics, and social properties such as number of households. The choice of variables was based on published studies – i.e., we selected the same variables as those found in other studies to be responsible, in the main, for drivers' parking choices. Before the policy was introduced, drivers' choice of parking spaces was affected by the total supply of on-road parking spaces – i.e. they could choose parking spaces anywhere along the road. After the introduction of the policy, residents in a traffic zone could be negatively affected by increased parking fees as their choice was now limited.

Population, number of households, and the proportion of residential land-use area were removed from the second model, due to multicollinearity effects. This new regression model has a higher explanatory power. In addition, the homoscedasticity problem that was observed with the first model was improved. Carrying out the same analysis after policy implementation revealed that drivers still preferred to occupy on-road parking spaces. Parking behaviour changed only slightly after the introduction of the new policy (away from on-street parking), indicating that drivers' preferences will stay much the same, despite a rise in the average parking fee in a traffic zone.

The traditional MLR model shows a significant heteroscedasticity problem, which could be overcome by a regionally weighted approach, such as a geographically weighted regression (GWR). The GWR makes use of the same variables as MLR model 2, analysing spatial patterns and impacts at local levels. As one example of the GWR analysis, correlation coefficients for

illegal parking are shown in Figure 6, for the periods before and after the policy implementation. Since on-road parking spaces are generally charged, some drivers will look for cheaper alternatives, and some will even park illegally along roads where parking is not allowed. Using the traditional regression model, it is not possible to identify the areas where this situation affects occupancy levels. Model 2 shows another effect, in which a decrease of illegal parking by 0.028 correlates with freeing one more kerb-side space for occupation (Figure 6). If we compare the situation before and after the introduction of the policy for each traffic zone, we see that drivers in each traffic zone show different preferences with regard to occupying the kerb-side spaces. Before the policy was implemented, they showed less preference for off-road supplies; after the average parking charge in the traffic zone was raised, they tended to park in kerb-side spaces. Also, illegal parking increased after the introduction of the policy.

Table 1: Comparison of Multiple Linear Regression (MLR) and Basic Geographically Weighted Regression (GWR) results before and after policy implementation. (RSS: residual sum of squares.)

	Before Policy		After Policy	
	MLR	Basic GWR	MLR	Basic GWR
R2	0.9362	0.9558	0.9354	0.9573
RSS	142,091.4	98,514.29	167,244.5	110,472

4 Summary and Conclusions

Considering today's dynamic urban environment and increasing sensitivity towards urban sustainability and mobility (Stubbs, 2002; Banister, 1998), parking policies need to be adaptive and reviewed on a regular basis to respond to the changing demands. The assessment of parking policies must be conducted using tools that can be readily applied, with indicators and metrics that can describe the actual situation (e.g., Barter, 2011). However, assessing parking situations in a uniform way across different traffic zones (or analogues thereof) poses a number of challenges, with respect to addressing not only the temporal dynamics, but also the influence of variables that are spatially as well as temporally dynamic.

The impact of the Taipei City government's new parking policy was assessed through a series of spatial analyses which aimed to gain a better understanding of the situation before and after the policy's introduction in 2015. A further aim was to (potentially) identify variables within their spatial contexts that might prove useful for future policy reviews and developments in response to changing traffic demands.

Despite many strategic improvements and a wider availability of tools to manage parking and develop car-parking policies, management decisions do not always address the actual dynamics of parking behaviour, due to the complexity of interdependencies, the lack of representative and meaningful (or even consistent) data, and new objectives that have to be integrated for a more sustainable urban environment. An analysis of the parking data that is currently available

for investigating parking in Taipei City showed pronounced clusters of parking places with high parking charges but limited demand as derived from hotspot, cluster and outlier analyses.

In this study, spatial analyses were complemented by a Multiple Linear Regression (MLR) in order to identify variables that influence parking behaviour within a traffic zone, and to gain a better understanding of the effectiveness of the policy employed. It turned out that the choice of specific variables (which was based on a literature review) and the application of an MLR led to the appearance of pronounced multicollinearity effects. These effects had to be addressed by adapting the regression model, removing variables originally deemed relevant. A Geographically Weighted Regression (GWR) emerged as a more accurate approach to capture drivers' responses to the policy adjustment.

Before the policy was implemented, drivers reacted less to off-road availability of spaces; following a rise in the average parking charge in a traffic zone, they tended to use the kerb-side parking spaces. In addition, the use of illegal parking spaces increased after the introduction of the policy.

For all traffic zones across the city, drivers show a preference for on-road parking, which might be related to their daily habits. For every 7 to 10 on-road parking spaces, there are about 10 drivers who would prefer to park at an indoor location.

According to the empirical results, parking behaviour has changed since 2015. However, in most districts, drivers are still willing to occupy kerb-side spaces even though the parking fees have risen. Hence, it seems safe to state that targeting charges in an attempt to adjust parking behaviour might have limited success in improving a parking situation or regulating traffic. It could also be seen in a few districts that further parking choices (e.g. off-road parking, or carparks attached to specific buildings or workplaces) can improve the problem of the high demand for on-road parking. Introducing more restrictions and customizing the parking policy for individual administrative districts may be other feasible options. Since Taipei has introduced experimental smart parking in several districts, new real-time data could soon be available that would provide higher temporal resolution of drivers' responses to parking adjustments.

The initial analytical procedure presented here could support discussions on policy impact, and enhance understanding of the relationships between parking behaviour and the attractiveness of locations. Ultimately, the approach could influence the design of parking infrastructure in order to address new needs in the context of sustainable city development.

Acknowledgements

The authors wish to thank the organizers and three anonymous reviewers for their comments and critical questions that have helped to improve the manuscript. We also wish to thank Mary Rigby for her extraordinarily detailed and helpful copyediting.

Reference

- ADB (2011). Parking policy in Asian cities. Asian Development Bank, Mandaluyong City, Philippines; 112 pp.
- Anselin, L. (1995). Local Indicators of Spatial Association - LISA. *Geographical Analysis* 27(2): 93–115.
- Banister, D. (1998). Barriers to the implementation of urban sustainability. *International Journal of Environment and Pollution*, 10(1): 65-83, doi:10.1504/IJEP.1998.002231.
- Barter, P.A. (2011). On-Street Parking Management - An International Toolkit. Sustainable Urban Transport Technical Document #14; Deutsche Gesellschaft fuer Internationale Zusammenarbeit, Federal Ministry for Economic Cooperation and Development; 120 pp.
- Barter, P.A. (2012). Off-street parking policy surprises in Asian cities, *Cities*, 29(1): 23-31, doi: 10.1016/j.cities.2011.06.007.T
- Barter, P.A. (2018). Parking Policies in Asian cities: Conventional but instructive. In D. Shoup (Ed.), *Parking and the City* (pp. 161–170). New York, NY: Routledge.
- Barter, P.A. (2015). A parking policy typology for clearer thinking on parking reform, *International Journal of Urban Sciences*, 19:2, 136-156, doi: 10.1080/12265934.2014.927740.
- Biswas, S., Chandra, S. and Ghosh, I. (2017). Effects of On-Street Parking In Urban Context: A Critical Review, *Transportation in Developing Economies*, 3:1-14.
- Brooke, S. (2016). Factors influencing urban on-street parking search time using a multilevel modelling approach, PhD thesis, Architecture, Building and Civil Engineering, Loughborough University, UK.
- Brooke, S., Ison, S. & Quddus, M. (2014). On-Street Parking Search, *Journal of the Transportation Research Board*, 2469:65-75.
- Brunsdon C., Fotheringham A. S. & Charlton M. E. (1996). Geographically weighted regression: a method for exploring spatial nonstationarity, *Geographical Analysis* 28:281-298; doi:10.1111/j.1538-4632.1996.tb00936.x
- Chan, C. C. (2019). Global Perspective: Taipei in Motion - A Proposal of Voluntary Local Review for SDG Progress; presentation on 18 March 2019, New York.
- Chaturvedi M., 2012, *Parking in Balance: A Geospatial Analysis of Efficiency of the Parking System of Enschede*, The Netherlands, University of Twente Faculty of Geo-Information and Earth Observation (ITC).
- Clements, R. (2019). Parking and the City, *Planning Theory & Practice*, 20:3, 456-465, DOI: 10.1080/14649357.2019.1627120
- Feeney, B. P. (1989). A review of the impact of parking policy measures on travel demand; *Transportation Planning and Technology*, 13:4, 229-244, doi: 10.1080/03081068908717403.
- Fotheringham A. S. & Brunsdon C. (1999). Local forms of spatial analysis; *Geographical Analysis*, 31(4):340-358.
- Fotheringham A. S., Brunsdon C. & Charlton M. (2002). *Geographically Weighted Regression: The Analysis of Spatially Varying Relationships*, 284 pp., Wiley.
- Getis, A. and J.K. Ord (1992). The Analysis of Spatial Association by Use of Distance Statistics. *Geographical Analysis* 24(3).
- Ma, X., Sun, X., He, Y. & Chen, Y. (2013). Parking Choice Behavior Investigation: A Case Study at Beijing Lama Temple. *Procedia - Social and Behavioral Sciences*, 96:2635-2642.
- Marsden, G. (2014). Parking Policy, Parking Issues and Policies. *Transport and Sustainability*, 5: 11-32. doi:10.1108/S2044-994120140000005016.
- MOI (2021). Taiwan Ministry of the Interior. Statistical Yearbook of Interior. Internet: <https://www.moi.gov.tw/english> (accessed 2021-01-25).
- Ord, J.K. and A. Getis (1995). Local Spatial Autocorrelation Statistics: Distributional Issues and an Application. *Geographical Analysis* 27(4).

- Osborne J. & Waters E. (2002). Four Assumptions of Multiple Regression that Researchers Should Always Test. *Practical Assessment, Research & Evaluation*, 8(2); doi: 10.7275/r222-hv23.
- Shoup D. (1997). The High Cost of Free Parking, *Journal of Planning Education and Research* 17:3-20.
- Shoup, D. (2020). The Pseudoscience of Parking Requirements. 8 pp., *Zoning Practice*, American Planning Association, 2, Practice Parking Reform.
- Stubbs, M. (2002) Car Parking and Residential Development: Sustainability, Design and Planning Policy, and Public Perceptions of Parking Provision. *Journal of Urban Design*, 7(2): 213-237. doi: 10.1080/1357480022000012249.
- UN (2015). *Transforming our World: The 2030 Agenda for Sustainable Development*. A/RES/70/1, 41 pp., United Nations, Geneva.
- Uyanık G. K. & Güler N., (2013). A Study on Multiple Linear Regression Analysis, *Procedia - Social and Behavioral Sciences*, 106:234-240.
- Young, W. (1988). A review of parking lot design models - Foreign summaries; *Transport Reviews*, 8(2): 161-181. doi: 10.1080/01441648808716682.
- Young, W., R. G. Thompson & M. A. P. Taylor (1991). A review of urban car parking models. *Transport Reviews*, 11(1), 63–84. doi:10.1080/01441649108716773.
- Yun, M., Lao, Y., Ma, Y. & Yang, X. (2009). Optimization Model on Scale of Public Parking Lot Considering Parking Behavior; *Eighth International Conference of Chinese Logistics and Transportation Professionals (ICCLTP)*, 2692-2699. doi:10.1061/40996(330)398.

Putting Pedestrians First: Sidewalk Infrastructures, Width Patterns and COVID-19

Victoria Fast and Jiaao Guo
University of Calgary, Canada

Abstract

As the COVID-19 crisis has forced people to adhere to social distancing, the proximity to each other of pedestrians on the sidewalk suddenly becomes meaningful: do pedestrians have enough space to safely move within cities? With decades of urban planning prioritizing roads and automobiles, the answer is 'no'. Cities all over the world have been forced to make urgent changes to pedestrian infrastructure in order to make it safe for people to move about public spaces during the pandemic.

In this study, using the sidewalk infrastructure from the Canadian city of Calgary as an example, we model sidewalk widths and then analyse the spatial patterns across the city. Our results reveal that Calgary's sidewalk widths vary substantially and form clusters of narrow sidewalks among residential zones, while wide sidewalks are typically found in downtown, and in some parks and recreational areas.

We recommend that the City of Calgary, and all cities, re-evaluate their sidewalk and pathway development patterns, and upgrade sidewalk infrastructures in those narrow-sidewalk communities. By developing more robust methods for modelling and analysing sidewalk width, paired with adequate sidewalk data, cities can make informed decisions that lead to more inclusive, pedestrian-safe, cities.

Keywords:

sidewalk width, pedestrians, accessibility, spatial pattern, health equity

1 Introduction

The global COVID-19 pandemic has forced us to rethink the role of pedestrian spaces, such as pathways and sidewalks, in an urban environment to keep the community safe and healthy. Local governments across the globe are taking decisive action to support pedestrian safety during the pandemic. For instance, traffic signals are set to be automatic for pedestrians, without the need for their physical contact with the traffic light buttons, in Brisbane, Australia (Brisbane, 2020). The Mayor of London, England announced the 'StreetSpace Plan' creating temporary cycling lanes (Simon, 2020). Thousands of kilometers of temporary 'corona' cycleways have popped-up across Europe, and arguments are being put forward to permanently adopt these as improvements to pedestrian and cyclist infrastructure (Reid, 2020).

In Canada, local policies are also adapting to ensure pedestrian and cyclist safety in response to COVID-19. The City of Toronto has opened kerb-side pedestrian lanes in areas that are identified as walking hotspots (Rider, 2020); the City of Winnipeg is reserving some automobile lanes for pedestrians practising physical distancing (Frew, 2020); and the City of St. John's council voted to widen the lanes for pedestrians' and cyclists' safety (Mercer, 2020). As early as March 2020, the City of Calgary closed roads to vehicular traffic in order to accommodate pedestrians who were going out for fresh air (Castillo, 2020). More recently, the mayor of Calgary announced that only pedestrians and cyclists will be allowed on certain popular downtown streets (Knight, 2020). As part of their COVID-19 relief plans, some local governments have gone as far as limiting public access to pedestrian sidewalks and bikeways in order to avoid overcrowding (District of North Vancouver, 2020).

Who do, and do not, have access to safely use the pedestrian infrastructure varies geographically, and the patterns relate directly to health equity (i.e. fair access for all to reach their full health potential). Spatial health inequality occurs when fair and safe access is restricted by social, economic and cultural forces, such as income, gender, race and disability. For example, areas where there is a higher incidence of road traffic accidents involving pedestrians have been associated with low-income neighbourhoods, where there is already lower spatial accessibility to active modes of transit (Khakh et al., 2019; Khakh, Fast, and Shahid, 2019). In studying our often racist urban past, Klein (2020) observed that 90% of high-income areas have sidewalks, while less than 50% of low-income communities do. Scholars have attributed systemic inequality, rather than simply high density, to the spread of COVID-19 (Jacobson, 2020). Observationally, COVID-related pedestrian interventions, such as street closures to cars, have disproportionately favoured downtowns and frequently-used public spaces over suburban or lower-income areas.

Motivated by gaining a better understanding of the spatial inequality of sidewalk interventions, we ask: where do pedestrians have enough space to safely move within cities? To answer this question, we use the City of Calgary to model the width of sidewalks and pathways for pedestrians (Section 2). Next, using aggregates (Section 3.1) and clusters (3.2), we analyse sidewalk-width patterns in order to reveal the spatial distribution of sidewalk widths across the city. Overall, a better understanding of sidewalk systems can contribute to more equitable planning in response to the pandemic and beyond for local government.

2 Modelling Sidewalks

The sidewalk represents one of the most common infrastructures for pedestrian use in an urban setting. Typically, a sidewalk occupies the space between residential (or other) buildings and the roadway proper. In some extreme cases, residential sidewalks can be found in the middle of a ten-lane road in Calgary (Figure 1a), further highlighting that the movement of cars has been the focus of transportation engineering and urban planning.

One of the most simple but powerful indexes of sidewalk design, illustrated by the architect Meli Harvey for New York City (Harvey, 2020), is sidewalk width. In the context of the global pandemic, sidewalk width is a direct indicator of the potential for pedestrians to maintain appropriate social distancing. A distance of 2 metres or 6 feet was adopted by the City of

Calgary (2020), and cities and public health agencies across the world, as a safe distance to reduce the spread of COVID-19. However, before pandemic-distancing measures, sidewalk-width standards had already established 2 metres as being appropriate for people with disabilities and wheelchair users (see Table 1). This width classification system is also checked against the accessibility standards specified by the Americans with Disabilities Act (ADA; 2010) and the guidance by the Rick Hansen Foundation when taking wheelchairs into consideration (Rick Hansen Foundation, 2020).

Table 1: Classification scheme for sidewalk width

Width	Sidewalk Width Standard
< 0.9 m	Wheelchair inaccessible, difficult to maintain physical distancing
0.9-1.5 m	0.9 m (36 inches) is minimum sidewalk width legislated by the ADA (Americans with Disabilities Act, 2010)
1.51-2.0 m	1.5 metres is meaningfully accessible for people with disabilities because it enables 2 wheelchair users to pass each other (Rick Hansen Foundation, 2020)
2.1-3.0 m	2 metres required for COVID physical distancing (City of Calgary, 2020)
3.1-4.0 m	Enough pedestrian space
> 4.0 m	Abundant pedestrian space

We used the City of Calgary’s 2019 sidewalk data, which include polygons of sidewalk shapes and sidewalk centrelines that were digitized from aerial surveys (Figure 1a). Open-source data such as OpenStreetMap’s footway data were not used (as we had initially intended) due to their inconsistency and lack of width values. Inspired by Harvey & Whong (2020), we calculated the average sidewalk width by 1) creating a midpoint from each centreline segment using Feature Vertices To Points in ArcGIS (ESRI, 2020a); 2) using Split Line at Point in ArcGIS (ESRI, 2020b) to split each centreline segment into two parts; 3) repeating steps 1 and 2 until midpoints of centrelines could be found on all sides of street blocks; 4) converting sidewalk polygons into polylines (edges only) and calculating the ‘Near’ statistics (ESRI, 2019) from each point to the closest edge ($\frac{1}{2}W$); 5) multiplying the nearest proximity (perpendicular to the edge) of each point by two to get the full sidewalk width (W).

To facilitate viewing the sidewalk-width data in detail, we created a web-map application: <https://arcg.is/1fj4LK1>. While the map should not be used for navigation (the data is out of date, and the model does not represent all walkway types), an interactive view supports data browsing at ‘pedestrian’ level, and the data is useful for analysing overall sidewalk patterns throughout the city.

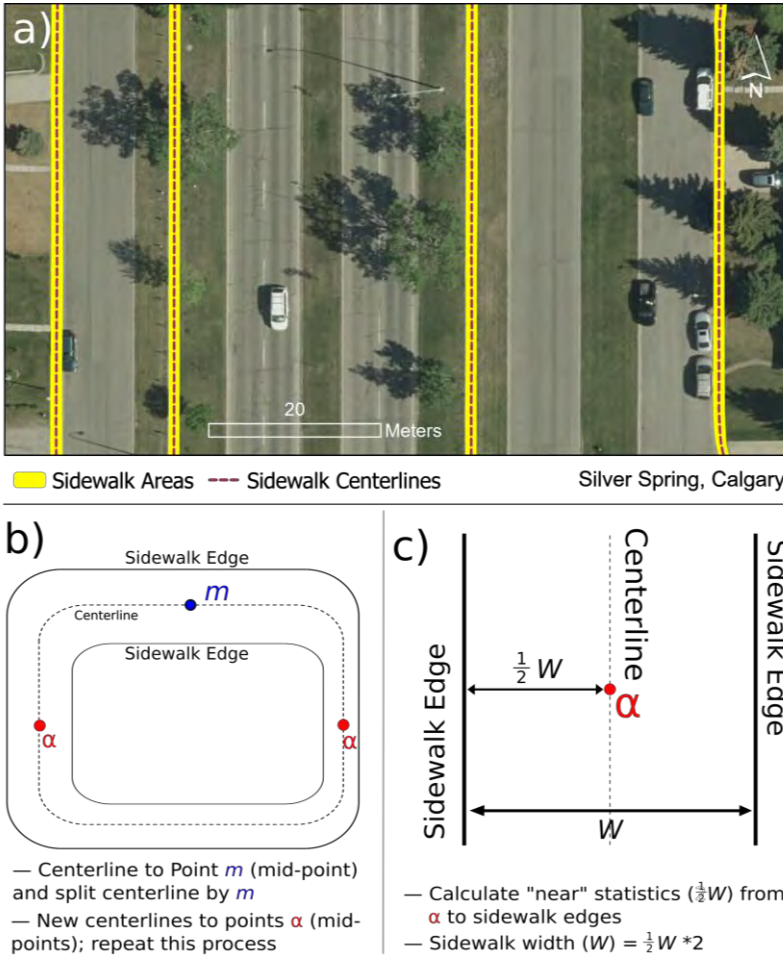


Figure 1: a) An aerial view of the sidewalks (yellow) and their centrelines (dashed line, red) in Silver Spring, Calgary; b) Sidewalk centrelines split by mid-points; c) sidewalk 'width' (W) generation from the mid-point of each segment of the centreline.

3 Analysing Sidewalk Patterns

Calgary is known for its unusual population density patterns due to its sprawling growth (Guo and Fast, 2019), especially compared to other major Canadian cities (Guo and Fast, 2020). Using aggregates and clusters, here we investigate how Calgary’s sidewalk widths vary across the city.

3.1 Aggregated Sidewalk Widths

First, we analysed the average sidewalk widths by aggregating individual sidewalk segments into different enumeration areas: by community (a neighbourhood governed by a community association); 400 x 400m grid; and the finest-grained census unit in Canada, the dissemination

block (Statistics Canada, 2017). The average sidewalk widths in Calgary vary substantially (Figure 2). At all viewing levels, downtown Calgary contains the widest sidewalks in the city. At dissemination-block level, we observe many blocks that do not meet the threshold for meaningfully accessible sidewalks (<1.5m), or even the absolute minimum sidewalk width of 0.91m required for wheelchair access (in red). The instances of red blocks, especially in the northeast of Calgary, align with patterns of traffic accidents involving pedestrians observed in Calgary by Khakh et al. (2019). Further study is required to test the strength of the association between sidewalk width and road accidents involving pedestrians.

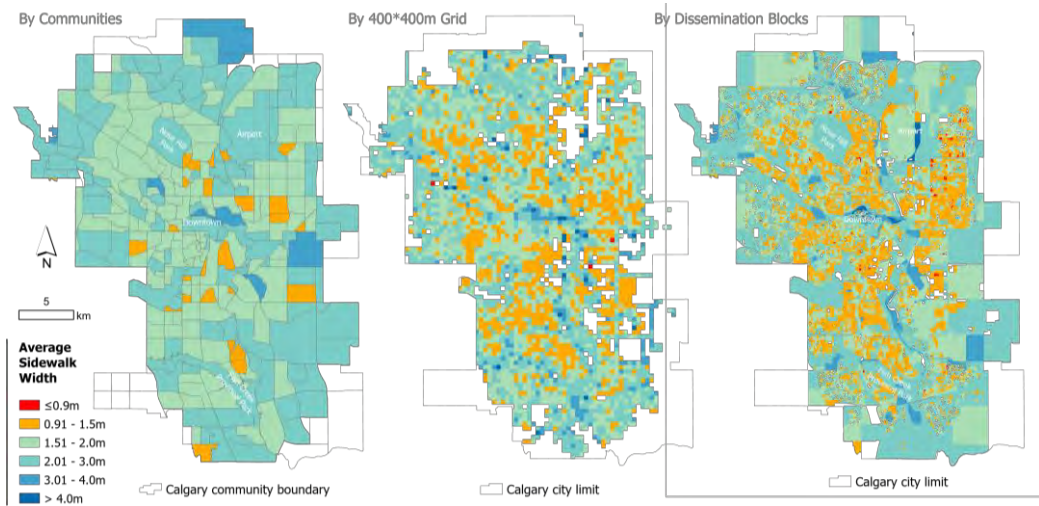


Figure 22: Calgary's average sidewalk width for three different aggregation units: community, 400m grid, and dissemination block.

3.2 Clusters of Similar-width Sidewalks

Recognizing that sidewalks vary not just across the city but within local neighbourhoods, we next applied spatial autocorrelation (SA) to test for local clusters of similar-width sidewalks. We used the average sidewalk widths at a 50 x 50m aggregation level, with searching distances of 1,500 m and 3,000 m. SA is a fundamental concept in spatial analysis: it reveals how geographical objects are correlated or uncorrelated with each other (Getis, 2008). Using Anselin Local Moran's I index (Anselin, 1995), SA can reveal the 'spatial inequality' of sidewalk width across a study area (Zhang, Luo, Xu & Ledwith, 2008) (see Figure 3). A positive local Moran's I value represents a location with a high or low value similar to that of its neighbours, which together are also known as 'spatial clusters' (Yuan, Cave, and Zhang, 2018). SA was calculated as follows:

$$I_i = \frac{z_i - \bar{z}}{\sigma^2} \sum_{j=1, j \neq i}^n [w_{ij}(z_j - \bar{z})] \quad (1)$$

where z_i represents the value of variable z at location i ; \bar{z} is the average value of z with n samples; σ^2 is the variance of all z variables; z_j represents the value of z at all other locations within a certain radius; and w_{ij} is the weight as the inverse of distance d_{ij} between z_i and z_j (Zhang et al., 2008).

In this study, the high and low values are wide and narrow sidewalks, respectively. The results show that various sidewalk widths are clustered throughout the city, and that narrow or wide sidewalks are often surrounded by each other (Figure 4). In particular, clusters of wide sidewalks (high Moran's I value; green) can be seen distinctly in downtown Calgary and near large public green spaces (such as Fish Creek Provincial Park and Nose Hill Park), at both search distances. Neighbourhoods that have clusters of narrow sidewalks are found throughout the city limit, but they are typically located in suburban areas. These results suggest that different areas of the city are differently, and unequally, served by sidewalk infrastructure. Residents living in areas with narrow sidewalks would have to travel to a different part of the city to walk safely without worrying about physical distancing issues. Our analysis can be extended further by overlaying sidewalks with population distribution.

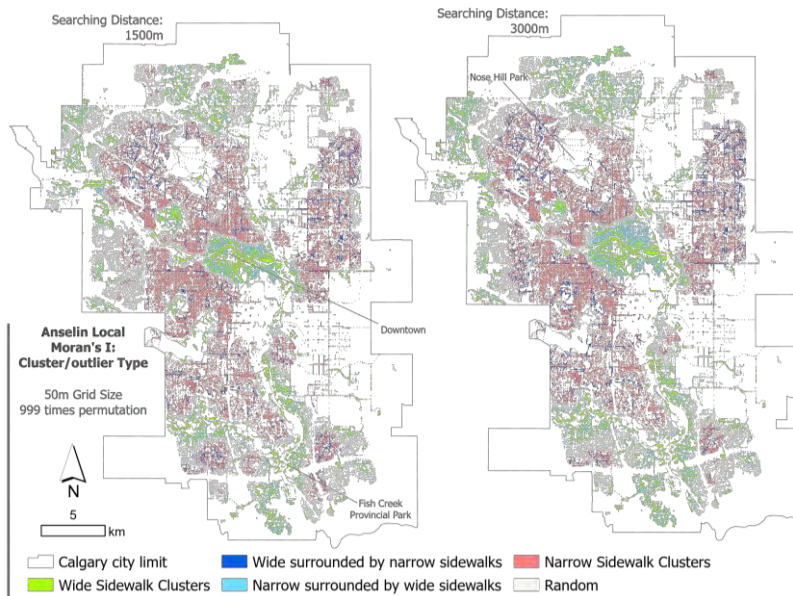


Figure 3: The spatial autocorrelation product of sidewalk widths using Anselin Local Moran's I with two searching distances at 50m x 50m resolution. Statistically significant positive Moran's I values are classified into: 1) wide sidewalks, and 2) narrow sidewalks. Statistically significant negative Moran's I values are classified into: 3) wide sidewalks surrounded by narrow sidewalks, and 4) narrow sidewalks surrounded by wide sidewalks. 5) Statistically non-significant Moran's I values (close to 0) are classified as random.

4 Discussion and Recommendations

During GI_Forum 2021, organizers asked how data and spatial analytics can support the achievement of Sustainable Development Goals (SDGs). Informed by this research, in order for urban data science to reduce inequalities (goal 10) and create more sustainable cities and communities (goal 11), we need: 1) better pedestrian-level data, and 2) to analyse the entire city system. We heard during the conference that many participants do not have access to sidewalk data, and often use roads as proxies in their city or community. Roads do not capture the pedestrian perspective, and even sidewalk width is an oversimplified way of understanding pedestrian space. Data and urban mobility analysis have served the automobile for far too long. It is time to put all pedestrians first. Data on sidewalks, ramps, stairs, public washrooms and pathway obstacles, among other features, are required to properly model pedestrian space. As spatial scientists, we need to create, share and advocate for data that are inclusive of the pedestrian perspective to make the SDGs measurable and to inform future urban interventions.

Second, we need to consider the entire city system in our analyses. In response to the COVID pandemic, the City of Calgary has prioritized pedestrian initiatives, such as road closures, only in only selected parts of the city (e.g. downtown). While an extensive network of pedestrian pathways and bridges have made the city's downtown iconic, the pandemic has reminded us that pedestrian mobility must extend beyond the core, because the city's historic development strategy has promoted the expansion of low-density, automobile-oriented communities. This is where the majority (80%+) of residents live. Wherever there are residents, there needs to be equitable sidewalk infrastructure to create a pedestrian-friendly environment. We suggest that the City of Calgary, and all cities, should re-evaluate – and prioritize – development plans for sidewalks and pedestrian infrastructure more broadly (e.g. pathways and bikeways) by taking into account population densities and distributions in the city. Overall, urban data science needs to measure and analyse the pedestrian infrastructure within our cities, with a view beyond the COVID-19 pandemic, to achieve urban livability improvements for all pedestrians.

Acknowledgements

We gratefully acknowledge that this work was supported by the Social Science and Humanities Research Council of Canada Grant 430-2018-00432: Accessible Mobility: Getting Around in the Smart City.

References

- Americans with Disabilities Act [ADA]. (2010). 2010 ADA Standards for Accessible Design. Retrieved from <https://www.ada.gov/regs2010/2010ADASTandards/2010ADASTandards.htm>
- Anselin, L. (1995). Local Indicators of Spatial Association—LISA. *Geographical Analysis*. <https://doi.org/10.1111/j.1538-4632.1995.tb00338.x>
- Brisbane. (2020). Updates to automatic pedestrian traffic signals. Retrieved from <https://www.brisbane.qld.gov.au/community-and-safety/community-safety/disasters-and-emergencies/coronavirus-council-updates-and-impacts/updates-to-automatic-pedestrian-traffic-signals>
- Castillo, C. K. de. (2020). Road closures planned for Calgary to give more room for pedestrians and cyclists, 28 March. Retrieved from <https://globalnews.ca/news/6744420/road-closures-calgary-cyclists-pedestrians-social-distancing-coronavirus/>
- City of Calgary. (2014). 2014 Complete Streets Guide. Calgary, Alberta, Alberta. Retrieved from <https://www.calgary.ca/content/dam/www/ca/city-clerks/documents/council-policy-library/tp021-complete-streets-policy.pdf>
- City of Calgary. (2020). COVID-19 - Physical distancing and self-isolation. Retrieved from <https://www.calgary.ca/csps/cema/covid19/safety/covid19-social-distancing-self-isolation.html>
- District of North Vancouver. (2020). Facilities, parks, and services impacted by COVID-19. Retrieved from <https://www.dnv.org/programs-services/facilities-parks-and-services-impacted-covid-19#Park>
- ESRI. (2019). Near. Retrieved from <https://desktop.arcgis.com/en/arcmap/10.3/tools/analysis-toolbox/near.htm>
- ESRI. (2020a). Feature Vertices To Points (Data Management). Retrieved from <https://pro.arcgis.com/en/pro-app/latest/tool-reference/data-management/feature-vertices-to-points.htm>
- ESRI. (2020b). Split Line at Point. Retrieved from <https://desktop.arcgis.com/en/arcmap/10.3/tools/data-management-toolbox/split-line-at-point.htm>
- Frew, N. (2020). City of Winnipeg to open 4 active transportation routes for pedestrians, cyclists early. Retrieved from <https://www.cbc.ca/news/canada/manitoba/city-winnipeg-active-transportation-routes-1.5516549>
- Getis, A. (2008). A history of the concept of spatial autocorrelation: A geographer's perspective. *Geographical Analysis*, 40(3), 297–309. <https://doi.org/10.1111/j.1538-4632.2008.00727.x>
- Guo, J., and Fast, V. (2019). Spatial insights on urban density: A case study of Calgary. *CEUR Workshop Proceedings*, 2323(3). Retrieved from <http://ceur-ws.org/Vol-2323/>
- Guo, J., and Fast, V. (2020). Growing up, growing out: comparing spatial patterns of urban populations in Canada. *Geomatica*, 74(1). <https://doi.org/https://doi.org/10.1139/geomat-2020-0003>
- Harvey, M. (2020). Sidewalk Widths NYC. Retrieved from <https://www.sidewalkwidths.nyc/#13/40.714/-74.005>
- Harvey, M., and Whong, C. (2020). Github: Sidewalk Widths NYC. Retrieved from <https://www.sidewalkwidths.nyc/#13/40.714/-74.005>
- Jacobson, A. (2020). “Idiocy of our current urban systems”: Inequality, not high-density cities, to blame for COVID-19’s spread. Retrieved from <https://www.cbc.ca/radio/spark/idiocy-of-our-current-urban-systems-inequality-not-high-density-cities-to-blame-for-covid-19-s-spread-1.5544528>
- Khakh, A., Fast, V., Lee, C., Rogers, N., Nasca, F., and St.Pierre, M. (2019). Toward Active Neighbourhoods: Analyzing Pedestrian Collisions and Socio-Economic Status In Three Canadian Cities. In Canadian Association of Road Safety Professionals. Calgary, Alberta. Retrieved from

- <http://www.carsp.ca/research/research-papers/research-papers-search/download-info/toward-active-neighbourhoods-analysing-pedestrian-collisions-and-socio-economic-status-in-three-canadian-cities/>
- Khakh, A. K., Fast, V., and Shahid, R. (2019). Spatial accessibility to primary healthcare services by multimodal means of travel: Synthesis and case study in the city of calgary. *International Journal of Environmental Research and Public Health*, 16(2). <https://doi.org/10.3390/ijerph16020170>
- Klein, G. (2020, June). To fix our cities, we must reckon with our racist urban past. Retrieved from <https://www.washingtonpost.com/opinions/2020/06/12/fix-our-cities-we-must-reckon-with-our-racist-urban-past/>
- Knight, D. (2020). Calgary to limit vehicles on Stephen Avenue to make room for pedestrians, patios. Retrieved from <https://globalnews.ca/news/6998483/stephen-avenue-traffic-restrictions-patio-extensions-coronavirus/>
- Mercer, J. (2020). St John’s council votes to widen lanes for pedestrian, cyclist safety during COVID-19 pandemic. *The Telegram*. Retrieved from <https://www.thetelegram.com/news/local/st-johns-council-votes-to-widen-lanes-for-pedestrian-cyclist-safety-during-covid-19-pandemic-446158/>
- Reid, C. (2020). Pop-Up Coronavirus Cycleways Deliver \$3 Billion In Annual Health Benefits Across Europe. *Forbes*. Retrieved from <https://www.forbes.com/sites/cartonreid/2020/08/18/pop-up-coronavirus-cycleways-deliver-3-billion-in-annual-health-benefits-across-europe/?sh=32a3728a6ad7>
- Rick Hansen Foundation. (2020). A Guide to Creating Accessible Play Spaces. Retrieved from <https://www.rickhansen.com/sites/default/files/2020-03/sch-35913-guide-creating-accessible-play-spacesen2020web.pdf>
- Rider, D. (2020). Toronto to open some traffic lanes to pedestrians in congestion ‘hot spots.’ Retrieved from https://www.thestar.com/news/city_hall/2020/04/27/toronto-traffic-lanes-to-be-closed-for-pedestrians-in-hot-spots.html
- Simon, M. (2020). Mayor announces “radical” plans for London. Retrieved from <https://lcc.org.uk/articles/mayor-announces-radical-plans-for-london>
- Statistics Canada. (2017). Dissemination block (DB). Retrieved from <https://www150.statcan.gc.ca/n1/pub/92-195-x/2011001/geo/db-id/db-id-eng.htm>
- Yuan, Y., Cave, M., and Zhang, C. (2018). Using Local Moran’s I to identify contamination hotspots of rare earth elements in urban soils of London. *Applied Geochemistry*, 88, 167–178. <https://doi.org/10.1016/j.apgeochem.2017.07.011>
- Zhang, C., Luo, L., Xu, W., and Ledwith, V. (2008). Use of local Moran’s I and GIS to identify pollution hotspots of Pb in urban soils of Galway, Ireland. *Science of the Total Environment*, 398(1–3), 212–221. <https://doi.org/10.1016/j.scitotenv.2008.03.011>

Innovation for Sustainable Cities: The Effects of Nudging and Gamification Methods on Urban Mobility and Sustainability Behaviour

Claudia Luger-Bazinger and Veronika Hornung-Prähauser
Salzburg Research, Austria

Abstract

For more sustainable urban behaviour and mobility, innovative methods are needed to change behaviour. We discuss the results of an explorative study of the use of a personal mobility tracker (a digital, data-based tool) to motivate users to adopt a more sustainable city lifestyle. We examine motivational techniques that can influence citizens' personal mobility on a day-to-day basis. Using a personal mobility app that incorporates gamified elements and nudging, citizens become part of a community. They are motivated to cycle more and to explore sustainable services in the city through tours and visiting points of interest. We present the first results of a trial of this mobile app: characteristics of users, and empirical data that indicate a change in cycling behaviour. We also show effects of nudging on personal mobility.

Keywords:

sustainability, nudging, mobility behaviour, mobility tracker

1 Introduction

Cities are trying to integrate the UN's Sustainable Development Goals into their policies in order to promote sustainable (urban) living and fight climate change. Cities face multiple issues regarding sustainability. One of the biggest challenges is adjusting the modal split in transport, as car use still dominates in cities and their surroundings (European Platform on Mobility Management, 2018); transport accounts for a quarter of Europe's GHG emissions (European Environment Agency, 2018). Therefore, cities need to find ways to change citizens' mobility behaviour. However, it appears that pure promotion of, or information on, more sustainable behaviour alone do not motivate sufficiently (Huber et al., 2017). Nudging (i.e. guiding behaviour while still leaving room for personal choices) (Thaler & Sunstein, 2008) has started to establish itself as a promising method in governance and policy instrumentation. It is of great importance that new tools using nudging are created in such a way that their impact and efficiency can be evaluated. Thus, our key research question is how, using data from a personal mobility tracker, can motivational techniques be used to influence citizens' personal mobility?

This paper discusses the results of an explorative study concerned with the use of a digital, data-based tool to promote more active urban mobility at the same time as citizens are discovering other facets of sustainability (e.g. locally produced goods or locally grown food) within a city. Building on our previous theoretical work (Klieber et al., 2020), we are now able to present empirical data. The use of data is crucial in designing the tools necessary for triggering a more sustainable lifestyle, but also for measuring actual behavioural change.

First, we provide a theoretical overview of the data-based nudging approach, supported by a mobile app. Second, we report results on the effects of this approach.

2 Fostering sustainability goals through data-based interventions

Within a European research project (SimpliCITY, www.simplicity-project.eu), two cities are developing effective strategies to stimulate sustainable behaviour among citizens, who are engaged through behavioural nudges and gamified features in a personal mobility app. With the mobile app, the user becomes part of a community and is motivated to show more sustainable behaviour. They explore sustainable offers (e.g. locally produced goods, local environmental protection services) within the city via cycling. The use of data, for guiding behaviour (i.e. nudging), for gamification elements (e.g. location-based services, mobility tracker) as well as for measuring changes towards more sustainable behaviour, is central to the project. The following sections describe how the gamification and nudging elements in the app are planned and implemented, and how behavioural change is measured (see also Klieber et al., 2020, for a more detailed description of the methods).

2.1 Gamification

Gamification uses elements taken from gaming in other contexts, and has been successfully implemented in mobile apps for smart-city initiatives in order to keep citizens engaged (Kazhamiakin et al., 2016). Gamification can motivate users to engage more regularly, and can incite them to modify their behaviour (Engel, 2017; Hamari et al., 2014). In the personal mobility app discussed here, users earn reward points ('heartbeats') for carrying out activities – e.g. tours in their neighbourhood, visiting points of interest such as urban gardening spaces, solving quizzes and riddles, and using the mobility tracker when cycling. Active mobility is used for exploring sustainable services in the city. Users collect reward points for the specific neighbourhood of which they are part.

2.2 Nudging

Nudging can be described as a strategy to change people's behaviour without threat or severe economic consequences (i.e. fines). Nudging uses interventions that are 'easy and cheap to avoid' (Thaler & Sunstein, 2008, p. 6), while seeking to alter the way choices in relation to local environments are presented and made (Ly & Soman, 2013). It aims to guide people's behaviour in a desired direction while they are still free to make their own decisions. Interest in the method was sparked in various contexts (Lehner et al., 2016; Sunstein, 2014). In general,

people seem to be in favour of nudging, at least if the nudge fits with the interests and values of the majority of people (Reisch & Sunstein, 2016).

Insights into digital nudges show promising results (Meske, 2017; Schneider et al., 2018). In the context of developing our particular personal mobility app, we also investigate the effect of social comparison. Social comparison theory (Festinger, 1954) states that people tend to compare their own opinions, abilities and behaviour to those of other people for evaluation. Social influences can be successful in changing individual behaviour, notably in terms of sustainable living (Abrahamse & Steg, 2013). More specifically, people tend to modify their behaviour after seeing that a specific social group is showing a particular behaviour. Quite famously in the nudging literature, Nudge Lebanon (2019) demonstrated that a letter to people stating that most of their neighbours paid their electricity bill on time helped to improve the overall timeliness of payments. If there is strong identification with the relevant social group, the nudge has a greater effect (Doran et al., 2017). In our case, the community using the personal mobility app could serve as the relevant social group.

2.3 Measuring change in sustainable behaviour

Ajzen's (1991) theory of planned behaviour explains that behaviour is influenced by attitudes and subjective norms, as well as by people's perceived ability to behave in a particular way. These factors lead to an intention and subsequently to an actual behaviour. The theory of planned behaviour often informs efforts to change behaviour regarding the environment and sustainability (Macovei, 2015).

However, the effectiveness of an intervention can be evaluated only if the desired target behaviour can be measured in a valid manner. For the present study, we rely on self-reported behaviour in a before-and-after design, as well as on tracked (i.e. measured) mobility and sustainability behaviour.

3 Method

A personal mobility tracker, in the form of a mobile app, was tested from the beginning of August 2020 to end of September 2020; for the nudging phase, it was used again in April to May 2021.

Users downloaded the app to their smartphone, and after a sign-up were then part of the community. The main activities for users of the app focus on active mobility and exploring sustainability (see Figure 1); they use the mobility tracker when cycling, and can take tours around the city (which include points of interest and involve quizzes). They can explore regional and sustainable services (as a virtual list or as points of interest in the city), such as local shops or environmental organizations. Five different city tours were offered, which included a total of 18 points of interest (visiting these was logged through geolocation), and 114 regional and sustainable services that were represented in the community, such as local non-profit organizations, urban gardening spaces and second-hand stores.

The personal mobility tracker serves both to measure behaviour (i.e. the tracker for cycling), as well as a way to influence behaviour (awarding ‘heartbeats’, and sending notifications and reminders to individual users).

The data analysed included logs of each user’s activities, as well as user-profile information (e.g. age, gender). Data was analysed using R Studio.



Figure 1: Screenshot from the mobile app: activities within the app.

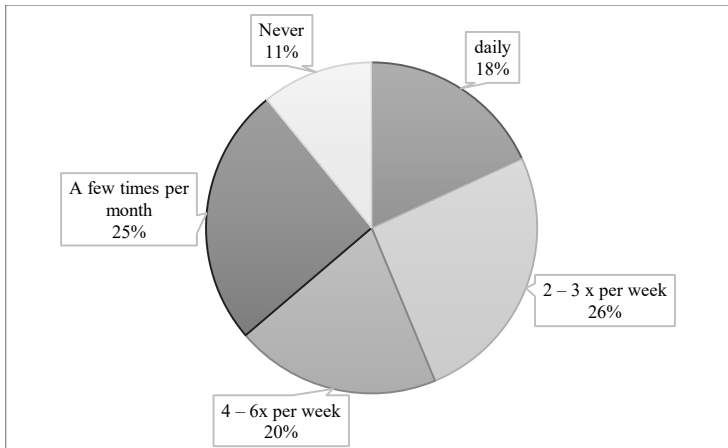


Figure 2: Habits of users: How often do you ride your bicycle?

4 Results

4.1 User characteristics

587 users in Salzburg, Austria, took part in the trial. Information from the user profiles showed that most were women (59.5% females, 38.6% male, 1.9% inter/diverse), with over half of the users (53%) aged between 26 and 45, and almost a quarter (22%) between 18 and 25. Almost two-thirds ride their bikes at least 2–3 times per week (see Figure 2). While this indicates a group that is already using active forms of mobility, more than a third of users ride their bike just a few times per month or never. This shows that the app is not simply “preaching to the converted”, but is also reaching a broader group of citizens.

4.2 Effects of gamification

When users carry out activities using the app, they are rewarded with gamified ‘heartbeats’. They collected a total of 1,969 heartbeats. Factors like gender or age influence the effect of gamification on engagement and behaviour (Koivisto & Hamari, 2014). We therefore looked at whether there are significant differences between men and women: men collected a total of 1,045 heartbeats, women collected 900, but no significant difference between the mean collected heartbeats was found ($t(312) = -0.99, p = .32$).

The mobility trackers revealed that users cycled 1,493 km in total. On average, men cycled 28 km over the course of the test period, and women 21 km. Statistically, however, the difference is not significant: ($t(57) = -0.53, p = .60$).

In order to estimate any effect on behaviour, some kind of comparison needs to be made. Simply looking at overall bicycle use within the app does not necessarily indicate a behavioural change, as the baseline for cycling within the sample was unknown (i.e. users perhaps cycled a lot already). For the first trial, a comparison with a self-reported estimate of alternative behaviours was made. After users finished tracking their cycle ride, they could indicate whether

they would usually have taken their car or the bus for this journey. This allows an estimation of the effect of the app on mobility behaviour. For 117 km cycled, users indicated that they would usually have taken the bus. For 207 km cycled, they would normally have taken the car.

4.3 Effects of nudging

Using a subset of users, we relaunched the app to test the effectiveness of social comparison as a data-based nudging method ($N = 202$). Over a period of two weeks from April to May 2021, users were sent six nudges (notifications) via the app. Each nudge focused on the comparison of their own cycling behaviour with that of other users (e.g. ‘Your neighbours are leaving you behind on their bikes! Catch up and use the mobility tracker today!’). We compared the distances cycled before, during and after the nudges were sent, defining a two-week period for each condition. In the two weeks before nudging, cyclists covered a total of 469.3 km. During nudging, they cycled 600.8 km, which seems to indicate a positive effect of the nudging. After the nudging, they covered 652.7 km. However, it is unclear whether this was a result of the nudging, as the longer-term effects of nudging are unknown (Marteau et al., 2011). The weather could play a role, as before the nudges the average temperature was a little lower (5.6°C, 27.1 mm of rainfall) than the period during which the nudges were sent out (12.1°C, 11.6 mm).¹ The two weeks after the nudging were the warmest, but they also had the highest rainfall (12.4°C, 62.6 mm). However, it seems that more users were motivated to get on their bikes when the nudges were sent out than during the period that followed: 28 tracked their cycling during the nudging period, compared to 11 in the following two weeks.

5 Conclusion

In sum, our preliminary results are encouraging regarding the effectiveness of using nudging and gamification techniques within a personal mobility app to foster cycling within a city. There is some evidence to suggest that nudging was successful, but more contextual factors (e.g. the weather) need to be taken into account; a combination of contextual data and nudging could be the most successful. In addition, nudges could be moderated by identification with the relevant community. As users become part of a neighbourhood, their engagement with activities can be logged in the app (e.g. the number of POIs in the neighbourhood that they have visited). Our first results might help to inform how nudging using digital tools could help foster behavioural change. However, before nudging is implemented on a broad scale, especially in combination with collecting personal data, it is essential to evaluate the ethical and legal implications.

¹ <https://meteostat.net/de/station/11150?t=2021-04-22/2021-05-03> (accessed 8 November 2021)

Acknowledgements

This research has received funding in the framework of the Joint Programming Initiative Urban Europe (Making Cities Work, project SimpliCITY). Funding for Austria was received from the Austrian Federal Ministry of Climate Action, Environment, Energy, Mobility, Innovation and Technology, and for Sweden from Vinnova.

References

- Abrahamse, W., & Steg, L. (2013). Social influence approaches to encourage resource conservation: A meta-analysis. *Global Environmental Change*, 23(6), 1773–1785.
<https://doi.org/10.1016/J.GLOENVCHA.2013.07.029>
- Ajzen, I. (1991). The theory of planned behavior. *Organizational Behavior and Human Decision Processes*, 50(2), 179–211. [https://doi.org/10.1016/0749-5978\(91\)90020-T](https://doi.org/10.1016/0749-5978(91)90020-T)
- Doran, R., Hanss, D., & Øgaard, T. (2017). Can Social Comparison Feedback Affect Indicators of Eco-Friendly Travel Choices? Insights from Two Online Experiments. *Sustainability* 2017, Vol. 9, Page 196, 9(2), 196. <https://doi.org/10.3390/SU9020196>
- Engel, T. (2017). Influencing the choice of means of transportation by Gamification. *ATZ Worldwide* 2017 119:5, 119(5), 70–72. <https://doi.org/10.1007/S38311-017-0053-9>
- European Environment Agency. (2018). Greenhouse gas emissions from transport in Europe. <https://www.eea.europa.eu/data-and-maps/indicators/transport-emissions-of-greenhouse-gases-7>
- European Platform on Mobility Management. (2018). Mobility Management Strategy Book. EPOMM. http://epomm.eu/sites/default/files/files/EPOMM_strategy_book.pdf
- Festinger, L. (1954). A Theory of Social Comparison Processes: *Human Relations*, 7(2), 117–140. <https://doi.org/10.1177/001872675400700202>
- Hamari, J., Koivisto, J., & Sarsa, H. (2014). Does gamification work? - A literature review of empirical studies on gamification. Proceedings of the Annual Hawaii International Conference on System Sciences, 3025–3034. <https://doi.org/10.1109/HICSS.2014.377>
- Huber, L. R., Sloof, R., & Van Praag, M. (2017). The effect of incentives on sustainable behavior: evidence from a field experiment. *Labour Economics*, 45, 92–106. <https://doi.org/10.1016/J.LABECO.2016.11.012>
- Kazhamiakin, R., Marconi, A., Martinelli, A., Pistore, M., & Valetto, G. (2016). A gamification framework for the long-term engagement of smart citizens. 1–7. <https://doi.org/10.1109/ISC2.2016.7580746>
- Klieber, K., Luger-Bazinger, C., Hornung-Prähauser, V., Geser, G., Wieden-Bischof, D., Paraschivoiu, I., Layer-Wagner, T., Mostegl, N., Huemer, F., & Rosen, J. (2020). Nudging sustainable behaviour: Data-based nudges for smart city innovations. The ISPIM Innovation Conference – Innovating in Times of Crisis, 7-10 June 2020. https://conferencesubmissions.com/ispim/proceedings/individual_papers/1118544199_Paper.pdf
- Koivisto, J., & Hamari, J. (2014). Demographic differences in perceived benefits from gamification. *Computers in Human Behavior*, 35, 179–188. <https://doi.org/10.1016/J.CHB.2014.03.007>
- Lehner, M., Mont, O., & Heiskanen, E. (2016). Nudging – A promising tool for sustainable consumption behaviour? *Journal of Cleaner Production*, 134, 166–177. <https://doi.org/10.1016/j.jclepro.2015.11.086>
- Ly, K., & Soman, D. (2013). Nudging Around The World. https://inside.rotman.utoronto.ca/behaviouraleconomicsinaction/files/2013/12/Nudging-Around-The-World_Sep2013.pdf

- Macovei, O.-I. (2015). Applying the Theory of Planned Behavior in Predicting Pro-environmental Behavior: The Case of Energy Conservation. *Acta Universitatis Danubius. (Economica)*, 11(4). <http://journals.univ-danubius.ro/index.php/oeconomica/article/view/2958/2830>
- Marteau, T. M., Ogilvie, D., Roland, M., Suhrcke, M., & Kelly, M. P. (2011). Judging nudging: can nudging improve population health? *BMJ*, 342(7791), 263–265. <https://doi.org/10.1136/BMJ.D228>
- Meske, C. (2017). Digital Nudging – Wie User zu besseren Entscheidungen „angestupst“ werden können – Competence Center Connected Organization. <https://connected-organization.de/2017/07/nudging-wie-user-zu-besseren-entscheidungen-angestupst-werden-koennen/>
- Nudge Lebanon. (2019). Improving Timely Payment of Electricity Bills. <https://nudgelebanon.org/2019/01/24/improving-timely-payment-of-electricity-bills/>
- Reisch, L. A., & Sunstein, C. R. (2016). Do Europeans like nudges? *Judgment and Decision Making*, 11(4), 310–325.
- Schneider, C., Weinmann, M., & vom Brocke, J. (2018). Digital nudging: Guiding online user choices through interface design. *Communications of the ACM*, 61(7), 67–73. <https://doi.org/10.1145/3213765>
- Sunstein, C. (2014). Nudging: A Very Short Guide. *Journal of Consumer Policy*, 37(4), 583–588. <https://doi.org/10.1007/S10603-014-9273-1>
- Thaler, R. H., & Sunstein, C. R. (2008). Nudge: Improving decisions about health, wealth, and happiness. In *Nudge: Improving Decisions about Health, Wealth, and Happiness*. Yale University Press.